

RNA-binding proteins balance neuronal activity



Dissertation der Fakultät für Biologie
der Ludwig-Maximilians-Universität München

Rico Schieweck

München, 2020

Diese Dissertation wurde unter der Leitung von
Prof. Dr. Michael Kiebler und Prof. Dr. Heinrich Leonhardt
im Bereich Zellbiologie – Anatomie III des Biomedizinischen Centrums (BMC) der Ludwig-
Maximilians-Universität München angefertigt

Erstgutachter: Prof. Dr. Heinrich Leonhardt

Zweitgutachter: Prof. Dr. Christof Osman

Tag der Abgabe: 17.03.2020

Tag der mündlichen Prüfung: 21.07.2020

Eidesstattliche Erklärung

Ich versichere hiermit an Eides statt, dass die vorgelegte Dissertation von mir selbständig und ohne unerlaubte Hilfe angefertigt ist.

München, den 16.09.2020 Rico Schieweck
(Unterschrift)

Erklärung

Hiermit erkläre ich, *

- dass die Dissertation nicht ganz oder in wesentlichen Teilen einer anderen Prüfungskommission vorgelegt worden ist.
- dass ich mich anderweitig einer Doktorprüfung ohne Erfolg **nicht** unterzogen habe.
- dass ich mich mit Erfolg der Doktorprüfung im Hauptfach
und in den Nebenfächern
bei der Fakultät für der
(Hochschule/Universität)
unterzogen habe.
- dass ich ohne Erfolg versucht habe, eine Dissertation einzureichen oder mich der Doktorprüfung zu unterziehen.

München, den 16.09.2020 Rico Schieweck
(Unterschrift)

*) Nichtzutreffendes streichen

Table of content

Abbreviations	1
List of Publications	2
<i>Research articles</i>	2
<i>Review articles</i>	2
<i>Book chapters</i>	3
<i>Submitted/ In preparation</i>	3
Summary	4
Zusammenfassung	6
1. Introduction	8
1.1 <i>Synaptic transmission and plasticity</i>	8
1.2 <i>RNA-binding proteins as critical regulators of synaptic functioning</i>	10
1.3 <i>Translation as regulatory hub for neuronal homeostasis and synaptic transmission</i>	13
1.4 <i>Pumilio2 and its role in synaptic balancing</i>	18
1.5 <i>The RNA transport RBP Staufen2 crucially contributes to synaptic functioning</i>	19
1.6 <i>RBPs and their role in balancing neuronal activity: the aims of my Ph.D. thesis</i>	20
2. Discussion	21
2.1 <i>The complex regulatory potential of RBPs</i>	21
2.1.1 <i>Pum2 and Stau2 selectively shape the neuronal proteome</i>	22
2.2 <i>Synaptic protein expression is controlled by Pum2 and Stau2</i>	25
2.2.1 <i>Pum2 activates GABAergic protein expression</i>	25
2.2.1.1 <i>Pum2 and the maturation of the GABAergic system</i>	29
2.2.1.2 <i>GABA regulates Pum2 expression</i>	30
2.2.2 <i>Stau2 functionally regulates synaptic organization</i>	31
2.3 <i>Pum2 and Stau2 are needed for circuit homeostasis and plasticity</i>	33
2.3.1 <i>Knock-down of Pum2 causes epileptic seizures</i>	33
2.3.2 <i>Stau2 is necessary for motor learning and novelty response</i>	34
2.4 <i>The RBP network as key to understand neuropsychiatric and neurological diseases? An outlook</i>	35
2.4.1 <i>The RBP network to regulate synaptic homeostasis: what we know and where we go</i>	35
2.4.2 <i>RBPs and their therapeutic potential</i>	37
3. References	39
Appendices	54
<i>Publication I: Pumilio2-deficient mice show a predisposition for epilepsy</i>	54

<i>Publication II: Staufen2 deficiency leads to impaired response to novelty in mice</i>	55
<i>Publication III: Altered Glutamate Receptor Ionotropic Delta Subunit 2 Expression in Stau2-Deficient Cerebellar Purkinje Cells in the Adult Brain</i>	56
<i>Publication IV: Posttranscriptional Gene Regulation of the GABA Receptor to Control Neuronal Inhibition</i>	57
<i>Manuscript I (Publication V): The RNA-binding protein Pumilio2 controls translation of the GABA_A receptor subunit GABRA2 to regulate neuronal excitation</i>	58
<i>Manuscript II (Publication VI): The RNA-binding protein Pumilio2 regulates GABAergic transmission</i>	59
Acknowledgments	60
Curriculum Vitae	61

Abbreviations

3'-UTR	3'-untranslated region
Ago	Argonaute
ALS	Amyotrophic lateral sclerosis
AMPA	α -amino-3-hydroxy-5-methyl-4-isoxazolepropionic acid
ASD	Autism spectrum disorders
CDS	Coding sequence
CLIP	Crosslinking and immunoprecipitation
E	Excitation
EPSC	Excitatory postsynaptic current
FDA	Food & Drug Administration
FMRP	Fragile X mental retardation protein
FTD	Frontotemporal dementia
GABA	γ -aminobutyric acid
I	Inhibition
IPSC	Inhibitory postsynaptic current
LTP	Long-term potentiation
LTD	Long-term depression
miRNA	microRNA
mRNA	messenger RNA
NOR	Novel object recognition
NMDA	<i>N</i> -Methyl-D-aspartate
Pum2	Pumilio2
RBP	RNA-binding protein
RNP	Ribonucleoprotein particle
SMA	Spinal muscle atrophy
SMN1	Survival motor neuron 1
Stau2	Staufen2
tRNA	transfer RNA
WT	Wildtype

List of Publications

Research articles

1. **Schieweck R.***, Kiebler M.A.* (2019) Posttranscriptional gene regulation of the GABA receptor to control neuronal inhibition. *Front Mol Neurosci.* 12, 152 (*corresponding authors)
2. Pernice H.F., **Schieweck R.**, Jafari M., Straub T., Bilban M., Kiebler M.A. and Popper B. (2019). Altered Glutamate Receptor Ionotropic Delta Subunit 2 Expression in Stau2-Deficient Cerebellar Purkinje Cells in the Adult Brain. *Int J Mol Sci.* 20, 1797
3. Popper B., Demleitner A., Bolivar V.J., Kusek G., Snyder-Keller A., **Schieweck R.***, Temple S., Kiebler M.A.* (2018) Stauf2 deficiency leads to impaired response to novelty in mice. *Neurobiol Learn Mem.* 150, 107-115 (*corresponding authors)
4. Berger S.M., Fernández-Lamo I., Schöning K., Fernandez-Moya S.M., Ehses J., **Schieweck R.**, Clementi S., Enkel T., von Bohlen Und Halbach O., Segura I.*, Delgado-García J.M., Gruart A., Kiebler M.A.* and Bartsch D.* (2017) Forebrain-specific, conditional silencing of Stauf2 alters synaptic plasticity, learning, and memory in rats. *Genome Biol.* 18, 222 (*corresponding authors)
5. Follwaczny P.*, **Schieweck R.***, Demleitner A., Straub T., Klemm A.H., Riedemann T., Bilban M., Sutor B., Popper B. and Kiebler M.A. (2017). Pumilio2-deficient mice show a predisposition for epilepsy in mice. *Dis Model Mech.* 10, 1333-1342 (*shared first authors)

Review articles

1. **Schieweck R.**, Ninkovic J. and Kiebler M.A. (2019). Balance at the synapse – lessons from the biology of RNA-binding proteins. *Physiol Rev.* *under revision.*
2. Pernice H.F., **Schieweck R.**, Kiebler M.A. and Popper B. (2016). mTOR and MAPK: from localized translation control to epilepsy. *BMC Neurosci.* 17, 73
3. **Schieweck R.**, Popper B. and Kiebler M.A. (2016). Co-Translational Folding: A Novel Modulator of Local Protein Expression in Mammalian Neurons? *Trends Genet.* 32, 788-800

Book chapters

1. **Schieweck R.**, Ang F.Y., Fritzsche R. and Kiebler M.A. (2018). Isolation and Characterization of Endogenous RNPs from Brain Tissues. In: Gaspar I. (eds.) RNA Detection. *Methods in Molecular Biology*, Vol 1649. Humana Press, New York, NY

Submitted/ In preparation

1. **Schieweck R.**, Riedemann T., Forné I., Rieger D., Demleitner A.F., Popper B., Sutor B., Imhof A. and Kiebler M.A. (2020). The RNA-binding protein Pumilio2 regulates GABAergic transmission.
2. **Schieweck R.** and Kiebler M.A. (2020). The RNA-binding protein Pumilio2 controls translation of the GABA_A receptor subunit *Gabra2* to regulate neuronal excitation.
3. Frey S.*, **Schieweck R.***, Forne I., Imhof A., Straub T., Popper B. and Kiebler M.A. (2020). Physical activity dynamically regulates the hippocampal proteome along the dorsoventral axis: implications for adult neurogenesis. (*shared first authors)

Summary

Neuronal activity and network excitability crucially rely on the balance between excitation (E) and inhibition (I). Dysregulation of this tightly controlled E/I ratio is thought to be the molecular cause of many neurological and neuropsychiatric diseases such as epilepsy and autism spectrum disorders (ASD). Elucidating the control mechanisms guiding this balance is a prerequisite to understand these diseases. Therefore, upstream regulators of the E/I ratio need to be identified and characterized. RNA-binding proteins (RBPs) are promising candidates since (i) depletion of certain RBPs causes severe pathological deficits such as ASD or epilepsy, (ii) RBPs bind to and control the expression of numerous mRNAs and (iii) they are able to bind transcripts coding for both excitatory and inhibitory synaptic signaling molecules.

The aim of this PhD thesis is to unravel the impact of two different RBPs, *i.e.* Pumilio2 (Pum2) and Stauf2 (Stau2), on balancing neuronal activity. I exploited complementary approaches consisting of transcriptome/proteome analysis, microscopy, electrophysiology and behavioral assays using primary neuronal cell cultures, brain tissues and transgenic mouse lines. Altogether, my data strongly suggest that Pum2 and Stau2 control different aspects of neuronal activity.

Pum2 has a dual role in regulating neuronal excitability. It is known to repress the expression of voltage-gated sodium channels such as Nav1.2 (*Scn2a*) and Nav1.6 (*Scn8a*) to inhibit neuronal excitation. In my work, I have identified that Pum2 regulates several key proteins for neuronal inhibition such as Gephyrin (Gphn) and the $\alpha 2$ subunit of the GABA_A receptor (Gabra2). Thereby, Pum2 enhances Gphn, but represses Gabra2 expression. Gphn is the postsynaptic scaffolding protein of glycine and GABA_A receptors. Interestingly, Gphn expression drops in dendrites, but not in the soma of Pum2 deficient neurons. Accordingly, spontaneous synaptic miniature inhibitory postsynaptic currents (mIPSCs) are significantly reduced while general (IPSCs) are unaffected. Together, these findings argue for a crucial role of Pum2 in GABAergic transmission. In the case of the $\alpha 2$ subunit of the GABA_A receptor (Gabra2), Pum2 selectively represses Gabra2 expression both in cultured neurons and in mouse brain. Importantly, double knock-down of *Gabra2* and *Pum2* leads to enhanced excitatory synaptic transmission. These findings suggest that Gabra2 upregulation serves as a compensatory effect to counterbalance increased neuronal excitability in Pum2 depleted neurons. Together, these results establish Pum2 as a key regulator to balance neuronal activity. Supportive for this notion is the finding that Pum2 knock-down (KD) mice show a

predisposition to develop epileptic seizures, a neurological disease characterized by an imbalance in neuronal network activity.

To evaluate whether the effect of Pum2 on GABAergic transmission was selective for this specific RBP, I also investigated the RBP Stau2. Stau2 is a crucial regulator of gene expression. Upon depletion of Stau2 in cortical neurons, GABAergic proteins remain mostly unaffected. Proteins involved in neurotransmitter release, however, such as Complexin1 (Cplx1) and the ionotropic glutamate receptor AMPA1 (Gria1), are significantly downregulated. Cplx1 and Gria1 are both essential for synaptic transmission and plasticity. Strikingly, a recently established Stau2 KD rat model in the lab shows an imbalance in the long-term potentiation (LTP) to long-term depression (LTD) ratio suggesting that Stau2 acts as a regulatory hub to balance plasticity. In line with this, Stau2 KD mice show spatial memory deficits and impaired novelty response. Moreover, another neurotransmitter receptor, the glutamate receptor ionotropic delta subunit 2 (GluD2 or Grid2), shows enhanced expression upon physical training of Stau2 KD animals, when compared to control mice. GluD2 is essential for synaptic transmission in the cerebellum and important for motor learning. Strikingly, Stau2 KD animals exhibit a delay in motor learning indicating an impact on synaptic plasticity in the cerebellum. Together, my PhD thesis establishes the RBPs Pum2 and Stau2 as crucial regulators to balance neuronal activity in the brain. While Pum2 fine-tunes GABAergic inhibition and voltage-gated sodium channel mediated excitation, Stau2 controls the balance in synaptic plasticity. Understanding the underlying mechanisms controlling synaptic balancing is key to develop new therapies for treating neurological and neuropsychiatric disorders such as epilepsy and ASD.

Zusammenfassung

Neuronale Aktivität und Netzwerk-Erregbarkeit hängen im besonderen Maße von einem Gleichgewicht zwischen Erregung (E) und Inhibition (I), dem sogenannten E/I Quotienten, ab. Ein Verschieben dieses Gleichgewichts wurde bisher mit verschiedenen neurologischen und neuropsychiatrischen Krankheiten wie Epilepsie und Autismus in Verbindung gebracht. Ein Verständnis der molekularen Mechanismen, die diese Balance etablieren, ist Voraussetzung um diese Krankheiten verstehen zu können. Dabei ist es besonders wichtig, Schlüsselregulatoren zu identifizieren, die das E/I Verhältnis beeinflussen. Hierfür sind RNA-Bindeproteine (RBP) aus mehreren Gründen vielversprechende Kandidaten. Erstens, genetische Deletion von bestimmten RBPs verursacht schwere neurologische und neuropsychiatrische Krankheiten wie Epilepsie und Autismus. Zweitens, RBPs binden und regulieren zahlreiche verschiedene Transkripte. Und drittens, sie sind in der Lage, sowohl mRNAs kodierend für erregende als auch hemmende Rezeptoren zu binden.

Das Ziel dieser Doktorarbeit war es zu klären, ob und wie die beiden RBPs Pumilio2 (Pum2) und Stau2 (Stau2) das E/I Verhältnis regulieren. Um diese Fragestellung zu beantworten, verwendete ich einen komplementären experimentellen Ansatz, der sowohl Transkriptom- und Proteom-Analysen, sowie Mikroskopie und Elektrophysiologie, als auch Verhaltenstests an verschiedenen Mauslinien enthielt. Meine Daten zeigen deutlich, dass Pum2 und Stau2 unterschiedliche Aspekte der neuronalen Aktivität regulieren können.

Pum2 hat eine Doppelfunktion in dieser Regulation. Aus anderen Studien ist bekannt, dass es die Expression von spannungsabhängigen Natriumkanälen wie $\text{Na}_v1.2$ (*Scn2a*) und $\text{Na}_v1.6$ (*Scn8a*) inhibiert. Damit unterdrückt Pum2 indirekt die neuronale Erregbarkeit. Meine Arbeit zeigt nun, dass verschiedene Schlüsselmoleküle, lokalisiert an inhibitorischen Synapsen, wie z.B. Gephyrin (Gphn) und die $\alpha 2$ Untereinheit des GABA_A Rezeptors (Gabra2), von Pum2 reguliert werden. Hierbei fördert Pum2 die Expression von Gphn, inhibiert jedoch die von Gabra2.

Gphn ist ein Verankerungsmolekül, das Glyzin- und GABA_A -Rezeptoren in der Membran fixiert. Interessanterweise sinkt das Gphn Proteinlevel nur in den Dendriten, aber nicht im Soma von Pum2-defizienten Neuronen. Als Konsequenz zeigen spontane inhibitorische synaptische Ströme eine reduzierte Amplitude. Diese Daten belegen eindeutig, dass Pum2 die GABA_A synaptische Übertragung steuert. Ein weiteres Zielmolekül von Pum2 ist die $\alpha 2$ Untereinheit des GABA_A Rezeptors (Gabra2). Hierbei unterdrückt Pum2 die Expression von Gabra2 in

kultivierten kortikalen Neuronen und im Mausgehirn. Dieser Effekt ist hochselektiv. Die Runterregulation von Pum2 und Gabra2 führt zu einer Erhöhung der neuronalen Aktivität. Basierend auf diesen Daten lässt sich folgendes Modell herleiten: die Hochregulation von Gabra2 in Pum2-defizienten Neuronen inhibiert die neuronale Aktivität und puffert somit die erhöhte Erregbarkeit dieser Neurone ab. Das bedeutet, die Pum2-abhängige translationelle Kontrolle von Gabra2 repräsentiert einen kompensatorischen Effekt. Zusammenfassend lassen meine Daten den Schluss zu, dass Pum2 ein wichtiger Regulator ist, um neuronale Aktivität auszubalancieren. Im Einklang mit diesem Modell sind *in vivo* Daten von Pum2-defizienten Mäusen. Diese Tiere zeigen spontane epileptische Anfälle, welche durch ein Ungleichgewicht der neuronalen Aktivität gekennzeichnet sind.

Um die Selektivität der Pum2 vermittelten Kontrolle der GABAergen Inhibition einschätzen zu können, habe ich diesbezüglich auch Stau2 untersucht. Stau2 ist ein weiteres RBP sowie ein wichtiger Regulator der Genexpression. Nach der Depletion von Stau2 in kortikalen Neuronen sind Proteine für die GABAerge Transmission weitergehend unverändert. Jedoch zeigen Proteine, die für die Freisetzung von Neurotransmittern wichtig sind, wie z.B. Complexin1 (Cplx1), als auch der AMPA1 Rezeptor eine Verminderung der Expression. Beide Proteine sind essentiell für die synaptische Übertragung und Plastizität. Von besonderer Bedeutung sind in diesem Zusammenhang *in vivo* Daten aus einer Stau2 KD Rattenlinie. Diese Ratte zeigt ein Ungleichgewicht zwischen LTP und LTD. Diese Daten deuten darauf hin, dass Stau2 ein zentraler Regulator der synaptischen Plastizität ist. Übereinstimmend mit diesen molekularen Daten sind Verhaltenstests mit einer Stau2-defizienten Maus. Diese zeigt Defizite im räumlichen Gedächtnis und in ihrer kognitiven Flexibilität. Des Weiteren zeigt ein anderer Neurotransmitterrezeptor, die Untereinheit Delta 2 des ionotropen Glutamaterezeptors (GluD2), nach körperlichem Training eine erhöhte Expression in Stau2-defizienten Mäusen. GluD2 ist essentiell für die synaptische Übertragung im Kleinhirn und wichtig für das Motorlernen. Interessanterweise zeigen Stau2 KD Mäuse eine Verzögerung im Motorlernen, was auf eine gestörte synaptische Plastizität hindeutet.

Zusammenfassend hat meine Doktorarbeit gezeigt, dass Pum2 und Stau2 entscheidend neuronale Aktivität regulieren. Während Pum2 die GABAerge Inhibition als auch die Natriumkanal-abhängige Erregbarkeit steuert, balanciert Stau2 synaptische Plastizität. Das Verständnis über die zugrundeliegenden Mechanismen, die das Gleichgewicht der neuronalen Aktivität regulieren, ist Voraussetzung, um zukünftig neue Therapiestrategien gegen neurologische und neuropsychiatrische Krankheiten wie Autismus und Epilepsie entwickeln zu können.

1. Introduction

1.1 Synaptic transmission and plasticity

Neuronal communication relies on the transmission of currents through chemical synapses. Intense research in the last decades has unraveled the principles of synaptic transmission at inhibitory and excitatory contact sites. This effort has been awarded by 17 Nobel prizes so far. It is generally accepted that sufficient dendritic (but also somatic) stimulation generates an action potential in the presynaptic neuron. This action potential moves along its axon and induces calcium dependent exocytosis of neurotransmitters at presynaptic buttons (1). These transmitters diffuse through the synaptic cleft to activate synaptic receptors in the postsynaptic neuron. Importantly, the action of a certain neurotransmitter on neuronal activity depends on both the nature of the neurotransmitter and the composition of the postsynaptic receptors. The activation of postsynaptic receptors can either stimulate a neuron or dampen its activity (1, 2). The two main opponent neurotransmitters in the brain are glutamate for excitation and GABA (γ -aminobutyric acid) for inhibition. The fine-tuned ratio of excitation (E) and inhibition (I) is the basis for both proper neuronal development and neuronal circuit homeostasis in the adult brain (3).

Importantly, the Cl^- ion concentration gradient conveys neuronal inhibition. Thus, intracellular Cl^- concentration ($[\text{Cl}^-]_i$) determines whether GABA is excitatory or inhibitory (4, 5). For instance, early postnatal neurons highly express the Cl^- ion intruder Solute carrier family 12 member 2, also called Bumetanide-sensitive sodium-(potassium)-chloride cotransporter 2 (*Slc12a2* or NKCC1). NKCC1 imports Cl^- from the extracellular environment. Thus, in immature neurons, activation of the GABA_A receptor, which is a Cl^- channel itself, leads to a net efflux of Cl^- ions and thereby to neuronal depolarization. However, during postnatal maturation, the main Cl^- ion extruder Solute carrier family 12 member 5, also called K/Cl cotransporter 2 (*Slc12a5* or KCC2) is expressed. KCC2 exports Cl^- ions and establishes the gradient that is necessary for neuronal hyperpolarization upon GABA stimulation (6). The opposing expression profiles of KCC2 and NKCC1 are essential to drive neuronal maturation through the establishment of GABA as neuronal inhibitor: the so-called GABA switch (4, 5). It has been shown that excitatory GABA enhances calcium influx through the NMDA receptor during development (7). Complementary, the NMDA receptor enhances inhibitory synapse formation in immature neurons (8). Hence, the balance between the glutamatergic and

GABAergic systems during development is essential for proper neuronal functioning in the adult brain. In line with this notion are findings showing that the imbalance between NKCC1 and KCC2 causes ASD and schizophrenia (9, 10).

In the adult brain, the E/I ratio determines net synaptic currents. In general, the strength of synaptic transmission is defined by its frequency and the corresponding amplitude. As an approximation, the frequency is determined by the number of presynaptic vesicles and their probability to release neurotransmitters. In contrast, the amplitude is crucially influenced by the activation of postsynaptic receptors. These two parameters crucially influence both excitatory and inhibitory postsynaptic currents (EPSCs and IPSCs, respectively). Hence, the interplay between pre- and postsynaptic activity as well as the E/I ratio decide about the stimulation efficiency of the target neuron. In addition to its role as receptor ligands, the downstream signaling induced by the neurotransmitters, such as serotonin, has the capacity to posttranslationally modify proteins. This process crucially regulates histone proteins and thereby transcription (11), linking synaptic stimulation with transcriptional activity.

Synaptic activity induces different downstream signaling pathways in the postsynaptic neuron that can strengthen or weaken the transmission. This phenomenon is called ‘synaptic plasticity’ (12). Intense research in the last decades has identified numerous molecules that control synaptic plasticity (12–14). The two main types of synaptic plasticity are long-term potentiation (LTP) and long-term depression (LTD). It is generally accepted that LTP enhances transmission efficiency while LTD decreases it. Together, they provide the basis for learning, memory formation and cognitive flexibility (12, 13, 15, 16). Importantly, both LTP and LTD depend, at least partly, on translation (17, 18) (see also *section 1.3 Translation as regulatory hub for neuronal homeostasis and synaptic transmission*). Similar to the E/I ratio, LTP and LTD need to be balanced to allow flexibility of the neuronal network. Of note, both forms of plasticity are conveyed by changes in the synaptic actin cytoskeleton network. These changes are equally important for the decay of memory, a process that has been termed forgetting (19).

In summary, the molecular basis for balancing neuronal activity and plasticity is already being established during development. Moreover, it is the basis for neuronal circuit homeostasis (20). This homeostasis is a prerequisite for adjusting and fine-tuning memory acquisition and decay. Therefore, identification of key regulators is crucial to understand these fundamental processes.

1.2 RNA-binding proteins as critical regulators of synaptic functioning

Research in the last decades has clearly established that certain RBPs are crucial for synaptic function (21). RBPs bind their target mRNAs preferentially in the 3'-untranslated region (3'-UTR) (22). Thereby, they control different aspects of the RNA life cycle such as splicing, RNA stability and localization as well as translation (23, 24). Importantly, mRNAs can be bound by several RBPs (25) indicating a certain degree of cooperativity or competition between RBPs to control gene expression. This cooperativity is thought to be a complex interplay between RBPs and might account for compensatory (or indirect) effects observed upon knocking out a single RBP (Schieweck *et al.*, *Physiol. Rev.* *under revision*). To date, several hundred RBPs have been identified exploiting different experimental approaches such as UV crosslinking of RBPs to RNA and immunoprecipitation (CLIP) or density gradient centrifugation (26, 27). The ever-growing list of RBPs raises the question about their manifold functional implications in neurons.

In this context, RBPs might play a pivotal role in regulating the synaptic balance for several reasons. First, knock-out (KO) or KD of certain RBPs such as the Fragile X Mental Retardation Protein (FMRP), Rbfox1 or Pumilio2 (Pum2) in mice lead to severe alterations in neuronal network activity resulting in mental retardation and epilepsy (28–31). Second, RBPs have the ability to regulate numerous steps in the RNA life cycle such as RNA decay, transport and translation (23, 24). Thereby, in the absence of a certain functional RBP, multiple transcripts are affected, which is characteristic for complex multigenic disorders. Third, different mRNAs coding for subunits of GABA_A (32) and glutamatergic receptors are bound by several RBPs (Schieweck *et al.*, *Physiol. Rev.* *under revision*). Fourth, RBPs such as FMRP and Rbfox1 regulate GABAergic transmission through different mechanisms, including receptor transport (33, 34), indicating distinct effects on excitability regulation.

To date, only few RBPs have been tested for their *in vivo* role in neuronal transmission and synaptic plasticity. One of the best characterized RBPs regarding its impact on excitatory and inhibitory synaptic transmission is Rbfox1 (28, 34, 35). The absence of Rbfox1 in mouse brain increases excitatory synaptic transmission efficiency (28). Moreover, it is essential for development and required for establishing the connectivity of inhibitory interneurons. Therefore, interneuron specific KO of Rbfox1 leads to a decrease in frequency and amplitude of inhibitory synaptic currents (35). In line with this notion is the finding that brain-wide KO of Rbfox1 increases the E/I ratio (34), which might be a molecular explanation for the epileptic seizures observed in Rbfox1 KO mice (28). Another example for an RBP regulating the E/I

ratio is TAR-DNA binding protein 43, also known as TDP-43. Mutant TDP-43 is well-known to cause neurodegeneration as observed in amyotrophic lateral sclerosis (ALS) and frontotemporal dementia (FTD) (36, 37). Interestingly, presymptomatic mice carrying mutant TDP-43 show increased frequency of EPSCs, while IPSCs remain unaffected, leading to an increase in the E/I ratio (38) similar to *Rbfox1* KO mice. In contrast to *Rbfox1* and TDP-43, FMRP KO mice exhibit a reduction in both frequency and amplitude of EPSCs (39). This finding might be the molecular basis for mental retardation observed in fragile X mental retardation patients (40).

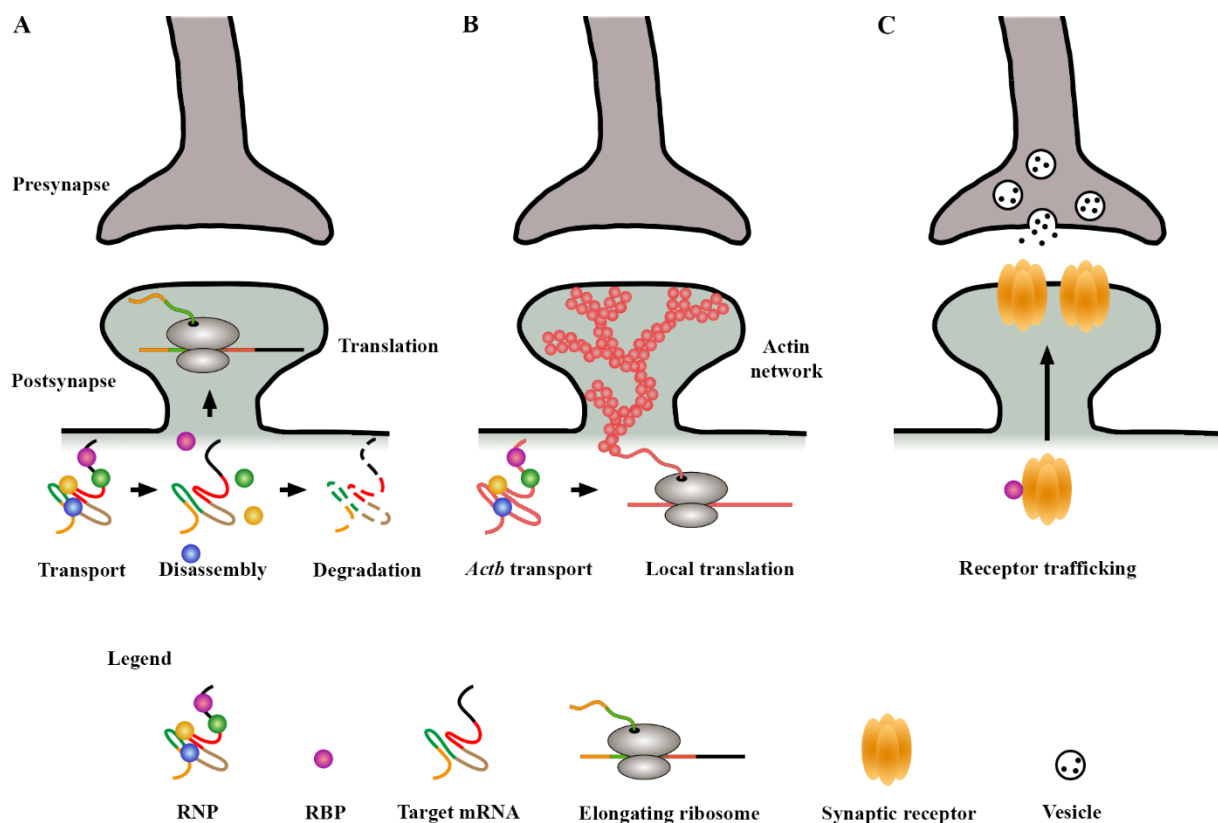


Figure 1: RBPs regulate synaptic transmission through different mechanisms.

(A) Transcripts coding for synaptic receptors or components of their downstream signaling cascade such as $\text{CaMKII}\alpha$ are transported in RNA granules, also termed RNPs. Synaptic activation leads to disassembly of these RNA granules. Localized mRNAs are subsequently translated near and/or at synapses. Locally, newly synthesized proteins modify synaptic transmission efficiency. mRNAs might be degraded locally or repacked into RNPs in order to limit the protein supply.

(B) Remodeling the synaptic actin network is necessary for synaptic plasticity. RBPs can regulate the actin organization through delivery and translational control of $\beta\text{-actin}$ (*Actb*) or essential actin remodelers such as *Cofilin-1*.

(C) In addition to its role in RNA transport, degradation and translation, RBPs might regulate receptor trafficking to postsynaptic densities through direct protein-protein interactions.

In the cerebellum, however, FMRP KO leads to enhanced release of GABA from the basket cells to inhibit Purkinje cells (33), suggesting a role for FMRP in balancing neuronal excitation

and inhibition. Moreover, FMRP also regulates the GABA switch during development. Depletion of FMRP leads to a delay of the inhibitory action of GABA due to the accumulation of NKCC1 (41) suggesting a complex impact of FMRP on neuronal activity.

The three mentioned examples, *i.e.* Rbfox1, TDP-43 and FMRP, clearly show that RBPs might be essential to balance neuronal activity. Even though the underlying mechanisms of posttranscriptional gene regulation might be different (**Fig. 1**), some aspects are commonly shared between different RBPs. First, RBPs control neuronal excitation by regulating expression of synaptic proteins, cytoskeleton or receptor organization. Rbfox1 for example regulates the expression of the presynaptic vSNARE protein Vamp1 through antagonizing miRNA mediated repression (34). In brief, Rbfox1 binds the 3'-UTR of *Vamp1* and thereby blocks binding of *miRNA-9* that would otherwise induce *Vamp1* mRNA degradation through the Ago pathway (42). Vamp1 is expressed in inhibitory interneurons and it is important for GABA release (34). Another example is FMRP. This RBP regulates the activity-dependent expression of Cofilin-1 (43), a protein that regulates the dynamics of the actin cytoskeleton, essential for dendritic spine maturity (44). Upon chemical induction of LTP, *Cofilin-1* mRNA is decreased in dendrites. In FMRP KO neurons, the effect is absent, which might explain the impaired dynamics of dendritic spine morphology observed upon LTP induction (43). In addition to its ability to bind mRNAs, FMRP can directly control transmitter release through the interaction with ion channels such as the potassium channel K_v1.2 (33) (**Fig. 1C**). Second, in the brain RBPs can be expressed both in pyramidal cells and inhibitory interneurons (45) suggesting cell type specific roles and mRNA targets (**Fig. 2**). This might explain their distinct impact on excitation and inhibition as discussed above. And third, different RBPs share some of their mRNA targets such as the glutamate and the GABA receptors as well as additional ion channels (Schieweck *et al.*, *Physiol. Rev.* *under revision*) (**Fig. 3**). Together, this provides the platform to either synergistically or antagonistically regulate their expression.

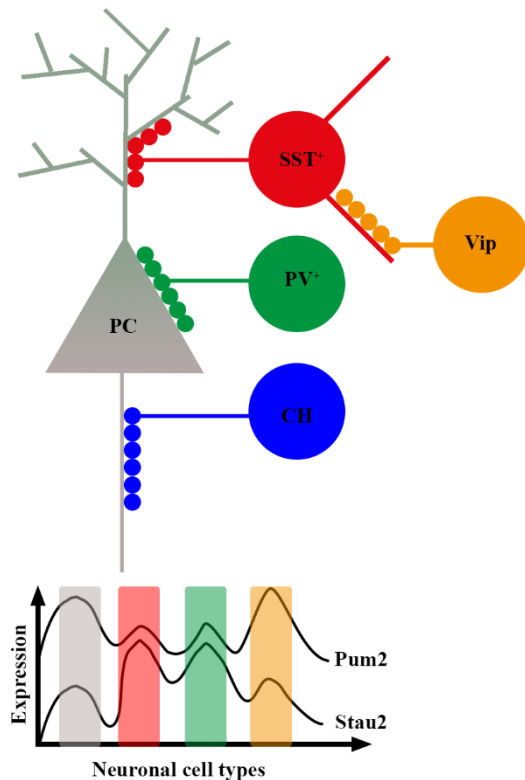


Figure 2: Neuronal cell type specific expression of RBPs.

Excitatory pyramidal cells (PC) are inhibited by different types of inhibitory interneurons. Thereby, somatostatin positive (SST⁺) interneurons target dendrites, parvalbumin positive (PV⁺) interneurons form synapses with the soma and chandelier cells (CH) with the axon initial segment (46). Importantly, within a negative feedback loop, vasointestinal peptide positive (Vip) interneurons inhibit SST⁺ cells. The coordinated interplay between PCs and interneurons is essential for homeostatic excitability. Interestingly, RBPs such as Pum2 and Stau2 show distinct expression profiles in different neuronal cell types (45).

1.3 Translation as regulatory hub for neuronal homeostasis and synaptic transmission

Numerous studies have unraveled by now that translation is a central regulatory hub for protein homeostasis (*proteostasis*) in cells (47). The classical view of translation as a biochemical process to synthesize proteins is certainly too simplistic. This process not only regulates protein levels, but also protein and mRNA stability as well as protein folding (48, 49). By exploiting different technologies such as ribosome profiling (50), polysome profiling (51) or translating ribosome affinity purification (TRAP) (52), different aspects of neuronal translation dynamics have been elucidated. To date, distinct sequences and structure elements embedded in an mRNA have been identified as regulators of translation. In particular for localized mRNAs, the 3'-UTR is of utmost importance for translation control (22) and protein localization (53). For instance, it has been shown that the median 3'-UTR length of localized mRNAs that are targets of the RBP Stau2 is significantly longer compared to the median length of the 3'-UTRs of the transcriptome (54). A possible explanation for this expansion is the evolutive addition of regulatory elements, such as different RBP binding motifs (**Fig. 3**) as well as miRNA binding sites (22, 55). The collectivity of these elements decides whether, where and how much a transcript is translated. Moreover, some transcripts contain retained introns in their 3'-UTR. These introns are necessary for mRNA localization (56) and translation control through the induction of the non-sense mediated decay pathway (NMD) (57). Importantly, one of the

transcripts that contain a retained intron in the 3'-UTR and is targeted for NMD is the activity-regulated cytoskeleton associated protein (*Arc*). *Arc* is needed for the actin cytoskeleton remodeling, which occurs during LTP (58). Neuronal stimulation enhances *Arc* mRNA localization to dendrites (59) and increases *Arc* protein levels (57) suggesting a complex role of NMD in regulating protein expression. Of note, pioneer studies suggest that the 3'-UTR holds a certain coding capacity. This conclusion is based on a significant ribosome density found in the 3'-UTR (60) and the detection of translated 3'-UTR sequences separated from the mRNA body in aging neurons (61). The encoded peptides might convey important regulations. Future studies are clearly necessary to unravel their potential role in cells. Together, these findings clearly show that the 3'-UTR harbors an immense regulatory potential to control different aspects of the RNA life cycle.

Similar to the 3'-UTR, the 5'-end of a transcript also contains regulatory elements. In addition to 5'-UTR length and structure (55), upstream open reading frames (uORF) tightly regulate translation of the main open reading frame (mORF) (62). The presence of uORFs leads to accumulation of ribosomes in the 5'-UTR. Interestingly, a redistribution of ribosomes from the 5'-UTR to the mORF is observed during neuronal differentiation indicating an important functional role of uORFs in development (51). The translation rate of the mORF is critically regulated by the phosphorylation of initiation factor 2 α (eIF2 α). eIF2 α is a component of the ternary complex that delivers GTP and the initiator tRNA to initiating ribosomes to start translation. Upon eIF2 α phosphorylation, the GDP to GTP exchange by eIF2b is impaired. This mechanism inhibits global translation. uORF containing transcripts, however, show a higher ribosome occupancy of the mORF (62), even though this theory was challenged by a recent finding demonstrating that there is no dependency translome-wide between translational activity of uORF and mORF (63). Interestingly, eIF2 α phosphorylation is needed to regulate synaptic plasticity and long-term memory (64). At the molecular level, activation of the metabotropic glutamate receptor induces phosphorylation of eIF2 α . In turn, global translation rate is decreased while the synthesis rate of uORF containing transcripts increases. This pathway is essential for learning and memory formation (65).

In addition to 5'- and 3'-UTRs, the coding sequence (CDS) itself harbors regulatory elements that influence protein synthesis and folding rate. Thereby, the codon usage frequency that reflects tRNA levels crucially determines the speed of elongating ribosomes (66). Rare codons correspond to low-abundant tRNAs. Variations in the elongation speed promote or impair co-translational folding (48, 49), indicating that finely adapted tRNA levels are essential for proteostasis (47). In line with this notion is the finding that deficiencies in tRNA homeostasis

lead to neurodegeneration probably through the accumulation of misfolded proteins (67, 68). In addition to co-translational folding, ribosomes can influence protein folding and identity through frameshifting. Frameshifting can be caused by depletion of cognate tRNAs during translation. Higher abundant tRNAs recognizing codons in the +1 and/or -1 frame enhance the frameshifting frequency of the ribosome. This has been observed for *Huntingtin (Htt)*. Expansion of the CAG codon stretch in the *Htt* gene causes long poly-glutamine stretches that induce Htt aggregation and leads to Chorea Huntington, a neurodegenerative disease (47). Translation of the CAG stretch depletes cognate tRNAs. Consequently, the ribosome shifts to the +1 or -1 frame of *Htt* resulting in a poly-serine or poly-alanine stretch containing proteins, respectively, that influence the aggregation of Htt (69, 70). Another example for CDS mediated translational aberrations is FMRP and its contribution to the neurodegenerative disorder fragile X tremor ataxia syndrome (FXAS) (71). Unlike fragile X syndrome, the expansion of a CGG stretch within the 5'-UTR of *Fmr1* (the mRNA coding for FMRP) does not cause complete transcriptional shutdown in FXAS patients. Instead, mutant *Fmr1* mRNA is expressed (71). Interestingly, repeat associated non-AUG-initiated translation (RAN) is induced by the mutant *Fmr1* mRNA leading to the production of a poly-glycine containing FMRP protein found in inclusion bodies (72–74). These examples show that translational homeostasis is critically needed to ensure neuronal function and survival.

In addition to its molecular complexity, the spatial organization of the translational apparatus provides an elegant possibility to control protein expression in a spatially defined manner. From the first evidence (75) to transcriptome-wide screenings for locally translated mRNAs (76), different studies experimentally addressed how localized translation contribute to cellular functioning in developing and mature neurons. Importantly, localized translation depends on mRNA localization. According to the *RNA granule hypothesis*, transcripts are transported embedded in RNA granules (also known as RNPs) that contain a certain subset of RBPs (21). These granules are diverse in their mRNA and protein composition (21). It is generally accepted that translation is repressed during transport (77). This model, however, has been challenged by recent studies (78, 79). RNA granules deliver mRNAs that are translated at synapses. This theory, in turn, raises the question, which synapses are provided with mRNAs for translation. According to the *synaptic tagging* theory, activation of a single synapse creates a labile synaptic tag that subsequently recruits proteins needed for remodeling (80). This theory can be applied to RNA granules. Hence, synaptic activation leads to recruitment of RNA granules to the synapse (81, 82) that are then unpacked thereby releasing their embedded mRNAs for translation (Schieweck *et al.*, *Physiol. Rev.*, *under revision*). Arguably, one of the best

characterized localized and locally translated transcripts is β -actin (*Actb*). *Actb* mRNA is bound by the RBP Zipcode-binding protein 1 (ZBP1) (83, 84). Studies published by the Singer lab clearly show that *Actb* mRNA is transported to synapses and locally translated upon activation of NMDA receptors (81, 85, 86). Thereby, phosphorylation of ZBP1 might serve as a molecular switch to release *Actb* mRNA from binding and translational repression (84). Actin cytoskeleton remodeling is needed to establish synaptic long-term changes such as LTP and LTD (20). Thus, it is plausible to propose that activity-dependent delivery of *Actb* mRNA and its local translation support synaptic remodeling. In line with this notion are pioneer experiments showing that translation inhibitors impair both LTP and LTD in the hippocampus (87). LTP can be divided into an early and late LTP (e- and l-LTP), respectively. Only l-LTP depends on protein synthesis while e-LTP does not require newly synthesized proteins, but a rearrangement of existing receptors in the plasma membrane (88). Similarly, LTD also requires translation (89). In line with this finding, chemical induction of LTD causes phosphorylation of eIF2 α and a global shutdown of translation. In turn, this effect leads to translational upregulation of uORF containing transcripts (65). Of note, translation and protein degradation need to be balanced for synaptic changes to occur. This has been shown for LTP as well as LTD (89–91). Even though it has not been experimentally shown that local translation is indeed needed for LTP and LTD, it is plausible that locally made proteins modify synaptic transmission to allow long-term synaptic changes. Supportive for this idea is the finding that the mRNA of essential regulators and components of the signaling cascade are localized at post- and presynaptic sites (92, 93). Importantly, most studies on RNA localization and translation to date focused on the impact of glutamatergic stimulation (56, 81, 82, 85). According to a pioneer study, however, it is plausible that GABA_A receptor activation drives mRNA localization as well (94). In addition, ribosomes in axon terminals of inhibitory interneurons are able to translate localized mRNAs, although the number of translationally active compartments is significantly smaller for inhibitory presynaptic terminals than postsynaptic dendritic spines (93). Functionally speaking, translation is necessary for plasticity of GABA release at inhibitory presynaptic terminals (95). Together, these pioneer studies suggest that (localized) translation is equally important for inhibitory synapses as for excitatory synapses. Supportive for this notion is a recent study showing that deletion of the translation repressor eIF4E-binding protein 2 (4E-BP2) in inhibitory GABAergic interneurons causes autism-associated behavior in mice (96). Even though it is unknown, which transcripts are affected by 4E-BP2 KO, this finding clearly shows that translational homeostasis in inhibitory interneurons is essential for normal

circuit functioning. How translation is regulated at inhibitory postsynaptic sites and how it impacts GABAergic transmission is, however, basically unknown (see also *Discussion*).

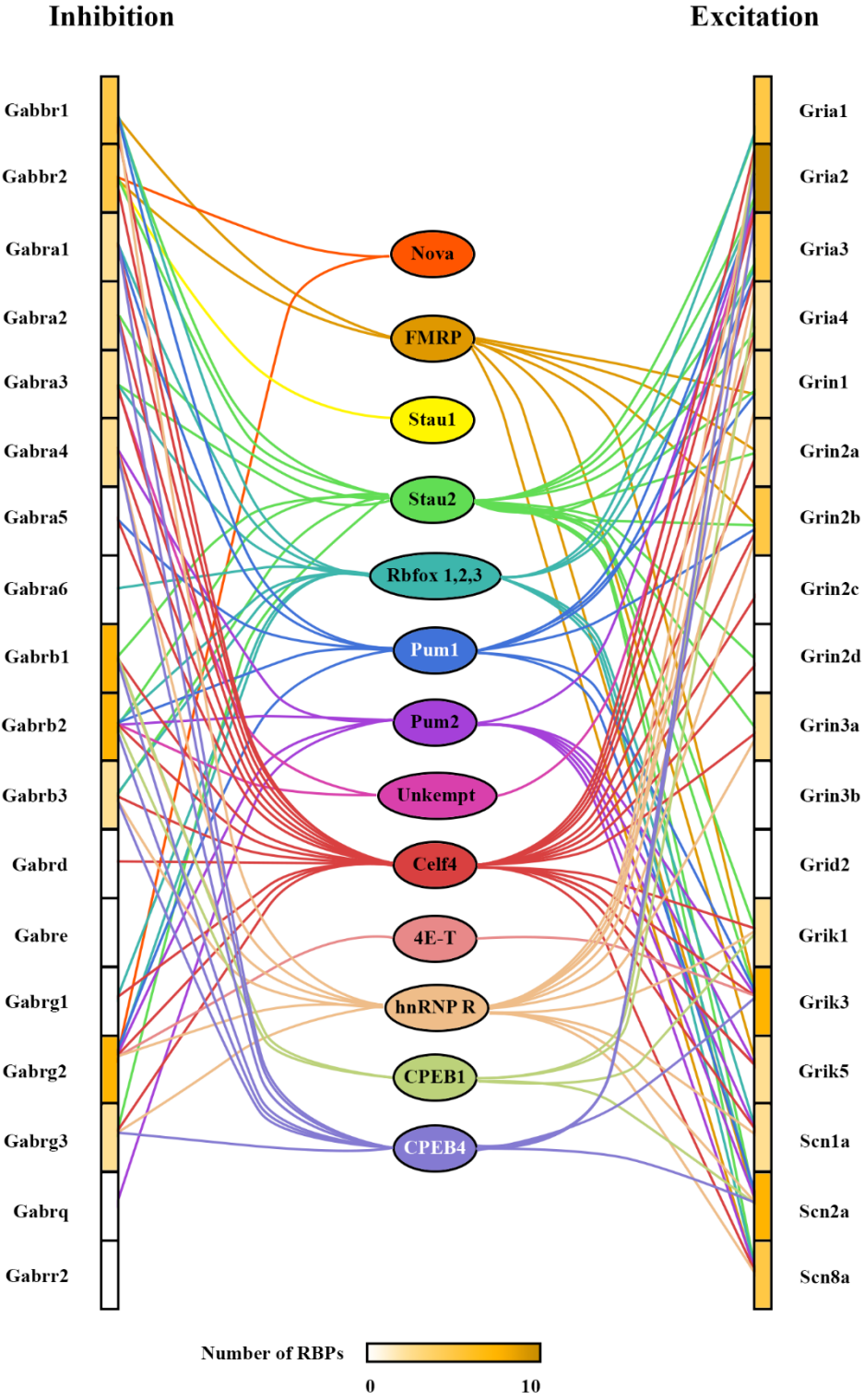


Figure 3: RBPs share mRNA targets coding for ‘excitatory’ and ‘inhibitory’ proteins. Published CLIP and RIPseq datasets (54, 56, 97–108) reveal that RBPs show a certain degree of convergence in their target mRNA binding. Additionally, they interact with transcripts coding for proteins involved both in neuronal excitation and inhibition suggesting a role in balancing synaptic activity. Color code reveals number of RBPs binding to depicted transcripts.

1.4 *Pumilio2* and its role in synaptic balancing

Pum2 belongs to the PUF (Pumilio/FBF) RBP family (109). It binds a short nucleotide sequence (UGUANAUA) (110) in the 3'-UTR of its target mRNAs (107). Pum2 regulates different aspects in the RNA life cycle including transport (111, 112), stability and translation (109). Numerous studies have unraveled the possible mechanisms of how Pum2 regulates mRNA expression. By recruiting the main polyadenylation complex CCR4-NOT (113, 114), Pum2 can destabilize its target mRNAs (113). Moreover, it is able to bind the 5'-cap of mRNAs in *Xenopus* oocytes. Thereby, it competes with the initiation factor eIF4E for cap recognition, which is essential to start translation (115). This finding suggests that Pum2 represses translation initiation. An *in vitro* study, however, showed that (nematode and) mammalian Pum2 binds to Ago and the translation elongation factor eEF1A to inhibit ribosome elongation (116). Importantly, the diversity of RBPs, their stoichiometry and target mRNAs in different model organisms might influence how Pum2 regulates mRNA expression. These limitations impeded general conclusions drawn from these studies. Moreover, the impact of Pum2 on global protein expression is also unknown, raising the question about the precise cellular function of this RBP. This question is of particular interest for neurons. Knock-down of Pum2 leads to spontaneous epileptic seizures in mice (31, 117), one of the most severe neurologic conditions affecting millions of people worldwide (118). This drastic phenotype strongly suggests that Pum2 has distinct and numerous functions to regulate neuronal homeostasis. A first possible molecular explanation was suggested by the Baines lab. They found that Pum2 represses translation of the voltage-gated sodium channels $Na_v1.6$ (*Scn8a*), a known risk gene for epilepsy (119, 120). Supportive for this model is the finding that downregulation of Pum2 increases the sodium current in these neurons (121). Of note, *Scn8a* is a common mRNA target of FMRP (102) and Rbfox1 (28) as well. In addition, Rbfox1 KO mice also exhibit epileptic seizures (28), and synaptic hyperexcitability was reported in FMRP KO mice (122). Thus, it is tempting to speculate that different RBPs act together to control the expression of particular mRNAs that might explain similar phenotypes in KO or KD animal models (see *Discussion*). In addition to its effect on $Na_v1.6$ expression, Pum2 regulates excitatory synapse formation. Upon Pum2 knock-down, the number of post- and presynaptic sites increases. In addition, the frequency of excitatory currents is significantly elevated (123). Moreover, immunoprecipitation experiments using antibodies specific for Pum2 revealed that *Scn1a* mRNA, encoding $Na_v1.1$ (another voltage-gated sodium channel), is another target of Pum2 (123). This finding is of particular interest as $Na_v1.1$ is highly expressed in parvalbumin positive inhibitory interneurons

(45). In addition, 80% of patients suffering from Dravet syndrome, an infantile disorder characterized by early-onset seizures beginning around 5 months of age, carry mutations in the *Scn1a* gene (124). At the molecular level, reduced Na_v1.1 mediated sodium currents diminish the excitation of inhibitory interneurons. This effect, in turn, decreases neuronal inhibition and might lead to epilepsy (125). Together, these findings suggest a role of Pum2 in regulating neuronal inhibition and excitation, probably acting in different neuronal cell types. Additionally, it has been suggested that the interaction of different RBPs crucially controls the transcriptome in a cell type and development specific manner (Schieweck *et al.*, *Physiol. Rev.*, *under revision*). Thus, elucidating the interaction network of RBPs is a prerequisite to understand the regulatory role of RBPs (see *Discussion*). The underlying molecular mechanisms are, however, basically unknown.

1.5 The RNA transport RBP Stau2 crucially contributes to synaptic functioning

One of the protein interactors of Pum2 is Stau2 (77). Stau2 is a double-stranded RBP that is enriched in nerve cells (126). Importantly, the orthologues of Stau2 and Pum2 were identified in a memory screening in *Drosophila* as crucial factors for learning and memory formation (127). Moreover, Stau2 has a key role in regulating cortical neurogenesis in embryos (128, 129) and mature neurons (130, 131). It serves as a critical regulator for RNA transport (56, 82). It associates with microtubules to enable RNA transport (132, 133). Importantly, a significant subset of dendritically localized mRNAs are Stau2 targets (54). In addition, overexpression of a mutant version of Stau2 reduces a significant proportion of dendritically localized mRNAs (134). Thus, elucidating the role of Stau2 in neurons is key to understand local expression control and dynamics as well as synaptic transmission that crucially relies on mRNA supply. Pioneer studies aiming at identifying the role of Stau2 in synaptic transmission showed that downregulation of this RBP significantly alters – amongst others – the actin cytoskeleton. Concomitantly, a reduction in number of mature dendritic spines and in the amplitude of excitatory currents was observed (130). Supportive for a role of Stau2 in synaptic transmission is the finding that some of its mRNA targets code for proteins involved in the metabotropic glutamate receptor (mGluR) pathway (54). In line with this finding is the effect of Stau2 on mGluR dependent LTD. Downregulation of Stau2 impairs LTD in cultured hippocampal neurons (135). Moreover, Stau2 regulates the dendritic localization of *Calm3* (56), one of three mRNA isoforms that code for the protein Calmodulin, which is essential for downstream

signaling upon synaptic stimulation (56). These findings suggest that Stau2 regulates downstream synaptic signaling to control synaptic transmission.

1.6 RBPs and their role in balancing neuronal activity: the aims of my Ph.D. thesis

The ability to regulate neuronal activity through a finely tuned balance between excitation and inhibition as well as long-term synaptic strengthening or weakening is a prerequisite for synaptic plasticity in the brain. Neurological and neuropsychiatric diseases such as epilepsy, ASD or learning and memory deficits have been linked to an impaired synaptic balance (3, 30, 136). As discussed above, RBPs have the potential to regulate synaptic transmission and plasticity through numerous mechanisms and pathways. For only few RBPs their impact on balancing neuronal activity has yet been experimentally validated. Due to their prevalence and importance for controlling protein expression, RBPs are essential regulators of synaptic homeostasis (137). Thus, elucidating the role in neurons is key to understand complex neurological and neuropsychiatric diseases.

In this PhD thesis, I focused on the RBPs Pum2 and Stau2 to unravel their role in synaptic balancing. The aims of this PhD thesis are:

- (i) to investigate their roles in expression control in the brain and in cultured neurons,
- (ii) to identify and characterize their impact on synaptic transmission and
- (iii) to link their regulatory potential with the behavior of their respective knock-down animals.

Together, these aims allowed me to elucidate the role of Pum2 and Stau2 in balancing synaptic activity and plasticity.

2. Discussion

2.1 The regulatory potential of RBPs

RBPs regulate essentially all steps in the RNA life cycle (23, 24) including transcription, splicing, RNA export/transport, translation and degradation (**Fig. 4**). Thereby, they are shaping the neuronal transcriptome and translatoome. In this context, it is important to note that mRNAs often contain multiple binding sites for different RBPs suggesting that cooperative and antagonistic binding occurs (25). Moreover, RBPs regulate different steps in the RNA life cycle by exploiting distinct mechanisms (23). Finally, some steps of the RNA life cycle occur in parallel rather than sequentially. This allows antagonistic and synergistic effects to occur at the same time, such as transcription and splicing or translation and RNA degradation (**Fig. 4**). It is therefore tempting to speculate that a complex regulatory network for protein expression exists at the level of RBPs.

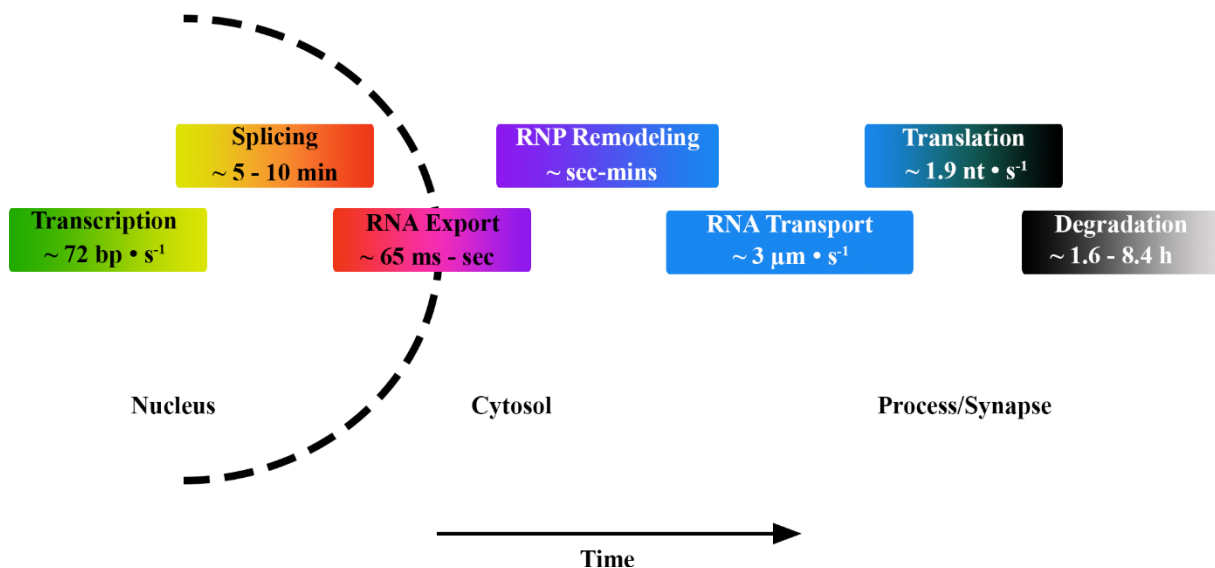


Figure 4: The life cycle of RNA molecules.

The RNA life cycle starts with transcription (138). Upon splicing (139), mRNAs are exported (140) into the cytosol, where their RBP composition is remodeled (141). This remodeling is thought to control the RNA fate. Transcripts are then transported to their destination (82) where they are translated (142) and/or degraded (143, 144). Importantly, all these steps do not proceed sequentially but also occur in parallel. This phenomenon allows a given RBP to regulate multiple steps in the RNA life cycle. Moreover, each step requires a different duration. This fact is particularly important for local expression control, where protein expression also depends on the supply of transcripts. Of note, all these steps are interconnected through feedback-loops that are not shown here.

Hence, the RBP regulatory network crucially influences translation and, in turn, protein expression. Therefore, for some transcripts translational adaptation occurs, a phenomenon that

is called ‘translational buffering’. In brief, to outbalance altered transcript levels, the number of translating ribosomes is adjusted to produce similar amounts of protein (145). This means that downregulated mRNAs are bound to an increased number of elongating ribosomes while upregulated transcripts exhibit a lower number. Translational buffering has been described in FMRP KO cells (145). Thus, it is plausible that deletion of a given RBP has a more complex impact on protein expression levels. In line with this notion is the observation that RBP deletion affects also non-target mRNAs (Schieweck *et al.*, *Physiol. Rev.*, *under revision*). This effect, in turn, might result in compensatory, indirect effects that mask direct effects caused by the deletion itself (**Fig. 5**, Schieweck *et al.*, *Physiol. Rev.*, *under revision*). Additionally, mRNA steady-state levels (RNA-seq) or ribosomal occupancy (Ribo-seq) of transcripts show both only weak correlation with the levels of their corresponding encoded proteins (63, 146). Therefore, conclusions drawn from RNA-seq or Ribo-seq data are limited and might not fully represent the impact of a certain RBP on the resulting proteome. To overcome this limitation, investigating primarily the protein levels might be a more reliable strategy to identify the pathways regulated by a specific RBP. Therefore, I decided in my PhD thesis to exploit quantitative mass spectrometry to address the effect of Pum2 and Stau2 downregulation on cultured cortical neurons.

2.1.1 Pum2 and Stau2 selectively shape the neuronal proteome

According to published individual-nucleotide resolution CLIP datasets, Pum2 and Stau2 appear to regulate multiple but distinct subsets of mRNAs in neuronal progenitors or nerve cells (56, 107). Therefore, I anticipate a broad impact of these two RBPs on neuronal protein expression. According to my hypothesis, hundreds of proteins were dysregulated in Pum2 and Stau2 depleted neurons. Importantly, only a minor overlap between both data sets was observed: 16% and 5% for Pum2 and Stau2 deficient neurons, respectively. Moreover, depletion of these two RBPs seems to impact translation in different directions. While Pum2 depletion results in a global downregulation of proteins, Stau2 downregulation selectively enhances levels of a subset of proteins (see **Fig. 3D-F**, in *Manuscript 2*). In line with this observation are results from polysome profiling experiments showing that Pum2 depletion decreases the polysome-to-monosome ratio, an indication for decreased translational activity (see **Fig. 2C-E**, in *Manuscript 2*). For Stau2, in contrast, a general increase was observed in both monosome and polysome fractions (Schieweck & Kiebler, *unpublished*). Based on these results, it is tempting

to speculate that Pum2 is needed for general translational activation, while Stau2 is predominately involved in repression of certain targets.

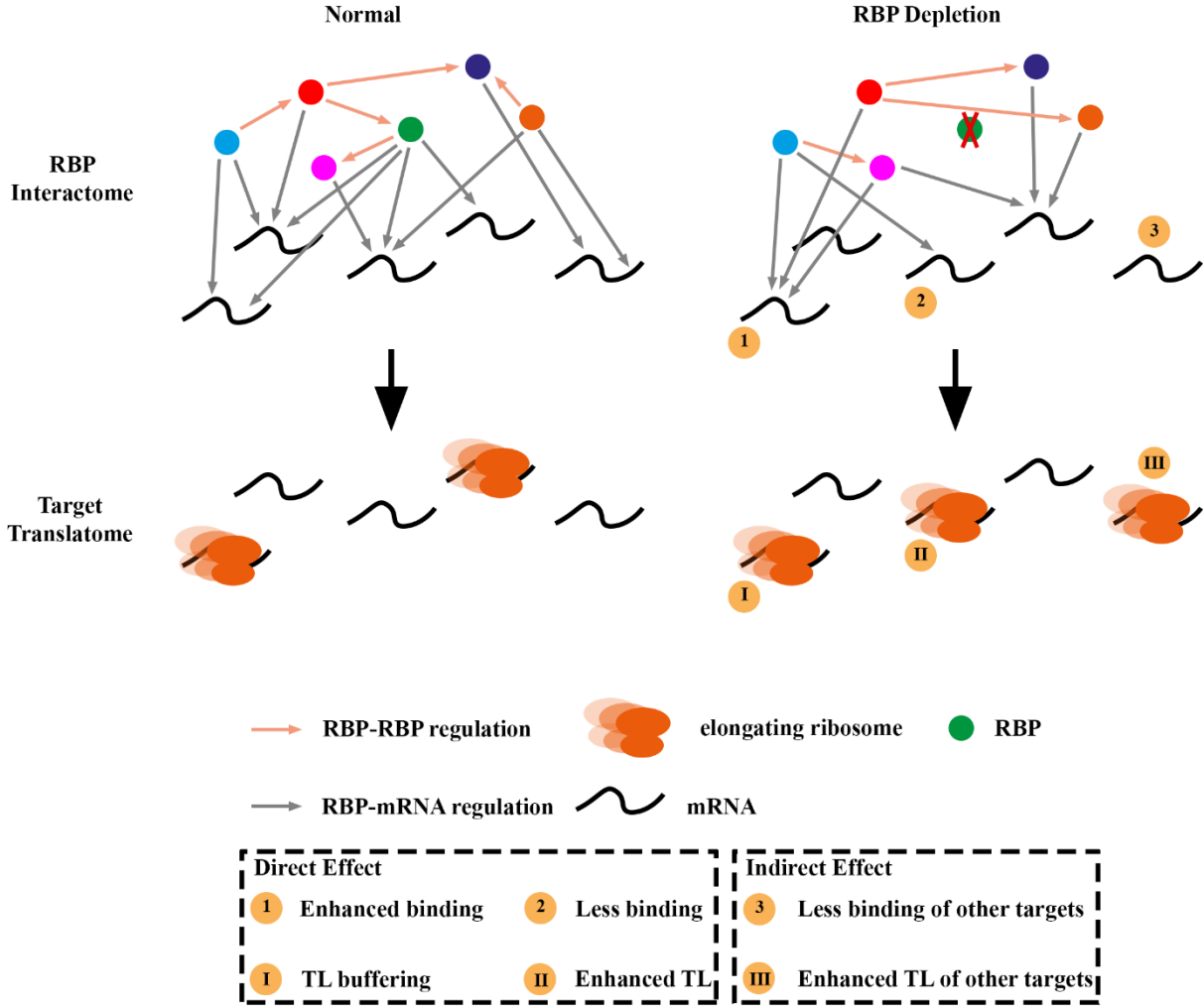


Figure 5: Compensatory effects occur upon depletion of RBPs.

Neuronal protein expression is regulated through a network of different RBPs that share common mRNA targets (RBP-mRNA regulation) and that control each other (RBP-RBP regulation). Together, this network of RBPs defines translational activity of the transcriptome. Upon depletion of a particular RBP, direct targets lose their regulation conveyed by a particular RBP. Instead, some transcripts are increasingly bound by other RBPs within the network. Consequently, they bind less well to their own targets (indirect effects). Alterations in the mRNA-RBP interactome network crucially influence the translatome. Here, some transcripts can compensate changes at mRNA steady-state levels through translational buffering. Together, these effects lead to various indirect effects in neurons. These indirect effects are a consequence of a shift in the RBP network interactome and regulatome. TL: Translation.

For Pum2, this effect seems to be counterintuitive as this RBP has been shown to repress translation both *in vitro* as well as in different cellular contexts (109). The impact of Pum2, however, on global translation in neurons has never been experimentally addressed yet. Thus, while Pum2 might repress translation of certain transcripts, its effect on global translation might

differ. Supportive for this notion is a recent study addressing the impact of the Pumilio interactor FMRP (107) on global translation in *Drosophila* oocytes. FMRP has been identified as a translational repressor (147) that inhibits translation elongation on its target mRNAs through direct interaction with the ribosome (102, 148, 149). However, in *Drosophila* oocytes FMRP activates global translation. To address this effect, the authors exploited ribosome profiling, a method to determine ribosome positions on mRNAs in a transcriptome-wide manner (50). Interestingly, FMRP KO preferentially affects longer CDS meaning that larger proteins are translationally activated by FMRP (150). Interestingly, proteins downregulated by Pum2 knock-down tend to have a shorter polypeptide chain when compared to upregulated proteins. In contrast, proteins downregulated in Stau2 deficient neurons tend to have a longer polypeptide chain, similar to FMRP (Schieweck & Kiebler, *unpublished*). Compared to other RBPs such as FUS or TDP-43, Stau2 shows a higher binding to the CDS (56). Thus, Stau2 might – similar to FMRP – regulate translation of long transcripts through binding to the CDS. This length bias might represent another regulatory mechanism as it has been described for the RBP PCF11 and its impact on intronic polyadenylation of long genes (151). In summary, the loss of Pum2 mediated translational repression might turn into a global shutdown of protein synthesis as part of a stress response. This might be the reason, why most of the mRNAs coding for dysregulated proteins in Pum2 depleted neurons are not bound by Pum2 (see **Fig. 3G**, in *Manuscript 2*). Interestingly, Stau2 binds most of the mRNAs encoding dysregulated proteins indicating that it conveys a more direct regulation of protein expression (Schieweck & Kiebler, *unpublished*).

Drosophila Staufen activates the translation of *oskar* mRNA (152) at the posterior pole. A similar effect has been reported for Stau1 in an *in vitro* translation assay (153). Moreover, depletion of Stau2 in cortical neurons leads to an upregulation of chaperons that facilitates protein folding and thereby enhances protein stability (154). Thus, the higher number of upregulated proteins in Stau2 depleted neurons might, therefore, be due to an indirect effect. In addition, Stau2 is needed for the localization of a significant number of mRNAs (134). Thus, Stau2 knock-down might cause mRNA accumulation in the soma, where they would be then translated. This means that mRNA mislocalization might drive protein upregulation in certain cellular compartments as it has been shown for Pum2 (111). Future studies are clearly needed to unravel the exact mechanism of how Pum2 and Stau2 regulate translation.

In summary, Pum2 and Stau2 differently impact neuronal protein expression. These results indicate that both RBPs might indeed exploit different mechanisms to regulate the neuronal

proteome. Even when we do not (yet) understand the underlying mechanisms in detail, it appears that Pum2 enhances, whereas Stau2 rather represses global translation.

2.2 Synaptic protein expression is controlled by Pum2 and Stau2

Pioneer studies have shown that Pum2 and Stau2 selectively regulate synaptic transmission (123, 130). In this context, loss of Pum2 increases the frequency, while Stau2 deficiency leads to a reduction in the amplitude of excitatory postsynaptic currents (EPSCs) indicating that both RBPs are indeed involved in the regulation of distinct synaptic pathways or at least distinct steps. Moreover, depletion of Pum2 leads to epileptic seizures in adult mice (29, 31). Epilepsy is characterized by neuronal hyperexcitability due to an increase in excitation and/or a decrease in inhibition. Stau2 deficiency results in learning and memory deficits in mouse and rat models (131, 155). Together, these findings strongly point towards a role of Pum2 and Stau2 in regulating synaptic homeostasis.

Therefore, to get further insight into synaptic pathways that are functionally controlled by these RBPs, I took advantage of the list of dysregulated proteins found in Pum2 and Stau2 depleted neurons to identify synaptic pathways regulated by these RBPs.

2.2.1 Pum2 activates GABAergic protein expression

To get new insight into the Pum2 regulated proteome, I initially performed bioinformatic analysis to cluster functionally related proteins. Gene Ontology (GO) analysis of dysregulated proteins revealed a strong cluster enrichment for GABAergic synapses (see **Fig. 3C**, in *Manuscript 2*). Here, in Pum2 depleted neurons Gephyrin (*Gphn*), Vesicular inhibitory amino acid transporter (*Vgat*, *Slc32a1*), Sodium- and chloride-dependent GABA transporter 1 (*Gat1*, *Slc6a1*), Glutamate decarboxylase 1 (*Gad1*) and Somatostatin (*SST*) were all found to be downregulated (see **Fig. 4A**, in *Manuscript 2* and **Fig. 6**). These proteins convey different aspects of neuronal inhibition. *Gphn* is an essential scaffolding protein for the postsynaptic GABA_A receptor (156). *Vgat* is presynaptically localized and transports GABA into synaptic vesicles (157). *Gat1* reuptakes GABA into presynaptic terminals to terminate its action, while *Gad1* synthesizes GABA in inhibitory interneurons (2). Importantly, proteins localized at excitatory postsynaptic sites remained unaffected (see **Fig. 4B**, in *Manuscript 2*). Interestingly, an *in vitro* binding assay using recombinantly expressed and purified Pum2 revealed that *Gphn*, *Gad1* and *Slc6a1* but not *Slc32a1* are mRNA targets of Pum2 (Schieweck & Kiebler,

unpublished). This finding indicates that not all affected proteins are direct Pum2 targets. In addition to the altered Gphn and Gad1 protein levels, also the corresponding transcripts showed less expression. *Slc32a1*, *SST* and *Slc6a1* were unaffected at the mRNA level. Pum2 has the potential to destabilize its target mRNAs (113, 114). Neither *Gphn* nor *Gad1*, however, showed altered transcript stability (Schieweck & Kiebler, *unpublished*). Together, these results suggest that Pum2 might have a direct role in transcriptional regulation as well. In line with this idea is a study showing that Pum2 is necessary for maintaining genomic stability (158). Even though the Pum2 dependent impact on the genome described in this study is indirect, a proximity-ligation approach, so-called BioID (159), suggests that Pum2 might regulate transcription of its target mRNAs as it interacts with components of polymerases and the mRNA processing machinery (Schieweck & Kiebler, *unpublished*). Notably, the binding motifs of some components of the cleavage and polyadenylation complex that is required for 3'-end processing of nascent transcripts show a remarkable similarity to the Pum2 recognition site. The cleavage stimulating factor 64 (CstF-64) recognizes the polyadenylation signal AAUAAA, while the cleavage factor I 68 (CF I 68) rather binds the motif UGUA (160, 161). Interestingly, Pum2 recognizes an eight nucleotide motif located in the 3'-UTR, UGUANAUA (110). Due to the sequence similarity, it is plausible that Pum2 might interfere with the cleavage and polyadenylation complex to regulate the 3'-UTR length of its target mRNAs.

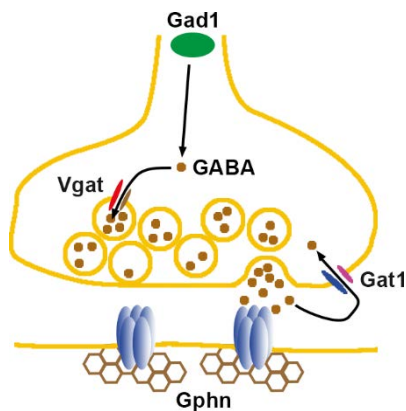


Figure 6: Components of GABAergic transmission regulated by Pum2.

Gphn, Vgat, Gat1 and Gad1 are all found to be downregulated in Pum2 deficient neurons. These proteins all convey different aspects of neuronal inhibition. Gphn (brown hexagons) is an essential scaffold protein for the postsynaptic GABA_A receptor (blue cigars). Vgat, Gat1 and Gad1 are specifically expressed in inhibitory interneurons. Gad1 synthesizes GABA, Vgat imports GABA into presynaptic vesicles and Gat1 terminates the action of GABA by transporting it from the synaptic cleft into presynaptic terminals. Somatostatin, a marker for a subtype of inhibitory interneurons, is not shown.

In addition to Gphn, Gad1, Gat1 and Vgat, SST was found to be downregulated as well. SST is a neuropeptide that has been linked to numerous processes including motor activity, sleep regulation and cognitive processes (162). In addition, it is a marker protein for a certain subclass of inhibitory interneurons (163). This finding strongly suggests that Pum2 regulates protein expression in inhibitory interneurons. Moreover, my data points toward a dual role of this RBP in regulating GABAergic transmission at the post- and the presynaptic site.

Importantly, downregulation of Pum2 led to an increase in the protein expression of sodium channel subunit beta-3 (*Scn3b*) and voltage-gated sodium channel type 2 subunit alpha ($\text{Na}_v1.2$, *Scn2a*) in rat cortical neurons in culture. In addition, $\text{Na}_v1.2$ is also upregulated in the hippocampus of Pum2 depleted mouse brains (29). In conclusion, these findings show that Pum2 can regulate key components of both neuronal inhibition and excitation. Another protein that regulates both excitation and inhibition is the Slit-Robo Rho GTPase 2 (SRGAP2), also known as formin-binding protein 2 (164). Strikingly, SRGAP2 protein interacts with Pum2 in cortical neurons according to the BioID results (Schieweck & Kiebler, *unpublished*). SRGAP2 regulates the number of Gphn positive inhibitory synapses (164). In addition, *Gphn* mRNA is bound by Pum2 (108). Moreover, Gphn is essential for GABAergic transmission (156). Therefore, I focused on Gphn to elucidate the impact of Pum2 on its expression. Interestingly, Gphn protein levels were unaffected in the soma of Pum2 depleted neurons, but showed a significant decrease in dendrites (see **Fig. 4D,E**, in *Manuscript 2*). These findings suggest a local expression control of Gphn protein. The assembly of synapses partially depends on the self-assembly ability of postsynaptic density proteins (165). However, the number of dendritic Gphn clusters remained unaffected (Schieweck & Kiebler, *unpublished*). This finding indicates a selective effect of Pum2 on Gphn expression, but not on the assembly of inhibitory synapses. Importantly, Gphn is essential for modifying inhibitory currents (166). Therefore, I asked the question whether downregulation of Pum2 impacts GABAergic transmission. Electrophysiological recordings revealed that the amplitude, but not the frequency of synaptic IPSCs is reduced in Pum2-depleted rat cortical neurons (see **Fig. 4G,H**, in *Manuscript 2*). The amplitude of inhibitory currents is thought to be regulated from the postsynaptic site while the frequency is mainly controlled presynaptically. Thus, Pum2 impacts GABAergic transmission preferentially from the postsynaptic side. This notion is in line with the finding that the KO of Gphn, the postsynaptic scaffold protein (156), leads to a reduction in the amplitude of GABA response (167). Moreover, an increased decay time of the GABA response was observed (see **Fig. 4I**, in *Manuscript 2*). This finding is mirrored by the downregulation of Gat1. Supportive for this notion is the finding that Gat1 KO mice show an increased decay time of the GABA response. Importantly, the amplitude is unaffected in these mice suggesting that Gphn and Gat1 regulate GABA response by two functionally independent pathways (168). Together, my results suggest a postsynaptic impact on GABAergic transmission via Gphn expression and/or a presynaptic effect via Gat1. It has been shown that Pum2 protein is not really expressed in axons (111). Thus, it is tempting to speculate that Pum2 impacts GABAergic transmission preferentially at the postsynaptic side, most likely through expression control of Gphn. In turn,

decrease in Gat1 expression might be a compensatory effect to counterbalance the drop in IPSC amplitude. An alternative explanation might be that Pum2 affects SST positive interneurons. The observed decrease in SST expression in Pum2 deficient neuronal cultures suggests that the number of this class of inhibitory interneurons is reduced. Following this idea, less SST positive interneurons would target less pyramidal cells and, in turn, form less inhibitory synapses on dendrites. This model would explain the drop in Vgat, Gat1 and Gad1 expression (**Fig. 6**). Moreover, it would also be a plausible explanation for the downregulation of dendritic Gphn, since SST positive interneurons target only dendrites of pyramidal cells (163). Supportive for a role of Pum2 in inhibitory interneuron signaling is the finding that Pum2 binds *Gad1* mRNA *in vitro* (Schieweck & Kiebler, *unpublished*). *Gad1* is a general inhibitory interneuron marker. A Pum2 mediated activation of *Gad1* expression in interneurons would be a plausible explanation for the reduced inhibition of pyramidal cells observed in the hippocampus of Pum2 KD mice (29). Future studies are clearly needed to distinguish between these two interesting scenarios. Important to note is that these two possibilities are not mutually exclusive, as Pum2 is expressed in both pyramidal cells and inhibitory interneurons (45). Hence, Pum2 might play a post- and presynaptic role in controlling circuit excitability.

As discussed above, Gphn is crucial for GABA_A receptor clustering (156). To investigate the effect of Pum2 depletion on the GABA_A receptor, I tested all subunits for their mRNA expression in Pum2 depleted brains. Strikingly, the $\alpha 2$ subunit of the GABA_A receptor (*Gabra2*) was the only one significantly upregulated at the mRNA level in Pum2 depleted brains (see **Fig. 1B**, in *Manuscript 1*). Moreover, *Gabra2* protein levels were starkly upregulated (see **Fig. 1D**, in *Manuscript 1*), while the $\alpha 1$ subunit (*Gabra1*) remained unaffected (Schieweck & Kiebler, *unpublished*). Complementary, cultured cortical Pum2 depleted neurons recapitulated these effects (see **Fig. 2C,D** in *Manuscript 1*). Furthermore, *Gabra2* mRNA was found to be enriched in Pum2 granules (see **Fig. 1E,F**, in *Manuscript 1*). Supportive for these observations is the finding that there are two computationally predicted Pum2 binding sites present in the *Gabra2* 3'-UTR. *Gabra2* is known to interact with numerous proteins in brain. One of its protein interactors is Ephexin1 (*Ngef*) (169), a guanine nucleotide exchange factor which modulates growth cone collapse in neurons (170, 171). Based on these interesting and promising findings, I speculate that *Gabra2* might serve as a binding platform for Ephexin1 to modulate dendrite outgrowth. In brief, downregulation of Pum2 leads to translationally upregulation of *Gabra2*. *Gabra2* protein is subsequently incorporated into the assembled GABA_A receptor. Through protein-protein interaction, *Gabra2* recruits Ephexin-1 that, in turn, reduces the number of dendritic growth cones and inhibits dendritic branching of mature

neurons. Supportive for this idea is the genetic interaction of *Gabra2* and *Ngef*. Downregulation of *Gabra2* leads to a drop in *Ngef* expression (Schieweck & Kiebler, *unpublished*). In line with this idea, double knock-down of *Pum2* and *Gabra2* rescued the deficits in dendritic complexity observed in *Pum2* depleted neurons (see **Fig. 3A-C**, in *Manuscript 1*). Importantly, dendrites receive excitatory or inhibitory inputs from presynaptic neurons (172). Thus, it is tempting to speculate that reduced dendritic complexity in *Pum2* depleted neurons diminishes synaptic input that, in turn, will decrease the frequency of excitatory action potentials. Strikingly and in line with my working hypothesis, *Pum2* and *Gabra2* double knock-down led to a strong increase in the number of c-Fos positive neurons, a marker for neuronal activation in epilepsy models (28) (see **Fig. 4A,B**, in *Manuscript 1*). Together, these results suggest that upregulation of *Gabra2* serves as a rescue mechanism to balance increased excitability of *Pum2* depleted neurons. Therefore, I would like to propose the following working model: *Pum2* is essential for efficient GABAergic transmission as well as for reduction in sodium channel mediated action potentials. This regulation is important for neuronal excitability regulation (173). In addition to this regulatory hub, a second pathway would have been established during evolution: *Gabra2* mediated reduction in synaptic input that is controlled by *Pum2*. Hence, loss of *Pum2* leads to a reduction in GABAergic transmission with a concomitant upregulation of *Gabra2* accompanied by a reduction in synaptic input (see **Fig. 4C**, in *Manuscript 1*). In this model, *Pum2* balances neuronal excitation and inhibition. In addition, it also regulates synaptic input and output through *Gabra2*. Together, these findings suggest that *Pum2* balances two important determinants of neuronal excitability: excitation through sodium channels and inhibition through the GABAergic signaling cascade as well as the ratio between synaptic input and output through the complexity of the dendritic tree. In sum, my data provide first molecular and mechanistic insight into posttranscriptional regulation of key components of inhibitory synapses through a RBP. Moreover, my results show the complex impact of RBPs in balancing neuronal activity.

2.2.1.1 *Pum2* and the maturation of the GABAergic system

Pum2 has an important role during neuronal development. It has been shown that Pumilio proteins are necessary for the survival of neuronal stem cells and that, in particular, *Pum2* is needed for neuronal specification (107, 108). These findings are of utmost importance to understand neurological diseases that require a certain developmental window to manifest pathological alterations in synaptic transmission. For epilepsy, this process is called

epileptogenesis (174). As discussed above, GABAergic inhibition crucially relies on the balanced expression of KCC2 and NKCC1 during development (see also *1.1 Synaptic transmission and plasticity*). Thus, an imbalance in the KCC2-to-NKCC1 ratio has been discussed to be causal for epileptic seizures in adults (175). Supportive for this notion are pioneer studies showing that altered expression of KCC2 and NKCC1 is linked with epilepsy and Schizophrenia (10, 176). Interestingly, downregulation of Pum2 in developing cortical neurons leads to an increased KCC2-to-NKCC1 ratio indicating an accelerated maturation of the GABAergic system (Schieweck & Kiebler, *unpublished*). Importantly, knock-down of FMRP leads to a delayed maturation of the GABAergic system (41) indicating that the effect of Pum2 on the KCC2-NKCC1 ratio is not a general effect of RBPs. This maturation involves the switch from a depolarizing to a hyperpolarizing action of GABA (so-called GABA switch, see also *1.1 Synaptic transmission and plasticity*). An increased KCC2 expression in newly fertilized zebrafish embryos, when endogenous KCC2 is not expressed, perturbs neuronal development (177). This effect might also explain the reduction in axon outgrowth in developing Pum2 depleted neurons (111). Moreover, a single seizure period in neonatal mice induces a higher surface expression of KCC2 (178). This, in turn, leads to a higher Cl⁻ ion extrusion, which might compensate the higher neuronal excitability (175). In addition, Pum2 knock-down in developing neurons also reduces *Gphn* expression indicating impaired GABAergic signaling (Schieweck & Kiebler, *unpublished*). Based on these findings, it is plausible that the increase in KCC2 expression in developing Pum2 deficient neurons represents an indirect effect to compensate for deficits in the GABAergic system. Together, it is tempting to speculate that the impact of Pum2 on the maturation of GABAergic signaling critically contributes to epileptogenesis that would cause seizures in the adult animals. Moreover, this effect might also explain deficits observed in Pum2 depleted animals during development (107, 108).

2.2.1.2 GABA regulates Pum2 expression

Neurotransmitters have the potential to directly regulate gene expression as it has been shown for serotonin (11). In this context, RBPs might also be regulated by neurotransmitters to directly couple posttranscriptional gene regulation with synaptic activity. For Pum2, it was shown that its expression levels are adjusted according to neuronal activity (121). Here, enhanced activity increases Pum2 expression, while decreased neuronal activity reduces its protein level (121). The exact mechanism of this process, however, is unclear. Since Pum2 is involved in the

regulation of GABAergic signaling, it is tempting to speculate that GABA has the potential to control Pum2 expression. Indeed, treatment of cultured cortical neurons with GABA for one hour significantly reduced Pum2 expression levels. Interestingly, this effect was not observed upon thirty minutes or two hours of treatment suggesting a narrow time window for the regulation. In addition, *Pum2* mRNA levels were unaffected (Schieweck & Kiebler, *unpublished*). A possible explanation for this drop in protein expression might be that Pum2 is cleaved by Calpain proteases. Calpains belong to the family of cytosolic calcium-dependent proteases (179). Interestingly, Calpain-1 cleaves Gphn upon calcium influx indicating the importance of Calpain proteases for inhibitory synapses (180). Supportive for this model is the finding that Calpain-2 was identified as a Pum2 protein interactor in a BioID screening (Schieweck & Kiebler, *unpublished*). Due to the ability of the GABA_A receptor to induce depolarization in dendrites (4), it is plausible that GABA treatment of cortical neurons would lead to depolarization in dendrites. This, in turn, might activate voltage-gated calcium channels and lead to calcium influx. Consequently, Calpain-2 would be activated, yielding to Pum2 cleavage. Even though this model is purely hypothetical, it would provide an elegant feedback mechanism to restrict the expression of key components of GABAergic synapses to terminate the action of GABA. Supportive for this idea is the finding that the Pum2 target *Gad1* exhibits reduced mRNA expression upon one hour of GABA treatment, but not upon thirty minutes or two hours of incubation, concomitant with the decrease in Pum2 protein expression (Schieweck & Kiebler, *unpublished*). Together, these results indicate that Pum2 is regulated by GABA and that this regulation might be a regulatory feedback loop to restrict GABA availability.

2.2.2 *Stau2* functionally regulates synaptic organization

Research in the Kiebler lab has shown that Stau2 binds and regulates mRNA coding for proteins involved in the mGluR pathway (54). Moreover and particularly important in this context are two key signaling pathways involving either serotonin or dopamine receptors, both have been previously linked with learning and memory (181, 182).

GO term analysis of downregulated proteins in Stau2 depleted neurons revealed an enrichment for 'neurotransmitter secretion' and 'action potential' (Schieweck & Kiebler, *unpublished*). One of the proteins essential for neurotransmitter secretion and significantly downregulated in Stau2 depleted neurons is Complexin1 (Cplx1). *Cplx1* mRNA is bound and regulated by Stau2 (54). Importantly, Cplx1 is located at presynaptic terminals and regulates neurotransmitter release (183), while Stau2 is preferentially postsynaptic (133). These apparently contradictory

results suggest that Stau2 might regulate Cplx1 expression in the cell body or control *Cplx1* mRNA localization through retaining the transcript in the soma as shown for Pum2 targets (111). However, a recent study has suggested that a fraction of Cplx1 is also located at the postsynaptic side, where it might regulate AMPA receptor exocytosis during LTP (184). Consequently, this fraction might be under the control of postsynaptic Stau2.

Moreover, components of the actin cytoskeleton were also significantly downregulated in Stau2 depleted neurons. This observation is in line with the finding that the actin cytoskeleton network is found to be fundamentally reorganized, when Stau2 is depleted in primary hippocampal neurons (130). The actin cytoskeleton is a key remodeler of synaptic organization and important for synaptic transmission as well as long-term plasticity (185).

Additionally, a reduction in the AMPA1 receptor (*Gria1*) was observed. *Gria1* is bound by Stau2 (56). Importantly, KO of *Gria1* in mice leads to alterations in hippocampal space coding and synaptic plasticity (186–188). Complementary to these findings, Stau2 depletion caused a reduction in the density of excitatory synapses (130). The impact of Stau2 on Cplx1, the actin cytoskeleton and *Gria1* expression strongly suggests that Stau2 regulates synaptic transmission. The reduction of presynaptic vesicle release proteins such as Cplx1 and postsynaptic receptors such as *Gria1* in Stau2 knock-down neurons suggests an impact on synaptic scaling (137). Here, a drop in postsynaptic protein expression would simultaneously downregulate presynaptic components as part of a homeostatic feedback loop. Thus, it is plausible that the downscaling of synaptic proteins represents a feedback mechanism causing a lower threshold to induce long-term synaptic changes. Strikingly, such a lower threshold for LTP induction has been observed in a Stau2 depleted rat model (131). Importantly, both LTP and LTD are not two isolated mechanistic phenomena, but rather two sides of the same coin, which has been taken into consideration in the BCM theory (189). Consequently, loss of Stau2 shifts the LTP-to-LTD ratio favoring LTP over LTD. This finding suggests that Stau2 controls the balance between synaptic strengthening and weakening and promotes synaptic strengthening (131).

To further elucidate the role of Stau2 in synaptic transmission, I exploited a *Stau2* knock-down mouse model (155). To test for transcripts that are dysregulated upon learning, *Stau2* KD mice – as their corresponding control mice – underwent a battery of behavior assays (see also 2.3.2 *Stau2 is necessary for motor learning and novelty response*) (155). Transcriptome-wide analysis of naïve and trained animals revealed a significant upregulation of the mRNAs coding for *cerebellin1* (*Cbln1*) and *glutamate receptor ionotropic delta subunit 2* (*GluD2* or *Grid2*) upon training (190) (see **Fig. 1B-D** and **Fig. 4**, in *Publication III*). Interestingly, *Cbln1* and *GluD2* are both core components of cerebellar synapses. Thereby, *Cbln1* appears to be the

bridging molecule that binds postsynaptic GluD2 in Purkinje cells and connects it with presynaptic neurexin in granule cells (191). To serve as a bridging molecule, Cbln1 is secreted by granule cells (191, 192). This synaptic connection mediated by the interaction between GluD2, Cbln1 and neurexin is essential for motor learning and coordination (192). *Grid2* is bound and regulated by *Stau2* (56, 190). Moreover, *Stau2* is strongly expressed in Purkinje cells (see **Fig. 2A**, in *Publication III*) indicating that the primary effect on cerebellar synapse organization is mediated via postsynaptic GluD2 rather than presynaptically secreted Cbln1 (190). Therefore, it is tempting to speculate that *Stau2* regulates synaptic transmission from granule cells towards Purkinje cells in the cerebellum.

Together, these results suggest that *Stau2* balances both synaptic potentiation (LTP) and depression (LTD). These two types of synaptic plasticity are not only essential for learning and memory formation in the hippocampus (193), but also in the cerebellum (194). Thus, it is tempting to speculate that *Stau2* critically contributes to distinct aspects of learning such as spatial and motor learning in the mouse brain, again highlighting its importance for memory formation *in vivo*.

2.3 *Pum2* and *Stau2* are needed for circuit homeostasis and plasticity

The presented proteomics and transcriptomics data together with the electrophysiology experiments presented in this PhD thesis strongly argue that *Pum2* and *Stau2* are needed for homeostatic excitability and synaptic plasticity. To test this novel and exciting hypothesis and to understand their physiological role *in vivo*, *Pum2* and *Stau2* KD mouse lines as well as a *Stau2*-depleted rat line were investigated.

2.3.1 Knock-down of *Pum2* causes epileptic seizures

My work has established *Pum2* as an essential regulator for GABAergic transmission. In addition, it has been shown that it also regulates sodium channel mediated action potentials (121). Thus, the impact of *Pum2* on neuronal excitation *ex vivo* might reflect the effect on circuit excitability in the brain. Indeed, adult *Pum2* knock-down mice exhibit epileptic seizures starting between three and five months of age (29, 31). Interestingly, electrophysiological recordings reveal that general excitation appears not to be affected in these mice. *Pum2* deficient mice, however, show reduced paired-pulse inhibition suggestive for impaired GABAergic inhibition (see **Fig. 3A-I**, in *Publication I*) (29), which is in line with the *in vitro* results discussed above.

Importantly, the effect of Pum2 on neuronal excitability seems to be evolutionary conserved as seizures can be prevented through increased Pumilio expression in *Drosophila* (195). Together, these findings clearly state an essential role of Pum2 in seizure control in different experimental models. Moreover, a recent study has found that Pum2 is downregulated in patients suffering from temporal lobe epilepsy (196). This finding clearly indicates that understanding Pum2 controlled expression is key for the development of future medical applications towards seizure treatment. Of note, epilepsy shows a high comorbidity with autism spectrum disorders (ASD) (197). Interestingly, Pum2 targets such as *Scn1a*, *Scn2a*, *Scn8a* and *Gphn* are known genes mutated and/or dysregulated in patients suffering from ASD (SFARI database, <https://gene.sfari.org>). Together, these results suggest that Pum2 has a role in the pathology of ASD as well. Of note, other RBPs that are involved in the ASD pathology either interact with Pum2, *e.g.* FMRP (107), or regulate the same target mRNAs, *e.g.* Rbfox1 (28). Hence, Pum2 might be an important hub within a common RBP regulatory network (**Fig. 5**) that crucially controls ASD relevant mRNAs. Further studies, however, are clearly needed to unravel the precise role of Pum2 in ASD.

2.3.2 *Stau2* is necessary for motor learning and novelty response

Recent studies have established that *Stau2* is necessary for synapse formation and organization (126). Thus, it is tempting to speculate that *Stau2* crucially contributes to memory formation. Indeed, knock-down of *Stau2* in mice leads to impaired spatial detection in a spatial memory assay, the so-called Barnes maze (see **Fig. 4A-F**, in *Publication II*) (155). A possible molecular explanation for this behavior might be the drop in *Gria1* expression observed in *Stau2* depleted neurons. *Gria1* is known to be necessary for proper spatial detection (187). Similarly, *Stau2* KD rats show altered response to spatial memory (131). Moreover, *Stau2* knock-down mice show impaired novelty response in novel object recognition (NOR) assays (see **Fig. 3B,C**, in *Publication II*) (155). NOR requires the hippocampus as well as additional brain regions such as the cerebral cortex (198, 199). Impaired novelty response indicates altered synaptic transmission between different hippocampal areas (155). Indeed, *Stau2* KD rats exhibit an imbalance between LTP and LTD, thereby favoring LTP. Therefore, it is tempting to speculate that increased synaptic potentiation might interfere with novelty recognition and memory formation.

In addition to hippocampus-dependent learning, motor learning depends on coordinated synaptic transmission and plasticity. Here, synapses formed between parallel fibers originated

from granule cells and Purkinje cells are crucial for motor learning and motor coordination (194). Interestingly, Stau2 KD mice show impaired motor coordination when tested on a rotarod (see **Fig. 3C,D**, in *Publication III*) (190), a motor learning assay (200). Strikingly, Stau2 KD mice display a significant improvement in their rotarod performance when compared to WT controls upon training (see **Fig. 3C,D**, in *Publication III*). This suggests an increase in synaptic transmission efficiency. In line with this finding is the observed upregulation of the known synaptic organizers GluD2 and Cbln1 (190). Together, these results clearly establish Stau2 as critical for synaptic plasticity and a prerequisite for proper memory acquisition.

2.4 The RBP network as key to understand neuropsychiatric and neurological diseases? An outlook

Immense effort has been made to identify and characterize key RBPs during the last 20-30 years. Thanks to these studies, it becomes more and more clear that RBPs act through a complex interplay between different RBPs and between RBPs and their target mRNAs: the RBP network. In this last section, I focus on this network idea and discuss obvious gaps in the RBP field. A special focus will be on the role of RBPs to explain neurological and neuropsychiatric diseases.

2.4.1 The RBP network to regulate synaptic homeostasis: what we know and where we go

The findings discussed in this PhD thesis clearly show the potential of RBPs to regulate synaptic transmission as well as synaptic plasticity. Future studies are therefore necessary to unravel the precise mechanisms how Pum2 and Stau2 control synaptic homeostasis. Special emphasis should be put on the interaction between different RBPs such as Rbfox1, FMRP, Stau2 and Pum2. RBPs form RNA granules that are distinct in both their contained mRNAs and protein interactors (77), indicating a differential impact on mRNA target expression depending on the RNA granule identity. For instance, Stau2 and Pum2 bind both to FMRP as well as to each other (77, 107). Moreover, RBPs share a significant set of common mRNAs (32) (Schieweck *et al.*, *Physiol. Rev.*, *under revision*, **Fig. 3**). Based on these results, it is plausible that they can partially compensate for each other. Thus, elucidating the underlying RBP regulatory network is key for understanding complex regulations of cellular pathways (**Figs. 5,7**). Therefore, future studies should focus on the dynamic interaction between RBPs and their respective target mRNAs. To address these important questions, proximity ligation assays (PLA) using biotin

ligases to biotinylate both protein and RNA interactors appear as ideal approaches (159, 201–203). Pilot experiments in this direction yielded a list of high-confidence Pum2 protein interactors in cortical neurons (Schieweck & Kiebler, *unpublished*). Moreover, by exploiting the MS2 system to tag specific mRNAs in cells (82) combined with PLA allowed to identify the interactome of a single mRNA (25). These assays will clearly give novel insight into the dynamics of RBP network regulation. As a complementary approach, genetic studies using double or triple knock-down mouse lines will provide valuable information on the RBP regulatome. In particular, their ability to compensate each other can be investigated using these models.

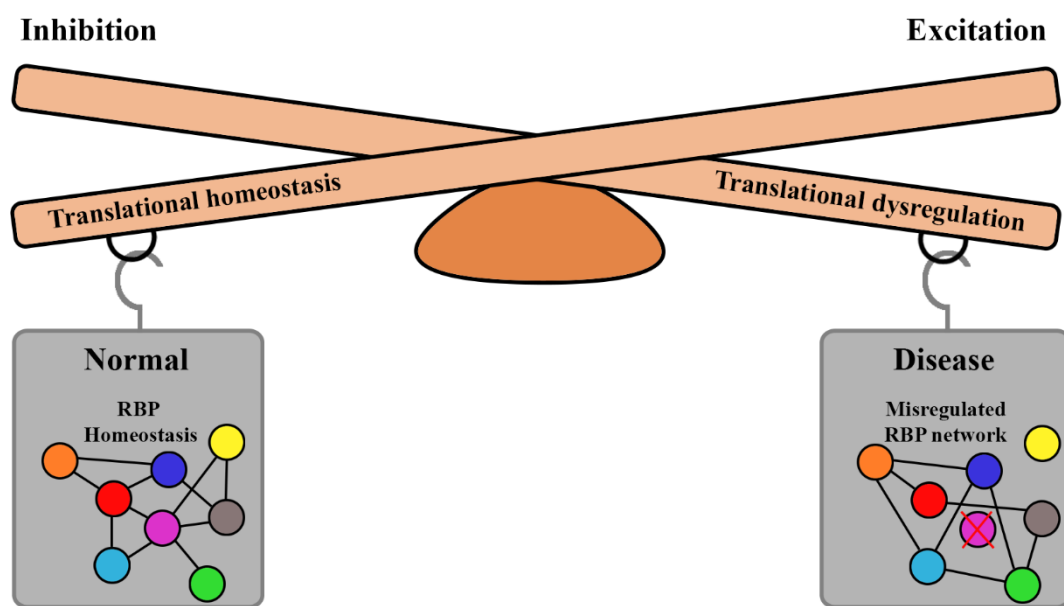


Figure 7: RBPs and their potential to balance neuronal excitability.

The neuronal transcriptome is critically regulated by a network of different RBPs that bind either antagonistically or synergistically to their target mRNAs. Under normal conditions, this leads to translational homeostasis, which means a balanced supply with newly synthesized proteins according to the physiological demands. By disruption of RBP binding and/or regulatory functions, this network will be rearranged. Consequently, expression of a wide range of transcripts will be altered. This, in turn, would lead to general translation dysregulation and, in some cases, to an imbalance in neuronal activity.

In summary, research during the last twenty years has shown that RBPs have an immense regulatory potential. In neurons, they shape the transcriptome and crucially regulate the translome to eventually establish translational homeostasis in the cell. Consequently, they are needed for numerous key neuronal pathways such as synaptic transmission and plasticity. Importantly, recent findings strongly suggest that it is not a single RBP conveying co- and posttranscriptional regulation but the collectivity of RBPs, the “RBPome”, that controls these cellular pathways. Therefore, it is of utmost importance to understand the underlying dynamic

interactions and how they change during development, in health and disease, as well as upon aging (**Fig. 7**).

2.4.2 RBPs and their therapeutic potential

As discussed above, RBPs are promising targets for the development of new therapeutic approaches to treat patients suffering from epilepsy or ASD. Different RBPs such as FMRP, Rbfox1, Pum2 and CPEB4 have been linked to neurological and neuropsychiatric diseases (29, 31, 99, 102, 106, 147). Arguably, one of the best therapeutic strategies to treat multigenic diseases is gene therapy. Here, the WT locus of a particular RBP is delivered through a viral vector. A prominent example for gene therapy based restoring of RBP expression is ZOLGENSMA[®], a FDA approved drug (204) to treat spinal muscle atrophy (SMA). SMA is caused by mutation in the survival motor neuron 1 (*SMN1*) gene. SMN1 is a RBP and acts preferentially as a chaperone for RNP assembly (205–207). The exact pathomechanism of how loss of SMN1 induces neuronal death is still unknown. However, a pioneer study suggested that translational misregulation might contribute to the phenotype in presymptomatic mice (208). Even though gene therapy for SMA seems to be promising, there are several limitations and gaps that need to be addressed for other RBPs in the future. First, RBPs show a certain degree of cell type specificity. Although RBPs such as FMRP, Pum2, Stau2 and Rbfox1 are ubiquitously expressed in different neuronal cell types (45), their target mRNA expression profile is distinct between different neuronal cell types. Moreover, a significant fraction of RBPs control translation of their targets. A pioneer study has shown that translational activity exhibit a certain degree of cell type specificity meaning that reduction in protein synthesis rate affects one cell type over others (209). Thus, expression of an RBP in different cell types might differently impact the cellular translome. Second, except for some splicing factors, it is essentially unknown how RBPs are regulated. However, this information is crucial for future therapeutic approaches, since RBPs also affect the expression of other RBPs (**Fig. 5**). To overcome this problem, their regulatory pathways need to be identified. Third and in line with the aforementioned regulation of RBPs, adjusting the expression levels of these proteins is essential for their regulation. Many RBPs tend to aggregate (210). Overexpression might promote this effect leading to nonfunctional and toxic protein assemblies.

In conclusion, these obstacles currently limit the usage of RBPs for gene therapy available to date. Future studies are clearly needed to provide sufficient information for the development of

new strategies to treat patients. Nevertheless, targeting RBPs seem to be an elegant and effective approach to treat multigenic and complex neurological and neuropsychiatric diseases.

3. References

1. J. E. Lisman, S. Raghavachari, R. W. Tsien, The sequence of events that underlie quantal transmission at central glutamatergic synapses. *Nat. Rev. Neurosci.* **8**, 597–609 (2007).
2. D. F. Owens, A. R. Kriegstein, Is there more to GABA than synaptic inhibition? *Nat. Rev. Neurosci.* **3**, 715–727 (2002).
3. J. L. R. Rubenstein, M. M. Merzenich, Model of autism: increased ratio of excitation/inhibition in key neural systems. *Genes Brain Behav.* **2**, 255–267 (2003).
4. A. T. Gullledge, G. J. Stuart, Excitatory actions of GABA in the cortex. *Neuron.* **37**, 299–309 (2003).
5. Y. Ben-Ari, Excitatory actions of GABA during development: The nature of the nurture. *Nat. Rev. Neurosci.* **3**, 728–739 (2002).
6. I. Medina *et al.*, Current view on the functional regulation of the neuronal K⁺-Cl⁻ cotransporter KCC2. *Front. Cell. Neurosci.* **8**, 1–18 (2014).
7. D. D. Wang, A. R. Kriegstein, GABA regulates excitatory synapse formation in the neocortex via NMDA receptor activation. *J. Neurosci.* **28**, 5547–5558 (2008).
8. X. Gu, L. Zhou, W. Lu, An NMDA Receptor-Dependent Mechanism Underlies Inhibitory Synapse Development. *Cell Rep.* **14**, 471–478 (2016).
9. R. Tyzio *et al.*, Oxytocin-mediated GABA inhibition during delivery attenuates autism pathogenesis in rodent offspring. *Science.* **343**, 675–679 (2014).
10. J. Y. Kim *et al.*, Interplay between DISC1 and GABA signaling regulates neurogenesis in mice and risk for schizophrenia. *Cell.* **148**, 1051–1064 (2012).
11. L. A. Farrelly *et al.*, Histone seronylation is a permissive modification that enhances TFIID binding to H3K4me3. *Nature.* **567**, 535–539 (2019).
12. G. Neves, S. F. Cooke, T. V.P. Bliss, Synaptic plasticity, memory and the hippocampus: a neural network approach to causality. *Nat. Rev. Neurosci.* **9**, 1030–1034 (2012).
13. A. Holtmaat, K. Svoboda, Experience-dependent structural synaptic plasticity in the mammalian brain. *Nat. Rev. Neurosci.* **10**, 647–658 (2009).
14. C. M. Alberini, E. R. Kandel, The regulation of transcription in memory consolidation. *Cold Spring Harb. Perspect. Biol.* **7**, 1–18 (2015).
15. A. Kemp, D. Manahan-Vaughan, Hippocampal long-term depression and long-term

- potentiation encode different aspects of novelty acquisition. *Proc. Natl. Acad. Sci. U. S. A.* **101**, 8192–8197 (2004).
16. S. J. Martin, P. D. Grimwood, R. G. M. Morris, SYNAPTIC PLASTICITY AND MEMORY: An Evaluation of the Hypothesis. *Annu. Rev. Neurosci.* **23**, 649–711 (2000).
 17. M. E. Klein, P. E. Castillo, B. a. Jordan, Coordination between translation and degradation regulates inducibility of mGluR-LTD. *Cell Rep.* **10**, 1459–1466 (2015).
 18. C. Gkogkas, N. Sonenberg, M. Costa-Mattioli, Translational Control Mechanisms in Long-lasting Synaptic Plasticity and Memory. *J. Biol. Chem.* **285**, 31913–31917 (2010).
 19. R. L. Davis, Y. Zhong, The Biology of Forgetting—A Perspective. *Neuron.* **95**, 490–503 (2017).
 20. L. a Colgan, R. Yasuda, Plasticity of dendritic spines: subcompartmentalization of signaling. *Annu. Rev. Physiol.* **76**, 365–85 (2014).
 21. M. A. Kiebler, G. J. Bassell, Neuronal RNA granules: movers and makers. *Neuron.* **51**, 685–90 (2006).
 22. C. Andreassi, A. Riccio, To localize or not to localize: mRNA fate is in 3'UTR ends. *Trends Cell Biol.* **19**, 465–74 (2009).
 23. M. W. Hentze, A. Castello, T. Schwarzl, T. Preiss, A brave new world of RNA-binding proteins. *Nat. Rev. Mol. Cell Biol.* **19**, 327–341 (2018).
 24. H. Jung, C. G. Gkogkas, N. Sonenberg, C. E. Holt, Remote control of gene function by local translation. *Cell.* **157**, 26–40 (2014).
 25. J. Mukherjee *et al.*, β -Actin mRNA interactome mapping by proximity biotinylation. *Proc. Natl. Acad. Sci. U. S. A.* **116**, 12863–12872 (2019).
 26. M. Caudron-Herger *et al.*, R-DeeP: Proteome-wide and Quantitative Identification of RNA-Dependent Proteins by Density Gradient Ultracentrifugation. *Mol. Cell.* **75**, 184–199.e10 (2019).
 27. A. Castello *et al.*, Resource Insights into RNA Biology from an Atlas of Mammalian mRNA-Binding Proteins. *Cell.* **149**, 1393–1406 (2012).
 28. L. T. Gehman *et al.*, The splicing regulator Rbfox1 (A2BP1) controls neuronal excitation in the mammalian brain. *Nat. Genet.* **43**, 706–711 (2011).
 29. P. Follwaczny *et al.*, Pumilio2-deficient mice show a predisposition for epilepsy. *Dis. Model. Mech.* **10**, 1333–1342 (2017).
 30. M. W. Antoine, T. Langberg, P. Schnepel, D. E. Feldman, Increased Excitation-

- Inhibition Ratio Stabilizes Synapse and Circuit Excitability in Four Autism Mouse Models. *Neuron*. **101**, 648-661.e4 (2019).
31. H. Siemen, D. Colas, H. C. Heller, O. Brustle, R. A. Reijo Pera, Pumilio -2 Function in the Mouse Nervous System. *PLoS One*. **6**, 1–14 (2011).
 32. R. Schieweck, M. A. Kiebler, Posttranscriptional gene regulation of the GABA receptor to control neuronal inhibition. *Front. Mol. Neurosci*. **12**, 1–10 (2019).
 33. Y. M. Yang *et al.*, Identification of a molecular locus for normalizing dysregulated GABA release from interneurons in the Fragile X brain. *Mol. Psychiatry*. **1–19** (2018), doi:10.1038/s41380-018-0240-0.
 34. C. K. Vuong *et al.*, Rbfox1 Regulates Synaptic Transmission through the Inhibitory Neuron-Specific vSNARE Vamp1. *Neuron*. **98**, 127-141.e7 (2018).
 35. B. Wamsley *et al.*, Rbfox1 Mediates Cell-type-Specific Splicing in Cortical Interneurons. *Neuron*. **100**, 846-859.e7 (2018).
 36. H. Ederle, D. Dormann, TDP-43 and FUS en route from the nucleus to the cytoplasm. *FEBS Lett*. **591**, 1489–1507 (2017).
 37. S. Alberti, D. Dormann, Liquid–Liquid Phase Separation in Disease. *Annu. Rev. Genet*. **53**, 1–19 (2019).
 38. M. J. Fogarty *et al.*, Cortical synaptic and dendritic spine abnormalities in a presymptomatic TDP-43 model of amyotrophic lateral sclerosis. *Sci. Rep*. **6**, 1–13 (2016).
 39. A. Suvrathan, C. A. Hoeffler, H. Wong, E. Klann, S. Chattarji, Characterization and reversal of synaptic defects in the amygdala in a mouse model of fragile X syndrome. *Proc. Natl. Acad. Sci. U. S. A*. **107**, 11591–11596 (2010).
 40. A. J. M. H. Verkerk *et al.*, Identification of a Gene (FMR-1) Containing a CGG Repeat Coincident with a Breakpoint Cluster Region. *Cell*. **65**, 905–914 (1991).
 41. Q. He, T. Nomura, J. Xu, A. Contractor, The developmental switch in GABA polarity is delayed in fragile X mice. *J. Neurosci*. **34**, 446–450 (2014).
 42. K. S. Kosik, The neuronal microRNA system. *Nat. Rev. Neurosci*. **7**, 911–920 (2006).
 43. J. Feuge, F. Scharkowski, K. Michaelsen-Preusse, M. Korte, FMRP Modulates Activity-Dependent Spine Plasticity by Binding Cofilin1 mRNA and Regulating Localization and Local Translation. *Cereb. Cortex*. **29**, 1–13 (2019).
 44. P. Hotulainen *et al.*, Defining mechanisms of actin polymerization and depolymerization during Dendritic spine morphogenesis. *J. Cell Biol*. **185**, 323–339 (2009).

45. E. Furlanis, L. Traunmüller, G. Fucile, P. Scheiffele, Landscape of ribosome-engaged transcript isoforms reveals extensive neuronal-cell-class-specific alternative splicing programs. *Nat. Neurosci.* **22**, 1709–1717 (2019).
46. E. Favuzzi *et al.*, Neurodevelopment: Distinct molecular programs regulate synapse specificity in cortical inhibitory circuits. *Science*. **363**, 413–417 (2019).
47. M. Kapur, C. E. Monaghan, S. L. Ackerman, Regulation of mRNA Translation in Neurons—A Matter of Life and Death. *Neuron*. **96**, 616–637 (2017).
48. R. Schieweck, B. Popper, M. A. Kiebler, Co-Translational Folding: A Novel Modulator of Local Protein Expression in Mammalian Neurons? *Trends Genet.* **32**, 788–800 (2016).
49. G. Hanson, J. Coller, Translation and Protein Quality Control: Codon optimality, bias and usage in translation and mRNA decay. *Nat. Rev. Mol. Cell Biol.* **19**, 20–30 (2018).
50. N. T. Ingolia, S. Ghaemmaghami, J. R. S. Newman, J. S. Weissman, Genome-wide analysis in vivo of translation with nucleotide resolution using ribosome profiling. *Science*. **324**, 218–23 (2009).
51. J. D. Blair, D. Hockemeyer, J. A. Doudna, H. S. Bateup, S. N. Floor, Widespread Translational Remodeling during Human Neuronal Differentiation. *Cell Rep.* **21**, 2005–2016 (2017).
52. J. P. Doyle *et al.*, Application of a Translational Profiling Approach for the Comparative Analysis of CNS Cell Types. *Cell*. **135**, 749–762 (2008).
53. B. D. Berkovits, C. Mayr, Alternative 3' UTRs act as scaffolds to regulate membrane protein localization. *Nature*. **522**, 363–367 (2015).
54. J. E. Heraud-Farlow *et al.*, Staufen2 regulates neuronal target RNAs. *Cell Rep.* **5**, 1511–8 (2013).
55. S. N. Floor, J. A. Doudna, Tunable protein synthesis by transcript isoforms in human cells. *Elife*. **5**, 1–25 (2016).
56. T. Sharangdhar *et al.*, A retained intron in the 3'-UTR of Calm3 mRNA mediates its Staufen2- and activity-dependent localization to neuronal dendrites. *EMBO Rep.* **18**, 1762–1774 (2017).
57. C. Giorgi *et al.*, The EJC factor eIF4AIII modulates synaptic strength and neuronal protein expression. *Cell*. **130**, 179–191 (2007).
58. S. Kim, H. Kim, J. W. Um, Synapse development organized by neuronal activity-regulated immediate-early genes. *Exp. Mol. Med.* **50**, 1–7 (2018).
59. S. Farris, G. Lewandowski, C. D. Cox, O. Steward, Selective localization of Arc

- mRNA in dendrites involves activity- and translation-dependent mRNA degradation. *J. Neurosci.* **34**, 4481–4493 (2014).
60. T. P. Miettinen, M. Bjorklund, Modified ribosome profiling reveals high abundance of ribosome protected mRNA fragments derived from 3' untranslated regions. *Nucleic Acids Res.* **43**, 1019–1034 (2014).
 61. P. H. Sudmant, H. Lee, D. Dominguez, M. Heiman, C. B. Burge, Widespread Accumulation of Ribosome-Associated Isolated 3' UTRs in Neuronal Cell Populations of the Aging Brain. *Cell Rep.* **25**, 2447-2456.e4 (2018).
 62. F. Gebauer, M. W. Hentze, Molecular mechanisms of translational control. *Nat. Rev. Mol. Cell Biol.* **5**, 827–35 (2004).
 63. S. van Heesch *et al.*, The Translational Landscape of the Human Heart. *Cell.* **178**, 242-260.e29 (2019).
 64. M. Costa-Mattioli *et al.*, eIF2 α Phosphorylation Bidirectionally Regulates the Switch from Short- to Long-Term Synaptic Plasticity and Memory. *Cell.* **129**, 195–206 (2007).
 65. G. V. Di Prisco *et al.*, Translational control of mGluR-dependent long-term depression and object-place learning by eIF2 α . *Nat. Neurosci.* **17**, 1073–82 (2014).
 66. C. H. Yu *et al.*, Codon Usage Influences the Local Rate of Translation Elongation to Regulate Co-translational Protein Folding. *Mol. Cell.* **59**, 744–754 (2015).
 67. J. W. Lee *et al.*, Editing-defective tRNA synthetase causes protein misfolding and neurodegeneration. *Nature.* **443**, 50–55 (2006).
 68. R. Ishimura *et al.*, RNA function. Ribosome stalling induced by mutation of a CNS-specific tRNA causes neurodegeneration. *Science.* **345**, 455–9 (2014).
 69. H. Girstmair *et al.*, Depletion of Cognate Charged Transfer RNA Causes Translational Frameshifting within the Expanded CAG Stretch in Huntingtin. *Cell Rep.* **3**, 148–159 (2013).
 70. P. Saffert, F. Adaml, R. Schieweck, J. F. Atkins, Z. Ignatova, An expanded CAG repeat in huntingtin causes +1 frameshifting. *J. Biol. Chem.* **291**, 18505–18513 (2016).
 71. R. J. Hagerman, P. Hagerman, Fragile X-associated tremor/ataxia syndrome-features, mechanisms and management. *Nat. Rev. Neurol.* **12**, 403–412 (2016).
 72. P. K. Todd *et al.*, CGG repeat-associated translation mediates neurodegeneration in fragile X tremor ataxia syndrome. *Neuron.* **78**, 440–455 (2013).
 73. C. Sellier *et al.*, Translation of Expanded CGG Repeats into FMRpolyG Is Pathogenic and May Contribute to Fragile X Tremor Ataxia Syndrome. *Neuron.* **93**, 331–347 (2017).

74. M. Boivin, R. Willemsen, R. K. Hukema, C. Sellier, Potential pathogenic mechanisms underlying Fragile X Tremor Ataxia Syndrome: RAN translation and/or RNA gain-of-function? *Eur. J. Med. Genet.* **61**, 674–679 (2018).
75. O. Steward, W. B. Levy, Preferential localization of polyribosomes under the base of dendritic spines in granule cells of the dentate gyrus. *J. Neurosci.* **2**, 284–91 (1982).
76. T. Shigeoka *et al.*, Dynamic Axonal Translation in Developing and Mature Visual Circuits. *Cell.* **166**, 181–192 (2016).
77. R. Fritzsche *et al.*, Interactome of two diverse RNA granules links mRNA localization to translational repression in neurons. *Cell Rep.* **5**, 1749–1762 (2013).
78. T. E. Graber *et al.*, Reactivation of stalled polyribosomes in synaptic plasticity. *Proc. Natl. Acad. Sci. U. S. A.* **110**, 1–6 (2013).
79. J. J. Langille, K. Ginzberg, W. S. Sossin, Polysomes identified by live imaging of nascent peptides are stalled in hippocampal and cortical neurites. *Learn. Mem.* **26**, 351–362 (2019).
80. U. Frey, R. G. M. Morris, Synaptic tagging and long-term potentiation. *Nature.* **385**, 533–536 (1997).
81. Y. J. Yoon *et al.*, Glutamate-induced RNA localization and translation in neurons. *Proc. Natl. Acad. Sci. U. S. A.* **113**, E6877–E6886 (2016).
82. K. E. Bauer *et al.*, Live cell imaging reveals 3'-UTR dependent mRNA sorting to synapses. *Nat. Commun.* **10**, 1–13 (2019).
83. J. a. Chao *et al.*, ZBP1 recognition of b-actin zipcode induces RNA looping. *Genes Dev.* **24**, 148–158 (2010).
84. S. Hüttelmaier *et al.*, Spatial regulation of β -actin translation by Src-dependent phosphorylation of ZBP1. *Nature.* **438**, 512–515 (2005).
85. A. R. Buxbaum, B. Wu, R. H. Singer, Single b-Actin mRNA Detection in Neurons Reveals a Mechanism for Its Translatability. *Science.* **343**, 419–422 (2014).
86. B. Wu, A. R. Buxbaum, Z. B. Katz, Y. J. Yoon, R. H. Singer, Quantifying Protein-mRNA Interactions in Single Live Cells. *Cell.* **162**, 211–220 (2015).
87. I. J. Cajigas, T. Will, E. M. Schuman, Protein homeostasis and synaptic plasticity. *EMBO J.* **29**, 2746–52 (2010).
88. T. V. P. Bliss, G. L. Collingridge, R. G. M. Morris, K. G. Reymann, Long-term potentiation in the hippocampus: Discovery, mechanisms and function. *Neuroforum.* **24**, A103–A120 (2018).
89. M. E. Klein, P. E. Castillo, B. A. Jordan, Coordination between translation and

- degradation regulates inducibility of mGluR-LTD. *Cell Rep.* **10**, 1459–1466 (2015).
90. C. Hanus, E. M. Schuman, Proteostasis in complex dendrites. *Nat. Rev. Neurosci.* **14**, 638–48 (2013).
 91. B. Bingol, E. M. Schuman, Activity-dependent dynamics and sequestration of proteasomes in dendritic spines. *Nature.* **441**, 1144–8 (2006).
 92. I. J. Cajigas *et al.*, The local transcriptome in the synaptic neuropil revealed by deep sequencing and high-resolution imaging. *Neuron.* **74**, 453–66 (2012).
 93. A. S. Hafner, P. G. Donlin-Asp, B. Leitch, E. Herzog, E. M. Schuman, Local protein synthesis is a ubiquitous feature of neuronal pre- and postsynaptic compartments. *Science.* **364**, 1–12 (2019).
 94. W. C. Oh, S. Lutz, P. E. Castillo, H. B. Kwon, De novo synaptogenesis induced by GABA in the developing mouse cortex. *Science.* **353**, 1037–1040 (2016).
 95. T. J. Younts *et al.*, Presynaptic Protein Synthesis Is Required for Long-Term Plasticity of GABA Release. *Neuron.* **92**, 479–492 (2016).
 96. S. Wiebe *et al.*, Inhibitory interneurons mediate autism-associated behaviors via 4E-BP2. *Proc. Natl. Acad. Sci. U. S. A.* **16**, 18060–18067 (2019).
 97. G. Yang, C. A. Smibert, D. R. Kaplan, F. D. Miller, An eIF4E1/4E-T complex determines the genesis of neurons from precursors by translationally repressing a proneurogenic transcription program. *Neuron.* **84**, 723–739 (2014).
 98. C. Scheckel *et al.*, Regulatory consequences of neuronal ELAV-like protein binding to coding and non-coding RNAs in human brain. *Elife.* **5**, 1–35 (2016).
 99. A. Parras *et al.*, Autism-like phenotype and risk gene mRNA deadenylation by CPEB4 mis-splicing. *Nature.* **560**, 441–446 (2018).
 100. M. Briese *et al.*, hnRNP R and its main interactor, the noncoding RNA 7SK, coregulate the axonal transcriptome of motoneurons. *Proc. Natl. Acad. Sci. U.S.A.* **115**, E2859–E2868 (2018).
 101. J. Ule *et al.*, Identifies Nova-Regulated RNA Networks in the Brain. *Science.* **302**, 1212–1215 (2003).
 102. J. C. Darnell *et al.*, FMRP stalls ribosomal translocation on mRNAs linked to synaptic function and autism. *Cell.* **146**, 247–61 (2011).
 103. Y. Sugimoto *et al.*, hiCLIP reveals the in vivo atlas of mRNA secondary structures recognized by Staufen 1. *Nature.* **519**, 491–494 (2015).
 104. J. Murn *et al.*, Control of a neuronal morphology program by an RNA-binding zinc finger protein, Unkempt. *Genes Dev.* **29**, 501–512 (2015).

105. J. L. Wagon *et al.*, CELF4 Regulates Translation and Local Abundance of a Vast Set of mRNAs, Including Genes Associated with Regulation of Synaptic Function. *PLoS Genet.* **8**, e1003067 (2012).
106. J. A. Lee *et al.*, Cytoplasmic Rbfox1 Regulates the Expression of Synaptic and Autism-Related Genes. *Neuron.* **89**, 113–128 (2016).
107. M. Zhang *et al.*, Post-Transcriptional Regulation of Mouse Neurogenesis by Pumilio Proteins. *Genes Dev.* **31**, 1354–1369 (2017).
108. S. K. Zahr *et al.*, A Translational Repression Complex in Developing Mammalian Neural Stem Cells that Regulates Neuronal Specification. *Neuron.* **97**, 520-537.e6 (2018).
109. A. C. Goldstrohm, T. M. T. Hall, K. M. McKenney, Post-transcriptional Regulatory Functions of Mammalian Pumilio Proteins. *Trends Genet.* **34**, 972–990 (2018).
110. E. K. White, T. Moore-Jarrett, H. E. Ruley, PUM2, a novel murine puf protein, and its consensus RNA-binding site. *RNA.* **7**, 1855–1866 (2001).
111. J. C. Martínez *et al.*, Pum2 Shapes the Transcriptome in Developing Axons through Retention of Target mRNAs in the Cell Body. *Neuron.* **104**, 1–16 (2019).
112. M. Hotz, W. J. Nelson, Pumilio-dependent localization of mRNAs at the cell front coordinates multiple pathways required for chemotaxis. *Nat. Commun.* **8**, 1–9 (2017).
113. J. Van Etten *et al.*, Human Pumilio proteins recruit multiple deadenylases to efficiently repress messenger RNAs. *J. Biol. Chem.* **287**, 36370–83 (2012).
114. A. C. Goldstrohm, B. a Hook, D. J. Seay, M. Wickens, PUF proteins bind Pop2p to regulate messenger RNAs. *Nat. Struct. Mol. Biol.* **13**, 533–9 (2006).
115. Q. Cao, K. Padmanabhan, J. D. Richter, Pumilio 2 controls translation by competing with eIF4E for 7-methyl guanosine cap recognition. *RNA.* **16**, 221–227 (2010).
116. K. Friend *et al.*, A conserved PUF–Ago–eEF1A complex attenuates translation elongation. *Nat. Struct. Mol. Biol.* **15**, 98–116 (2014).
117. P. Follwaczny *et al.*, Pumilio2-deficient mice show a predisposition for epilepsy. *Dis. Model. Mech.* **10**, 1333–1342 (2017).
118. H. F. Pernice, R. Schieweck, M. A. Kiebler, B. Popper, mTOR and MAPK: from localized translation control to epilepsy. *BMC Neurosci.* **17**, 1–10 (2016).
119. M. S. Martin *et al.*, The voltage-gated sodium channel Scn8a is a genetic modifier of severe myoclonic epilepsy of infancy. *Hum. Mol. Genet.* **16**, 2892–2899 (2007).
120. M. G. Blanchard *et al.*, De novo gain-of-function and loss-of-function mutations of SCN8A in patients with intellectual disabilities and epilepsy. *J. Med. Genet.* **52**, 330–

- 337 (2015).
121. H. E. Driscoll, N. I. Muraro, M. He, R. A. Baines, Pumilio-2 Regulates Translation of Nav1.6 to Mediate Homeostasis of Membrane Excitability. *J. Neurosci.* **33**, 9644–9654 (2013).
 122. A. Contractor, V. A. Klyachko, C. Portera-Cailliau, Altered Neuronal and Circuit Excitability in Fragile X Syndrome. *Neuron.* **87**, 699–715 (2015).
 123. J. P. Vessey *et al.*, Mammalian Pumilio 2 regulates dendrite morphogenesis and synaptic function. *Proc. Natl. Acad. Sci. U. S. A.* **107**, 3222–7 (2010).
 124. A. C. Bender, R. P. Morse, R. C. Scott, G. L. Holmes, P.-P. Lenck-santini, SCN1A mutations in Dravet syndrome: Impact on interneuron dysfunction on neural networks and cognitive outcome. *Epilepsy Behav.* **23**, 177–186 (2012).
 125. F. H. Yu *et al.*, Reduced sodium current in GABAergic interneurons in a mouse model of severe myoclonic epilepsy in infancy. *Nat. Neurosci.* **9**, 1142–1149 (2006).
 126. J. E. Heraud-Farlow, M. A. Kiebler, The multifunctional Staufen proteins: conserved roles from neurogenesis to synaptic plasticity. *Trends Neurosci.* **37**, 470–9 (2014).
 127. J. Dubnau, A. Chiang, L. Grady, The staufen/pumilio pathway is involved in *Drosophila* long-term memory. *Curr. Biol.* **13**, 286–296 (2003).
 128. G. Kusek *et al.*, Asymmetric segregation of the double-stranded RNA binding protein Staufen2 during mammalian neural stem cell divisions promotes lineage progression. *Cell Stem Cell.* **11**, 505–16 (2012).
 129. J. P. Vessey *et al.*, An asymmetrically localized Staufen2-dependent RNA complex regulates maintenance of mammalian neural stem cells. *Cell Stem Cell.* **11**, 517–28 (2012).
 130. B. Goetze *et al.*, The brain-specific double-stranded RNA-binding protein Staufen2 is required for dendritic spine morphogenesis. *J. Cell Biol.* **172**, 221–31 (2006).
 131. S. M. Berger *et al.*, Forebrain-specific, conditional silencing of Staufen2 alters synaptic plasticity, learning, and memory in rats. *Genome Biol.* **18**, 1–13 (2017).
 132. M. Köhrmann *et al.*, Microtubule-dependent recruitment of Staufen-green fluorescent protein into large RNA-containing granules and subsequent dendritic transport in living hippocampal neurons. *Mol. Biol. Cell.* **10**, 2945–2953 (1999).
 133. M. A. Kiebler *et al.*, The Mammalian Staufen Protein Localizes to the Somatodendritic Domain of Cultured Hippocampal Neurons: Implications for Its Involvement in mRNA Transport. *J. Neurosci.* **19**, 288–297 (1999).
 134. S. J. Tang, D. Meulemans, L. Vazquez, N. Colaco, E. Schuman, A role for a rat

- homolog of stau1 in the transport of RNA to neuronal dendrites. *Neuron*. **32**, 463–475 (2001).
135. G. Lebeau *et al.*, Stau1 regulates mGluR long-term depression and Map1b mRNA distribution in hippocampal neurons. *Learn. Mem.* **18**, 314–26 (2011).
 136. K. Staley, Molecular mechanisms of epilepsy. *Nat. Neurosci.* **18**, 367–372 (2015).
 137. G. Turrigiano, Homeostatic synaptic plasticity: Local and global mechanisms for stabilizing neuronal function. *Cold Spring Harb. Perspect. Biol.* **4**, 1–17 (2012).
 138. X. Darzacq *et al.*, In vivo dynamics of RNA polymerase II transcription. *Nat. Struct. Mol. Biol.* **14**, 796–806 (2007).
 139. J. Singh, R. A. Padgett, Rates of in situ transcription and splicing in large human genes. *Nat. Struct. Mol. Biol.* **16**, 1128–1133 (2009).
 140. J. P. Siebrasse, T. Kaminski, U. Kubitscheck, Nuclear export of single native mRNA molecules observed by light sheet fluorescence microscopy. *Proc. Natl. Acad. Sci. U. S. A.* **109**, 9426–9431 (2012).
 141. Y. Shin *et al.*, Spatiotemporal Control of Intracellular Phase Transitions Using Light-Activated optoDroplets. *Cell*. **168**, 159-171.e14 (2017).
 142. N. T. Ingolia, L. F. Lareau, J. S. Weissman, Ribosome profiling of mouse embryonic stem cells reveals the complexity and dynamics of mammalian proteomes. *Cell*. **147**, 789–802 (2011).
 143. I. Horvathova *et al.*, The Dynamics of mRNA Turnover Revealed by Single-Molecule Imaging in Single Cells. *Mol. Cell*. **68**, 615-625.e9 (2017).
 144. G. Tushev *et al.*, Alternative 3' UTRs Modify the Localization, Regulatory Potential, Stability, and Plasticity of mRNAs in Neuronal Compartments. *Neuron*. **98**, 495-511.e6 (2018).
 145. B. Liu *et al.*, Regulatory discrimination of mRNAs by FMRP controls mouse adult neural stem cell differentiation. *Proc. Natl. Acad. Sci. U.S.A.* **115**, E11397–E11405 (2018).
 146. B. Schwanhäusser *et al.*, Global quantification of mammalian gene expression control. *Nature*. **473**, 337–342 (2011).
 147. J. C. Darnell, E. Klann, The translation of translational control by FMRP: therapeutic targets for FXS. *Nat. Neurosci.* **16**, 1530–6 (2013).
 148. S. S. Tran *et al.*, Widespread RNA editing dysregulation in brains from autistic individuals. *Nat. Neurosci.* **22**, 25–36 (2019).
 149. E. Chen, M. R. Sharma, X. Shi, R. K. Agrawal, S. Joseph, Fragile X mental retardation

- protein regulates translation by binding directly to the ribosome. *Mol. Cell.* **54**, 407–417 (2014).
150. E. J. Greenblatt, A. C. Spradling, Fragile X mental retardation 1 gene enhances the translation of large autism-related proteins. *Science.* **361**, 709–712 (2018).
 151. R. Wang, D. Zheng, L. Wei, Q. Ding, B. Tian, Regulation of Intronic Polyadenylation by PCF11 Impacts mRNA Expression of Long Genes. *Cell Rep.* **26**, 2766-2778.e6 (2019).
 152. D. R. Micklem, Distinct roles of two conserved Staufen domains in oskar mRNA localization and translation. *EMBO J.* **19**, 1366–1377 (2000).
 153. S. Dugré-Brisson *et al.*, Interaction of Staufen1 with the 5' end of mRNA facilitates translation of these RNAs. *Nucleic Acids Res.* **33**, 4797–4812 (2005).
 154. H.-C. Tai, E. M. Schuman, Ubiquitin, the proteasome and protein degradation in neuronal function and dysfunction. *Nat. Rev. Neurosci.* **9**, 826–38 (2008).
 155. B. Popper *et al.*, Staufen2 deficiency leads to impaired response to novelty in mice. *Neurobiol. Learn. Mem.* **150**, 107–115 (2018).
 156. S. K. Tyagarajan, J. M. Fritschy, Gephyrin: A master regulator of neuronal function? *Nat. Rev. Neurosci.* **15**, 141–156 (2014).
 157. S. L. McIntire, R. J. Reimer, K. Schuske, R. H. Edwards, E. M. Jorgensen, Identification and characterization of the vesicular GABA transporter. *Nature.* **389**, 870–876 (1997).
 158. S. Lee *et al.*, Noncoding RNA NORAD Regulates Genomic Stability by Sequestering PUMILIO Proteins. *Cell.* **164**, 69–80 (2015).
 159. K. J. Roux, D. I. Kim, M. Raida, B. Burke, A promiscuous biotin ligase fusion protein identifies proximal and interacting proteins in mammalian cells. *J. Cell Biol.* **196**, 801–810 (2012).
 160. R. Elkon, A. P. Ugalde, R. Agami, Alternative cleavage and polyadenylation: Extent, regulation and function. *Nat. Rev. Genet.* **14**, 496–506 (2013).
 161. G. Martin, A. R. Gruber, W. Keller, M. Zavolan, Genome-wide Analysis of Pre-mRNA 3' End Processing Reveals a Decisive Role of Human Cleavage Factor I in the Regulation of 3' UTR Length. *Cell Rep.* **1**, 753–763 (2012).
 162. G. Martel, P. Dutar, J. Epelbaum, C. Viollet, Somatostatinergic systems: An update on brain functions in normal and pathological aging. *Front. Endocrinol. (Lausanne).* **3**, 1–15 (2012).
 163. R. Tremblay, S. Lee, B. Rudy, GABAergic Interneurons in the Neocortex: From

- Cellular Properties to Circuits. *Neuron*. **91**, 260–292 (2016).
164. M. Fossati *et al.*, SRGAP2 and Its Human-Specific Paralog Co-Regulate the Development of Excitatory and Inhibitory Synapses. *Neuron*. **91**, 356–369 (2016).
 165. M. Zeng *et al.*, Reconstituted Postsynaptic Density as a Molecular Platform for Understanding Synapse Formation and Plasticity. *Cell*. **174**, 1172-1187.e16 (2018).
 166. E. M. Petrini *et al.*, Synaptic recruitment of gephyrin regulates surface GABAA receptor dynamics for the expression of inhibitory LTP. *Nat. Commun.* **5**, 1–19 (2014).
 167. M. Kneussel *et al.*, Loss of postsynaptic GABA(A) receptor clustering in gephyrin-deficient mice. *J. Neurosci.* **19**, 9289–9297 (1999).
 168. L. Bragina *et al.*, GAT-1 regulates both tonic and phasic GABAA receptor-mediated inhibition in the cerebral cortex. *J. Neurochem.* **105**, 1781–1793 (2008).
 169. Y. Nakamura *et al.*, Proteomic characterization of inhibitory synapses using a novel phluorin-tagged γ -aminobutyric acid receptor, type a (GABAA), α 2 subunit knock-in mouse. *J. Biol. Chem.* **291**, 12394–12407 (2016).
 170. M. Sahin *et al.*, Eph-dependent tyrosine phosphorylation of ephexin1 modulates growth cone collapse. *Neuron*. **46**, 191–204 (2005).
 171. S. M. Shamah *et al.*, EphA receptors regulate growth cone dynamics through the novel guanine nucleotide exchange factor ephexin. *Cell*. **105**, 233–244 (2001).
 172. J. G. Nicholls *et al.*, *From Neuron to Brain, Fifth Edition* (Sinauer Associates, 2012).
 173. C. J. Mee, E. C. G. Pym, K. G. Moffat, R. A. Baines, Regulation of neuronal excitability through pumilio-dependent control of a sodium channel gene. *J. Neurosci.* **24**, 8695–703 (2004).
 174. A. Pitkänen, K. Lukasiuk, F. E. Dudek, K. J. Staley, Epileptogenesis. *Cold Spring Harb. Perspect. Med.* **5**, 1–17 (2014).
 175. A. S. Galanopoulou, S. W. Briggs, Altered GABA signaling in early life epilepsies. *Neural Plast.* **2011** (2011).
 176. A. Buchin, A. Chizhov, G. Huberfeld, R. Miles, B. S. Gutkin, Reduced Efficacy of the KCC2 Cotransporter Promotes Epileptic Oscillations in a Subiculum Network Model. *J. Neurosci.* **36**, 11619–11633 (2016).
 177. A. Reynolds *et al.*, Neurogenic role of the depolarizing chloride gradient revealed by global overexpression of KCC2 from the onset of development. *J. Neurosci.* **28**, 1588–1597 (2008).
 178. S. Khirug *et al.*, A single seizure episode leads to rapid functional activation of KCC2 in the neonatal rat hippocampus. *J. Neurosci.* **30**, 12028–12035 (2010).

179. M. Baudry, X. Bi, Calpain-1 and Calpain-2: The Yin and Yang of Synaptic Plasticity and Neurodegeneration. *Trends Neurosci.* **39**, 235–245 (2016).
180. S. K. Tyagarajan *et al.*, Extracellular Signal-regulated Kinase and Glycogen Synthase Kinase 3 b Regulate Gephyrin Postsynaptic Aggregation and GABAergic Synaptic Function in a Calpain-dependent. *J. Biol. Chem.* **288**, 9634–9647 (2013).
181. O. Stiedl, E. Pappa, Å. Konradsson-Geuken, S. O. Ögren, The role of the serotonin receptor subtypes 5-HT1A and 5-HT7 and its interaction in emotional learning and memory. *Front. Pharmacol.* **6**, 1–17 (2015).
182. A. Handler *et al.*, Distinct Dopamine Receptor Pathways Underlie the Temporal Sensitivity of Associative Learning. *Cell.* **178**, 60-75.e19 (2019).
183. R. A. Jorquera, S. Huntwork-Rodriguez, Y. Akbergenova, R. W. Cho, J. Troy Littleton, Complexin controls spontaneous and evoked neurotransmitter release by regulating the timing and properties of synaptotagmin activity. *J. Neurosci.* **32**, 18234–18245 (2012).
184. M. Ahmad *et al.*, Postsynaptic Complexin Controls AMPA Receptor Exocytosis during LTP. *Neuron.* **73**, 260–267 (2012).
185. P. Hotulainen, C. C. Hoogenraad, Actin in dendritic spines: Connecting dynamics to function. *J. Cell Biol.* **189**, 619–629 (2010).
186. J. C. Selcher, W. Xu, J. E. Hanson, R. C. Malenka, D. V. Madison, Glutamate Receptor Subunit GluA1 is Necessary for Long-term Potentiation and Synapse Unsilencing, but not Long-term Depression in Mouse Hippocampus. *Brain Res.* **1435**, 8–14 (2012).
187. E. Resnik, J. M. Mcfarland, R. Sprengel, B. Sakmann, M. R. Mehta, The effects of GluA1 deletion on the hippocampal population code for position. *J. Neurosci.* **32**, 8952–8968 (2012).
188. D. Zamanillo *et al.*, Importance of AMPA receptors for hippocampal synaptic plasticity but not for spatial learning. *Science.* **284**, 1805–1811 (1999).
189. L. N. Cooper, M. F. Bear, The BCM theory of synapse modification at 30: Interaction of theory with experiment. *Nat. Rev. Neurosci.* **13**, 798–810 (2012).
190. H. F. Pernice *et al.*, Altered glutamate receptor ionotropic delta subunit 2 expression in Stau2-deficient cerebellar purkinje cells in the adult brain. *Int. J. Mol. Sci.* **20**, 1–12 (2019).
191. K. Matsuda *et al.*, Cbln1 Is a Ligand for an Orphan Glutamate Receptor d2, a Bidirectional Synapse Organizer. *Science.* **328**, 363–369 (2010).
192. M. Yuzaki, A. R. Aricescu, A GluD Coming-Of-Age Story. *Trends Neurosci.* **40**, 138–150 (2017).

193. M. Segal, Dendritic spines and long-term plasticity. *Nat. Rev. Neurosci.* **6**, 277–284 (2005).
194. E. Hoxha, F. Tempia, P. Lippiello, M. C. Miniaci, Modulation, plasticity and pathophysiology of the parallel fiber-purkinje cell synapse. *Front. Synaptic Neurosci.* **8**, 1–16 (2016).
195. W. Lin, C. N. G. Giachello, R. A. Baines, Seizure control through manipulation of Pumilio: a key component of neuronal homeostasis. *Dis. Model. Mech.* **10**, 141–150 (2017).
196. X. L. Wu *et al.*, Reduced Pumilio-2 expression in patients with temporal lobe epilepsy and in the lithium-pilocarpine induced epilepsy rat model. *Epilepsy Behav.* **50**, 31–39 (2015).
197. Y. Sztainberg, H. Y. Zoghbi, Lessons learned from studying syndromic autism spectrum disorders. *Nat. Neurosci.* **19**, 1408–1418 (2016).
198. N. J. Broadbent, S. Gaskin, L. R. Squire, R. E. Clark, Object recognition memory and the rodent hippocampus. *Learn. Mem.* **17**, 5–11 (2010).
199. S. J. Cohen, R. W. Stackman, Assessing rodent hippocampal involvement in the novel object recognition task. A review. *Behav. Brain Res.* **285**, 105–117 (2015).
200. S. P. Brooks, R. C. Trueman, S. B. Dunnett, Assessment of Motor Coordination and Balance in Mice Using the Rotarod, Elevated Bridge, and Footprint Tests. *Curr. Protoc. Mouse Biol.* **2**, 37–53 (2012).
201. F. M. Fazal *et al.*, Atlas of Subcellular RNA Localization Revealed by APEX-Seq. *Cell.* **178**, 473-490.e26 (2019).
202. S. Markmiller *et al.*, Context-Dependent and Disease-Specific Diversity in Protein Interactions within Stress Granules. *Cell.* **172**, 590-604.e13 (2018).
203. J. Y. Youn *et al.*, High-Density Proximity Mapping Reveals the Subcellular Organization of mRNA-Associated Granules and Bodies. *Mol. Cell.* **69**, 517-532.e11 (2018).
204. FDA, “Approval Letter - ZOLGENSMA” (2019), (available at <https://www.fda.gov/vaccines-blood-biologics/zolgensma>).
205. P. G. Donlin-Asp *et al.*, The Survival of Motor Neuron Protein Acts as a Molecular Chaperone for mRNP Assembly. *Cell Rep.* **18**, 1660–1673 (2017).
206. L. Pellizzoni, Chaperoning ribonucleoprotein biogenesis in health and disease. *EMBO Rep.* **8**, 340–345 (2007).
207. B. R. So *et al.*, A U1 snRNP-specific assembly pathway reveals the SMN complex as a

- versatile hub for RNP exchange. *Nat. Struct. Mol. Biol.* **23**, 225–230 (2016).
208. P. Bernabò *et al.*, In Vivo Translatome Profiling in Spinal Muscular Atrophy Reveals a Role for SMN Protein in Ribosome Biology. *Cell Rep.* **21**, 953–965 (2017).
209. R. K. Khajuria *et al.*, Ribosome Levels Selectively Regulate Translation and Lineage Commitment in Human Hematopoiesis. *Cell.* **173**, 90-103.e19 (2018).
210. E. G. Conlon, J. L. Manley, RNA-binding proteins in neurodegeneration: Mechanisms in aggregate. *Genes Dev.* **31**, 1509–1528 (2017).

Appendices

Publication I: Pumilio2-deficient mice show a predisposition for epilepsy

This section contains the study published in *Disease Models & Mechanisms* (2017) entitled **Pumilio2-deficient mice show a predisposition for epilepsy** by

Philipp Follwaczny*, **Rico Schieweck***, Therese Riedemann, Antonia Demleitner, Tobias Straub, Anna H. Klemm, Martin Bilban, Bernd Sutor, Bastian Popper[‡] and Michael A. Kiebler[‡]

* shared first authors

‡ corresponding authors

Author contribution to this publication

Rico Schieweck, Bastian Popper and Michael A. Kiebler designed the experiments. Rico Schieweck initially characterized the Pum2 deficient mouse line (Fig. 1A,B). Martin Bilban and Rico Schieweck performed the microarray analysis (Fig. 2). Philipp Follwaczny, Rico Schieweck, Antonia Demleitner, Tobias Straub, Anna H. Klemm, Martin Bilban and Bastian Popper contributed to the analysis of the immunostainings and transcriptome-wide expression data (Figs. 4 and 5). Therese Riedemann and Bernd Sutor performed the electrophysiological recordings (Fig. 3). The manuscript was written and revised by Rico Schieweck, Bastian Popper and Michael A. Kiebler.

(Philipp Follwaczny)

(Rico Schieweck)

(Prof. Dr. Michael A. Kiebler)

(Prof. Dr. Heinrich Leonhardt)

RESEARCH ARTICLE

Pumilio2-deficient mice show a predisposition for epilepsy

Philipp Follwaczny^{1,*}, Rico Schieweck^{1,*}, Therese Riedemann², Antonia Demleitner¹, Tobias Straub³, Anna H. Klemm^{4,5}, Martin Bilban⁶, Bernd Sutor², Bastian Popper^{1,7,‡} and Michael A. Kiebler^{1,‡}

ABSTRACT

Epilepsy is a neurological disease that is caused by abnormal hypersynchronous activities of neuronal ensembles leading to recurrent and spontaneous seizures in human patients. Enhanced neuronal excitability and a high level of synchrony between neurons seem to trigger these spontaneous seizures. The molecular mechanisms, however, regarding the development of neuronal hyperexcitability and maintenance of epilepsy are still poorly understood. Here, we show that pumilio RNA-binding family member 2 (Pumilio2; Pum2) plays a role in the regulation of excitability in hippocampal neurons of weaned and 5-month-old male mice. Almost complete deficiency of Pum2 in adult *Pum2* gene-trap mice (Pum2 GT) causes misregulation of genes involved in neuronal excitability control. Interestingly, this finding is accompanied by the development of spontaneous epileptic seizures in Pum2 GT mice. Furthermore, we detect an age-dependent increase in *Scn1a* (Na_v1.1) and *Scn8a* (Na_v1.6) mRNA levels together with a decrease in *Scn2a* (Na_v1.2) transcript levels in weaned Pum2 GT that is absent in older mice. Moreover, field recordings of CA1 pyramidal neurons show a tendency towards a reduced paired-pulse inhibition after stimulation of the Schaffer-collateral-commissural pathway in Pum2 GT mice, indicating a predisposition to the development of spontaneous seizures at later stages. With the onset of spontaneous seizures at the age of 5 months, we detect increased protein levels of Na_v1.1 and Na_v1.2 as well as decreased protein levels of Na_v1.6 in those mice. In addition, GABA receptor subunit alpha-2 (*Gabra2*) mRNA levels are increased in weaned and adult mice. Furthermore, we observe an enhanced GABRA2 protein level in the dendritic field of the CA1 subregion in the Pum2 GT hippocampus. We conclude that altered expression levels of known epileptic risk factors such as Na_v1.1, Na_v1.2, Na_v1.6 and GABRA2 result in enhanced seizure susceptibility and manifestation of epilepsy in the hippocampus.

Thus, our results argue for a role of Pum2 in epileptogenesis and the maintenance of epilepsy.

KEY WORDS: RNA-binding protein, Pumilio2, PUM2, Epilepsy, Epileptogenesis, Risk factor

INTRODUCTION

Epilepsy is one of the most common neurological diseases in humans. It is characterized by the occurrence of spontaneous seizures (Pernice et al., 2016). These seizures can be caused by hyperexcitability of neurons as well as hypersynchronous network activity. Great effort has been made to identify possible risk factors responsible for epileptogenesis (Bertram, 2003). Among others, voltage-gated sodium and potassium channels as well as the γ -aminobutyric acid receptor A (GABA_A)-receptor family have particularly been linked to epilepsy in animal models and human patients (Staley, 2015). It remains elusive, however, how those proteins act together during development and maintenance of epilepsy in adulthood.

Research in the last decades unraveled that RNA-binding proteins (RBPs) control the expression of their target RNAs (Jung et al., 2014). Thereby, they provide another regulation level to guide remote protein expression. One of the best characterized RBPs is the fragile-X mental retardation protein (FMRP). Loss of FMRP causes fragile-X syndrome (Pieretti et al., 1991), a disease that is hallmarked by mental retardation and the occurrence of seizures (Darnell and Klann, 2013). Therefore, it has been suggested that RBPs play an important role in the development and maintenance of healthy homeostasis in the brain. The RBP pumilio RNA-binding family member 2 (Pumilio2; Pum2) is a posttranscriptional regulator whose function is conserved from yeast to human (Quenault et al., 2011). Pum2 binds an eight-nucleotide consensus sequence in the 3'-untranslated region (3'-UTR) of its target mRNAs (White et al., 2001). Thereby, it regulates the expression of the encoded protein. In addition, Pum2 controls the expression of the voltage-gated sodium channel (Na_v) Na_v1.6 and dendrite morphogenesis of dissociated hippocampal neurons (Driscoll et al., 2013; Vessey et al., 2010), indicating a role in the regulation of neuronal excitability. Furthermore, Pum2 was reported to be downregulated in two epilepsy models in *Drosophila* (Lin et al., 2017). Moreover, knockdown of Pum2 in mice has been shown to cause spontaneous epileptic seizures (Siemen et al., 2011). In the study presented here, we investigated the molecular mechanisms of Pum2-loss-induced spontaneous epileptic seizures and present the first evidence of how Pum2 deficiency might cause late-onset epilepsy in *Pum2* gene-trap (Pum2 GT) mice.

Here, we took advantage of a previously published Pum2 GT mouse model that shows Pum2 deficiency (Siemen et al., 2011). Male mice that are largely deficient of Pum2 develop spontaneous epileptic seizures in adulthood, mainly at the age of 5 months. In order to investigate the underlying mechanism of the development of spontaneous seizures, we analyzed mRNA levels of ion channels,

¹Biomedical Center (BMC), Department for Cell Biology, Faculty of Medicine, LMU, Munich, 82152 Planegg-Martinsried, Germany. ²Biomedical Center (BMC), Department of Physiological Genomics, Ludwig-Maximilians-University, Munich, 82152 Planegg-Martinsried, Germany. ³Biomedical Center (BMC), Core Facility Bioinformatics, Ludwig-Maximilians-University, Munich, 82152 Planegg-Martinsried, Germany. ⁴Biomedical Center (BMC), Core Facility Bioimaging, Ludwig-Maximilians-University, Munich, 82152 Planegg-Martinsried, Germany. ⁵Walter Brendel Centre of Experimental Medicine, Ludwig-Maximilians-University, 81377 Munich, Germany. ⁶Department of Laboratory Medicine and Core Facility Genomics, Medical University of Vienna, 1090 Vienna, Austria. ⁷Biomedical Center (BMC), Core Facility Animal Models, Ludwig-Maximilians-University, Munich, 82152 Planegg-Martinsried, Germany.

*These authors contributed equally to this work

‡Authors for correspondence (bastian.popper@med.uni-muenchen.de; mkiebler@lmu.de)

id B.P., 0000-0003-1517-695X; M.A.K., 0000-0002-8850-6297

This is an Open Access article distributed under the terms of the Creative Commons Attribution License (<http://creativecommons.org/licenses/by/3.0>), which permits unrestricted use, distribution and reproduction in any medium provided that the original work is properly attributed.

ion transporters and receptors that guide neuronal excitability, and found these to be dysregulated in the absence of Pum2. In detail, we observed age-dependent alterations of mRNA and protein levels for *Scn1a* ($Na_v1.1$) and *Scn8a* ($Na_v1.6$) in the brain of weaned and 5-month-old mice. Strikingly, we detected a twofold upregulation of γ -aminobutyric acid receptor A (GABA) subunit $\alpha 2$ (*Gabra2*) mRNA for both ages tested. Strikingly, electrophysiological recordings of the Schaffer-collateral-commissural (SCC) pathway revealed reduced paired-pulse inhibition. Furthermore, we observed enhanced dendritic localization of the GABRA2 subunit in hippocampal CA1 neurons. Together, these findings suggest a role of Pum2 in the development and maintenance of epilepsy in adulthood that is, *inter alia*, mediated by altered neuronal inhibition.

RESULTS

Brain-wide Pum2 knockdown leads to misregulation of genes associated with epilepsy

To investigate the effect of Pum2 knockdown on epilepsy risk-factor expression, we took advantage of an existing Pum2 GT mouse exhibiting reduced Pum2 expression levels (Siemen et al., 2011; Xu et al., 2007). Quantitative reverse-transcription PCR (qRT-PCR) of total RNA from brains revealed an 80% reduction of *Pum2* mRNA (Fig. 1A, left) and more than 90% for the corresponding protein (Fig. 1A, middle, quantification right). Similar results were obtained for Pum2 protein levels in the hippocampus (Fig. 1B, quantification

right). Immunohistochemistry of coronal hippocampal sections showed a prominent Pum2 signal in the pyramidal cell layers (CA3-CA1) and less intense in the granular cell layer [dentate gyrus (DG)] that was absent in the hippocampus of Pum2 GT mice (Fig. 1C).

In previous studies, it has been shown that *Pum2* mRNA targets *Scn1a* and *Scn8a* mRNAs (Driscoll et al., 2013; Vessey et al., 2010). In addition, bioinformatic analysis of known epileptic risk factors revealed a possible Pum2-binding site in the 3'-UTR of *Scn1a* and *Scn8a* mRNAs. These results suggest that Pum2 is involved in the regulation of voltage-gated sodium-channel expression and thereby might control neuronal excitability in mice. To get further insight into the expression levels of target mRNAs in the absence of Pum2, we performed a transcriptome-wide microarray analysis in Pum2 GT and wild-type (WT) brains at the age of 5 months, the time of onset of spontaneous epileptic seizures in Pum2 GT mice. Strikingly, we found mRNAs coding for proteins involved in cell communication and synaptic transmission to be upregulated (Fig. 2A). Among others, our microarray analysis revealed an altered expression level of transporters for sodium, potassium and calcium ions (Table S1). Interestingly, we also observed the translational repressors *Nanos2* and *Nanos3* to be upregulated and mRNAs encoding for components of the eukaryotic initiation factor 3 complex (eIF3) to be downregulated (Table S1). Strikingly, *Gabra2*, which has been linked to epilepsy in

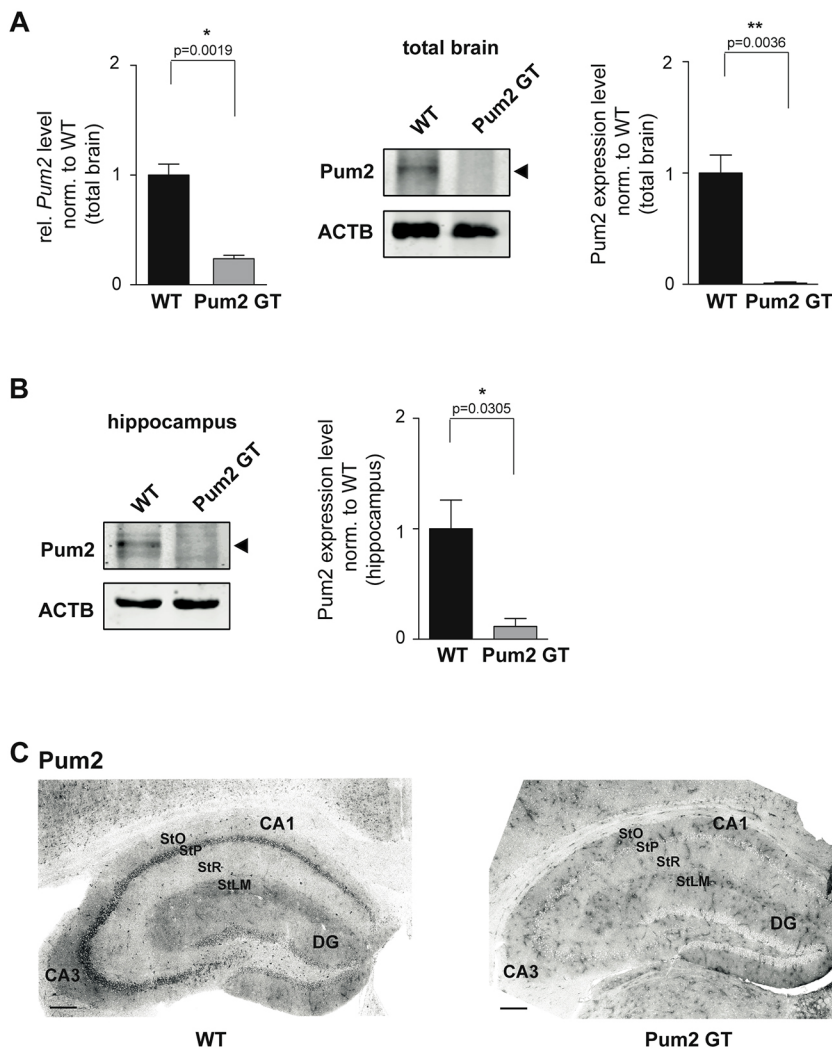


Fig. 1. Gene-trap (GT) vector insertion reduces Pum2 expression level in the hippocampus. (A) qRT-PCR of *Pum2* mRNA levels (left) and western blot analysis of *Pum2* protein levels (middle: representative western blot; right: quantification) of WT and Pum2 GT mouse brain lysates. β -actin (ACTB) was used as loading control ($n=3$ animals/group). Significance was determined using unpaired *t*-test. $*P<0.05$. (B) Representative western blot and quantification of *Pum2* protein levels in homogenates obtained from WT and Pum2 GT hippocampi. β -actin (ACTB) was used as loading control ($n=3$ animals/group). Significance was determined using unpaired *t*-test. $*P<0.05$. (C) Immunohistological stainings of WT and Pum2 GT hippocampus (coronal sections). Scale bars: 200 μ m. StO, stratum oriens; StP, stratum pyramidale; StR, stratum radiatum; StLM, stratum lacunosum-moleculare; DG, dentate gyrus.

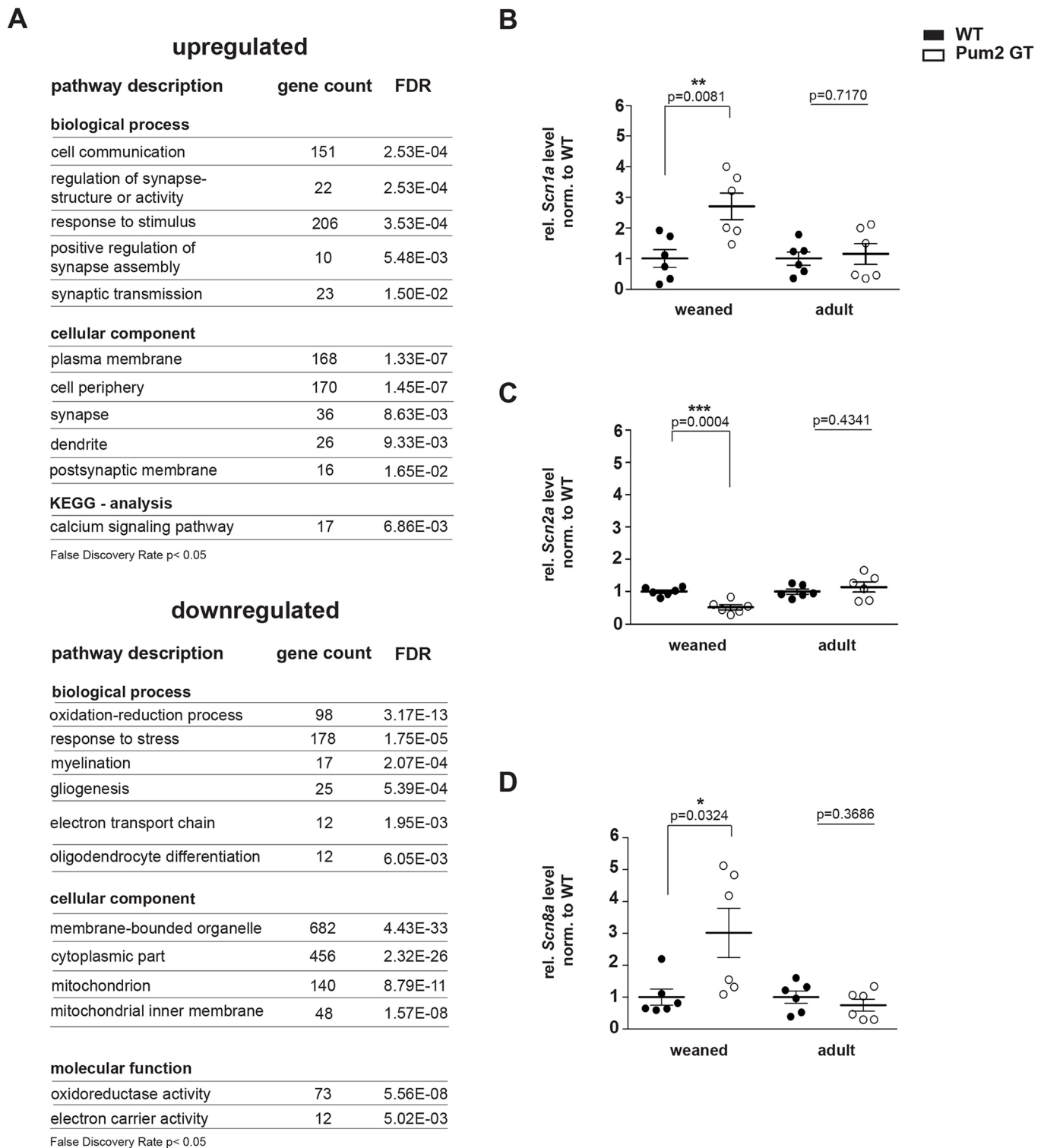


Fig. 2. Epileptogenic factors are misregulated in *Pum2* GT mice. (A) Gene ontology (GO) classification of mRNAs identified by microarray analysis that are upregulated (top) and downregulated (bottom) in *Pum2* GT compared to WT mice ($n=3$ animals/group). FDR, false discovery rate. (B-D) qRT-PCR mRNA expression analysis for *Scn1a* (B), *Scn2a* (C) and *Scn8a* (D) coding for $Na_v1.1$, $Na_v1.2$ and $Na_v1.6$, respectively, in total brain lysates obtained from weaned (3-week-old) and 5-month-old *Pum2* GT and WT mice ($n=6$ animals for all groups). Significance was determined using unpaired *t*-test. * $P < 0.05$, ** $P < 0.01$, *** $P < 0.001$.

humans (Loddenkemper et al., 2014), was upregulated twofold. For known *Pum2* targets such as *Scn1a* and *Scn8a*, we did not detect changes at the mRNA level in 5-month-old brains. The transcriptome data described above served as a starting point to

further test expression levels of these well-known epilepsy genes. Therefore, we performed qRT-PCR for *Scn1a* and *Scn8a*, coding for the voltage-gated sodium channels $Na_v1.1$ and $Na_v1.6$, as well as for the epilepsy gene *Scn2a*, coding for $Na_v1.2$, in brain lysates from

weaned and 5-month-old mice. Pum2 GT mice show spontaneous epileptic seizures at the age of 5 months (Siemen et al., 2011). We chose this age for mRNA quantification to investigate the onset of epileptic seizures. In addition, we analyzed mRNA levels of the above-mentioned targets in weaned animals [postnatal day 21 (P21)] in order to address the effect of Pum2 deficiency on the development and establishment of neuronal activity during late brain development (Fig. 2B-D). Interestingly, mRNAs coding for $Na_v1.1$ and $Na_v1.6$ showed a strong upregulation in weaned Pum2 GT mice compared to WT. We did not observe this effect in 5-month-old animals (Fig. 2B,D). In addition, *Scn2a* ($Na_v1.2$) mRNA levels were reduced in weaned Pum2 GT animals and returned to control values at the age of 5 months (Fig. 2C). Thus, our results suggest that *Scn1a*, *Scn2a* and *Scn8a* expression is dynamically regulated during postnatal development in response to Pum2 knockdown.

Increased paired-pulse ratios in CA1 pyramidal cells of Pum2 GT mice after SCC pathway stimulation

In order to get further insight into the development of spontaneous seizures in adult (P70-P84; no spontaneous epileptic seizures were yet observed at this age) Pum2 GT mice, we performed field recordings in acute hippocampal slices. Evoked population spikes in CA1 pyramidal neurons were recorded after SCC pathway stimulation. After correct positioning of the stimulation and recording electrode (Fig. 3A), we performed an input-output analysis and analyzed the normalized amplitudes of the presynaptic fiber volley (FV) as well as of the population spike (PS) as a function of the stimulation intensity (Fig. 3B,C). The stimulus-response relation of PS amplitudes in control and Pum2 GT mice were similar, indicating no alterations in the overall network excitability. This finding was further supported by the fact that we failed to detect significant differences in the magnitude of the FV or PS responses (Fig. 3D,E). However, in three out of five slices from Pum2 GT mice, we did detect a higher probability for multiple population spikes in response to afferent stimulation. Moreover, excitability was analyzed by plotting the PS amplitude as a function of the FV amplitude, and we detected no differences in WT and Pum2 GT mice (Fig. 3F). Next, in order to measure the ability of hippocampal interneurons to inhibit subsequent population responses, we performed paired-pulse stimulations at different interpulse intervals (IPIs), ranging from 750 ms to 20 ms IPI, at a stimulation intensity of around 60% (Fig. 3G,H). Paired-pulse ratios (PPRs) were plotted as a function of the IPI and we found a higher tendency in Pum2 GT mice for decreased paired-pulse inhibition compared to control mice, suggestive of reduced network inhibition (Fig. 3I). We conclude that this reduced network inhibition might be a cause for the development of spontaneous epileptic seizures.

Altered expression of sodium channels with the onset of spontaneous seizures

Pum2 is highly expressed in the hippocampus (Allen Brain Atlas: www.brain-map.org/). The occurrence of epileptic seizures and, eventually, epilepsy is caused by disturbed excitability mediated, *inter alia*, by voltage-gated sodium channels. Within those, $Na_v1.1$, $Na_v1.2$ and $Na_v1.6$ have been linked to epilepsy in human patients (Oliva et al., 2012). To test for protein expression levels of $Na_v1.1$, $Na_v1.2$ and $Na_v1.6$, we performed immunohistochemistry on coronal brain slices of the dorsal hippocampus (Fig. 4). All Na_v channels tested showed a staining pattern that followed the *in situ* hybridization results of the Allen Brain Atlas. In addition, we observed a clear dendritic localization for $Na_v1.6$ in the CA1

subregion in the WT hippocampus that is reduced in Pum2 GT mice (Fig. S2A). Strikingly, fluorescent signal quantifications showed significantly altered protein expressions of Na_v channels in the hippocampus of 5-month-old Pum2 GT mice. Whereas protein levels of $Na_v1.1$ and $Na_v1.2$ were increased, $Na_v1.6$ protein showed a reduced staining intensity. However, we did not detect statistically significant differences in staining intensity for $Na_v1.1$, $Na_v1.2$ and $Na_v1.6$ in the hippocampus of weaned mice (WT versus Pum2 GT) (Fig. S1).

Loss of Pum2 impacts GABRA2 expression levels and localization in CA1 pyramidal neurons

GABA_A receptors are chloride ion channels activated by the neurotransmitter GABA that have been linked to epilepsy (Loddenkemper et al., 2014). Our transcriptome analysis revealed a twofold upregulation of *Gabra2* levels in adult Pum2 GT mice that we confirmed by qRT-PCR in weaned and 5-month-old mice (Fig. 5A). This effect is specific for *Gabra2* and not a general effect of GABA receptor expression because γ -aminobutyric acid receptor B subunit 2 (*Gabbr2*), a member of the GABA_B-receptor family, remained unaffected (Fig. S2E). To test for alterations in protein levels, we performed immunohistochemistry on coronal slices of the dorsal hippocampus with antibodies specific for GABRA2 (Quadrato et al., 2014). Interestingly, we detected a significantly higher staining intensity in the dendritic field [stratum radiatum (StR)] of CA1 neurons compared to the pyramidal cell layer [stratum pyramidale (StP)] in 5-month-old Pum2 GT mice (Fig. 5B; Fig. S2B,C). Importantly, the expression levels of GABRA2 in pyramidal cells of the CA3-CA1 subregions and in granule cells in the DG as well as in the corresponding dendritic fields remained unaffected.

In summary, our expression analysis show that knockdown of Pum2 affects the expression of *Gabra2* age-independently, in contrast to the tested Na_v channels. Furthermore, Pum2 GT mice show reduced network inhibition. Thus, our results suggest that neuronal inhibition is mostly affected in Pum2 GT mice.

DISCUSSION

In this study, we investigated the age-dependent expression of known epileptogenic genes in Pum2-deficient mouse brains. In order to investigate the effect of Pum2 knockdown on mRNA levels, we performed a transcriptome-wide microarray analysis. Strikingly, gene ontology (GO) analysis revealed significantly enriched categories for genes involved in cell communication and synaptic transmission – two processes known to be affected in epilepsy models (Staley, 2015). Furthermore, Pum2 deficiency resulted in altered expression levels for a subset of genes coding for proteins involved in neuronal excitability. Among those genes, using microarray and qRT-PCR experiments, *Gabra2* levels were shown to be upregulated by 100% in weaned and adult Pum2 GT brains. Interestingly, we also detected altered *Scn1a*, *Scn2a* and *Scn8a* expression levels in weaned but not in 5-month-old Pum2 GT mice. According to binding-site screening in the 3'-UTR, all four candidate genes have a Pum2 consensus sequence in their 3'-UTR. It has been shown that Pum2 recruits the deadenylase complex CCR4-NOT (Van Etten et al., 2012), which has been linked to RNA decay (Collart, 2016). Therefore, it is tempting to speculate that the upregulation in expression levels for *Scn1a*, *Scn8a* and *Gabra2* might be caused by increased mRNA stability in the absence of Pum2.

Additionally, it has been shown that Pum2 regulates the translation of $Na_v1.6$ in dissociated hippocampal neurons (Driscoll et al., 2013). Therefore, we tested protein expression

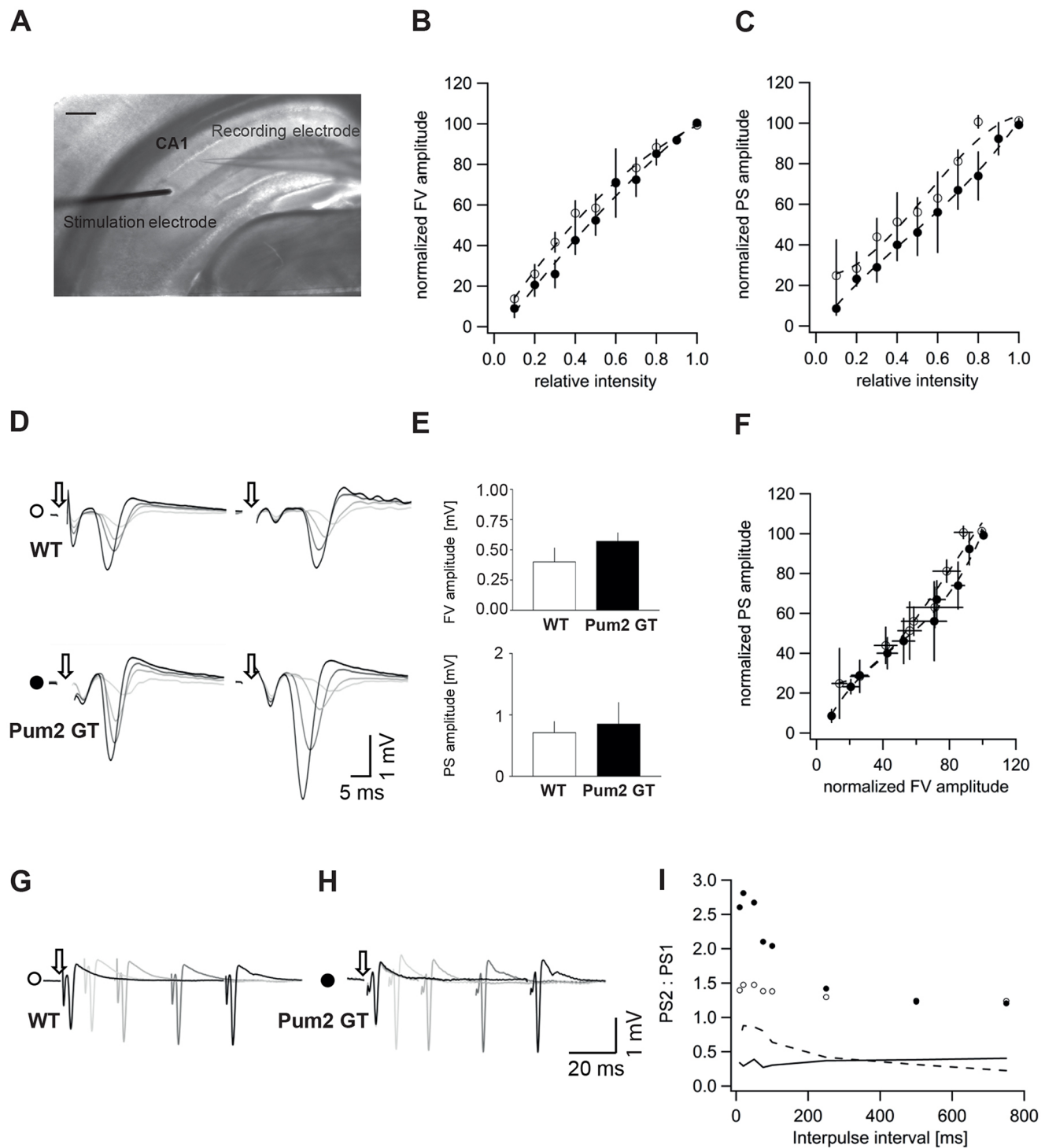


Fig. 3. Field recordings of acute hippocampal slices after Schaffer-collateral-commissural (SCC) pathway stimulation show reduced paired-pulse inhibition in Pum2 GT mice. (A) Representative bright-field image of the recording setup: a monopolar or bipolar stimulation electrode was placed onto the SCC pathway and the corresponding population spike was recorded from the pyramidal layer of the CA1 region of the hippocampus. Scale bar: 500 μ m. (B) Input-output analysis of evoked fiber volley (FV) responses in WT (white circles) and Pum2 GT (black circles) mice ($n=5$ animals/group), represented as the normalized FV amplitude (given as percentage of the maximal amplitude) as a function of the relative stimulation intensity (as percentage of the maximal current intensity). Data are means \pm s.e.m. (C) Input-output analysis of evoked population spike (PS) responses in WT (white circles) and Pum2 GT (black circles) mice. The normalized PS amplitude is plotted as a function of the relative current intensity ($n=5$ animals/group). (D) Representative single PS traces after stimulation with the following relative current intensities: 0.3 (light gray), 0.6 (medium gray), 0.8 (dark gray) and 1.0 (black) units. White circle: WT mouse; black circle: Pum2 GT mouse. Arrows indicate the stimulation onset; the stimulation artefact was removed from the single traces. (E) Overall FV (top) or PS (bottom) amplitudes in WT and Pum2 GT slides ($n=5$ animals/group). Data are means \pm s.e.m. (F) Normalized PS amplitude is plotted as a function of the normalized presynaptic FV amplitude ($n=5$ animals/group). Data are means \pm s.e.m. (G,H) Single traces of PS in WT mice (G) and Pum2 GT mice (H) after paired-pulse stimulations with different interpulse intervals (IPIs) are overlaid. Black trace: IPI 100 ms; dark gray trace: IPI 75 ms; medium gray trace: IPI 20 ms; light gray trace: IPI 10 ms. Arrows indicate the onset of stimulation; the stimulation artefact was truncated. (I) Ratio of the amplitude of the second PS (PS2) compared to the first one (PS1) as a function of the IPI. The black solid line indicates the coefficient of variance (CV) of recordings from WT mice; the dashed line indicates the CV of PS2:PS1 ratios in Pum2 GT mice. WT, white circles; Pum2 GT, black circles.

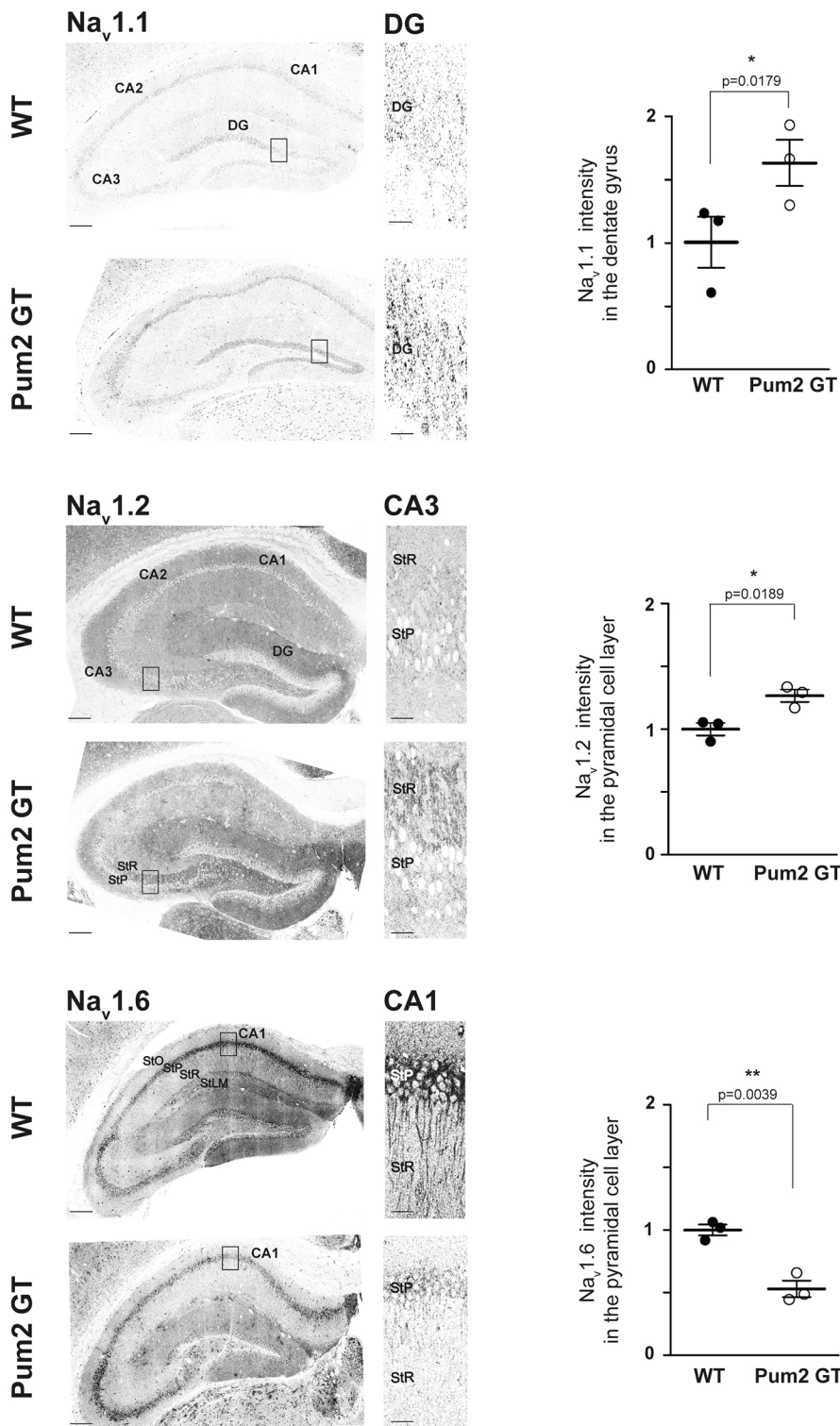


Fig. 4. Pum2 knockdown affects expression of Na_v channels in different hippocampal areas. Immunohistochemical stainings for Na_v1.1, Na_v1.2 and Na_v1.6 of the hippocampus of 5-month-old WT and Pum2 GT mice. Boxed areas indicate the magnified field that is shown. Quantification is shown for dentate gyrus (DG; Na_v1.1) and pyramidal cell layer (Na_v1.2, Na_v1.6) ($n=3$ animals for all groups). Scale bars: 200 μ m; insets: 20 μ m. Significance was determined using unpaired *t*-test. * $P<0.05$.

levels for Na_v1.1, Na_v1.2 and Na_v1.6 in the hippocampus. Interestingly, we observed higher Na_v1.1 and Na_v1.2 levels in both the DG and pyramidal cell layer, respectively, but reduced Na_v1.6 levels in the pyramidal cell layer in 5-month-old Pum2 GT brains. In weaned mice, protein levels are not significantly altered.

We suggest that there are at least two possible explanations for the differences in mRNA and protein levels for *Scn1a*, *Scn2a* and *Scn8a*: (i) protein levels for the sodium channels are significantly changed in weaned mice in extrahippocampal regions such as

forebrain or (ii) other translation repressors, such as *Nanos*, inhibit the translation of these sodium channels as a compensatory effect. For 5-month-old Pum2 GT mice, unaffected RNA levels but altered protein levels argue for translational regulation.

Next, in order to test for a functional impact of Pum2 knockdown on neuronal activity, we recorded evoked population spikes in CA1 pyramidal neurons after SCC pathway stimulation. Importantly, a previous study has shown that Pum2 GT animals show abnormal discharging in EEG recordings (Siemen et al., 2011). Our results

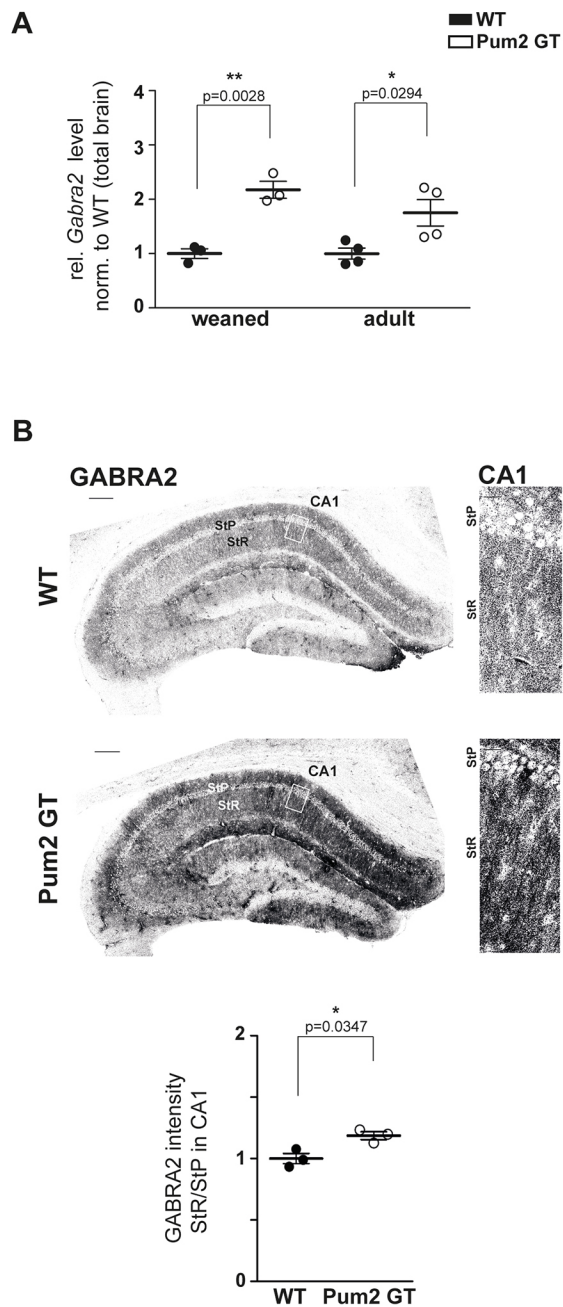


Fig. 5. GABRA2 shows increased mRNA levels and enhanced dendritic protein localization in the hippocampus of adult Pum2 GT mice.

(A) *Gabra2* mRNA levels are quantified by qRT-PCR in 3-month-old (weaned) and 5-month-old WT and Pum2 GT brains ($n \geq 3$ animals/group).

(B) Representative staining of GABRA2 in the hippocampus of 5-month-old WT and Pum2 GT animals, and quantification of GABRA2 protein expression in the stratum radiatum (StR) compared to stratum pyramidale (StP) in the CA1 area of WT and Pum2 GT mice. Scale bars: 200 μ m; insets: 20 μ m. Significance was determined using unpaired *t*-test. * $P < 0.05$.

suggest that Pum2 has no impact on overall neuronal activity. CA1 pyramidal neurons do not seem to exhibit a higher excitability level in Pum2 GT mice compared with WT. This is in line with our observation that weaned mice show no differences in the protein expression of $Na_v1.1$, $Na_v1.2$ and $Na_v1.6$. We found that Pum2 knockdown resulted in increased $Na_v1.1$ and $Na_v1.2$ levels in 5-month-old mice, a finding that could possibly be accompanied by a higher excitability of principal cells after afferent stimulation. A

likely explanation(s) for the fact that we did not observe increased excitability in Pum2 GT mice might be that: (i) principal cells as well as interneurons show a similar increase in Na_v protein levels, therefore maintaining the overall excitation to inhibition ratio; (ii) Na_v protein levels of β -subunits that regulate the gating behavior of their associated α -subunits are reduced/dysfunctional; or (iii) the analyzed young adult mice had not yet developed spontaneous seizures and, therefore, a clear phenotype is not yet detectable. We suggest that the generation of spontaneous seizures in 5-month-old Pum2 GT mice is likely due to reduced network inhibition and less likely due to increased neuronal excitability. This hypothesis is further supported by the finding that we detected a tendency towards reduced inhibition after paired-pulse stimulation in Pum2 GT mice compared to controls. In agreement with this interpretation, it is known that dysfunctional or loss of GABAergic inhibition can cause paroxysmal activity and a loss of paired-pulse inhibition (Kapur et al., 1989a,b; Sloviter and Brisman, 1995).

Loss of paired-pulse inhibition, indicative of reduced GABAergic inhibition, points towards a reduction of GABRA2 levels. However, we detected an upregulation of *Gabra2* levels in Pum2 GT brains. It remains to be investigated whether these increased GABRA2 levels are accompanied by increased expression of functional synaptic GABA_A receptors or whether this effect is specific for certain brain regions. Moreover, we detected an enhanced dendritic localization of GABRA2 in CA1 pyramidal neurons of Pum2 GT mice, possibly due to potentially higher neuronal input from CA3 neurons and/or the entorhinal cortex (Pettit and Augustine, 2009). Moreover, given the small volume of the dendritic compartment and thus a higher probability of a shift of its chloride equilibrium potential towards more positive values, increased dendritic localization of GABA_A receptors is able to actively contribute to action-potential induction in CA1 neurons of Pum2 GT mice (Jedlicka et al., 2011; Staley and Proctor, 1999). Moreover, depolarizing actions of GABA have been reported in neocortical pyramidal cells of adult mice (Gulledge and Stuart, 2003). Interestingly, a transition from dominant phasic GABAergic inhibition to dominant phasic GABAergic excitation has also been shown in a mouse model of epilepsy (Derchansky et al., 2008). Another possible explanation for reduced paired-pulse inhibition despite higher levels of dendritic GABA_A receptor expression could stem from findings showing that the function of chloride transporters that actively extrude chloride out of the cell can be impaired in epilepsy (Buchin et al., 2016; Conti et al., 2011; Doyon et al., 2016). It remains to be investigated whether chloride transporters, especially the K-Cl cotransporter KCC2, are affected by Pum2 knockdown.

It is generally believed that voltage-gated sodium channels and GABA_A receptors crucially contribute to the development and manifestation of epilepsy in human patients and animal models (Staley, 2015). In our study, we observed altered mRNA levels of *Scn1a*, *Scn2a* and *Scn8a* in weaned but not in adult mice. Based on our results, we conclude that brain-wide knockdown of Pum2 causes a predisposition in developing animals to develop epileptic seizures that might be mediated by altered mRNA levels of known epileptogenic factors. At this age, we did not observe differences on the corresponding protein level in the hippocampus. We speculate that this effect is, preferentially, due to increased translational repression. During epileptogenesis, mRNAs are released from repression, which then affects the protein levels in the hippocampus of adult, 5-month-old animals and leads to manifestation of spontaneous epileptic seizures (Siemen et al., 2011). In summary, the aim of the study presented here was to identify, in mice, epileptogenic risk factors during the development and maintenance

of epilepsy that are known to increase the risk for epilepsy when misregulated. Together with the fact that *Pum2* is downregulated in postmortem brains of patients who suffered from epileptic seizures (Wu et al., 2015), we conclude that *Pum2* is a key regulator of epileptogenic risk factors.

MATERIALS AND METHODS

Mice

For all experiments, male mice homozygous for GT-vector insertion [B6.129P2-*Pum2*^{GT(XE772)Byg}] in the *Pum2* locus (*Pum2* GT) and WT control animals (genetic background for WT and *Pum2* GT mice: C57Bl6/J) at the age of P21 (weaned) or 5 months (adult) were investigated. *Pum2* GT mice were a gift from Dr Eugene Xu (Northwestern University, IL, USA). Mice were kept under specified pathogen-free conditions and housed in groups of two to five animals in individually ventilated cages and a 12 h/12 h light/dark cycle. Mice had free access to water and standard rodent chow. All experiments were approved by the authors' institutional committee on animal care and were performed according to the German Animal Protection Law, conforming to international guidelines on the ethical use of animals.

Microarray analysis

RNA was isolated as described in qRT-PCR. Samples were processed according to the manufacturer's instructions (Affymetrix) and hybridized on a Mouse Gene 2.0 ST Array. Signal intensities were extracted and normalized using RMA (R/bioconductor package 'oligo'). Probesets with log₂-expression levels of >5 in at least three samples were subjected to differential expression analysis using limma and multiple-testing correction according to Benjamini and Hochberg (Benjamini and Hochberg, 1995) (R/bioconductor package 'limma'). GO analysis was performed using the STRING database (version 10.0; <http://string-db.org>). False discovery rate (FDR) was calculated according to the method of Benjamini and Hochberg (Benjamini and Hochberg, 1995; Franceschini et al., 2013).

Tissue preparation for fluorescent immunocytochemistry

For immunohistochemistry, mice were deeply anaesthetized with CO₂ and immediately prepared for tissue preservation. Mice were transcardially perfused with 1% PBS (pH 7.4) followed by 4% PFA (pH 7; Roti[®]-Histofix, Germany) for 12 min (Gage et al., 2012; Kohler et al., 1999). Brains were carefully removed and post-fixed in 4% PFA (pH 7; Roti[®]-Histofix) for 12–72 h at 4°C, then dehydrated in 30% sucrose in ddH₂O at 4°C for 24–48 h. Brains were cut into 30-µm coronal sections using a cryotome. Free-floating coronal brain sections were washed 3×10 min in 1% PBS (pH 7.4), blocked in blocking solution [1% (w/v) BSA, 0.5% (v/v) Triton X-100 in PBS] for 45 min at room temperature (RT; approx. 22°C) and incubated with primary antibody overnight at 4°C. Antibodies were diluted separately in blocking solution [polyclonal rabbit anti-Na_v1.1, 1:200; rabbit anti-Na_v1.2, 1:200; rabbit anti-Na_v1.6, 1:200; rabbit anti-GABRA2, 1:500 (all Alomone Labs, Israel)] and co-stained with chicken anti-NeuN (1:500; Millipore, Germany) or mouse anti-MAP2 (1:1000; Sigma-Aldrich, Germany). After overnight incubation, sections were washed 3×10 min in 1% PBS (pH 7.4) and incubated with secondary antibodies in blocking solution for 2 h at RT. Sections were incubated with donkey anti-rabbit IgG Alexa Fluor 488 (1:500) and goat anti-chicken IgY Alexa Fluor 647 (1:500) or donkey anti-mouse IgG Alexa Fluor 647 (1:500; all Life Technologies, Germany). To counterstain nuclei, sections were incubated with DAPI (2 µg/ml; Thermo Fisher, Germany) for 5 min at RT and washed 3×10 min in 1% PBS (pH 7.4). After washing, the sections were mounted with Fluomount (Sigma-Aldrich). Confocal microscopy was performed with an inverted Leica SP8 microscope equipped with lasers for 405, 488, 552 and 638 nm excitation. Images were acquired with a 40×1.3 oil objective; image pixel size was 80 nm. The following fluorescence settings were used for detection: DAPI: 430–470 nm; AF488: 500–550; AF555: 560–600; AF647: 650–700. Images were scanned in a sequential fashion to avoid bleed-through. AF488, AF555 and AF647 were recorded with hybrid photo detectors (HyDs), and DAPI with a conventional photomultiplier tube. Overview images with high resolution were obtained by stitching.

Acute slice preparation

Mice were deeply anaesthetized with CO₂ before decapitation. Brains were quickly removed and submerged in ice-cold cutting solution consisting of (in mM) 135 N-methyl-D-glucamine, 1.5 KCl, 1.5 KH₂PO₄, 23 NaHCO₃, 0.5 CaCl₂, 3.5 MgCl₂, 0.4 ascorbic acid and 25 D-glucose (pH at 28°C: 7.4; osmolarity: 310–330 mOsm) for 60 s. Coronal slices (slice thickness: 300 µm) were cut on a vibrating microtome (HM 650 V, Thermo Scientific Microm, Walldorf, Germany). Slices were collected and submerged in artificial cerebrospinal fluid (ACSF) containing (in mM): NaCl (125), KCl (3), NaH₂PO₄ (1.25), NaHCO₃ (25), CaCl₂ (2), MgCl₂ (2) and D-glucose (25), and left to recover for 1 h at 28°C and for another 1 h at RT. Both solutions were continuously perfused with 95% O₂/5% CO₂ to maintain a pH of 7.4. For electrophysiological analysis, slices were transferred to a recording chamber mounted on the stage of a microscope (Zeiss Axioskop FS with a 40×, 0.75 NA objective). The recording chamber was continuously perfused with artificial cerebrospinal fluid (ACSF). The recording temperature was maintained at 30°C with the help of a temperature controller (Automatic Temperature Controller TC-324B, Warner Instrument Corp., CT, USA).

Electrophysiological field recordings

The CA1 pyramidal cell layer was visualized and identified by means of an upright microscope equipped with differential interference contrast (DIC)-infrared optics. Infrared images were acquired with the help of a CCD camera and controller (Orca-ER, Hamamatsu, Shizouka, Japan). The electrodes for field recordings were fabricated from borosilicate glass capillaries (OD: 1.5 mm, ID: 0.86 mm; Hugo Sachs Elektronik-Harvard Apparatus, March-Hugstetten, Germany) and were filled with 1 mM NaCl solution. The electrodes were connected to the headstage of the amplifier (ELC; npi electronic, Tamm, Germany) via a chlorided silver wire. A silver/silver chloride pellet immersed into the recording solution served as reference electrode.

Electrode capacitance and resistance were compensated and bias and offset current were zeroed before the start of recordings. Evoked population spikes were recorded from CA1 pyramidal neurons after placing a monopolar or bipolar stimulation electrode in the SCC pathway. The stimulation intensity was increased in a stepwise fashion to obtain the optimal stimulation intensity (~60% of the maximal response).

Data acquisition and analysis

Recorded voltage signals were amplified (×20), filtered at 10 kHz and digitized at a sampling rate of 5 kHz. Data acquisition and generation of command pulses was accomplished by means of an analog-digital converter (CED Power1401; Cambridge Electronic Design, Cambridge, UK) in conjunction with the Signal data-acquisition software (version 6; Cambridge Electronic Design). Data analysis was performed using IGOR Pro 6 (WaveMetrics, Lake Oswego, OR, USA) together with the NeuroMatic IGOR plugin (www.neuromatic.thinkrandom.com).

Image analysis

Images of coronal hippocampal slices were analyzed with Fiji 1.50 g (Schindelin et al., 2015). Regions of interest were selected and quantified as mean pixel intensity. To identify the STP (CA1-CA3), NeuN images were thresholded using the mean gray value autothreshold after median filtering of the image (radius 15). For DG, mean pixel intensity of cell bodies in the stratum granulare (StG) were measured. For GABRA2, signal was measured in CA1 (StP) for cell bodies and in StR CA1 for the dendritic field. The inverse mask of the pyramidal cell layer was used to quantify signal intensity in the dendritic compartment. All values were normalized to WT. Intensities were measured on the original, non-filtered images.

qRT-PCR

Total mRNA was obtained from brain samples using TRIzol (Ambion) according to the manufacturer's protocol. DNA was depleted using the Mini RNeasy kit (Qiagen, Germany). cDNA was synthesized from purified mRNA by reverse transcription using Superscript III reverse transcriptase (Invitrogen) and random primers according to the

manufacturer's manual. For qPCR cDNA amplification, Hot Start Taq (New England Biolabs, MA, USA) was used with SYBR Green for amplicon detection. All primers were used with an optimal efficiency rate of 2.0 ± 0.5 . Target gene signal was normalized to *Ppia* as reference gene using the comparative $\Delta\Delta C_T$ method (Schmittgen and Livak, 2008). Normalization to *18S* gave similar results. Runs were performed on a Lightcycler 96 (Roche Bioanalytics, Germany). Primers used in this study were (5' to 3'): *Scn1a*, GAATCCCAAGCCAGACAAA and ACCATCTCTGGAGGAATGT; *Scn2a*, ACAGGAATTTACTTTTGAATCA and AGTATCATGACGTCAGACAG; *Scn8a*, CTTCAGTGTCATCATGATGG and GCCCACGATTGTCTTCA; *Gabra2*, GAAAGGCTCGTCATGATAC and GCTTGTCTCTGGCTTCTT; *Gabbr2*, CTACGACGGTCTTACTCTCA and GGCCTCTCTCTTTGTCTA; *Pum2*, AGCAACCAAGCACTAACC and CCAGGTCCATGAGAGAATAAAAG; *Ppia*, GTCAACCCACCGTGTCTT and CTGCTGTCTTTGGAACCTTG; and *18S*, GAAACTGCGAATGGCTCATTAATA and CCACAGTTATCCAAGTAGGAGAGGA.

Western blot

To analyze protein expression in *Pum2* GT mice, brains were homogenized in RIPA buffer [150 mM NaCl, 1.0 vol% NP-40, 0.5% (w/v) sodium deoxycholate, 0.1% (w/v) SDS, 50 mM Tris-HCl pH 8.0, complete protease inhibitor (Roche)]. Proteins were transferred to a nitrocellulose membrane (pore size 0.2 μ m). Membrane was blocked in blocking buffer [2% (w/v) BSA, 0.1% (v/v) Tween 20, 0.1% (w/v) sodium azide in 1 \times TBS pH 7.5] for 1 h. *Pum2* was detected by incubation with polyclonal rabbit anti-*Pum2* antibody (1:10,000; Abcam, Cambridge, UK) in blocking buffer. Protein bands for β -actin served as loading control and were detected with mouse anti- β -actin (anti-ACTB) antibody (1:2000; Sigma Aldrich). Proteins were visualized by incubation of the nitrocellulose membranes with secondary anti-rabbit antibody (1:10,000; Li-Cor, Germany) in blocking buffer. For quantification, the *Pum2* signal was normalized to the loading control. Quantification of optical density (OD) was performed using Image Studio Lite Software (Li-Cor).

Statistics

Data are presented as means \pm s.e.m. Statistics were calculated using the software GraphPad Prism (version 5; GraphPad, San Diego, CA, USA). Unpaired two-tailed Student's *t*-test was used to determine *P*-values. *P* < 0.05 was considered statistically significant if not stated otherwise.

Acknowledgements

We thank Dr Eugene Xu (Northwestern University, IL, USA) for providing *Pum2* GT mice; Ulrike Kring, Jessica Olberz and Christin Illig for excellent technical assistance; and all members of the Kiebler lab for helpful discussions. We also thank the Biomedical Center (BMC) core facilities involved in this study for kindly providing equipment and excellent services.

Competing interests

The authors declare no competing or financial interests.

Author contributions

Formal analysis: P.F., R.S., T.S., A.H.K., M.B., B.P.; Investigation: P.F., R.S., T.R., A.D., B.P.; Resources: M.A.K.; Writing - original draft: P.F., R.S., B.P., M.A.K.; Writing - review & editing: P.F., R.S., B.P., M.A.K.; Visualization: A.D.; Funding acquisition: B.P., M.A.K.

Funding

This work was supported by the Boehringer Ingelheim Fonds (BIF; to R.S.), the Förderprogramm für Forschung und Lehre – FöFoLe PhD program of the LMU Munich (Ludwig-Maximilians-Universität München; 12/2014 to A.D.), the Dr Hildegard und Heinrich Fuchs Stiftung scholarship (to P.F.), the DFG (Deutsche Forschungsgemeinschaft; FOR 2333 TP08 to M.A.K.) and the Friedrich-Baur-Stiftung (21/16 to A.H.K. and 02/14 to B.P.).

Supplementary information

Supplementary information available online at <http://dmm.biologists.org/lookup/doi/10.1242/dmm.029678.supplemental>

This article has an associated First Person interview with the first author of the paper available online at <http://dmm.biologists.org/lookup/doi/10.1242/dmm.029678.supplemental>.

References

- Benjamini, Y. and Hochberg, Y. (1995). Controlling the false discovery rate: a practical and powerful approach to multiple testing. *J. R. Stat. Soc. B* **57**, 289-300.
- Bertram, E. H. (2003). How epilepsy changes sodium channels. *Epilepsy Curr.* **3**, 72-73.
- Buchin, A., Chizhov, A., Huberfeld, G., Miles, R. and Gutkin, B. S. (2016). Reduced efficacy of the KCC2 cotransporter promotes epileptic oscillations in a subiculum network model. *J. Neurosci.* **36**, 11619-11633.
- Collart, M. A. (2016). The Ccr4-Not complex is a key regulator of eukaryotic gene expression. *Wiley Interdiscip. Rev. RNA* **7**, 438-454.
- Conti, L., Palma, E., Roseti, C., Lauro, C., Cipriani, R., de Groot, M., Aronica, E. and Limatola, C. (2011). Anomalous levels of Cl⁻ transporters cause a decrease of GABAergic inhibition in human peritumoral epileptic cortex. *Epilepsia* **52**, 1635-1644.
- Darnell, J. C. and Klann, E. (2013). The translation of translational control by FMRP: therapeutic targets for FXS. *Nat. Neurosci.* **16**, 1530-1536.
- Derchansky, M., Jahromi, S. S., Mamani, M., Shin, D. S., Sik, A. and Carlen, P. L. (2008). Transition to seizures in the isolated immature mouse hippocampus: a switch from dominant phasic inhibition to dominant phasic excitation. *J. Physiol.* **586**, 477-494.
- Doyon, N., Prescott, S. A. and De Koninck, Y. (2016). Mild KCC2 hypofunction causes inconspicuous chloride dysregulation that degrades neural coding. *Front. Cell. Neurosci.* **9**, 516.
- Driscoll, H. E., Muraro, N. I., He, M. and Baines, R. A. (2013). Pumilio-2 regulates translation of Nav1.6 to mediate homeostasis of membrane excitability. *J. Neurosci.* **33**, 9644-9654.
- Franceschini, A., Szklarczyk, D., Frankild, S., Kuhn, M., Simonovic, M., Roth, A., Lin, J., Minguez, P., Bork, P., von Mering, C. et al. (2013). STRING v9.1: protein-protein interaction networks, with increased coverage and integration. *Nucleic Acids Res.* **41**, D808-D815.
- Gage, G. J., Kipke, D. R. and Shain, W. (2012). Whole animal perfusion fixation for rodents. *J. Vis. Exp.* **65**, e3564.
- Gulledge, A. T. and Stuart, G. J. (2003). Excitatory actions of GABA in the cortex. *Neuron* **37**, 299-309.
- Jedlicka, P., Deller, T., Gutkin, B. S. and Backus, K. H. (2011). Activity-dependent intracellular chloride accumulation and diffusion controls GABA_A receptor-mediated synaptic transmission. *Hippocampus* **21**, 885-898.
- Jung, H., Gkogkas, C. G., Sonenberg, N. and Holt, C. E. (2014). Remote control of gene function by local translation. *Cell* **157**, 26-40.
- Kapur, J., Stringer, J. L. and Lothman, E. W. (1989a). Evidence that repetitive seizures in the hippocampus cause a lasting reduction of GABAergic inhibition. *J. Neurophysiol.* **61**, 417-426.
- Kapur, J., Bennett, J. P., Wooten, G. F. and Lothman, E. W. (1989b). Evidence for a chronic loss of inhibition in the hippocampus after kindling: biochemical studies. *Epilepsy Res.* **4**, 100-108.
- Kohler, I., Meier, R., Busato, A., Neiger-Aeschbacher, G. and Schatzmann, U. (1999). Is carbon dioxide (CO₂) a useful short acting anaesthetic for small laboratory animals? *Lab. Anim.* **33**, 155-161.
- Lin, W.-H., Giachello, C. N. G. and Baines, R. A. (2017). Seizure control through genetic and pharmacological manipulation of Pumilio in *Drosophila*: a key component of neuronal homeostasis. *Dis. Model. Mech.* **10**, 141-150.
- Loddenkemper, T., Talos, D. M., Cleary, R. T., Joseph, A., Sánchez Fernández, I., Alexopoulos, A., Kotagal, P., Najm, I. and Jensen, F. E. (2014). Subunit composition of glutamate and gamma-aminobutyric acid receptors in status epilepticus. *Epilepsy Res.* **108**, 605-615.
- Oliva, M., Berkovic, S. F. and Petrou, S. (2012). Sodium channels and the neurobiology of epilepsy. *Epilepsia* **53**, 1849-1859.
- Pernice, H. F., Schieweck, R., Kiebler, M. A. and Popper, B. (2016). mTOR and MAPK: from localized translation control to epilepsy. *BMC Neurosci.* **17**, 73.
- Pettit, D. L. and Augustine, G. J. (2009). Distribution of functional glutamate and GABA receptors on hippocampal pyramidal cells and interneurons. *J. Neurophysiol.* **84**, 28-38.
- Pieretti, M., Zhang, F., Fu, Y.-H., Warren, S. T., Oostra, B. A., Caskey, C. T. and Nelson, D. L. (1991). Absence of expression of the FMR-1 gene in fragile X syndrome. *Cell* **66**, 817-822.
- Quadrato, G., Elnaggar, M. Y., Duman, C., Sabino, A., Forsberg, K. and Di Giovanni, S. (2014). Modulation of GABA_A receptor signaling increases neurogenesis and suppresses anxiety through NFATc4. *J. Neurosci.* **34**, 8630-8645.
- Quenault, T., Lithgow, T. and Travençolo, A. (2011). PUF proteins: repression, activation and mRNA localization. *Trends Cell Biol.* **21**, 104-112.
- Schindelin, J., Rueden, C. T., Hiner, M. C. and Eliceiri, K. W. (2015). The ImageJ ecosystem: an open platform for biomedical image analysis. *Mol. Reprod. Dev.* **82**, 518-529.

- Schmittgen, T. D. and Livak, K. J.** (2008). Analyzing real-time PCR data by the comparative CT method. *Nat. Protoc.* **3**, 1101-1108.
- Siemen, H., Colas, D., Heller, H. C., Brüstle, O. and Reijo Pera, R. A.** (2011). *Pumilio-2* function in the mouse nervous system. *PLoS ONE* **6**, e25932.
- Sloviter, R. S. and Brisman, J. L.** (1995). Lateral inhibition and granule cell synchrony dentate gyrus in the rat hippocampal. *J. Neurosci.* **15**, 811-820.
- Staley, K.** (2015). Molecular mechanisms of epilepsy. *Nat. Neurosci.* **18**, 367-372.
- Staley, K. J. and Proctor, W. R.** (1999). Modulation of mammalian dendritic GABA_A receptor function by the kinetics of Cl⁻ and HCO₃⁻ transport. *J. Physiol.* **519**, 693-712.
- Van Etten, J., Schagat, T. L., Hrit, J., Weidmann, C. A., Brumbaugh, J., Coon, J. J. and Goldstrohm, A. C.** (2012). Human *Pumilio* proteins recruit multiple deadenylases to efficiently repress messenger RNAs. *J. Biol. Chem.* **287**, 36370-36383.
- Vessey, J. P., Schoderboeck, L., Gingl, E., Luzi, E., Riefler, J., Di Leva, F., Karra, D., Thomas, S., Kiebler, M. A. and Macchi, P.** (2010). Mammalian *Pumilio 2* regulates dendrite morphogenesis and synaptic function. *Proc. Natl. Acad. Sci. USA* **107**, 3222-3227.
- White, E. K., Moore-Jarrett, T. and Ruley, H. E.** (2001). PUM2, a novel murine puf protein, and its consensus RNA-binding site. *RNA* **7**, 1855-1866.
- Wu, X.-L., Huang, H., Huang, Y.-Y., Yuan, J.-X., Zhou, X. and Chen, Y.-M.** (2015). Reduced *Pumilio-2* expression in patients with temporal lobe epilepsy and in the lithium-pilocarpine induced epilepsy rat model. *Epilepsy Behav.* **50**, 31-39.
- Xu, E. Y., Chang, R., Salmon, N. A. and Reijo Pera, R. A.** (2007). A gene trap mutation of a murine homolog of the *Drosophila* stem cell factor *Pumilio* results in smaller testes but does not affect litter size or fertility. *Mol. Reprod. Dev.* **74**, 912-921.

Publication II: Staufen2 deficiency leads to impaired response to novelty in mice

This section contains the study published in *Neurobiology of Learning and Memory* (2018) entitled **Staufen2-deficiency leads to impaired response to novelty in mice** by

Bastian Popper*, Antonia Demleitner*, Valerie J. Bolivar, Gretchen Kusek, Abigail Snyder-Keller, **Rico Schieweck**[‡], Sally Temple, Michael A. Kiebler[‡]

* shared first authors

[‡] corresponding authors

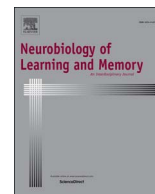
Author contribution to this publication

Bastian Popper, Rico Schieweck and Michael A. Kiebler conceptualized and designed the study. Bastian Popper and Antonia Demleitner performed behavior tests with *Staufen2* deficient mice (Figs. 2, 3 and 4). Valerie J. Bolivar, Gretchen Kusek, Abigail Snyder-Keller and Sally Temple generated the *Staufen2* deficient mouse line. Antonia Demleitner and Rico Schieweck initially characterized the *Staufen2* deficient mouse line (Fig. 1). Bastian Popper, Rico Schieweck and Michael A. Kiebler wrote and revised the manuscript.

(Rico Schieweck)

(Prof. Dr. Michael A. Kiebler)

(Prof. Dr. Heinrich Leonhardt)



Staufen2 deficiency leads to impaired response to novelty in mice

Bastian Popper^{a,b,1}, Antonia Demleitner^{a,1}, Valerie J. Bolivar^{c,d}, Gretchen Kusek^e,
Abigail Snyder-Keller^{c,d}, Rico Schieweck^{a,*}, Sally Temple^e, Michael A. Kiebler^{a,*}

^a Biomedical Center (BMC), Department for Cell Biology & Anatomy, Medical Faculty, Ludwig-Maximilians-University, Munich, Germany

^b Biomedical Center (BMC), Core Facility Animal Models, Ludwig-Maximilians-University, Munich, Germany

^c Wadsworth Center, New York State Department of Health, Albany, NY, USA

^d Department of Biomedical Sciences, University at Albany School of Public Health, State University of New York, Albany, NY, USA

^e Neural Stem Cell Institute, Regenerative Research Foundation, Rensselaer, NY, USA

ARTICLE INFO

Keywords:

Staufen2
RNA-binding protein
Gene-trap mouse
Behavior
Novelty response
Spatial memory

ABSTRACT

Staufen2 (Stau2) is a double-stranded RNA-binding protein (RBP) involved in posttranscriptional gene expression control in neurons. In flies, *stau2* contributes to learning and long-term memory formation. To study the impact of mammalian *Stau2* on behavior, we generated a novel gene-trap mouse model that yields significant constitutive downregulation of *Stau2* (*Stau2*^{GT}). In order to investigate the effect of *Stau2* downregulation on hippocampus-dependent behavior, we performed a battery of behavioral assays, *i.e.* open field, novel object recognition/location (NOR/L) and Barnes maze. *Stau2*^{GT} mice displayed reduced locomotor activity in the open field and altered novelty preference in the NOR and NOL paradigms. Adult *Stau2*^{GT} male mice failed to discriminate between familiar and newly introduced objects but showed enhanced spatial novelty detection. Additionally, we observed deficits in discriminating different spatial contexts in a Barnes maze assay. Together, our data suggest that *Stau2* contributes to novelty preference and explorative behavior that is a driver for proper spatial learning in mice.

1. Introduction

Plasticity of neuronal circuits is the key for learning and memory formation and its maintenance (Kandel, Dudai, & Mayford, 2014). Consequently, any dysfunction in these networks may cause neurological disorders (Paoletti, Bellone, & Zhou, 2013). Two distinct mechanisms critically enable neurons to alter the long-term efficacy of individual synapses within neural networks: the activation of gene transcription in the nucleus and the experience dependent synthesis of key proteins at selected synapses (Doyle & Kiebler, 2011; Govindarajan, Kelleher, & Tonegawa, 2006). To allow for the latter in the postsynaptic compartment, selected mRNAs become localized into dendrites, near synapses (Holt & Bullock, 2009). This is achieved by a set of RNA-binding proteins (RBPs) that recognize and bind to *cis*-elements preferentially within the 3'-untranslated region (3'-UTR) of target mRNAs (Nakielnny, Fischer, Michael, & Dreyfuss, 1997) allowing the assembly of ribonucleoprotein particles (RNPs). With the help of molecular motor proteins, these RNPs are then transported along the neuronal cytoskeleton towards synapses. Upon synaptic activation RBPs then critically contribute to regulate local translation of localized mRNAs (Jung,

Gkogkas, Sonenberg, & Holt, 2014; Kiebler & Bassell, 2006). Importantly, RBPs also contribute to posttranscriptional control of protein expression in the cell body (Hutten, Sharangdhar, & Kiebler, 2014; Jung et al., 2014). One of the best studied examples of RBPs which mediate the posttranscriptional expression control is the fragile X mental retardation protein (FMRP). Its loss-of-function or knock-out are associated with increased metabotropic glutamate receptor signaling, which has been hypothesized to contribute to the intellectual disability and mental illness associated with its mutation in human patients (Antar, Afroz, Dichtenberg, Carroll, & Bassell, 2004; Bear, Huber, & Warren, 2004; Darnell & Klann, 2013), highlighting the importance of RBPs for memory formation and maintenance.

Staufen2 (*Stau2*) is a known multifunctional RBP involved in various aspects of posttranscriptional control of protein expression in different neuronal cell types (Heraud-Farlow & Kiebler, 2014). In neuronal progenitor cells, *Stau2* is important for cortical neurogenesis through the asymmetric segregation of its target mRNAs during neurogenic progenitor cell divisions (Kusek et al., 2012; Vessey et al., 2012). In mature neurons, it contributes to dendritic mRNA localization dependent on synaptic signaling (Sharangdhar et al., 2017). Isolation of

* Corresponding authors at: Biomedical Center, Department for Cell Biology & Anatomy, Medical Faculty, Ludwig-Maximilians-University, 82152 Planegg-Martinsried, Germany.

E-mail addresses: rico.schieweck@med.uni-muenchen.de (R. Schieweck), mkiebler@lmu.de (M.A. Kiebler).

¹ Authors contributed equally.

Stau2-containing RNA granules from rat brain revealed an enrichment of transcripts that are involved in synaptic transmission and function (Heraud-Farlow et al., 2013). Furthermore, the presence of a series of translational regulators in these granules suggested that transported transcripts are translationally repressed in these neuronal RNPs (Fritzsche et al., 2013). In line with these findings, Stau2 is required for dendritic spine morphogenesis (Goetze et al., 2006; Berger et al., 2017) and the establishment of miniature excitatory postsynaptic currents in cultured hippocampal neurons (Goetze et al., 2006). In addition, weakening of synaptic connections, a process called long-term depression (LTD), has been indicated to be regulated by Stau2 in organotypic slices *in vitro* (Lebeau et al., 2011). Moreover, LTD is impaired and long-term potentiation (LTP) is enhanced in Stau2 deficient rats (Berger et al., 2017). Together, these studies strongly suggest that Stau2 critically contributes to synaptic morphogenesis and function. However, the impact of Stau2 on hippocampus dependent learning and memory formation on the organismic level is not well understood.

Here, we have generated a novel gene-trap mouse model showing a Stau2 deficiency of approx. 40% and investigated hippocampus-dependent behavior such as novelty response and spatial learning in these mice. A battery of different behavioral tests such as open field, novel object recognition/location and the Barnes maze assay revealed that Stau2 deficiency significantly impacted novelty preference and reduced performance in a spatial learning assay.

2. Materials and Methods

2.1. Generation and housing of Stau2^{GT} mice

All experiments were approved by the authors' institutional committees on animal care and were performed according to the American and German Animal Protection Laws, conforming to international guidelines on the ethical use of animals. Stau2^{GT} mice (B6.129P2-Stau2^{GT(RRG396)Byg}) were generated from a gene-trap cell line purchased from the gene-trapping resource BayGenomics (Stryke et al., 2003). The gene-trap cassette inserted in Stau2, intron 7 of transcript ENSMUST0000027052.12 predicted to result in a C-terminally truncated Stau2 protein. ES cells were injected into blastocysts and transferred into pseudo-pregnant recipients to generate chimeric male mice. Germline transmission was assessed by breeding chimeric male mice with wildtype (WT) females. Animals were mated with C57BL/6NTac mice (Taconic Biosciences) before initiating a backcross to C57BL/6J (The Jackson Laboratory) for at least 5 generations. Genetic background characterization of Stau2^{GT} mice using a panel of 1450 single nucleotide polymorphisms (SNPs) across inbred strains (Taconic Biosciences) revealed animals to be congenic ranging from 99.2% to 99.5% of the C57BL/6J genome. Mixed and non-C57BL/6 genomes remain only on chromosome 1, near the Stau2 locus, and on SNPs known to differentiate between C57BL/6N and C57BL/6J. To differentiate homozygous vs heterozygous animals, Stau2^{GT} mice were genotyped via two separate PCR reactions using primers that span from the intronic DNA into the integrated gene-trap sequence as follows: WT allele Stau2-F: 5'-ACAGTGTCCACTGAAAGCTGGT-3' and Stau2-R 5'-TGGGTCCGCTGTCCCAGTTATT-3' (400 bp product); Gene-trap allele Stau2-F (as above) and Stau2GTVect-R: 5'-TCCAACCTCCGCAAACCTCCTAT-3' (210 bp product).

2.2. Behavioral analysis

For behavioral tests, we used mature adult males (4 months old). For behavioral tests of younger mice carried out in Albany, please refer to [Supplementary Material](#). Stau2^{GT} mice were tested for homozygous gene-trap vector insertion in Stau2 loci before doing behavioral tests. Mice were housed under specific pathogen free conditions in groups of 2–5 animals of the same sex, if not stated otherwise, with a 12-hour light, 12-hour dark light cycle and they had free access to water and

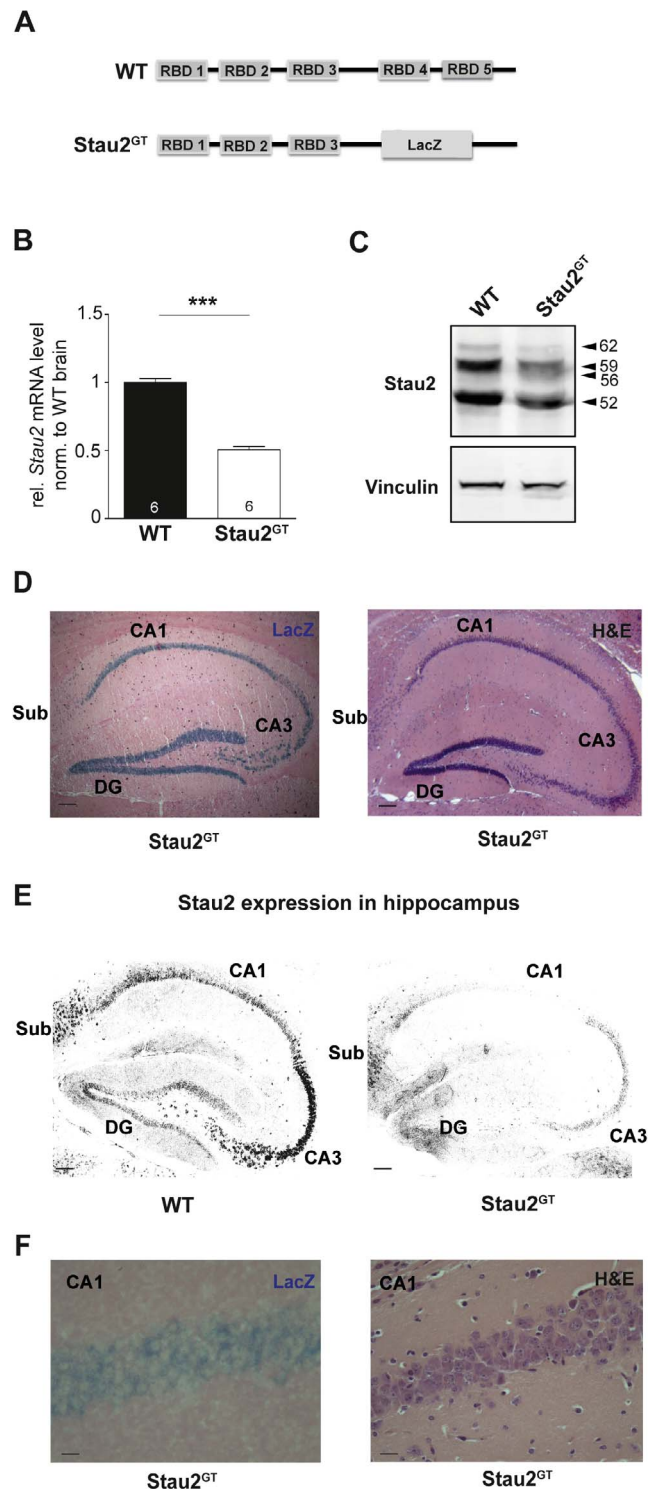


Fig. 1. Gene-trap vector insertion reduces Stau2 expression level in mouse brains. (A) Scheme of the WT Stau2 and the resulting Stau2-β-galactosidase fusion protein upon gene-trap vector insertion in the Stau2 gene locus. (B) Stau2 mRNA levels in WT and Stau2^{GT} mouse brains (n = 6 animals/group). Significance was determined using the Mann-Whitney U-Test. Mean + SEM. ***p < 0.001. (C) Representative Western blot of Stau2 protein in adult WT and Stau2^{GT} brain lysates. Vinculin was used as loading control (n = 3 animals/group). (D) Detection of the β-galactosidase activity encoded by the LacZ gene of the gene-trap vector (left). HE staining of Stau2^{GT} hippocampus (right). Sub: subiculum, DG: dentate gyrus. Scale bar: 200 μm. (E) Immunohistochemistry of Stau2 protein in the hippocampus of WT (left) and Stau2^{GT} (right) brains. Scale bar: 200 μm. (F) Magnification of β-galactosidase activity (left) and HE (right) stained slices of the CA1 region. Scale bar: 50 μm.

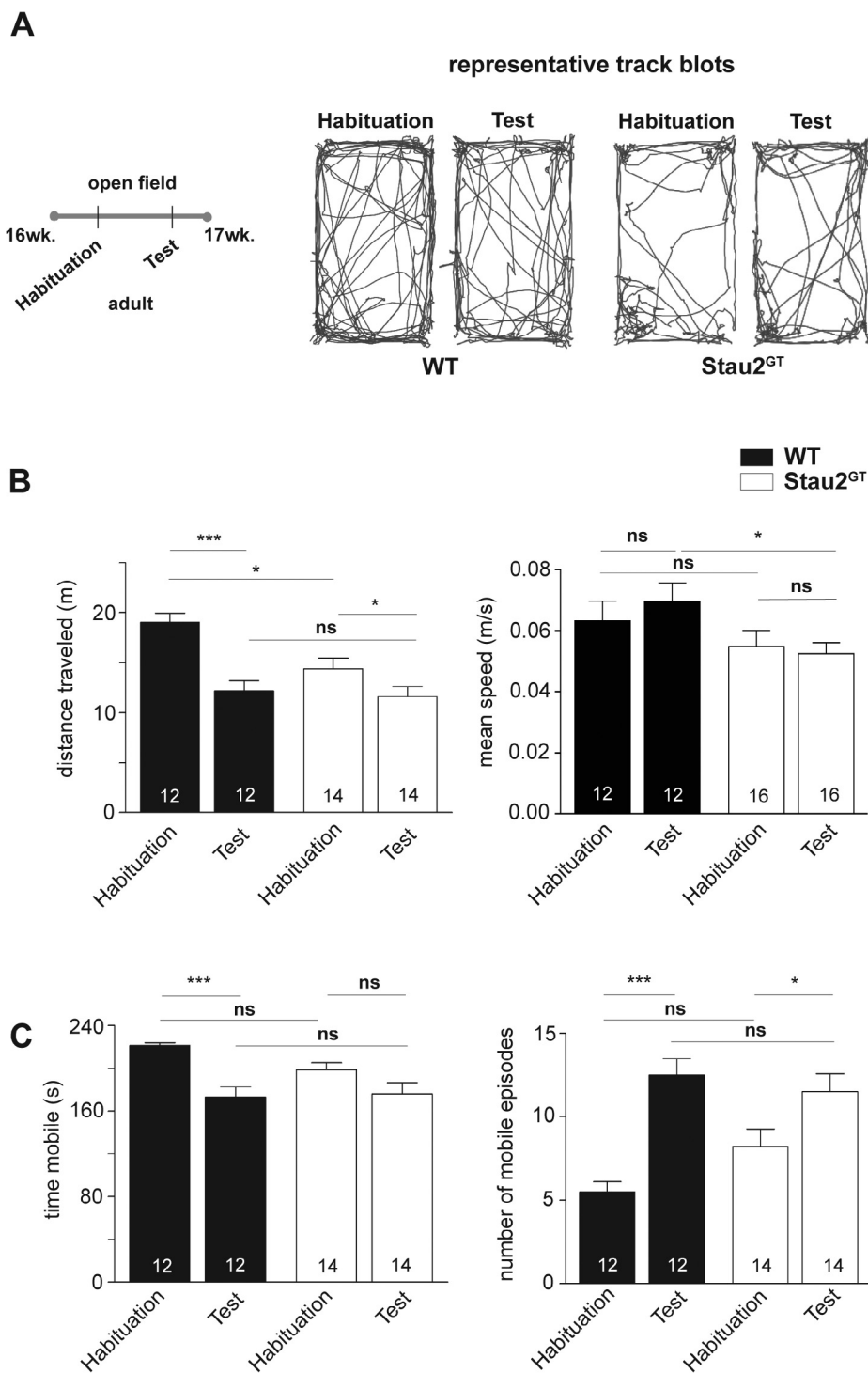


Fig. 2. Adult Stau2^{GT} mice are less active in the open field test. (A) Time line for open field tests of adult mice (left) and representative track blots for WT and Stau2^{GT} animals during habituation and test phases (right). (B and C) Quantification of total distance traveled (B, left), mean speed (B, right), time mobile (C, left) and number of mobile episodes defined as number of transitions from immobile to mobile (C, right) between the two test groups during the habituation and test phase. N numbers are depicted. Significance for all tests was determined using the Wilcoxon rank test for repeated measures or the Mann-Whitney U-Test. Mean + SEM. *p < 0.05, ***p < 0.001, ns = not significant.

food.

Between individual testing phases (see time line in Fig. 2A, 3A and 4A), animals were kept in their familiar housing cages. All mice underwent a standardized four-weeks behavior training starting at the age of 16 weeks. AnyMaze Software (Stoelting Co., USA) and automated activity monitors were used to track the locomotor activity of mice and to analyze the data, if not stated otherwise.

Open field (OF): The first week of behavioral testing of 4-month

Stau2^{GT} mice started with the OF. For habituation, mice were placed in the center of the 80 x 40 cm OF box and were allowed to freely investigate the testing environment for 4 min. With a 24-hour delay (second day), mice were re-tested in the OF for 4 min. Locomotor activity was investigated using AnyMaze Software (Stoelting Co., USA).

Novel object recognition/location assays (NOR/NOL): In the second week of testing, adult Stau2^{GT} mice, NOR/NOL tests were performed in the already familiar open field environment (Leger et al., 2013). Testing

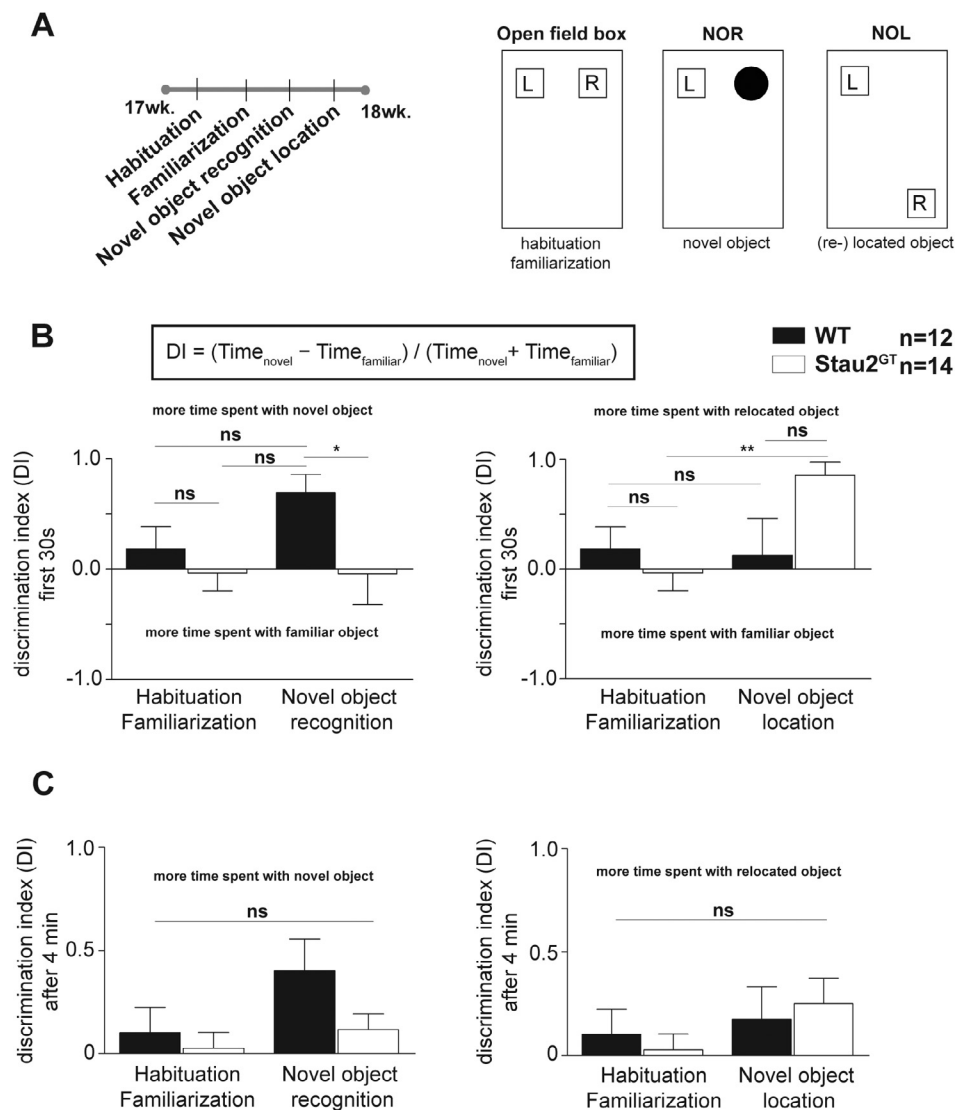


Fig. 3. Downregulation of Stau2 impairs novelty detection in adult male mice. (A) Time line for novel object recognition and location (NOR/L) (left). Scheme for NOR/L test setup with a 24 h delay between individual test phases (right). (B and C) The discrimination indexes for NOR (left) and NOL (right) were calculated with the indicated formula for the first 30 s for each test condition (B) as well as for the entire test phase of 4 min (C) as depicted. N numbers are depicted. Significance was determined using the Mann-Whitney U-Test. Mean + SEM. **p* < 0.05, ***p* < 0.01, ns = not significant.

consisted of habituation and familiarization trials on the first two consecutive days with a 24 h delay, a NOL assay on day three and NOR assay on day four (Vogel-Ciernia & Wood, 2014). As described previously, mice were placed in the center of the OF box and were allowed to investigate the objects for 4 min for each trial. During habituation/familiarization trials, two identical objects (identical in size, shape and color) were placed in the same location of the OF box (Fig. 3A, right panel). For NOR, one of the objects was replaced by a novel one differing in size, shape and color in the same location. NOL was performed on day four with one novel object and one familiar object in the opposite corner of the OF box (Fig. 3A, right panel). Based on the total time spent with the familiar and novel object, the discrimination index (DI) was calculated (Antunes & Biala, 2012). For habituation/familiarization, a discrimination index was calculated comparing the left to the right object, respectively.

Barnes maze: Behavioral experiments were performed as previously described (Barnes, 1979) using the Barnes maze platform adapted to mice. Stau2^{GT} mice were placed in the center of the platform (starting point) for a total test duration of 4 min. The Barnes maze platform (Stoelting Europe, Ireland) consists of a circular surface (diameter 91 cm) with 20 circular holes (diameter 5 cm) around its circumference.

The table surface is brightly lit by overhead lightning (900 lx), under one hole is a “flight box” (diameter 5 cm, depth 6 cm, length of the flight box: 15 cm). For each trial, mice had 240 s to find the target zone and hide in the flight box (Fig. 4B). Recording was stopped either when the mouse entered the flight box or automatically after 240 s. One week before testing, mice were trained in 2 trials per day on 4 consecutive days. The test set up was not changed along the training and test phase. No extra maze cues were used, and all surfaces were carefully cleaned with water after each individual.

2.3. Histology

Whole animal perfusion fixation was performed as described previously (Calzolari et al., 2015). In brief, mice were deeply anaesthetized with CO₂ and intracardially perfused with PBS followed by 4% PFA (pH 7, Roti®-Histofix, Carl Roth, Germany) in PBS (Gage, Kipke, & Shain, 2012; Kohler, Meier, Busato, Neiger-Aeschbacher, & Schatzmann, 1999). Dissected brains were dehydrated in increasing ethanol gradient (50–100% steps) and embedded in paraffin. Sections (approx. 5 μm thickness) were cut on a Reichert Jung Microtome (Leica, Germany). Subsequently, sections were mounted on glass slides (Wenzel,

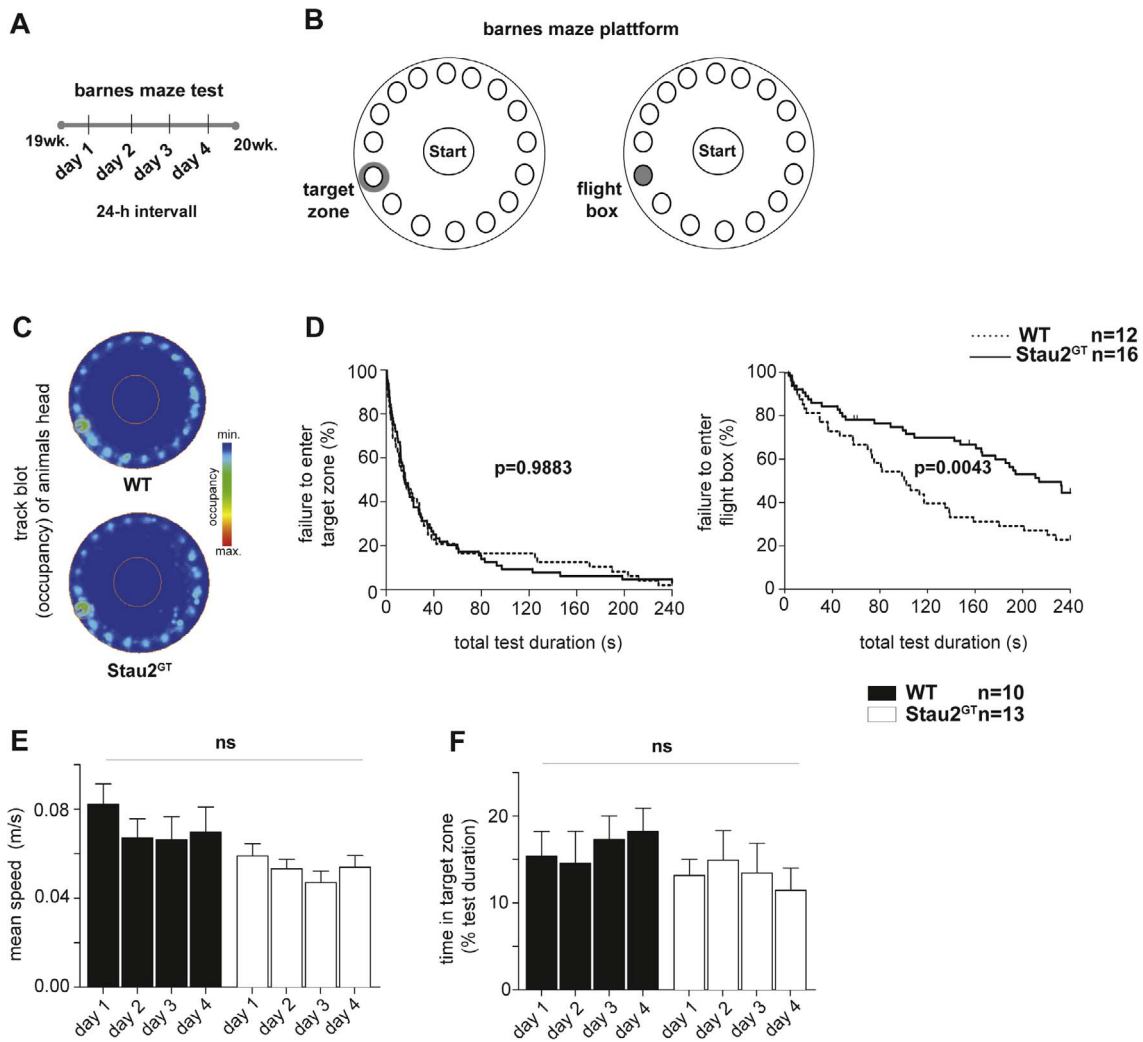


Fig. 4. Stau2 downregulation impacts long-term memory. (A) For long-term memory formation, adult WT and Stau2^{GT} mice were tested for 4 consecutive days with a 24 h delay. (B) Scheme for Barnes maze behavior testing. Mice were located in the “start” arena and had to find a target zone and enter a flight box located below one of the 20 holes. (C) Occupancy blots of WT and Stau2^{GT} mice (all individual blots merged) represented as heat maps. (D) Kaplan-Meier curves for WT and Stau2^{GT} mice for successful entry in the target zone (left) and subsequently in the flight box (right) are depicted. P-values were calculated using log-rank test. (E and F) Mean speed (E) and time in target zone (F) for WT and Stau2^{GT} mice. N numbers are depicted. P-values for repeated observations on day 1 to 4 (WT vs. Stau2^{GT}) were calculated using Friedman’s test followed by Dunn’s multiple comparison. Mean + SEM. ns = not significant.

Germany), deparaffinized in decreasing ethanol gradient (100–50% steps) and rehydrated, stained with hematoxylin, eosin (Sigma-Aldrich, Germany) and mounted with Histomount (Roth, Germany). Pictures were taken with a Leica DM2500 microscope equipped with a DMC2900 CMOS camera (Leica, Germany). Images were processed as previously described (Follwaczny et al., 2017).

Immunohistochemistry: After FA perfusion, dissected brains were post-fixed in 4% PFA in PBS for 12–72 h at 4 °C, then cryoprotected in 30% sucrose in ddH₂O for at least 48–72 h at 4 °C and then embedded in Tissue Tek OCT (Sakura/ Science Services). Brains were cut in 30 μm coronal sections on a Leica cryotome and immunostained as described previously (Calzolari et al., 2015). In brief, slices were washed three times in PBS, blocked in blocking solution (1% (w/v) BSA, 0.5% (v/v) Triton X-100 in PBS) for 45 min at room temperature (RT) and incubated with primary antibody in blocking solution overnight at 4 °C. Selfmade polyclonal rabbit anti-Stau2 antibody (Heraud-Farlow et al., 2013) was diluted 1:200. Sections were washed three times in PBS and incubated for 2 h at RT with secondary donkey anti-rabbit IgG antibody conjugated with Alexa Fluor 488 (Life Technologies, Germany) diluted 1:500 in blocking solution. Nuclei were counterstained by 5 min incubation in 4',6-diamidino-2-phenylindole (DAPI, Carl Roth, Germany) solution. Slices were washed 3 times in PBS and mounted in Fluomount

(Sigma-Aldrich). Confocal microscopy was performed with an inverted Leica SP8 microscope (Leica).

LacZ-staining: To monitor gene-trap cassette insertion, we detected LacZ expression by determining the encoded β-galactosidase activity in slices of Stau2^{GT} mouse brains according to the manufacturers’ manual (LacZ tissue staining kit from InvivoGen, Germany). In brief, brains of PBS perfused animals were carefully removed and stored in cold PBS (4–5 h). Brains were cut with a cryotome in 30 μm sagittal sections and fixed in 2% glutaraldehyde (Sigma-Aldrich). Samples were washed in PBS and stained with staining solution at 37 °C followed by rinsing in PBS. Pictures were taken with a Leica DM2500 microscope equipped with a DMC2900 CMOS camera (Leica).

2.4. Expression analysis

qRT-PCR: RNA was isolated from whole brain samples according to the manufacturers manual using TRIzol (Ambion, Germany). DNA was depleted with the Mini RNeasy kit (Qiagen). For cDNA synthesis from 1 μg RNA Superscript III reverse transcriptase (Invitrogen) was used. For qPCR, HotStart polymerase (New England Biolabs, MA, USA) for cDNA amplification and SYBR-green for detection were used. Target gene signal was normalized to *PPIA* or *18S*, respectively, as reference

genes. Sets of primers used for qRT-PCR: *Stau2* F: 5'-AGTTGCGACTG GAACAGGAC-3' R: 5'-TGGACCACTCCATCCTTTGT-3'; *PPIA* F: 5'-GTC AACCCACCGTGTCTT-3' R: 5'-CTGCTGTCTTTGGAACCTTTG-3'; *18S* F: 5'-GAAACTGCGAATGGCTCATTA-3' R: 5'-CCACAGTTATCCAAGT AGGAGAGGA-3'

Western blot: To analyze expression levels of *Stau2*, brains were homogenized in RIPA buffer (150 mM NaCl, 1.0 vol% NP-40, 0.5% (w/v) sodium deoxycholate, 0.1% (w/v) SDS, 50 mM Tris-HCl pH 8.0, complete protease inhibitor from Roche, Germany). Samples were electrophoresed using 10% SDS-PAGE. For blotting, nitrocellulose (pore size 0.2 μ m) membrane was used. Polyclonal rabbit anti-*Stau2* (Fritzsch et al., 2013; Heraud-Farlow et al., 2013) and polyclonal anti-Vinculin antibody (Santa Cruz, USA). Secondary anti-rabbit antibodies (IRDye CW 800, LICOR, Germany) were used accordingly. Vinculin served as loading control.

2.5. Statistics

All data were first tested for Gaussian distribution. Normally distributed data were either analyzed by Student's *t*-test while data not showing a Gaussian distribution were analyzed by Mann-Whitney U Test or Wilcoxon rank test for repeated measures. For multiple comparisons of paired observations, Friedman's test followed by Dunn's multiple comparison was applied. Grubbs' test (GraphPad, San Diego, CA, USA) was used to determine outliers.

Significant differences between WT and *Stau2*^{GT} mice in Kaplan-Meier curves were calculated by using log-rank test. Data are presented as means + or \pm SEM. Statistics were calculated using the software GraphPad Prism (Version 5, GraphPad, San Diego, CA, USA) or Statview 5.0 (SAS Institute Inc., Cary, NC). $p < 0.05$ was considered statistically significant.

3. Results

3.1. *Stau2* protein expression is reduced in the hippocampus of *Stau2*^{GT} mice

To reduce normal *Stau2* protein expression levels in an unbiased manner, we exploited the gene-trap vector technology (Gossler, Joyner, Rossant, & Skarnes, 1989). The murine *Staufen2* gene was disrupted by inserting a gene-trap construct into the intronic region 7 yielding a C-terminally truncated *Stau2* protein that lacks the RNA-binding domains 4 and 5 as well as the tubulin-binding domain (see Materials and Methods and Fig. 1A). Examining whole brains of adult *Stau2*^{GT} mice (homozygous for the GT insertion), full-length *Stau2* mRNA levels were reduced by 50% (Fig. 1B). The corresponding protein level of all isoforms showed a reduction by 40% compared to WT animals (Fig. 1C). Importantly, we did not detect the *Stau2*- β Gal fusion protein on Western Blots from brain lysates of *Stau2*^{GT} mice (Fig. S1A) suggesting that the resulting fusion protein was not accumulated in the brains. However, we were able to detect β -galactosidase activity in *Stau2*^{GT} brain slices (Fig. 1D, left panel).

The reduced immunoreactivity of *Stau2* in the hippocampus of *Stau2*^{GT} mice (Fig. 1E) paralleled the staining pattern of β -galactosidase encoded by the gene-trap cassette in the pyramidal (CA3-CA1) and granular (DG) cell layers of the hippocampus (Fig. 1D, left). The gene-trap vector was also expressed in thalamic and cortical brain regions (Fig. S1B and C). Thus, the homozygous insertion of the gene-trap cassette into the endogenous *Stau2* locus significantly reduced *Stau2* expression level in the brain. Importantly, reduction of *Stau2* expression did not yield any obvious morphological abnormalities in the adult *Stau2*^{GT} hippocampus (Fig. 1D,F), thalamus or cortex (Fig. S1B and C). In addition, we failed to detect differences in expression of the glutamate receptor 1 (GluR1) and neuronal nitric oxide synthase (nNOS) in the amygdala of *Stau2*^{GT} brains which are misregulated in animals suffering from neurodevelopmental disorders (Fig. S1D and E).

3.2. Adult *Stau2*^{GT} males display reduced activity in the open field

Next, we performed the OF tests with 4-month-old WT and *Stau2*^{GT} mice (Fig. 2A, left panel). Although they did not show a difference in distance traveled during the test phase (Fig. 2A, right panel, B left panel), *Stau2* males showed a reduction in distance traveled during the habituation phase (Fig. 2B left panel). In contrast, younger *Stau2* males showed increased locomotor activity in the open field relative to WT mice (Fig. S2A), while their anxiety-like behavior in the elevated zero maze and social behavior in the three-chamber social preference test were unaffected (Fig. S2B and C). Interestingly, mature adult *Stau2*^{GT} males displayed a significant reduction in mean speed in comparison to WT mice during the test phase (Fig. 2B, right panel) while time mobile was unaffected (Fig. 2C, left panel). Furthermore, a significant increase in the number of mobile episodes was observed indicating that vigilance was not affected (Fig. 2C, right panel). In addition, we detected enhanced nesting skills of mature adult *Stau2*^{GT} males ruling out possible deficits in motor activity (Fig. S3A and B). Finally, we did not detect differences in body weight at either age ruling out the possibility that changes in body weight might affect locomotor activity (Fig. S3C). Together, the open field assays displayed reduced levels of locomotor and explorative activity in adult *Stau2*^{GT} mice.

3.3. Mature adult *Stau2* mice showed impaired novelty detection

Response to novelty and learning are two behavioral parameters that are known to depend on the hippocampus (Kandel et al., 2014; Van Kesteren, Ruiters, Fernández, & Henson, 2012). To address novelty preference in mature adult mice, we performed the novel object location (NOL) assay that requires predominantly hippocampal circuits and the novel object recognition (NOR) assay that relies not only on the hippocampus but also additional brain regions such as the cerebral cortex (Broadbent, Gaskin, Squire, & Clark, 2010; Cohen & Stackman, 2015) (Fig. 3A). Based on the ability of either *Stau2*^{GT} or WT mice to recognize novel objects or novel localization of familiar objects, we calculated their respective discrimination indices (Antunes & Biala, 2012). In the NOR test, the animal is assessed on its ability to recognize a novel object. During the first 30 s of testing, WT mice showed - as expected - an increased ability to discriminate a novel from a familiar object between familiarization and testing phases. In contrast, mature adult male *Stau2*^{GT} animals revealed no changes in the NOR discrimination index when comparing the familiarization and testing phases (Fig. 3B, left panel). After 4 min, *Stau2*^{GT} mice showed comparable attention to the newly introduced object (Fig. 3C, left panel).

In the NOL assay, a familiar object is changed in its position. NOL thereby addresses hippocampus-dependent spatial learning and memory. At the 30 s time point, *Stau2*^{GT} mice showed a stark increase in attention for the relocated familiar object compared to WT mice (Fig. 3B, right panel). Upon 4 min of recording, WT and *Stau2*^{GT} mice showed nearly the same degree of attention for the relocated object (Fig. 3C, right panel). Based on these behavioral experiments, we hypothesize that *Stau2* downregulation leads to an altered response to novelty in mature adult mice.

3.4. *Stau2* deficiency affects long-term memory formation

Based on our results from the NOR/L assays with mature adult animals, it is tempting to speculate that altered novelty preference might affect learning and memory formation. To test whether *Stau2*^{GT} animals had affected memory formation, we performed Barnes maze experiments with mature adult mice (Fig. 4A). This test does not use a strong aversive stimulus or food deprivation that might influence the animal's behavior (Barnes, 1979) and addresses hippocampus-dependent spatial learning. In the Barnes maze, rodents have to find a hidden escape box localized below one out of 20 holes in a circular platform. To quantify mouse activity during the test, we measured total test duration and

distance traveled. Therefore, we defined three general areas on the test platform (1: start zone, 2: target zone and 3: flight box; as depicted in Fig. 4B).

To investigate long-term memory formation, mice were tested once per day (24 h intertrial interval) on four consecutive days (Fig. 4A). Mice were tracked to measure total time and traveled distance. Both mature adult *Stau2^{GT}* and WT mice exploited a similar search strategy, which seemed to be directed towards the flight box with episodes of trial and error (Fig. 4C) and showed no difference in entering the target zone that surrounded the flight box (Fig. 4D, left panel). Furthermore, we did not observe any statistically significant differences between WT and *Stau2^{GT}* animals in either mean speed, time in the target zone (Fig. 4E and F) or total test duration and total distance traveled (Fig. S4A and B). *Stau2^{GT}* mice, however, showed a significantly higher failure to enter the escape hole than WT mice (Fig. 4D, right panel).

In summary, *Stau2^{GT}* mice showed a range of behavioral differences compared to WT mice. Adult *Stau2^{GT}* males displayed reduced locomotor activity and impaired recognition of newly introduced objects but enhanced interest to relocated objects. In addition, we found this impaired novelty detection to lead to higher incidence of *Stau2^{GT}* animals failing to complete the Barnes maze task. This, in turn, suggests that downregulation of *Stau2* impairs selective learning abilities.

4. Discussion

In the last few decades, detailed analysis on various RBPs have revealed their importance for neuronal functions. However, the impact of RBP dysfunction(s) on complex behaviors is sparse and has only been investigated for few RBPs (Bakker et al., 1994; Berger-Sweeney, 2006; Park et al., 2017). In this study, we have generated a novel constitutive *Stau2^{GT}* mouse model that shows a 40% reduction in *Stau2* protein levels, that allowed us to investigate the role of *Stau2* on hippocampus dependent behavior such as spatial learning and novelty response. Our behavior assays demonstrate that *Stau2* deficiency impacts explorative activity, novelty preference and spatial learning.

4.1. *Stau2* knock-down affects explorative activity

It has been shown that *Stau2* is necessary for dendritic spine formation in hippocampal neurons (Goetze et al., 2006; Berger et al., 2017). Furthermore, in *Drosophila* *staufen* has been linked to long-term memory (Dubnau, Chiang, & Grady, 2003). Thus, it is tempting to speculate that *Stau2* also guides neuronal circuit formation in mice. Explorative activity and social behavior rely on specific subregions of the limbic system such as the hippocampus (Inoue et al., 1996; Van Kesteren et al., 2012). Our results indicate that *Stau2* depletion may affect locomotor activity in mice. We hypothesize that the age-dependent effect on explorative activity is mainly driven by changes in neuronal circuit formation within the limbic system during aging. Clearly, these age-dependent effects need to be investigated in further detail before any significant conclusions can be drawn.

4.2. Altered novelty response in adult *Stau2^{GT}* males

To unravel the physiological role of *Stau2* in mice, we performed a series of behavioral assays to address spatial memory and novelty preference. Mice have a natural drive for novelty, so in the NOR test, WT mice spend more time with a newly introduced object compared to a familiar object. Thus, deficits in novelty detection would change this behavior towards an equal interest for both objects. In particular, the early phase of NOR is thought to be dependent on extra-hippocampal regions such as the perirhinal cortex (Antunes & Biala, 2012; Vogel-Ciernia & Wood, 2014), although with increasing sampling time memory is further strengthened by the involvement of the hippocampus. Our results revealed that *Stau2^{GT}* males showed no preference for the newly introduced object in contrast to WT animals. Surprisingly,

in the NOL assay we observed an increased preference for the relocated object. Importantly, according to hippocampus lesion experiments in rats NOR depends primarily on the hippocampus, but requires other brain regions such as the cerebral cortex in addition to hippocampus, while NOL depends primarily on the hippocampus (Broadbent, Squire, & Clark, 2004). It is generally believed that for object recognition, the hippocampus, the perirhinal and medial prefrontal cortex are essential brain structures (Warburton & Brown, 2015). In this context, the CA1 region receives inputs from the perirhinal cortex and the CA3 region and projects to the entorhinal cortex. Importantly, mice depleted of NMDA receptor subunit 1 in CA1 neurons show impaired NOR (Rampon et al., 2000). In this context, it is worth mentioning that two known physiological mRNA targets of *Stau2*, *Rgs2* and *Rgs4* (Heraud-Farlow et al., 2013) act in the adrenergic receptor pathway to modulate NMDA receptor function (Liu et al., 2006).

According to our immunohistochemistry results, the *Stau2^{GT}* CA1, CA3 and dentate gyrus (DG) regions show a prominent downregulation of *Stau2* expression. In our NOR assays, *Stau2^{GT}* mice revealed no preference between familiar or novel objects, indicating that adult *Stau2^{GT}* males failed to discriminate between them. We therefore hypothesize that altered synaptic transmission in CA1 neurons is responsible for the impaired NOR, possibly influenced by *Rgs4*. For NOL test paradigms, neurotoxic lesion experiments have shown that the DG-CA3 connection is essential for spatial novelty detection while CA1 lesioned mice showed only mild impairment of novelty detection (Lee, Hunsaker, & Kesner, 2005). Interestingly, adult *Stau2^{GT}* mice revealed enhanced preference for the relocated familiar object compared to control animals. We hypothesize that altered synaptic transmission between subregions responsible for spatial navigation and novelty detection, such as the DG-CA3 axis, results in enhanced spatial novelty detection in *Stau2^{GT}* mice.

4.3. Adult *Stau2^{GT}* males reveal impaired spatial learning

To investigate the effect of *Stau2* downregulation on hippocampus-dependent spatial learning, we performed Barnes maze tests. Our data suggests that adult *Stau2^{GT}* males were as efficient in finding the target area as WT controls. This is in line with the NOL results where mutant males revealed enhanced spatial novelty detection. However, we observed that a significant higher number of *Stau2^{GT}* animals fail to enter the flight box. Together with the NOR results we therefore speculate that *Stau2* downregulation leads to defects in discrimination in the open area of the Barnes maze platform and the flight box as novel spatial object. This, in turn, would cause a higher incidence of mutant male mice to fail.

In summary, our results demonstrate that *Stau2* might have (at least) two distinct roles for novelty detection addressing different hippocampal and extrahippocampal brain regions. Novel object recognition was impaired in male mice while they showed enhanced discrimination in relocation tasks. This, in turn, affected spatial learning and deficits in discriminating different spatial contexts in Barnes maze tests. We speculate that altered synaptic transmission in the hippocampal trisynaptic circuitry is responsible for the observed phenotype in *Stau2^{GT}* mice. In the course of this study, a conditional *Stau2* knock-down rat model in pyramidal neurons primarily displayed deficits in spatial learning (Berger et al., 2017). Our *Stau2^{GT}* mice displaying constitutive *Stau2* depletion enabled us to unravel another important behavioral deficits, namely altered novelty preference. We therefore speculate that *Stau2* may play a role in novelty detection. Future investigations are clearly necessary to unravel the molecular role of *Stau2* in synaptic transmission between different hippocampal subregions and connecting cortical areas.

Competing interests

The authors declare no competing or financial interests.

Author contributions

G.K. and S.T. generated gene-trap Stau2 mice. V.B. and S.T. designed the experiments regarding young adult mice. B.P., R.S. and M.A.K. designed all experiments regarding adult mice. A.D., V.B., A.S.-K., R.S., and B.P. performed experiments. A.D., R.S., B.P., V.B., S.T. and M.A.K. interpreted results. R.S., B.P. and M.A.K. wrote the manuscript. All authors read and approved the final version of the manuscript.

Acknowledgements

We thank the Wadsworth Center Transgenic and Gene Knockout and Mouse Behavioral Phenotype Analysis Cores. We thank Christin Illig, Jessica Olberz and Alexandra Hörmann for excellent technical support, Dr. Michael Doyle for initial experiments and Drs. Inmaculada Segura, Sandra Fernandez Moya, Leda Dimou and Carsten Wotjak for critical discussions. We also thank the BMC Imaging Core facility. The study was funded by the Friedrich-Baur-Stiftung (02/14 and 02/16, LMU Munich to B.P.), the Förderprogramm für Forschung und Lehre – FöFoLe M.D. program of the LMU Munich (12/2014 to A.D.), the Boehringer Ingelheim Fonds (to R.S.), the German Research Foundation (SPP1738 DFG, KI 502/2-1 and KI502/3-1, FOR2333) and by LMUexcellent (all to M.A.K.). The behavioral studies on young adult Stau2^{GT} mice were supported by the National Institute of Neurological Disorders and Stroke (R01NS074047 to ST), the National Institute of Mental Health (R21MH10368 to V.B) and the Wadsworth Center.

Appendix A. Supplementary material

Supplementary data associated with this article can be found, in the online version, at <http://dx.doi.org/10.1016/j.nlm.2018.02.027>.

References

- Antar, L. N., Afroz, R., Dichtenberg, J. B., Carroll, R. C., & Bassell, G. J. (2004). Metabotropic glutamate receptor activation regulates fragile x mental retardation protein and FMR1 mRNA localization differentially in dendrites and at synapses. *The Journal of Neuroscience: The Official Journal of the Society for Neuroscience*, *24*(11), 2648–2655. <http://dx.doi.org/10.1523/JNEUROSCI.0099-04.2004>.
- Antunes, M., & Biala, G. (2012). The novel object recognition memory: Neurobiology, test procedure, and its modifications. *Cognitive Processing*, *13*(2), 93–110. <http://dx.doi.org/10.1007/s10339-011-0430-z>.
- Bakker, C., Verheij, C., Willemsen, R., van der Helm, R., Oerlemans, F., Vermey, M., ... Willems, P. (1994). Fmr1 knockout mice: A model to study fragile X mental retardation. *Cell*, *78*(1), 23–33. [http://dx.doi.org/10.1016/0092-8674\(94\)90569-X](http://dx.doi.org/10.1016/0092-8674(94)90569-X).
- Barnes, C. A. (1979). Memory deficits associated with senescence: A neurophysiological and behavioral study in the rat. *Journal of Comparative and Physiological Psychology*, *93*(1), 74–104. <http://dx.doi.org/10.1037/h0077579>.
- Bear, M. F., Huber, K. M., & Warren, S. T. (2004). The mGluR1 theory of fragile X mental retardation. *Trends in Neurosciences*. <http://dx.doi.org/10.1016/j.tins.2004.04.009>.
- Berger-Sweeney, J. (2006). Reduced extinction of hippocampal-dependent memories in CPEB knockout mice. *Learning & Memory*, *13*(1), 4–7. <http://dx.doi.org/10.1101/lm.73706>.
- Berger, S. M., Fernández-lamo, I., Schöning, K., Moya, S. M. F., Ehses, J., Schieweck, R., ... Bartsch, D. (2017). Forebrain-specific, conditional silencing of Stauf2 alters synaptic plasticity, learning, and memory in rats. *Genome Biology*, *18*(222), 1–13. <http://dx.doi.org/10.1186/s13059-017-1350-8>.
- Broadbent, N. J., Gaskin, S., Squire, L. R., & Clark, R. E. (2010). Object recognition memory and the rodent hippocampus. *Learning & Memory (Cold Spring Harbor, New York)*, *17*(1), 5–11. <http://dx.doi.org/10.1101/lm.1650110>.
- Broadbent, N. J., Squire, L. R., & Clark, R. E. (2004). Spatial memory, recognition memory, and the hippocampus. *Proceedings of the National Academy of Sciences*, *101*(40), 14515–14520. <http://dx.doi.org/10.1073/pnas.0406344101>.
- Calzolari, F., Michel, J., Baumgart, E. V., Theis, F., Götz, M., & Ninkovic, J. (2015). Fast clonal expansion and limited neural stem cell self-renewal in the adult subependymal zone. *Nature Neuroscience*, *18*(4), 490–492. <http://dx.doi.org/10.1038/nn.3963>.
- Cohen, S. J., & Stackman, R. W. (2015). Assessing rodent hippocampal involvement in the novel object recognition task. A review. *Behavioural Brain Research*, *285*, 105–117. <http://dx.doi.org/10.1016/j.bbr.2014.08.002>.
- Darnell, J. C., & Klann, E. (2013). The translation of translational control by FMRP: Therapeutic targets for FXS. *Nature Neuroscience*, *16*(11), 1530–1536. <http://dx.doi.org/10.1038/nn.3379>.
- Doyle, M., & Kiebler, M. A. (2011). Mechanisms of dendritic mRNA transport and its role in synaptic tagging. *The EMBO Journal*, *30*(17), 3540–3552. <http://dx.doi.org/10.1038/emboj.2011.278>.
- Dubnau, J., Chiang, A., & Grady, L. (2003). The stauf/pumilio pathway is involved in *Drosophila* long-term memory. *Current Biology*, *13*(3), 286–296.
- Follwaczny, P., Schieweck, R., Riedemann, T., Demleitner, A., Straub, T., Klemm, A. H., ... Kiebler, M. A. (2017). Pumilio2-deficient mice show a predisposition for epilepsy. *Disease Models & Mechanisms*, *10*, 1333–1342. <http://dx.doi.org/10.1242/dmm.029678>.
- Fritzsche, R., Karra, D., Bennett, K. L., Ang, F. Y., Heraud-Farlow, J. E., Tolino, M., ... Kiebler, M. A. (2013). Interactome of two diverse RNA granules links mRNA localization to translational repression in neurons. *Cell Reports*, *5*(6), 1749–1762. <http://dx.doi.org/10.1016/j.celrep.2013.11.023>.
- Gage, G. J., Kipke, D. R., & Shain, W. (2012). Whole animal perfusion fixation for rodents. *Journal of Visualized Experiments: JoVE*, *65*, 1–9. <http://dx.doi.org/10.3791/3564>.
- Goetze, B., Tuebing, F., Xie, Y., Dorostkar, M. M., Thomas, S., Pehl, U., ... Kiebler, M. A. (2006). The brain-specific double-stranded RNA-binding protein Stauf2 is required for dendritic spine morphogenesis. *The Journal of Cell Biology*, *172*(2), 221–231. <http://dx.doi.org/10.1083/jcb.200509035>.
- Gossler, A., Joyner, A., Rossant, J., & Skarnes, W. (1989). Mouse embryonic stem cells and reporter constructs to detect developmentally regulated genes. *Science*, *244*(4903), 463–465. <http://dx.doi.org/10.1126/science.2497519>.
- Govindarajan, A., Kelleher, R. J., & Tonegawa, S. (2006). A clustered plasticity model of long-term memory engrams. *Nature Reviews Neuroscience*, *7*(7), 575–583. <http://dx.doi.org/10.1038/nrn1937>.
- Heraud-Farlow, J. E., & Kiebler, M. A. (2014). The multifunctional Stauf proteins: Conserved roles from neurogenesis to synaptic plasticity. *Trends in Neurosciences*, *37*(9), 470–479. <http://dx.doi.org/10.1016/j.tins.2014.05.009>.
- Heraud-Farlow, J. E., Sharangdhar, T., Li, X., Pfeifer, P., Tauber, S., Orozco, D., ... Kiebler, M. A. (2013). Stauf2 regulates neuronal target RNAs. *Cell Reports*, *5*(6), 1511–1518. <http://dx.doi.org/10.1016/j.celrep.2013.11.039>.
- Holt, C. E., & Bullock, S. L. (2009). Subcellular mRNA localization in animal cells and why it matters. *Science (New York, New York)*, *326*(5957), 1212–1216. <http://dx.doi.org/10.1126/science.1176488>.
- Hutten, S., Sharangdhar, T., & Kiebler, M. (2014). Unmasking the messenger. *RNA Biology*, *11*(8), 992–997. <http://dx.doi.org/10.4161/rna.32091>.
- Inoue, I., Yanai, K., Kitamura, D., Taniuchi, I., Kobayashi, T., Niimura, K., ... Watanabe, T. (1996). Impaired locomotor activity and exploratory behavior in mice lacking histamine H1 receptors. *Proceedings of the National Academy of Sciences of the United States of America*, *93*(23), 13316–13320. <http://dx.doi.org/10.1073/pnas.93.23.13316>.
- Jung, H., Gkogkas, C. G., Sonenberg, N., & Holt, C. E. (2014). Remote control of gene function by local translation. *Cell*, *157*(1), 26–40. <http://dx.doi.org/10.1016/j.cell.2014.03.005>.
- Kandel, E. R., Dudai, Y., & Mayford, M. R. (2014). The molecular and systems biology of memory. *Cell*, *157*(1), 163–186. <http://dx.doi.org/10.1016/j.cell.2014.03.001>.
- Kiebler, M. A., & Bassell, G. J. (2006). Neuronal RNA granules: Movers and makers. *Neuron*, *51*(6), 685–690. <http://dx.doi.org/10.1016/j.neuron.2006.08.021>.
- Kohler, I., Meier, R., Busato, A., Neiger-Aeschbacher, G., & Schatzmann, U. (1999). Is carbon dioxide (CO₂) a useful short acting anaesthetic for small laboratory animals? *Laboratory Animals*, *33*(2), 155–161. <http://dx.doi.org/10.1258/002367799780578390>.
- Kusek, G., Campbell, M., Doyle, F., Tenenbaum, S. A., Kiebler, M., & Temple, S. (2012). Asymmetric segregation of the double-stranded RNA binding protein Stauf2 during mammalian neural stem cell divisions promotes lineage progression. *Cell Stem Cell*, *11*(4), 505–516. <http://dx.doi.org/10.1016/j.stem.2012.06.006>.
- Lebeau, G., Miller, L. C., Tartas, M., McAdam, R., Laplante, I., Badaeu, F., ... Lacaille, J.-C. (2011). Stauf 2 regulates mGluR long-term depression and Map1b mRNA distribution in hippocampal neurons. *Learning & Memory (Cold Spring Harbor, New York)*, *18*(5), 314–326. <http://dx.doi.org/10.1101/lm.2100611>.
- Lee, I., Hunsaker, M. R., & Kesner, R. P. (2005). The role of hippocampal subregions in detecting spatial novelty. *Behavioral Neuroscience*, *119*(1), 145–153. <http://dx.doi.org/10.1037/0735-7044.119.1.145>.
- Leger, M., Quiedeville, A., Bouet, V., Haelewyn, B., Boulouard, M., Schumann-Bard, P., & Freret, T. (2013). Object recognition test in mice. *Nature Protocols*, *8*(12), 2531–2537. <http://dx.doi.org/10.1038/nprot.2013.155>.
- Liu, W., Yuen, E. Y., Allen, P. B., Feng, J., Greengard, P., & Yan, Z. (2006). Adrenergic modulation of NMDA receptors in prefrontal cortex is differentially regulated by RGS proteins and spinophilin. *PNAS*, *103*(48), 18338–18343.
- Nakiely, S., Fischer, U., Michael, W. M., & Dreyfuss, G. (1997). *RNA Transport. Annual Review of Neuroscience*, *20*, 269–301. <http://dx.doi.org/10.1146/annurev.neuro.20.1.269>.
- Paoletti, P., Bellone, C., & Zhou, Q. (2013). NMDA receptor subunit diversity: Impact on receptor properties, synaptic plasticity and disease. *Nature Reviews Neuroscience*, *14*(6), 383–400. <http://dx.doi.org/10.1038/nrn3504>.
- Park, A. J., Havekes, R., Fu, X., Hansen, R., Tudor, J. C., Peixoto, L., ... Abel, T. (2017). Learning induces the translin/trax RNase complex to express activin receptors for persistent memory. *eLife*, *6*, e27872. <http://dx.doi.org/10.7554/eLife.27872>.
- Rampon, C., Tang, Y. P., Goodhouse, J., Shimizu, E., Kyin, M., & Tsien, J. Z. (2000). Enrichment induces structural changes and recovery from nonspatial memory deficits in CA1 NMDAR1-knockout mice. *Nature Neuroscience*, *3*(3), 238–244. <http://dx.doi.org/10.1038/72945>.
- Sharangdhar, T., Sugimoto, Y., Heraud-Farlow, J., Fernández-Moya, S. M., Ehses, J., Ruiz de los Mozos, I., ... Kiebler, M. A. (2017). A retained intron in the 3'-UTR of *Calm3* mRNA mediates its Stauf2- and activity-dependent localization to neuronal dendrites. *EMBO Reports*, *18*(10), e201744334. <http://dx.doi.org/10.15252/embr.201744334>.
- Stryke, D., Kawamoto, M., Huang, C. C., Johns, S. J., King, L. A., Harper, C. A., ... Ferrin, T. E. (2003). BayGenomics: A resource of insertional mutations in mouse embryonic

- stem cells. Retrieved from *Nucleic Acids Research*, 31(1), 278–281. <<http://www.ncbi.nlm.nih.gov/pubmed/12520002>>.
- Van Kesteren, M. T. R., Ruiters, D. J., Fernández, G., & Henson, R. N. (2012). How schema and novelty augment memory formation. *Trends in Neurosciences*, 35(4), 211–219. <http://dx.doi.org/10.1016/j.tins.2012.02.001>.
- Vessey, J. P., Amadei, G., Burns, S. E., Kiebler, M. A., Kaplan, D. R., & Miller, F. D. (2012). An asymmetrically localized Staufen2-dependent RNA complex regulates maintenance of mammalian neural stem cells. *Cell Stem Cell*, 11(4), 517–528. <http://dx.doi.org/10.1016/j.stem.2012.06.010>.
- Vogel-Ciernia, A., & Wood, M. A. (2014). Examining object location and object recognition memory in mice. *Current Protocols in Neuroscience*, 69(8), <http://dx.doi.org/10.1002/0471142301.ns0831s69> 8.31.1-17.
- Warburton, E. C., & Brown, M. W. (2015). Neural circuitry for rat recognition memory. *Behavioural Brain Research*, 285, 131–139. <http://dx.doi.org/10.1016/j.bbr.2014.09.050>.

Publication III: Altered Glutamate Receptor Ionotropic Delta Subunit 2 Expression in Stau2-Deficient Cerebellar Purkinje Cells in the Adult Brain

This section contains the study published in *International Journal of Molecular Sciences* (2019) entitled **Altered Glutamate Receptor Ionotropic Delta Subunit 2 Expression in Stau2-Deficient Cerebellar Purkinje Cells in the Adult Brain** by

Helena F. Pernice, **Rico Schieweck**, Mehrnoosh Jafari, Tobias Straub, Martin Bilban, Michael A. Kiebler[‡] and Bastian Popper[‡]

[‡] corresponding authors

Author contribution to this publication

Bastian Popper, Rico Schieweck and Michael A. Kiebler designed the study. Helena F. Pernice and Mehrnoosh Jafari performed and analyzed immunostainings (Figs. 2 and 4). Rico Schieweck performed expression analysis (Fig. 1). Tobias Straub and Martin Bilban performed and analyzed microarray experiments (related to Fig. 1). Helena Pernice, Rico Schieweck, Bastian Popper and Michael A. Kiebler wrote and revised the manuscript.

(Rico Schieweck)

(Prof. Dr. Michael A. Kiebler)

(Prof. Dr. Heinrich Leonhardt)



Article

Altered Glutamate Receptor Iontropic Delta Subunit 2 Expression in Stau2-Deficient Cerebellar Purkinje Cells in the Adult Brain

Helena F. Pernice ¹, Rico Schieweck ¹, Mehrnoosh Jafari ², Tobias Straub ³, Martin Bilban ⁴,
Michael A. Kiebler ^{1,*} and Bastian Popper ^{1,5,*}

¹ Biomedical Center (BMC), Department for Cell Biology & Anatomy, Medical Faculty, Ludwig-Maximilians-University, 82152 Martinsried, Germany; Franziska.Pernice@med.uni-muenchen.de (H.F.P.); Rico.Schieweck@med.uni-muenchen.de (R.S.)

² Institute of Clinical Neuroimmunology, University Hospital and Biomedical Center, Ludwig-Maximilians-University, 81377 Munich, Germany; mehrnoosh.jafari@med.uni-muenchen.de

³ Biomedical Center (BMC), Core Facility Bioinformatics, Medical Faculty, Ludwig-Maximilians-University, 82152 Martinsried, Germany; tstraub@bmc.med.lmu.de

⁴ Department of Laboratory Medicine and Core Facility Genomics, Medical University of Vienna, 1090 Vienna, Austria; martin.bilban@meduniwien.ac.at

⁵ Biomedical Center (BMC), Core Facility Animal Models, Medical Faculty, Ludwig-Maximilians-University, 82152 Martinsried, Germany

* Correspondence: mkiebler@lmu.de (M.A.K.); bastian.popper@med.uni-muenchen.de (B.P.); Tel.: +49-89-2180-71996 (B.P.)

Received: 6 March 2019; Accepted: 8 April 2019; Published: 11 April 2019



Abstract: Staufen2 (Stau2) is an RNA-binding protein that is involved in dendritic spine morphogenesis and function. Several studies have recently investigated the role of Stau2 in the regulation of its neuronal target mRNAs, with particular focus on the hippocampus. Here, we provide evidence for Stau2 expression and function in cerebellar Purkinje cells. We show that Stau2 downregulation (Stau2^{GT}) led to an increase of glutamate receptor ionotropic delta subunit 2 (GluD2) in Purkinje cells when animals performed physical activity by voluntary wheel running compared with the age-matched wildtype (WT) mice (C57Bl/6J). Furthermore, Stau2^{GT} mice showed lower performance in motor coordination assays but enhanced motor learning abilities than did WT mice, concomitantly with an increase in dendritic GluD2 expression. Together, our results suggest the novel role of Stau2 in Purkinje cell synaptogenesis in the mouse cerebellum.

Keywords: staufen2; synaptogenesis; cerebellum; purkinje cells; GluD2

1. Introduction

Research over the last few decades has shown the importance of posttranscriptional regulation mechanisms in neuronal function, particularly for synaptogenesis [1]. Key players for these processes are RNA-binding proteins (RBPs) [2,3]. By binding to their target mRNAs, RBPs control different steps of the RNA life cycle, such as splicing, RNA export and localization, translation control and degradation [1] underlining their importance for neuronal functioning. Depletion of RBPs can cause severe neuropathologies, such as mental retardation or epilepsy, as well as motor defect disorders, such as amyotrophic lateral sclerosis (ALS) [4–7]. Staufen2 (Stau2) is an RBP involved in different regulatory networks ranging from embryonic neurogenesis to synaptic transmission and morphogenesis in mature hippocampal neurons [8]. Recent studies of Stau2-deficient mice and rats have shown that Stau2 is important for learning and memory formation [9,10]. In this study, we took advantage of

the previously reported *Stau2* gene trap mouse model (*Stau2*^{GT}), which shows a brain-wide *Stau2* downregulation of about 40% [9]. Transcriptome-wide analysis of differentially expressed RNA in the *Stau2*^{GT} mouse brain revealed an upregulation of *glutamate receptor ionotropic delta subunit 2* (*Grid2*) and *cerebellin1* (*Cbln1*) mRNAs when compared with wildtype (WT) mice during extensive learning and motor activity. These mRNAs code for glutamate receptor ionotropic delta subunit 2 (GluD2) and Cbln1, two components of the cerebellar synaptic apparatus [11,12]. GluD2 and Cbln1 are believed to connect the synapses of granule cell parallel fibers and Purkinje cell dendrites. While GluD2 is expressed in the postsynaptic membrane of Purkinje cells, Cbln1 is secreted from the presynaptic compartment, binds to presynaptic neurexins and postsynaptic GluD2, and therefore connects pre-synapses deriving from parallel fibers of granule cells with post-synapses of Purkinje cells [13,14]. The consolidation of synapses through the interaction of these molecules has been shown to be the basis of synaptic transmission in Purkinje cells. Furthermore, Cbln1 and GluD2 play relevant roles in motor coordination and learning, while deficits lead to motor impairment, such as ataxia in mouse models [15–17]. Interestingly, naive *Stau2*^{GT} showed reduced motor coordination in a rotor rod assay compared with age-matched WT animals. Strikingly, mutant animals displayed enhanced motor learning skills during repeated training. These effects were concomitant with an increased GluD2 expression, suggesting improved synaptic transmission in the cerebellum. Together, our results suggest that *Stau2* plays a role in motor activity-induced synaptogenesis in the mouse cerebellum.

2. Results

2.1. Adult *Stau2*^{GT} Mice Show an Upregulation of *Cbln1* and *GluD2* mRNA during Behavior Testing

To identify genes that are *Stau2*-dependently affected during training, 4-month-old *Stau2*^{GT} mice and age-matched WT controls were exposed to a battery of behavioral tests for 4 consecutive weeks, as previously described [8] (Figure 1A). Subsequently, the mouse brains were dissected, and microarray analysis was performed. Interestingly, compared with the WT mice, we detected a significant 15% increase in the *Stau2*^{GT} mice for *Cbln1* and *Grid2* mRNA expression in brain lysates, which code for cerebellar proteins involved in synaptogenesis [12,18]. In naive mice, in contrast, there was no apparent changes in the expression of these mRNAs detectable (Figure 1B). To validate the upregulation of *Cbln1* and *Grid2* mRNAs, qRT-PCR was performed on *Stau2*^{GT} and control brain lysates. Here, mRNA levels of *Cbln1* and *Grid2* showed a significant increase in the adult *Stau2*^{GT} mice that underwent behavioral experimentation (Figure 1C,D).

2.2. Reduced *Stau2* Expression in Cerebellar Purkinje Cells of Adult *Stau2*^{GT} Mice

The increase in expression of the cerebellar genes *Cbln1* and *Grid2* prompted us to examine *Stau2* expression in the mouse cerebellum. First, we performed immunostainings against *Stau2* in frontal cerebellar sections in adult WT mice. Co-staining for calbindin was used to clearly distinguish Purkinje cells from NeuN-expressing cells. *Stau2* staining was prominent in the somatic area of the Purkinje cell layer (StP) and the stratum moleculare (StM) (Figure 2A). To evaluate *Stau2* downregulation in the cerebellum of transgenic mice, we performed immunostainings against *Stau2* in cerebellar sections of *Stau2*^{GT} mice. Quantification of *Stau2* protein intensity in Purkinje cells showed a 50% reduction in adult *Stau2*^{GT} animals compared with the controls (Figure 2B). Furthermore, staining for the β -galactosidase activity encoded by the gene trap construct in *Stau2*^{GT} mice [9] revealed a strong expression in Purkinje cells, indicating a knockdown preferentially in the stratum purkinjense (Figure 2C) underlining our previous results (Figure 2B).

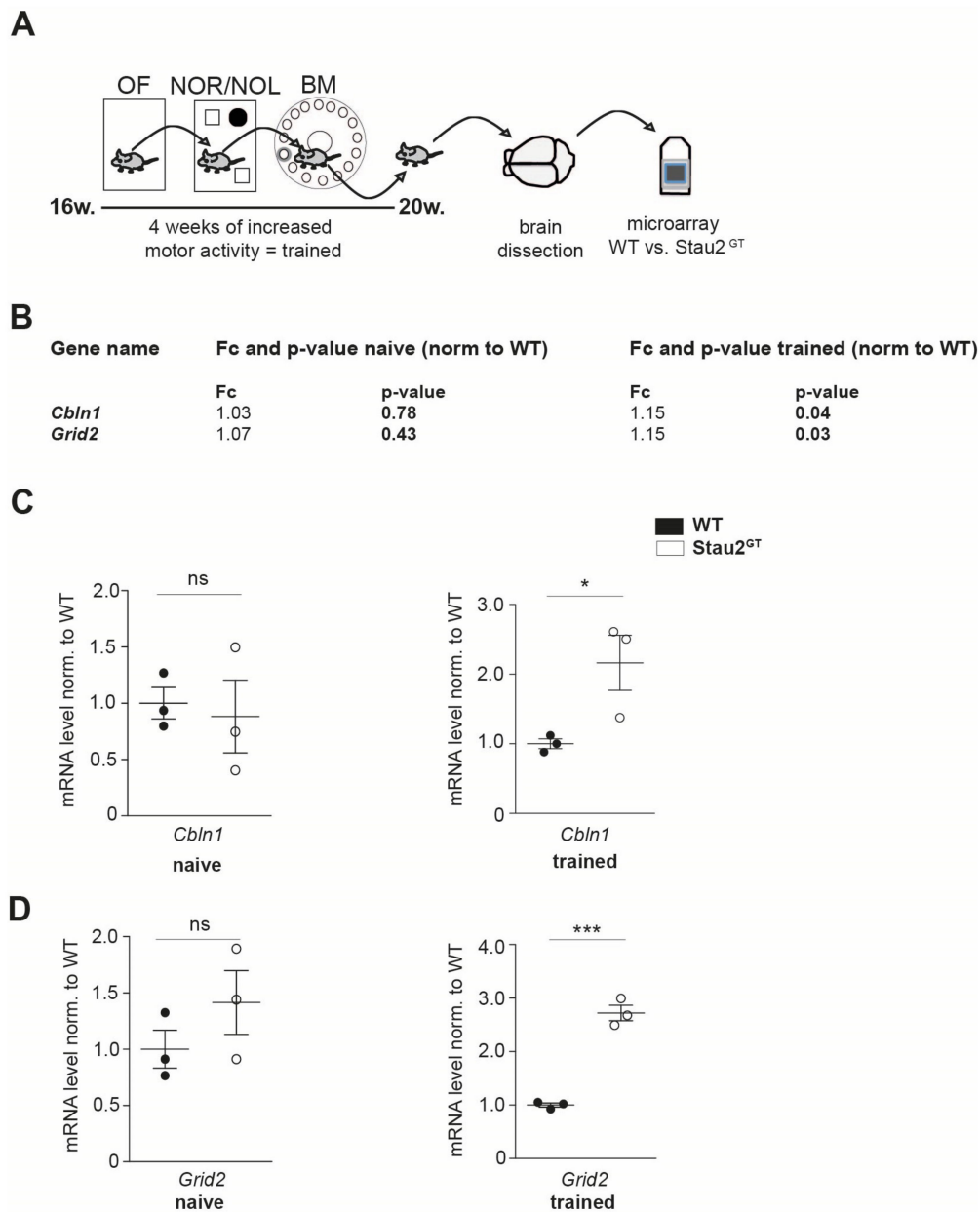


Figure 1. Adult Staufen2 knock-down (Stau2^{GT}) mice show an upregulation of *cerebellin1* (*Cbln1*) and *glutamate receptor ionotropic delta subunit 2* (*Grid2*) mRNA during behavioral tests. **(A)** Schematic representation of the experimental approach followed by the behavioral tests. Here, 4-month-old Stau2^{GT} and wildtype (WT) mice were exposed to a battery of behavioral tests (OF = open field test, NOR/NOL = novel object recognition/location test, and BM = Barnes maze), enabling physical trainings (= trained). Subsequently, the mouse brains were dissected, and microarray analysis was performed. **(B)** Microarray analysis of brain lysates of 5-month-old Stau2^{GT} and WT mice before and after training conditions. **(C,D)** Quantification of *Cbln1* (C) and *Grid2* (D) mRNA levels before (naive) and after behavioral tests (= trained) measured by qRT-PCR. $N = 3$ animals (**B–D**). Statistics: Students t-test. Mean + SEM, * $p < 0.05$, *** $p < 0.001$; ns = not significant (**B–D**).

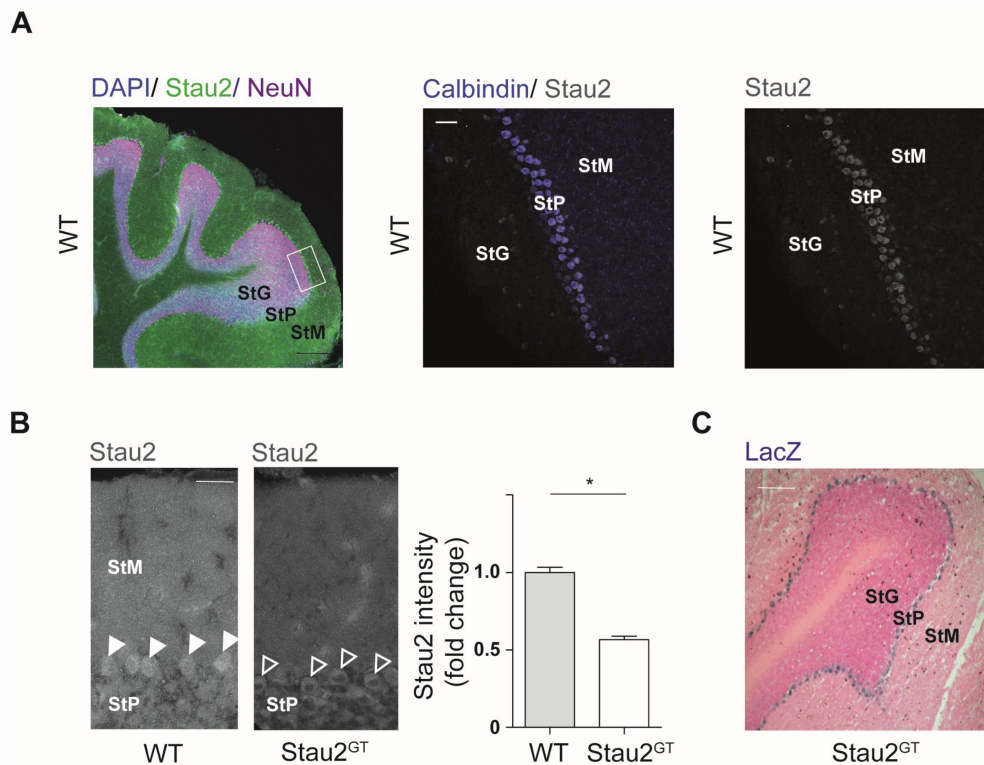


Figure 2. Stau2 expression in cerebellar Purkinje cells is reduced in adult Stau2^{GT} mice. (A) Representative confocal images of immunohistofluorescence staining for Stau2 (neuronal markers: NeuN and calbindin; nuclear marker: 4',6-diamidino-2-phenylindole (DAPI)) on frontal sections of cerebelli taken from 5-month-old WT mice. Scale bars = 200 μ m (left), 50 μ m (middle, right). (B) Representative confocal images of immunohistofluorescence staining against Stau2 on frontal sections of the cerebellum of 5-month-old Stau2^{GT} and WT mice (left) and relative Stau2 intensity (right). Scale bar = 20 μ m. (C) Light microscopic image of LacZ staining in a representative frontal section of Stau2^{GT} mouse cerebellum. Scale bar = 200 μ m. $N = 3$ (B). Statistics: Students *t*-test. Mean + SEM, * $p < 0.05$. StG, stratum granulare; StP, stratum pyramidale; and StM, stratum moleculare. Arrows point to Purkinje cell bodies (B).

2.3. Decreased Motor Coordination Abilities but Increased Motor Learning Capacity in Adult Male Stau2^{GT} Mice

The fact that Stau2 was found to be expressed in Purkinje cells and that its downregulation affected the gene expression of cerebellar proteins during behavior testing prompted us to investigate the impact of Stau2 depletion on motor activity and coordination. First, we measured the overall motor activity of adult Stau2^{GT} and WT mice exposed to a low-profile running wheel [19] during a three-week period (Figure 3A). Interestingly, the Stau2^{GT} mice showed a significantly higher tendency to use the running wheel at night (6 p.m.–6:00 a.m.) when compared with the tendency observed in the WT mice (Figure 3B), indicating that Stau2 does not affect general motor activity. To investigate the effect of Stau2 downregulation on motor coordination, we used the rotarod performance test [20] (Figure 3C). Then, 10-week-old Stau2^{GT} and WT mice were exposed to the rotarod running wheel. The duration of running until the animals fell from the wheel was measured in tests performed over two consecutive days. We observed that both Stau2^{GT} males and females showed a lower latency to fall than the age- and sex-matched controls on day 1 (Figure 3C,D). On day 2, male Stau2^{GT} mice improved significantly their test performance compared with the age-matched WT males (compare day 1 and day 2 for the Stau2^{GT} and WT animals), although the general performance was still lower in the Stau^{GT} mice (Figure 3C). Interestingly, for Stau^{GT} females, we did not observe a performance improvement during training (Figure 3D). Our expression analysis using mutant and WT brains from males (Figure 1) mirrored the effect that we observed in rotarod experiments. We therefore continued with male mice.

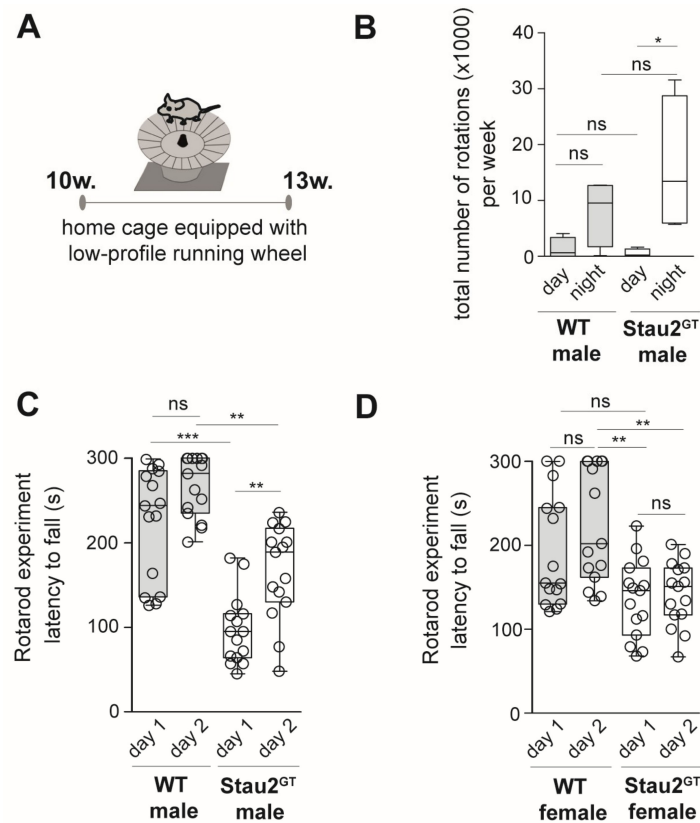


Figure 3. Adult male *Stau2*^{GT} mice show decreased motor coordination abilities but increased motor learning capacity. (A) Setup for voluntary wheel running experiments. Low-profile running wheels as depicted were placed into the home cages of 10-week-old *Stau2*^{GT} mice and age-matched WT controls for 3 weeks (w.). (B) Graph depicting the number of total rotations per week at night and day used by either the WT or *Stau2*^{GT} mice. (C) Quantification of rotarod running wheel testing. Here, 10-week-old male (left) or female (right) *Stau2*^{GT} mice, as well as age- and gender-matched controls, were set on the rotarod three times per day on two consecutive days and time until fall off was measured (the mean value per day was calculated). Mean latency to fall (in seconds) for either the WT or *Stau2*^{GT} male or female mice is plotted as boxplots. Individual data points represent different trials for single animals per day. *N* = 5 animals/group. Statistics: mean + SEM (B) or mean + min/max (C/D), one-way ANOVA and Bonferroni's multiple comparison test. * *p* < 0.05, ** *p* < 0.01, *** *p* < 0.001, ns. = not significant.

2.4. Increased Dendritic GluD2 Protein Expression in Adult *Stau2*^{GT} Mice after Motor Activity.

Based on our microarray and rotarod test results and because enhanced motor activity induces synaptogenesis in the cerebellum [21], we speculated that *Stau2* might play a role in this process. Therefore, we analyzed histological sections of the cerebellar cortex. We stained against GluD2 protein and vesicular glutamate transporter 1 (vGLUT1), a protein located at the presynaptic side of synapses between parallel fibers and Purkinje cells [22] (Figure 4A). Naive *Stau2*^{GT} mice (10 weeks old) showed weak expression of GluD2 in the StM and cell bodies of Purkinje cells. In contrast, motor activity by voluntary wheel running (3 weeks) increased GluD2 expression in the *Stau2*^{GT} mice by 50%, whereas no difference in GluD2 was observed in the WT animals. Furthermore, we detected elevated GluD2/vGLUT1 colocalization in the StM, suggesting an increase in the number of functional synapses in *Stau2*^{GT} mice after motor activity (Figure 4B,C). We next analyzed the GluD2 intensity in Purkinje cell dendrites of naive mice, as well as mice exposed to running wheels. Here, we detected higher levels of dendritically localized GluD2 protein in cerebellar Purkinje cells (Figure 4D). Naive 10-week-old WT and *Stau2*^{GT} mice, in contrast, showed no difference in GluD2 protein expression. Confirming previous experiments, the effect was much stronger in the *Stau2*^{GT} mice after motor activity than in the WT mice

(Figure 4D). In summary, the *Stau2^{GT}* mice showed higher voluntary motor activity, a steeper motor learning curve, and a more prominent increase of dendritic GluD2 expression after motor activity.

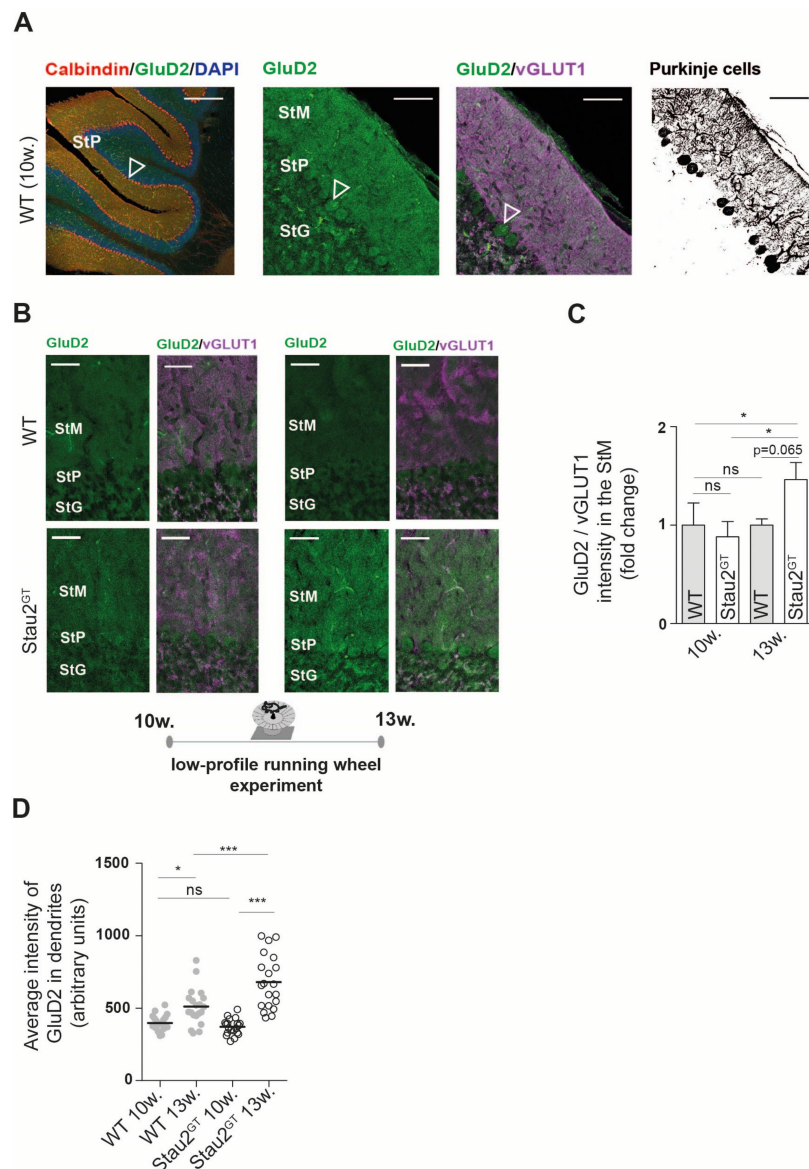


Figure 4. Dendritic GluD2 protein expression increases in adult *Stau2^{GT}* mice after motor activity. (A) Representative confocal images of immunofluorescent staining against GluD2, (vesicular glutamate transporter 1) vGLUT1, and calbindin (negative conversion for Purkinje cell morphology) on frontal sections of the cerebellum taken from 5-month-old WT mice. Scale bar = 200 μ m (left), 100 μ m (middle, right); arrow points to Purkinje cell bodies. (B) Representative confocal images of immunofluorescent staining against GluD2 and vGLUT1 in the *Stau2^{GT}* and WT mice before and after exposure to the running wheel (setup Figure 3). Scale bar = 40 μ m. (C) Quantification of the mean staining intensity of GluD2 normalized to the mean staining intensity of vGLUT1 before (10 w. = mice at the age of 10 weeks) and after (13 w. = mice at the age of 13 weeks) 3 weeks of voluntary wheel running. $N = 3$. Statistics: Student's t-test. Mean + SEM. (D) Histogram showing the average intensity of the GluD2 signal in calbindin-positive cerebellar Purkinje cell dendrites before (10 w.) and after (13 w.) running wheel exposure. The WT (filled grey circles) and *Stau2^{GT}* mice (empty black circles). $N = 20$ dendritic stretches in each group, from three different animals. Statistics: One-way ANOVA and Bonferroni's multiple comparison. Mean + SEM, * $p < 0.05$, ** $p < 0.01$, *** $p < 0.001$; ns. = not significant. StM, stratum moleculare; StP, stratum pyramidale; and StG, stratum granulare.

3. Discussion

Stau2 is an essential RNA-binding protein involved in posttranscriptional gene regulation in the brain [8,23,24]. Its role in hippocampus-dependent learning and memory formation has been studied in Stau2-deficient rat and mouse animal models [9,10]. However, little is known about its function in other brain regions. Here, we report a potential impact of Stau2 on synaptogenesis in the mouse cerebellum. Increased physical activity during behavior testing induced increased expression of *Grid2*, *Cbln1*, and *Cbln3* mRNA in adult Stau2^{GT} mice, which act together in the formation of parallel fiber-Purkinje cell synapses [11]. Interestingly, *Grid2* was detected in an iCLIP Stau2 study suggesting that it is a target of Stau2 [24]. Furthermore, the Stau2^{GT} mice showed lower motor coordination abilities but increased motor learning capacity in the rotarod test. Of note, we did not observe a similar effect in female Stau2^{GT} mice. Because we aimed at reducing the animal number used in our experiments, leading to a number of five mice per group, a larger cohort of females might be needed to observe enhanced motor learning skills. Similar to exposure to voluntary physical exercise experiments, these repeated rotarod trainings correlated to increased GluD2 protein expression in parallel fiber dendrites of cerebellar Purkinje cells.

The importance of GluD2 as a key component of the Purkinje cell post-synapse, thereby inducing synapse formation by interacting with presynaptic neurexins through secreted Cbln1, has been reported by several groups in the last few years [11–14,25]. GluD2 knockout (KO) mouse models have demonstrated a prominent motor dyscoordination and cerebellar ataxia [16,26,27]. Rotarod tests performed by GluD2 KO mice have resulted in a lower latency to fall [27], identifying GluD2 as an essential regulator of cerebellar synaptic transmission and, eventually, of motor coordination. Consequently, it is tempting to speculate that higher expression of GluD2 in Stau2^{GT} males during training contributes to the enhanced learning of motoric skills in these mice.

A possible basis of reduced motor coordination and motor learning in GluD2 KO mice is reduced long-term depression (LTD) in the cerebellum [28–30]. Interestingly, reduced Stau2 expression also leads to the disruption of LTD in the hippocampus [10,31]. Reduced LTD in the cerebellum caused by Stau2 deficiency might explain the generally weaker performance of adult Stau2^{GT} mice in rotarod tests compared with WT mice. Another possible reason for the lower test performance of Stau2^{GT} mice could be their generally reduced locomotor activity in a new environment, as has recently been reported [9].

Besides GluD2, we observed increases in *Cbln1* mRNA after stimulation of motor activity through behavioral tests in Stau2^{GT} mice when compared with WT mice. We interpret this result as a feedback response to enhanced synaptogenesis in adult Stau2^{GT} mice compared with WT animals after stimulation of motor activity. Cbln proteins are secreted by cerebellar granule cells and are predominantly expressed in the cerebellum, although involvement in other brain areas, such as the frontal brain have been reported [32–34]. *Cbln1*-null mice exhibit a cellular and physiological phenotype mimicking that of the GluD2 KO, underlining the tight functional interplay between these two proteins [32]. In another study, cerebellar ataxic gait in *Cbln1*-null mice was found to be clinically improved through Cbln1 injections into the cerebellum [35].

In summary, our results suggest that Stau2 is involved in Purkinje cell synaptogenesis in the adult mouse cerebellum and might contribute to the regulation of motor coordination and learning. These findings therefore hold consequences for new clinical approaches. For example, GluD2 mutations have been shown in cases of congenital cerebellar ataxia in patients [17]. A better understanding of the involvement of Stau2 in GluD2-dependent synapse formation could therefore provide new therapeutic options for cerebellar ataxia and similar disorders. It will be interesting to investigate further gender-specific differences in Stau2 function. Future studies are needed to unravel the impact of Stau2 in cerebellar synaptogenesis at the molecular level and its relevance for motor coordination and activity defects in humans.

4. Materials and Methods

4.1. Generation and Housing of *Stau2* Gene Trap Mice

All experiments were performed according to local animal protection laws and were approved by the district government of upper bavaria (55.2-1-54-2532-167-2013, 23 May 2014) Adult B6.129P2-*Stau2*^{Gt(RRG396)Byg} mice [9] and WT C57Bl/6J mice (aged 10–13 weeks and 16–20 weeks) were housed in groups of 2–5 animals with a 12-h light/12-h dark light cycle in individually ventilated cages. The mice had free access to autoclaved water and food.

4.2. Behavioral Analysis

All behavioral tests were performed under identical environmental conditions. Between individual testing phases, the animals were kept in their housing cages. First, 4-month-old male *Stau2*^{GT} and WT mice were exposed to a stimulation of exploratory and motor behavior for 4 consecutive weeks via different behavioral tests (open field, novel object recognition/location, Barnes maze) as described previously [9].

Running wheel: Low-profile running wheels (Med associates Inc, Fairfax, VT, USA) were placed in home cages of age- and gender-matched *Stau2*^{GT} and WT mice for a time period of 3 weeks. Motor activity was tracked by measuring total rotations of the running wheel per day.

Rotarod test: The rotarod test was performed as previously described [36]. Age- and gender-matched *Stau2*^{GT} and WT mice were set on a rotating rod (accelerating rotations during 5-min test duration), and the latency until fall from the rod was measured in seconds. The test was performed for two consecutive days. WT male and *Stau2*^{GT} males, as well as WT female and *Stau2*^{GT} female mice, were investigated.

4.3. Histology

Whole animal perfusion fixation was performed as previously described [37]. Cerebellar tissue was prepared as previously described [38].

Immunohistochemistry: Brains of perfusion fixed mice were postfixed, cryoprotected, cut in 30- μ m frontal sections, and immunostained as described previously [38]. Self-made rabbit polyclonal anti-*Stau2* antibody [39] was diluted 1:200, additionally anti-GluRD2 (rabbit polyclonal, Alomone, 1:200), anti-vGLUT1 (guinea pig polyclonal, Synaptic Systems, 1:500, Göttingen, Germany), calbindin (mouse monoclonal, Abcam, 1:500), and anti-NeuN (chicken polyclonal, Millipore, 1:500, Darmstadt, Germany) were used. To detect the primary antibody, sections were washed three times in PBS and incubated with secondary antibodies (goat anti-rabbit IgG Alexa Fluor 488 labeled (Jackson ImmunoResearch, Cambridgeshire, UK), goat anti-guinea pig IgG Cy3 labeled (Jackson ImmunoResearch), goat anti-chicken IgY Alexa Fluor 647 labeled (Life Technologies, Carlsbad, CA, USA), and donkey anti-mouse IgG Alexa Fluor 555 labeled (Life Technologies) diluted 1:500 in blocking solution for 2 h at room temperature. Nuclei were stained by 5-min incubation in 4',6-diamidino-2-phenylindole (DAPI) solution. Slices were washed three times in PBS and mounted in Fluomount (Sigma-Aldrich, Munich, Germany). Pictures were taken by a confocal SP8 microscope (Leica, Wetzlar, Germany).

Imaging: Dendritic stretches of cerebellar Purkinje cells were identified using calbindin staining and the Imaris software package (Bitplane, South Windsor, CT, USA). Fiji 1.50g (PMID 26153368) software was used to outline 20 randomly chosen dendritic stretches per group in the WT and *Stau2*^{GT} mice at 10 or 13 weeks, respectively. Immunofluorescence intensity of GluRD2 was measured in images taken at the same gain level by a confocal microscope (Leica, Germany).

LacZ-staining: To monitor gene trap vector insertion in murine brains, we detected LacZ expression by determining the encoded β -galactosidase activity in slices of *Stau2*^{GT} mouse brains according to the manufacturer's instructions (InvivoGen, San Diego, CA, USA). The procedure was performed as described previously [9].

4.4. RT-qPCR

Total mRNA was obtained from brain samples using TRIzol (Ambion, Carlsbad, CA, USA) according to the manufacturer's protocol. Genomic DNA was depleted using the Mini RNeasy kit (Qiagen). cDNA was synthesized from purified mRNA by reverse transcription using Superscript III reverse transcriptase (Invitrogen, Carlsbad, CA, USA) according to the manufacturer's instructions. For qPCR cDNA amplification, Hot Start Taq (New England Biolabs, Ipswich, MA, USA) was used with SYBR Green for amplicon detection. All primers were used with an optimal efficiency rate of 2.0 ± 0.05 . Runs were performed on a Lightcycler 96 (Roche Bioanalytics, Basel, Switzerland). Primers used in this study were (5' to 3'): *Cbln1*: GCTTCTCTGCCATCAGG and TCTGAGTCAAAGTTGTTCCC, *Grid2*: TGACACCATGAGGATAGAGG and ACCTCACTTATGAAGGATTTGG, *18S*: GAAACTGCGAATGGCTCATAAA and CCACAGTTATCCAAGTAGGAGAGGA.

4.5. Expression Analysis

Microarray analysis: RNA was isolated as described above. The samples were processed according to the manufacturer's instructions (Affymetrix, Santa Clara, CA, USA) and hybridized on a Mouse Gene 2.0 ST Array. Signal intensities were extracted and normalized using RMA (R/bioconductor package 'oligo'). Samples with log₂-expression levels of >5 in at least 3 samples were subjected to differential expression analysis using limma and multiple testing correction according to Benjamini and Hochberg (R/bioconductor package 'limma'). Data were deposited in the Gene Expression Omnibus (GEO) database (accession no. GSE126996).

4.6. Statistics

Data were first tested for Gaussian distribution using the KS-test. Normally distributed data were analyzed by Student's t-test or one-way ANOVA followed by Bonferroni's post-hoc test for multiple comparison. Data are presented as mean + SEM. Statistical analysis was performed using the software GraphPad Prism (Version 5, GraphPad, San Diego, CA, USA). $p < 0.05$ (*) was considered statistically significant if not stated otherwise.

Author Contributions: Conceptualization, H.F.P., R.S., and B.P.; Methodology and Experimentation, H.F.P., R.S., M.J., and B.P.; Data Analysis, H.F.P., R.S., M.B., T.S., M.A.K., and B.P.; Resources, M.A.K.; Writing, H.F.P., R.S., M.A.K., and B.P.; Supervision, M.A.K. and B.P.; Project Administration, M.A.K. and B.P., and Funding, M.A.K. and B.P.

Funding: This research was funded by the Boehringer Ingelheim Fund (BIF) granted to R.S., the Förderprogramm für Forschung und Lehre—FöFoLe PhD program of LMU Munich granted to H.P., the Friedrich-Baur-Stiftung (02/14 and 02/16 to B.P.), and the DFG (SPP1738, Kie 502/2-1 and FOR2333, Kie 502/3-1; all to M.A.K.).

Acknowledgments: We thank Jessica Weigel for her excellent technical assistance and all members of the Kiebler laboratory for their helpful discussions. We would also like to thank the BMC core facility for bioimaging for kindly providing equipment (SP8 Leica microscope) and excellent services.

Conflicts of Interest: The authors declare no conflicts of interest.

Abbreviations

Cbln1	Cerebellin1
GluD2	Glutamate receptor ionotropic delta subunit 2
KO	Knock out
LTD	Long-term depression
RBP	RNA-binding protein
Stau2	Staufen2
Stau2 ^{GT}	Staufen2 gene trap
StG	Stratum granulosum
StM	Stratum moleculare
StP	Stratum pyramidale
vGLUT1	Vesicular glutamate transporter 1
WT	Wild type

References

1. Jung, H.; Gkogkas, C.G.; Sonenberg, N.; Holt, C.E. Remote control of gene function by local translation. *Cell* **2014**, *157*, 26–40. [[CrossRef](#)]
2. Doyle, M.; Kiebler, M.A. Mechanisms of dendritic mRNA transport and its role in synaptic tagging. *EMBO J.* **2011**, *30*, 3540–3552. [[CrossRef](#)] [[PubMed](#)]
3. Kiebler, M.A.; Bassell, G.J. Neuronal RNA Granules: Movers and Makers. *Neuron* **2006**, 685–690. [[CrossRef](#)] [[PubMed](#)]
4. Jarero-Basulto, J.J.; Gasca-Martinez, Y.; Rivera-Cervantes, M.; Ureña-Guerrero, M.; Feria-Valesco, A.I.; Beas-Zarate, C. Interactions Between Epilepsy and Plasticity. *Pharmaceuticals* **2018**, *11*, 17. [[CrossRef](#)] [[PubMed](#)]
5. Liu-Yesucevitz, L.; Bassell, G.J.; Gitler, A.D.; Hart, A.C.; Klann, E.; Richter, J.D.; Warren, S.T.; Wolozin, B. Local RNA Translation at the Synapse and in Disease. *J. Neurosci.* **2011**. [[CrossRef](#)] [[PubMed](#)]
6. Swanger, S.A.; Bassell, G.J. Dendritic protein synthesis in the normal and diseased brain. *Neuroscience* **2013**, *232*, 106–127. [[CrossRef](#)] [[PubMed](#)]
7. Hanson, K.A.; Kim, S.H.; Tibbetts, R.S. RNA-binding proteins in neurodegenerative disease: TDP-43 and beyond. *Wiley Interdiscip. Rev. RNA* **2012**, 265–285. [[CrossRef](#)]
8. Heraud-Farlow, J.E.; Kiebler, M.A. The multifunctional Staufen proteins: Conserved roles from neurogenesis to synaptic plasticity. *Trends Neurosci.* **2014**, 470–479. [[CrossRef](#)] [[PubMed](#)]
9. Popper, B.; Demleitner, A.; Bolivar, V.J.; Kusek, G.; Snyder-Keller, A.; Schieweck, R.; Temple, S.; Kiebler, M.A. Staufen2 deficiency leads to impaired response to novelty in mice. *Neurobiol. Learn. Mem.* **2018**. [[CrossRef](#)]
10. Berger, S.M.; Fernández-Lamo, I.; Schönig, K.; Fernández Moya, S.M.; Ehses, J.; Schieweck, R.; Clementi, S.; Enkel, T.; Grothe, S.; von Bohlen und Halbach, O.; et al. Forebrain-specific, conditional silencing of Staufen2 alters synaptic plasticity, learning, and memory in rats. *Genome Biol.* **2017**, *18*, 222.
11. Hirano, T. Glutamate-receptor-like molecule GluR δ 2 involved in synapse formation at parallel fiber-Purkinje neuron synapses. *Cerebellum* **2012**, *11*, 71–77. [[CrossRef](#)]
12. Matsuda, K.; Miura, E.; Miyazaki, T.; Kakegawa, W.; Emi, K.; Narumi, S.; Fukazawa, Y.; Ito-Ishida, A.; Kondo, T.; Shigemoto, R.; et al. Cbln1 is a ligand for an orphan glutamate receptor δ 2, a bidirectional synapse organizer. *Science*. **2010**. [[CrossRef](#)]
13. Mishina, M.; Uemura, T.; Yasumura, M.; Yoshida, T. Molecular mechanism of parallel fiber-Purkinje cell synapse formation. *Front. Neural Circuits* **2012**, *6*, 90. [[CrossRef](#)] [[PubMed](#)]
14. Cheng, S.; Seven, A.B.; Wang, J.; Skiniotis, G.; Özkan, E. Conformational Plasticity in the Transsynaptic Neurexin-Cerebellin-Glutamate Receptor Adhesion Complex. *Structure* **2016**, *24*, 2163–2173. [[CrossRef](#)] [[PubMed](#)]
15. Hashizume, M.; Miyazaki, T.; Sakimura, K.; Watanabe, M.; Kitamura, K.; Kano, M. Disruption of cerebellar microzonal organization in GluD2 (GluR δ 2) knockout mouse. *Front. Neural Circuits* **2013**, *7*, 130. [[CrossRef](#)] [[PubMed](#)]
16. Miyoshi, Y.; Yoshioka, Y.; Suzuki, K.; Miyazaki, T.; Koura, M.; Saigoh, K.; Kajimura, N.; Monobe, Y.; Kusunoki, S.; Matsuda, J.; et al. A new mouse allele of glutamate receptor delta 2 with cerebellar atrophy and progressive ataxia. *PLoS ONE* **2014**, *9*, e107867. [[CrossRef](#)] [[PubMed](#)]
17. Coutelier, M.; Burglen, L.; Mundwiller, E.; Abada-Bendib, M.; Rodriguez, D.; Chantot-Bastaraud, S.; Rougeot, C.; Cournelle, M.A.; Milh, M.; Toutain, A.; et al. GRID2 mutations span from congenital to mild adult-onset cerebellar ataxia. *Neurology* **2015**, *84*, 1751–1759. [[CrossRef](#)]
18. Miura, E.; Matsuda, K.; Morgan, J.I.; Yuzaki, M.; Watanabe, M. Cbln1 accumulates and colocalizes with Cbln3 and GluR δ 2 at parallel fiber-Purkinje cell synapses in the mouse cerebellum. *Eur. J. Neurosci.* **2009**, *29*, 693–706. [[CrossRef](#)] [[PubMed](#)]
19. Walker, M.; Mason, G. A comparison of two types of running wheel in terms of mouse preference, health, and welfare. *Physiol. Behav.* **2018**. [[CrossRef](#)] [[PubMed](#)]
20. Brooks, S.P.; Trueman, R.C.; Dunnett, S.B. Assessment of Motor Coordination and Balance in Mice Using the Rotarod, Elevated Bridge, and Footprint Tests. *Curr. Protoc. Mouse Biol.* **2012**, *2*, 37–53.

21. Aguiar, A.S.; Castro, A.A.; Moreira, E.L.; Glaser, V.; Santos, A.R.S.; Tasca, C.I.; Latini, A.; Prediger, R.D.S. Short bouts of mild-intensity physical exercise improve spatial learning and memory in aging rats: Involvement of hippocampal plasticity via AKT, CREB and BDNF signaling. *Mech. Ageing Dev.* **2011**, *132*, 560–567. [[CrossRef](#)]
22. Fremeau, R.T.; Troyer, M.D.; Pahner, I.; Nygaard, G.O.; Tran, C.H.; Reimer, R.J.; Bellocchio, E.E.; Fortin, D.; Storm-Mathisen, J.; Edwards, R.H. The expression of vesicular glutamate transporters defines two classes of excitatory synapse. *Neuron* **2001**, *31*, 247–260. [[CrossRef](#)]
23. Goetze, B.; Tuebing, F.; Xie, Y.; Dorostkar, M.M.; Thomas, S.; Pehl, U.; Boehm, S.; Macchi, P.; Kiebler, M.A. The brain-specific double-stranded RNA-binding protein Stauf2 is required for dendritic spine morphogenesis. *J. Cell Biol.* **2006**, *172*, 221–231. [[CrossRef](#)] [[PubMed](#)]
24. Sharangdhar, T.; Sugimoto, Y.; Heraud-Farlow, J.; Fernández-Moya, S.M.; Ehses, J.; Ruiz de los Mozos, I.; Ule, J.; Kiebler, M.A. A retained intron in the 3′-UTR of *Calm3* mRNA mediates its Stauf2- and activity-dependent localization to neuronal dendrites. *EMBO Rep.* **2017**, *18*, 1762–1774. [[CrossRef](#)] [[PubMed](#)]
25. Uemura, T.; Lee, S.J.; Yasumura, M.; Takeuchi, T.; Yoshida, T.; Ra, M.; Taguchi, R.; Sakimura, K.; Mishina, M. Trans-synaptic interaction of GluRδ2 and neurexin through Cbln1 mediates synapse formation in the cerebellum. *Cell* **2010**, *18*, 1762–1774. [[CrossRef](#)]
26. Zanjani, H.S.; Vogel, M.W.; Mariani, J. Deletion of the GluRδ2 Receptor in the Hotfoot Mouse Mutant Causes Granule Cell Loss, Delayed Purkinje Cell Death, and Reductions in Purkinje Cell Dendritic Tree Area. *Cerebellum* **2016**, *15*, 755–766. [[CrossRef](#)] [[PubMed](#)]
27. Kashiwabuchi, N.; Ikeda, K.; Araki, K.; Hirano, T.; Shibuki, K.; Takayama, C.; Inoue, Y.; Kutsuwada, T.; Yagi, T.; Kang, Y.; et al. Impairment of motor coordination, Purkinje cell synapse formation, and cerebellar long-term depression in GluR delta 2 mutant mice. *Cell* **1995**, *81*, 245–252. [[CrossRef](#)]
28. Kakegawa, W.; Miyoshi, Y.; Hamase, K.; Matsuda, S.; Matsuda, K.; Kohda, K.; Emi, K.; Motohashi, J.; Konno, R.; Zaitzu, K.; et al. D-Serine regulates cerebellar LTD and motor coordination through the δ2 glutamate receptor. *Nat. Neurosci.* **2011**, *14*, 603–611. [[CrossRef](#)] [[PubMed](#)]
29. Hirai, H.; Launey, T.; Mikawa, S.; Torashima, T.; Yanagihara, D.; Kasaura, T.; Miyamoto, A.; Yuzaki, M. New role of delta2-glutamate receptors in AMPA receptor trafficking and cerebellar function. *Nat. Neurosci.* **2003**, *6*, 869–876. [[CrossRef](#)]
30. Uemura, T.; Mori, H.; Mishina, M. Direct interaction of GluRdelta2 with Shank scaffold proteins in cerebellar Purkinje cells. *Mol. Cell. Neurosci.* **2004**. [[CrossRef](#)]
31. Lebeau, G.; Miller, L.C.; Tartas, M.; McAdam, R.; Laplante, I.; Badeaux, F.; DesGroseillers, L.; Sossin, W.S.; Lacaille, J.C. Stauf2 regulates mGluR long-term depression and Map1b mRNA distribution in hippocampal neurons. *Learn. Mem.* **2011**, *18*, 314–326. [[CrossRef](#)]
32. Hirai, H.; Pang, Z.; Bao, D.; Miyazaki, T.; Li, L.; Miura, E.; Parris, J.; Rong, Y.; Watanabe, M.; Yuzaki, M.; et al. Cbln1 is essential for synaptic integrity and plasticity in the cerebellum. *Nat. Neurosci.* **2005**. [[CrossRef](#)] [[PubMed](#)]
33. Matsuda, K.; Yuzaki, M. Cbln1 and the delta2 glutamate receptor—An orphan ligand and an orphan receptor find their partners. *Cerebellum* **2012**, *11*, 78–84. [[CrossRef](#)] [[PubMed](#)]
34. Otsuka, S.; Konno, K.; Abe, M.; Motohashi, J.; Kohda, K.; Sakimura, K.; Watanabe, M.; Yuzaki, M. Roles of Cbln1 in Non-Motor Functions of Mice. *J. Neurosci.* **2016**, *36*, 11801–11816. [[CrossRef](#)] [[PubMed](#)]
35. Takeuchi, E.; Ito-Ishida, A.; Yuzaki, M.; Yanagihara, D. Improvement of cerebellar ataxic gait by injecting Cbln1 into the cerebellum of cbln1-null mice. *Sci. Rep.* **2018**, *8*, 6184. [[CrossRef](#)] [[PubMed](#)]
36. Hamm, R.J.; Pike, B.R.; O’Dell, D.M.; Lyeth, B.G.; Jenkins, L.W. The rotarod test: An evaluation of its effectiveness in assessing motor deficits following traumatic brain injury. *J. Neurotrauma* **1994**, *11*, 187–196. [[CrossRef](#)]
37. Calzolari, F.; Michel, J.; Baumgart, E.V.; Theis, F.; Götz, M.; Ninkovic, J. Fast clonal expansion and limited neural stem cell self-renewal in the adult subependymal zone. *Nat. Neurosci.* **2015**, *18*, 490–492. [[CrossRef](#)] [[PubMed](#)]

38. Follwaczny, P.; Schieweck, R.; Riedemann, T.; Demleitner, A.; Straub, T.; Klemm, A.H.; Bilban, M.; Sutor, B.; Popper, B.; Kiebler, M.A. Pumilio2-deficient mice show a predisposition for epilepsy. *Dis. Model. Mech.* **2017**, *10*, 1333–1342. [[CrossRef](#)] [[PubMed](#)]
39. Heraud-Farlow, J.E.; Sharangdhar, T.; Li, X.; Pfeifer, P.; Tauber, S.; Orozco, D.; Hörmann, A.; Thomas, S.; Bakosova, A.; Farlow, A.R.; et al. Staufen2 regulates neuronal target RNAs. *Cell Rep.* **2013**, *5*, 1511–1518. [[CrossRef](#)] [[PubMed](#)]



© 2019 by the authors. Licensee MDPI, Basel, Switzerland. This article is an open access article distributed under the terms and conditions of the Creative Commons Attribution (CC BY) license (<http://creativecommons.org/licenses/by/4.0/>).

Publication IV: Posttranscriptional Gene Regulation of the GABA Receptor to Control Neuronal Inhibition

This section contains the study published in *Frontiers in Molecular Neuroscience* (2019) entitled **Posttranscriptional Gene Regulation of the GABA Receptor to Control Neuronal Inhibition** by

Rico Schieweck[‡] and Michael A. Kiebler[‡]

[‡] corresponding authors

Author contribution to this publication

Rico Schieweck performed bioinformatic analysis (Figs. 1 and 2). Rico Schieweck and Michael A. Kiebler wrote and revised the manuscript.

(Rico Schieweck)

(Prof. Dr. Michael A. Kiebler)

(Prof. Dr. Heinrich Leonhardt)



Posttranscriptional Gene Regulation of the GABA Receptor to Control Neuronal Inhibition

Rico Schieweck* and Michael A. Kiebler*

Department of Cell Biology and Anatomy, Medical Faculty, Biomedical Center (BMC), Ludwig-Maximilians-University of Munich, Munich, Germany

Behavior and higher cognition rely on the transfer of information between neurons through specialized contact sites termed synapses. Plasticity of neuronal circuits, a prerequisite to respond to environmental changes, is intrinsically coupled with the nerve cell's ability to form, structurally modulate or remove synapses. Consequently, the synaptic proteome undergoes dynamic alteration on demand in a spatiotemporally restricted manner. Therefore, proper protein localization at synapses is essential for synaptic function. This process is regulated by: (i) protein transport and recruitment; (ii) local protein synthesis; and (iii) synaptic protein degradation. These processes shape the transmission efficiency of excitatory synapses. Whether and how these processes influence synaptic inhibition is, however, widely unknown. Here, we summarize findings on fundamental regulatory processes that can be extrapolated to inhibitory synapses. In particular, we focus on known aspects of posttranscriptional regulation and protein dynamics of the GABA receptor (GABAR). Finally, we propose that local (co)-translational control mechanism might control transmission of inhibitory synapses.

OPEN ACCESS

Edited by:

Andrea Barberis,
Istituto Italiano di Tecnologia, Italy

Reviewed by:

Carlos B. Duarte,
University of Coimbra, Portugal
Katharine R. Smith,
University of Colorado Denver,
United States

*Correspondence:

Rico Schieweck
rico.schieweck@med.
uni-muenchen.de
Michael A. Kiebler
mkiebler@lmu.de

Received: 25 March 2019

Accepted: 29 May 2019

Published: 25 June 2019

Citation:

Schieweck R and Kiebler MA
(2019) Posttranscriptional Gene
Regulation of the GABA Receptor to
Control Neuronal Inhibition.
Front. Mol. Neurosci. 12:152.
doi: 10.3389/fnmol.2019.00152

Keywords: posttranscriptional gene regulation, GABA receptors, inhibitory synapse, co-translational folding/assembly, RNA binding, RNA transport, local translation, RNA-binding proteins

INTRODUCTION

The enormous capacity of the brain to store information and respond to different environmental conditions and challenges crucially rely on underlying mechanisms like synaptic plasticity. This depends on the ability to modulate the strength of transmission between two nerve cells as well as the growth and removal of synapses. Synapses consist of (at least) hundreds of proteins that need to be organized and correctly assembled to ensure proper synaptic function. Changes in synaptic transmission and structure are accompanied and conveyed by local alterations in protein levels. Understanding the regulation of synaptic protein composition is, therefore, crucial to gain insight into complex neurological processes such as learning and memory and, eventually, into neuropsychiatric diseases such as autism spectrum disorders, schizophrenia and bipolar disorders.

In order to remodel the synaptic proteome, neurons exploit different mechanisms that allow spatial and temporal control of protein levels. Protein synthesis was one of the first molecular mechanisms that were discovered to be indispensable for memory formation (Hershkowitz et al., 1975; Shashoua, 1976). Pioneer experiments showed that inhibiting translation blocked the ability of an animal to remember after training (Flexner et al., 1963). In line with this observation, several experiments have shown that strengthening and weakening of synaptic transmission, so called long-term potentiation (LTP) and depression (LTD), respectively, need active translation in a time-dependent manner (Krug et al., 1984; Linden, 1996).

The spatial selectivity of synapses to undergo changes upon stimulation raised the question of how a cell knows, which synapse is destined for functional and structural remodeling. This inspired Frey and Morris (1997) to the idea of “synaptic tagging.” Repetitive activation of synapses, therefore, equips such a synapse with a labile molecular “tag.” Eventually, the synaptic tag allows the synapse to recruit newly synthesized proteins. The concept of “synaptic tagging” is a very elegant model to explain processes such as LTP and LTD at excitatory synapses (Frey and Morris, 1997). The precise identity of the tag(s) is still lacking. Furthermore, synaptic plasticity depends on additional processes such as mRNA localization, which is mainly independent of translation activity (Steward et al., 1998). mRNA transport and localization are important determinants of synaptic function (Jung et al., 2014). To date, it is generally believed that mRNAs are assembled into ribonucleoprotein particles (RNPs) consisting of mRNAs and RNA-binding proteins (RBPs). The protein and mRNA composition of these particles differ substantially (Kanai et al., 2004; Fritzsche et al., 2013) giving raise to the idea that different subtypes of particles or granules co-exist in a nerve cell. The function of these RNA granules is: (i) to transport mRNA—in a translationally dormant stage—along cytoskeletal elements such as microtubules to their destination at the synapse; and (ii) to regulate the translation of their target mRNAs. Activity-dependent disassembly of these RNA granules then allows the release of mRNAs and subsequent induction of translation. How neuronal stimulation, recruitment of mRNAs and unpacking of RNPs are synchronized is largely unknown. A pioneer study identified the kinase mechanistic target of rapamycin (mTOR) as a central hub to recruit RNAs. The authors suggest that mTOR might be the tag that controls mRNA recruitment at the synapse (Sosanya et al., 2015). mTOR is essential for proper neuronal function (Costa-Mattioli and Monteggia, 2013; Pernice et al., 2016). It needs to be experimentally verified though whether it might represent an universal synaptic tag or whether it might be specific for a subset of mRNAs.

Local protein expression control comprising mRNA transport, local protein synthesis and recruitment of newly synthesized protein remodel the synaptic proteome. Consequently, protein degradation is compulsive to complete synaptic remodeling. Synaptic protein degradation is induced in an activity-dependent manner (Bingol and Schuman, 2006). Moreover, it is tightly linked to translation to balance the protein need (Klein et al., 2015). In line with this finding, the translation repressor poly(A)-binding protein interacting protein 2A (PAIP2A) is degraded by calpain in neurons upon stimulation (Khoutorsky et al., 2013). Interestingly, calpain also degrades gephyrin (Gphn), a major scaffold protein at inhibitory synapses (Tyagarajan and Fritschy, 2014). This finding indicates that translational activation at excitatory synapses may modulate inhibitory synapses to alter transmission.

In this review article, we provide insight into posttranscriptional regulatory mechanisms that control synaptic protein expression. Since most of these studies investigated these processes at excitatory synapses, we aim to expand these fundamental aspects to inhibitory synapses. We speculate that

local expression control also regulates inhibitory transmission to balance neuronal excitation.

TO LOCALIZE OR NOT TO LOCALIZE—IT'S A MATTER OF RBP BINDING TO THE 3'-UTR

With the emergence of the individual-nucleotide resolution UV crosslinking and immunoprecipitation (iCLIP) technology (Huppertz et al., 2014), transcriptome-wide identification of RBP mRNA targets and binding site became experimentally addressable. iCLIP has now been performed for a series of RBPs (Tables 1, 2). Interestingly, most of the RBP binding occurs within the 3'-untranslated region (3'-UTR) of transcripts (Andreassi and Riccio, 2009). In addition, it was shown that the median of the 3'-UTR length of mRNAs bound to the RBP Staufen2 that is necessary for RNA transport (Heraud-Farlow and Kiebler, 2014) is longer than the median of the transcriptome (Heraud-Farlow et al., 2013). This finding indicates that a certain 3'-UTR length is needed to allow association with RBPs and, consequently, mRNA transport and/or expression control (Heraud-Farlow and Kiebler, 2014). To test whether mouse GABA receptor (GABAR) subunits show a similar tendency towards longer 3'-UTR length, we analyzed the nucleotide length of their 3'-ends of all GABA_A and GABA_B receptor subunit isoforms (see “Methods” section). Strikingly, GABAR subunits reveal a significant increase in their 3'-UTR compared to the total mouse 3'-UTRome (Figure 1A). Moreover, the 3'-UTR length was significantly extended when comparing the GABAR subunits with the 3'-UTRome of the somatic and neuropil layer of the hippocampal CA1 region (Cajigas et al., 2012; Figure 1A). An increase in 3'-UTR length is linked with decreased translational activity in HEK cells and human neurons (Floor and Doudna, 2016; Blair et al., 2017) probably due to a higher number of miRNA and RBP binding sites. In addition, 3'-UTR length is extended during neuronal development indicating increased translation regulation in mature neurons compared to developing nerve cells (Blair et al., 2017). Of note, GABAR subunits exhibited a trend towards longer 3'-ends when compared with ionotropic glutamate receptor subunits (Figure 1B). Together, these results suggest that GABAR subunit 3'-UTRs have a high(er) potential to be bound by RBPs. Supportive for this hypothesis is the fact that GABAR subunit mRNAs are enriched in the dendrite containing neuropil layer of CA1 neurons in the hippocampus (Cajigas et al., 2012) suggesting that these mRNAs are localized there. The recognition of mRNA targets by RBPs relies on binding sites within their 3'-UTRs and that each mRNA might have its own specific RNA signature. In detail, these binding sequences consist of both sequence and structural elements (Kiebler and Bassell, 2006; Doyle and Kiebler, 2011; Jung et al., 2014; Sugimoto et al., 2015). Interestingly, GABAR subunits exhibited a lower GC content compared to the total, somatic CA1 and neuropil 3'-UTRome (Figure 1C). Concomitantly, we observed a higher AT content (Figure 1C). Moreover, the same statistically significant effects were detected when comparing

TABLE 1 | Hand-selected list of RBPs with RNAs related to GABAR as targets.

Rbp	Method	Tissue	RNA targets related to GABAR	Reference
Nova	iCLIP	Brain	Gabbr2, Gabrg2	Ule et al. (2003)
FMRP	iCLIP	Brain	Gabbr1, Gabbr2	Darnell et al. (2011)
Staufen1	iCLIP	Brain	Gabbr2	Sugimoto et al. (2015)
Staufen2	RIP, iCLIP	Embryonic brain	Gabra2, Gabra3, Gabbr1, Gabbr2, Gabrb1, Gabrb2, Gabrb3, Gabrg3	Heraud-Farlow et al. (2013) and Sharangdhar et al. (2017)
Unkempt	iCLIP	Embryonic brain	Gabra3, Gabrb2	Murn et al. (2015)
Celf4	iCLIP	Brain	Gabra1, Gabra2, Gabra3, Gabra4, Gabra5, Gabrb1, Gabrb2, Gabrb3, Gabbr1, Gabbr2, Gabrg1, Gabrg2, Gabrg3, Gabrd	Wagnon et al. (2012)
Rbfox1, 2, 3	iCLIP	Brain	Gabra1, Gabra3, Gabra6, Gabbr1, Gabrb2, Gabrb3, Gabrg1, Gabrg2	Lee et al. (2016)
Pumilio1	iCLIP	Brain	Gabra1, Gabra5, Gabbr1, Gabrb2, Gabrg2	Zhang et al. (2017)
Pumilio2	iCLIP	Brain	Gabra4, Gabrb2, Gabrg2, Gabrg	Zhang et al. (2017) and Zahr et al. (2018)
4E-T	RIP	Embryonic brain	Gabrg2	Yang et al. (2014)
hnRNP R	iCLIP	Embryonic primary mouse motoneurons	Gabra4, Gabbr1, Gabrb1, Gabrb3, Gabrg2, Gabrg3	Briese et al. (2018)
CPEB1	RIP	Striatum	Gabrb1, Gabrb2	Parras et al. (2018)
CPEB4	RIP	Striatum	Gabra1, Gabra2, Gabra4, Gabrb1, Gabrb2, Gabrb3, Gabrg3	Parras et al. (2018)
nELAV	iCLIP	Human dorsolateral prefrontal cortex	Gabra4, Gabrb2, Gabrb3, Gabrg1, Gabrg3	Scheckel et al. (2016)

TABLE 2 | Hand-selected list of RBPs with RNAs related to scaffold protein, GABAR auxiliary and transport proteins as targets.

Rbp	Method	Tissue	RNA targets related to GABAR	Reference
Nova	iCLIP	Brain	Gphn	Ule et al. (2003)
FMRP	iCLIP	Brain	NSF, Trak2, Ubqln1	Darnell et al. (2011)
Staufen1	iCLIP	Brain	KCTD12, GABARAPL3, NSF, Argef2, Ubqln1	Sugimoto et al. (2015)
Staufen2	RIP, iCLIP	Embryonic brain	Gphn, Arhgef9, KCTD16, NSF, Argef2, GABARAPL1, Zdhhc3, Plcl1, Ubqln1	Heraud-Farlow et al. (2013) and Sharangdhar et al. (2017)
Rbfox1, 2, 3	iCLIP	Brain	Gphn, NSF, Argef2, Ubqln1	Lee et al. (2016)
Pumilio1	iCLIP	Brain	KCTD12, Trak2	Zhang et al. (2017)
Pumilio2	iCLIP	Brain	Gphn, KCTD12, Argef2, Trak2, Plcl1	Zhang et al. (2017) and Zahr et al. (2018)
4E-T	RIP	Embryonic brain	Gphn, Trak2	Yang et al. (2014)
hnRNP R	iCLIP	Embryonic primary mouse motoneurons	Gphn, Arhgef9, KCTD16, NSF, Argef2, Zdhhc3, Trak2, Plcl1	Briese et al. (2018)
CPEB1	RIP	Striatum	Argef2, Zdhhc3	Parras et al. (2018)
CPEB4	RIP	Striatum	Gphn, Argef2, Zdhhc3, Trak2, Ubqln1	Parras et al. (2018)
nELAV	iCLIP	Human dorsolateral prefrontal cortex	KCTD16, Plcl1	Scheckel et al. (2016)

ionotropic GluR and GABAR subunit mRNAs (**Figure 1D**). A lower GC content accounts for less stable secondary structures in the 3'-UTRs of GABAR compared to the total, somatic CA1 and neuropil 3'-UTRome as well as to GluR 3'-ends. Interestingly, the cytoplasmic polyadenylation binding element binding protein (CPEB) binds a short, AT-rich sequence within the 3'-UTR of target mRNAs to control translation and to induce the elongation of polyA tails (Mendez and Richter, 2001). By using RNA immunoprecipitation (RIP), it was shown that CPEB1 and 4 bind different GABAR subunits as well as mRNAs coding for scaffold protein such as Gphn (Parras et al., 2018; see also **Tables 1, 2**). Moreover, ELAV proteins, among others, bind so-called AU-rich elements (ARE) to stabilize its target mRNAs (Fan and Steitz, 1998; Peng et al., 1998). Therefore, it is tempting to speculate that ELAV proteins

also bind mRNAs coding for GABAR subunits to regulate their abundance. Supportive for this idea is an iCLIP-based ELAV target screen from human brain, which detected selective mRNAs encoding GABAR subunits, GABA_B receptor auxiliary proteins and GABAR transport proteins (Scheckel et al., 2016; see also **Tables 1, 2**).

To date, several GABAR subunits, scaffold, auxiliary and GABAR transport proteins have been detected as targets for RBPs by iCLIP or RIP (**Tables 1, 2**). Among those, known translation regulators such as fragile X mental retardation protein (FMRP), Pumilio1, 2, 4E-T as well as CPEB1 and 4 all bind GABAR subunit mRNAs. However, how these RBPs act together to locally control the expression of GABAR subunits in dendrites is still unknown. Future studies are clearly needed to unravel the role of RBP mediated protein expression control.

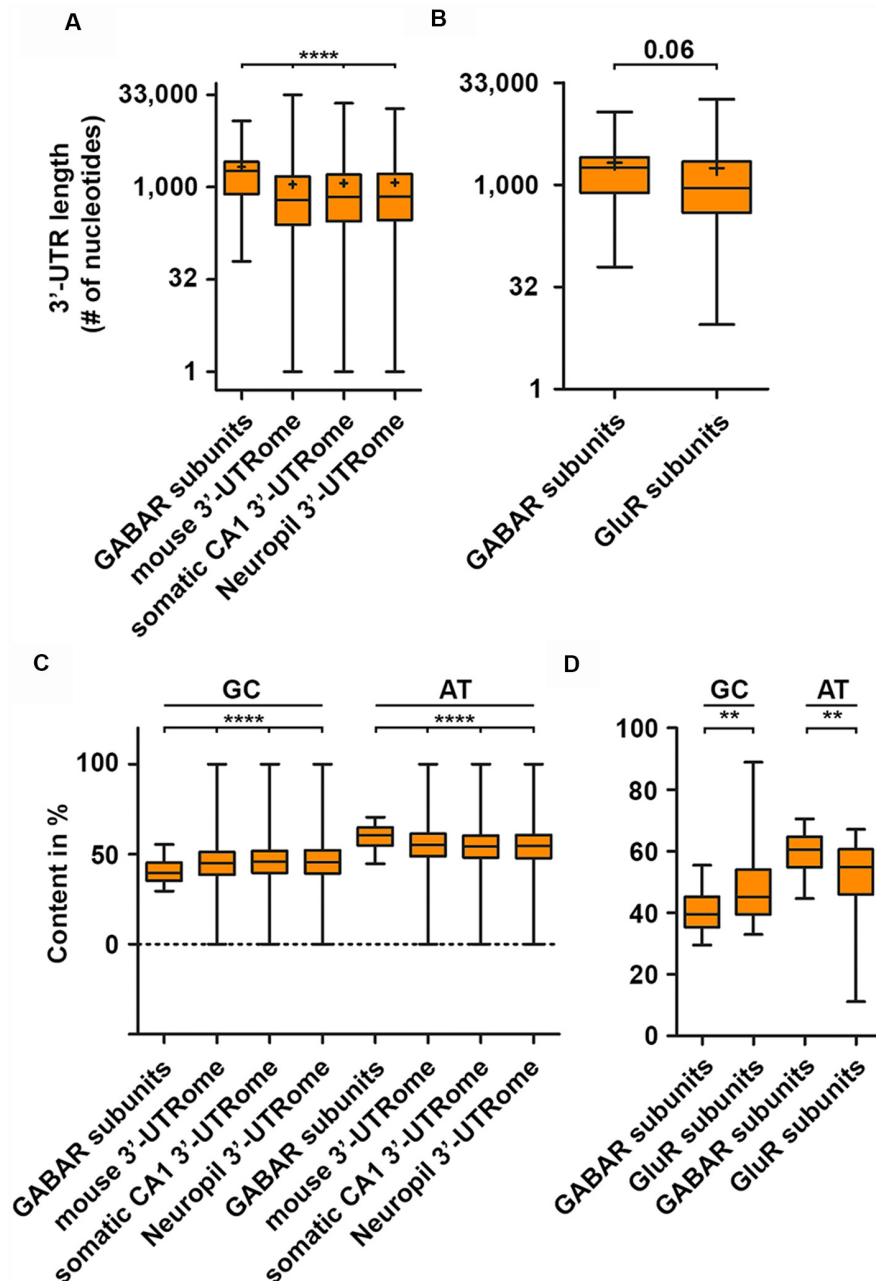


FIGURE 1 | GABA receptor (GABA_R) subunits exhibit extended 3'-untranslated region (3'-UTR) length. 3'-UTR lengths of GABA_R (GABA_A and GABA_B receptor) subunits compared to the global mouse, hippocampal CA1, neuropil 3'-UTRome (**A**) and the 3'-UTR lengths of ionotropic GluR subunits (**B**). GC and AT content of GABA_R subunits 3'-UTRs compared to the global mouse, hippocampal CA1 and neuropil 3'-UTRome (**C**) as well as ionotropic GluR subunits (**D**). Abbreviation: †represents the mean. *P*-values were calculated using the Mann-Whitney *U*-test, ***p* < 0.01, *****p* < 0.0001.

TRANSLATION CONTROL: A POSSIBLE REGULATION OF GABA RECEPTOR PROTEIN ABUNDANCE AND COMPLEX ASSEMBLY

Translation is a multistep process that is regulated by versatile proteins (Jackson et al., 2010). Different sequence features of the

mRNA that influence translation activity and association with ribosomal polysomes have been characterized in human cell lines (Floor and Doudna, 2016). In detail, the length and structural stability of the 3'-UTR, the number of miRNA binding sites as well as AU elements in the 3'-UTR are main drivers of translation activity located at the 3'-end of the untranslated region. An increase in these features is associated with decreased translation activity in non-neuronal cells (Floor and Doudna, 2016) as well

as nerve cells (Blair et al., 2017). For GABAR subunit 3'-UTRs, we observed an increase in 3'-UTR length and AT content (Figures 1A,C,D). These results suggest that translation of these subunits is strongly regulated. Supportive for this idea is the finding that GABAR subunit mRNAs are recognized and subsequently bound by different RBPs (Table 1). In the last decade, several studies revealed that RBPs control translation of their target mRNAs (Hentze et al., 2018). One extensively studied example is the FMRP. FMRP mediated translational control is crucial for neuronal homeostasis and function since loss-of-function leads to severe neurological impairments in synaptic plasticity which cause intellectual disability and social deficits hallmarked for autism spectrum disorders (Bassell and Warren, 2008; Darnell and Klann, 2013). Furthermore, recent studies showed that FMRP is needed for proper differentiation of neuronal stem cells (Castrén et al., 2005; Gao et al., 2018). FMRP has been shown to co-migrate with translationally active ribosomal polysomes (Stefani et al., 2004). However, this finding was challenged by the same study showing that polysomal co-migration is detergent sensitive (Stefani et al., 2004). A mechanistic study combining *in vitro* assays and cryoelectron microscopy reported that FMRP inhibits translation through binding to the ribosomal intersubunit space thereby precluding binding of tRNAs and translation elongation factors (Chen et al., 2014). A transcriptome-wide screen for FMRP targets associated with polysomes identified mRNAs coding for subunits of the GABA_B receptor complex (Darnell et al., 2011; see Table 1). Moreover, a recent study showed that the GABA_A receptor subunit δ was downregulated in an FMRP knock-out mouse model (Gantois et al., 2006). These findings suggest that FMRP may regulate selected subunits of the GABA_B and/or GABA_A receptor, most likely at the translational level. Another known translation regulator is Pumilio2 (Pum2). For Pum2, it was shown that it represses translation by competing with the eukaryotic initiation factor (eIF4E) for mRNA 5'-cap binding (Cao et al., 2010), an essential step to start translation initiation (Jackson et al., 2010). Moreover, Pum2 is able to form a complex with the miRNA binding protein Argonaute (Ago) and the eukaryotic translation elongation factor 1A to repress translation elongation (Friend et al., 2014). Next to its role as translation regulator, Pum2 regulates transcript stability through recruitment of the polyA deadenylase complex CCR4-NOT (Van Etten et al., 2012), which is the major protein complex to induce RNA degradation (Collart, 2016). Based on a published iCLIP dataset, Pum2 is able to bind subunits of the GABA_A and GABA_B receptor (Table 1). Interestingly, double knockdown of Pumilio1 and 2 lead to a decrease in the mRNA levels of certain GABAR subunits (Zhang et al., 2017) indicating that they may be regulated posttranscriptionally by Pumilio proteins. Another RBP that impacts the expression of GABA_A receptor subunits, is the non-octamer, POU-domain DNA-binding protein (NONO, also known as p54NRB). NONO belongs to the family of polypyrimidine tract-binding protein-associated splicing factors that are known to regulate various aspects of the RNA lifecycle including transcription regulation, splicing, RNA processing and RNA transport (Yarosh et al., 2015). Interestingly, mutations in the NONO locus causes intellectual disability in humans

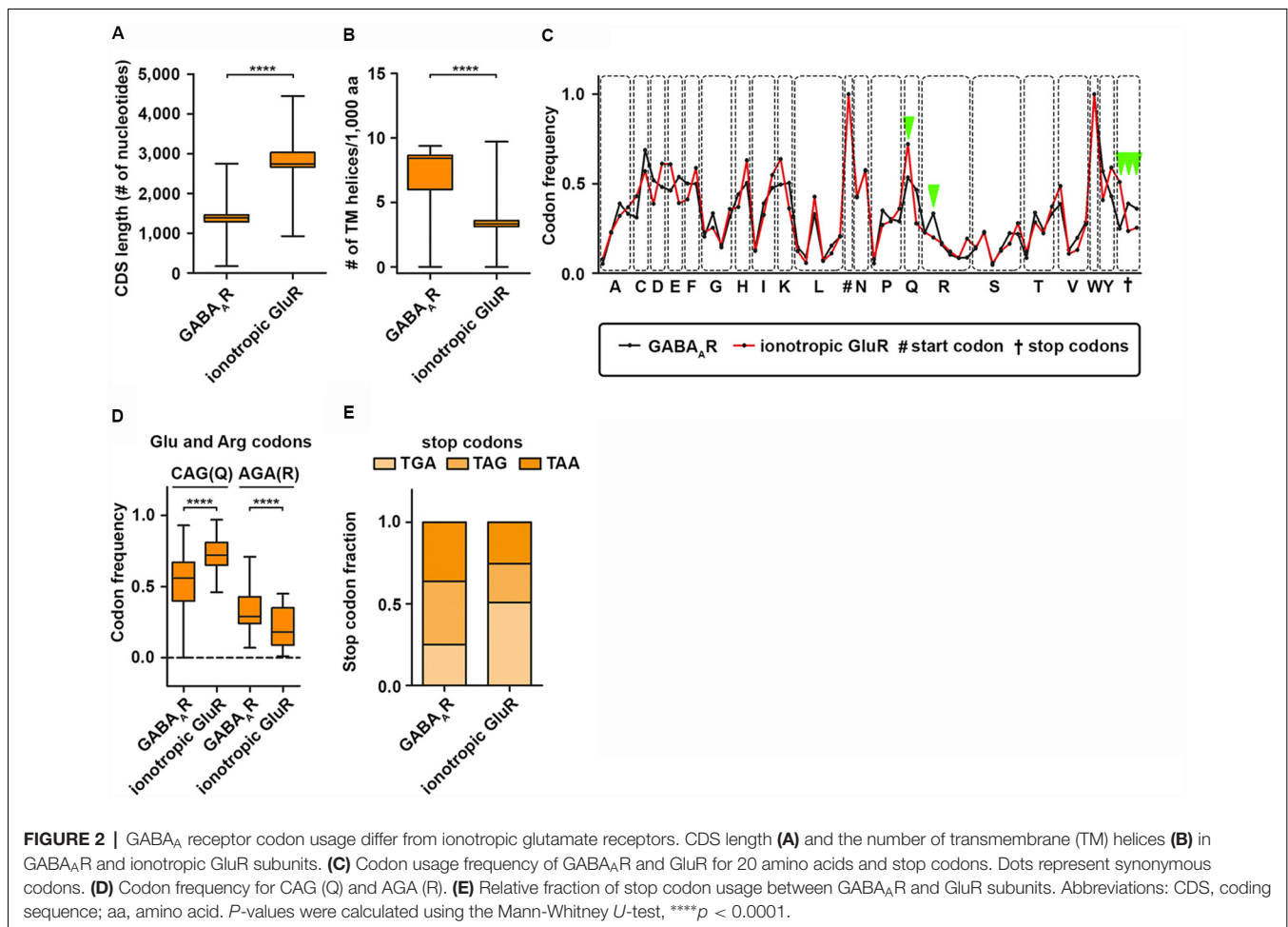
(Mircsof et al., 2015). Moreover, the authors found that the GABA_A receptor-mediated inhibition is mainly affected when NONO is depleted (Mircsof et al., 2015) suggesting that this RBP regulates directly or indirectly the expression of the GABA_A receptor. Nonetheless, it is widely unknown which GABAR subunits are translationally regulated. However, the binding of RBPs that are known to control RNA metabolism and translation, clearly suggests the existence of posttranscriptional gene regulation mechanisms for GABARs.

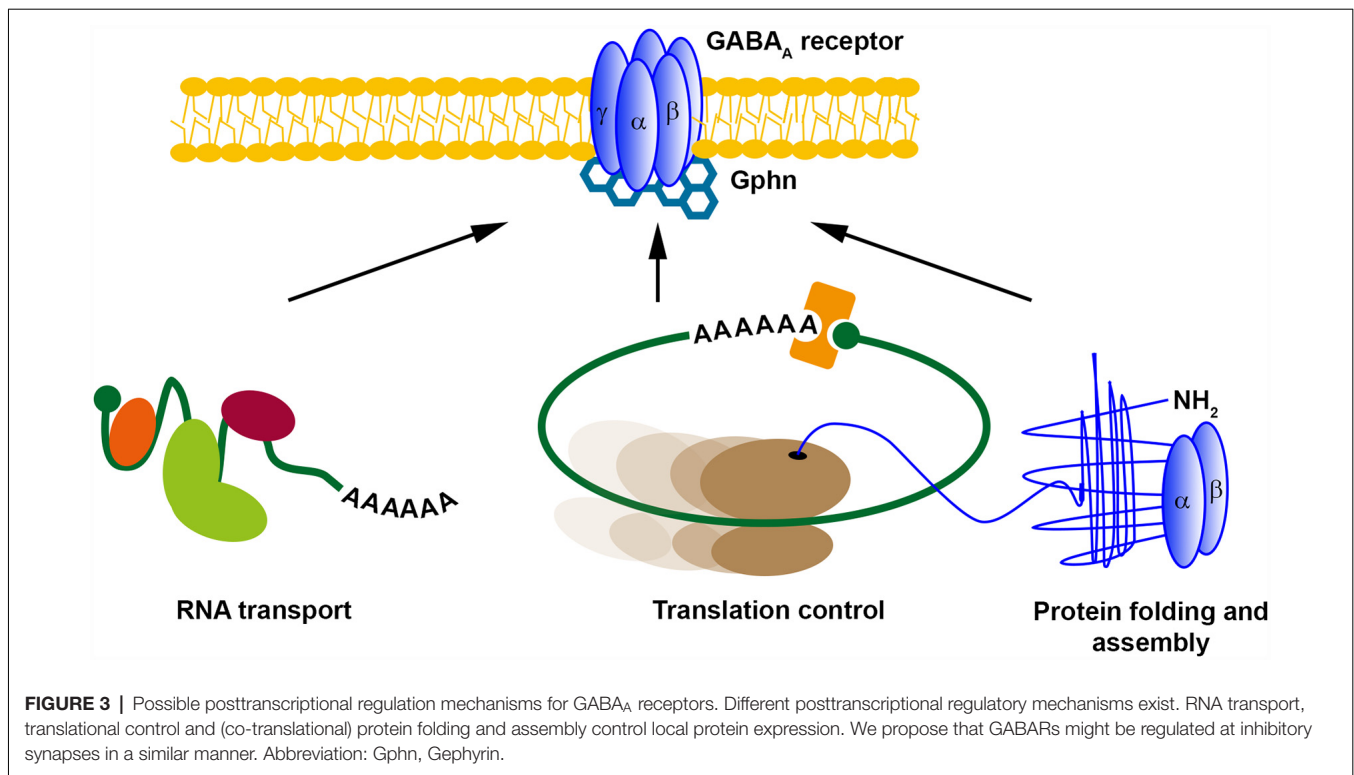
It is commonly accepted that the 3'-UTR allows for translational regulation of mRNAs. Research in the last years, however, has shown that the coding sequence (CDS) can also regulate protein synthesis rate, protein folding and protein complex assembly (Hanson and Collier, 2018). Dynamic translation regulation mediated by the CDS became experimentally accessible with the emergence of deep sequencing technologies and ribosome profiling protocols (Ingolia et al., 2009). Studies in cell lines and cultured neurons revealed that longer CDS are associated with translationally active "heavy" polyribosomes; most likely because a longer CDS can accumulate more ribosomes (Floor and Doudna, 2016; Blair et al., 2017). Interestingly, subunits of the GABA_AR receptor complex display a shorter CDS compared to ionotropic GluR subunits (Figure 2A) suggestive for differences in translation activity. Another exciting possibility to regulate protein synthesis rate and output is the usage of synonymous codons. Twenty-one amino acids are encoded by 64 codons including three stop codons in the eukaryotic genome (Alberts et al., 2014). This degeneration of the genetic code leads to a codon bias, the preferred usage of certain codons over others to encode the same amino acid. Research in the last decades has shown that the usage bias is not random, but in contrast is driven and influenced by certain features such as translation activity, mRNA stability, protein folding, protein assembly and transcription factor binding (Grantham et al., 1980; Stergachis et al., 2013; Hanson and Collier, 2018). Codons can influence translation speed (Sørensen and Pedersen, 1991) most likely through the levels of cognate and near-cognate tRNAs (Anderson, 1969; Zhang and Ignatova, 2011; Fedyunin et al., 2012; Yu et al., 2015; Hanson and Collier, 2018). Since the nascent chain initiates folding already in the ribosomal exit tunnel (Lu and Deutsch, 2005), the elongation rate can also influence protein folding and, thereby, the protein conformation as it has been shown for the Cystic Fibrosis Transmembrane Regulator (CFTR) in mammalian cells (Kirchner et al., 2017). In line with this finding, Yu et al. (2015) showed using an *in vitro* translation system that codon usage determines co-translational folding through variation in the elongation rate. In particular for a multi-domain protein, it has been suggested that cluster of rare codons flank the parts of the mRNA that code for protein domains. Thus, ribosomes attenuate at these sites allowing the nascent domains to fold first to prevent misfolding (Schieweck et al., 2016; Hanson and Collier, 2018). Protein domains, that are encoded by the downstream mRNA, can then interact with already folded protein substructures to form a functional complex. Moreover, codon usage dependent protein folding can also influence protein specificity, which

was reported for the Multi-Drug Resistance 1 protein (MDR1). A silent mutation in a rare codon changes the specificity of MDR1 (Kimchi-sarfaty et al., 2007). Together, these results strongly indicate that dynamics in the translation elongation rate determine trajectories of (co-)translational folding. Based on these results, an intriguing question raises: can codon usage influence protein folding of transmembrane proteins such as subunits of the GABA_A receptor? Interestingly, GABA_AR subunits contain more transmembrane helices compared to ionotropic GluR subunits (**Figure 2B**). This suggests that GABA_AR subunits may need more variation in translation speed to allow co-translational folding than ionotropic GluR subunits. Furthermore, GABA_AR subunits differ in their codon usage compared to GluR subunits (**Figure 2C**). Overall, the codon usage profiles between the two receptor groups are similar. For some codons, however, we detected significant differences in their frequency (**Figures 2D,E**). Interestingly, impaired translation of AGA codons leads to neurodegeneration in a mouse model (Ishimura et al., 2014). Moreover, GABA_AR and GluR subunits exploit different stop codons. While GABA_AR subunit mRNAs display an almost 1:1:1 ratio, GluR subunits prefer the TGA stop codon that yields the highest readthrough potential in mammalian cell lines (Howard et al., 2000; Bidou

et al., 2004; Loughran et al., 2014; Manuvakhova et al., 2014). In addition to co-translational folding, the assembly of large protein complexes can also occur co-translationally (Balchin et al., 2016). It has been shown that this process is crucial for the complex formation in eukaryotic cells (Shiber et al., 2018). It is tempting to speculate that for large neuronal protein complexes such as GABA_A receptors, a similar mechanism exists to ensure proper protein-protein interaction. Of note, codon usage and optimality differ dramatically in their impact on RNA stability comparing neurons and non-neuronal cells (Burrow et al., 2018). Therefore, a thorough analysis of the neuronal transcriptome and tRNAome is needed to understand the impact of codon usage on GABA_A receptor functioning.

To sum up, findings from different model organisms and cells demonstrate that translation is a highly dynamic process necessary for many aspects of the protein life cycle. For GABA_A receptors, it is widely unknown: (i) whether and how they are translationally regulated; and (ii) whether co-translational folding/assembly is necessary for proper GABA_A function. However, our bioinformatic predictions suggest that for some aspects, GABA_A receptors are prone to be subject to posttranscriptional regulation. Future studies will be clearly needed to unravel the dynamics and regulatory factors of their translation.





IS LOCAL PROTEIN SYNTHESIS A PREREQUISITE FOR PLASTICITY OF INHIBITORY SYNAPSES: A PERSPECTIVE

Since the discovery of LTP by Bliss and Lomo (1973), numerous studies have unraveled the plasticity of excitatory synapses in the brain aiming to explain the mechanism of learning and memory formation (Kandel et al., 2014). However, how inhibitory synapses undergo structural and molecular plasticity has been widely overlooked for some time (Gaiarsa and Ben-Ari, 2006). One of the first examples that inhibitory synapses show long-term plasticity was a study on Purkinje cells in the cerebellum published in 1998 (Aizenman et al., 1998). Since that time, various studies have addressed the mechanisms of how inhibitory LTP is conveyed (Castillo et al., 2011). Interestingly, in some aspects, inhibitory and excitatory LTP share similar mechanisms including the exchange of synaptic receptors (de Luca et al., 2017) as well as the importance of scaffold proteins for LTP (Petrini et al., 2014). In this context, it was shown that clustering of Gephyrin (Gphn), the major scaffold protein for inhibitory synapses (Tyagarajan and Fritschy, 2014), is essential for GABA_A receptor surface dynamics and iLTP (Petrini et al., 2014). In line with its importance for iLTP, Gphn is posttranslationally modified in response to neuronal activity (Flores et al., 2015; Ghosh et al., 2016), which may represent a molecular hub to control inhibitory transmission. Arguably, one of the most impressive examples showing the dynamics of inhibitory synapse formation is the study by Oh et al. (2016). Upon GABA stimulation, newly

formed Gphn cluster appear that are the structural basis for inhibitory synapse formation (Tyagarajan and Fritschy, 2014). Based on our bioinformatic predictions (Figures 1, 2) and RBP target screens (Tables 1, 2), it is tempting to speculate that the appearance of Gphn clusters upon GABA stimulation requires mRNA transport and, subsequently, translation. We propose that these mechanisms are necessary for inhibitory synapse formation (Figure 3). In general, future studies are clearly necessary to address the importance of posttranscriptional gene regulation for GABAergic synaptic transmission. Therefore, it needs to be investigated: (i) which GABAR component is regulated by RBPs; (ii) whether their expression is regulated at the translation, splicing and/or stability level; and (iii) whether their posttranscriptional regulation occurs locally at the synapse. Unraveling the role of RBPs in neuronal inhibition will clearly improve our understanding how neuronal networks are coordinated to find the balance between excitation and inhibition.

METHODS

For analysis, 3'-UTR sequences and length of transmembrane domains were extracted from the EMSEMBL database (genome assembly GRCm38.p6) using the Gene Ontology ID "GO:0016917" for GABARs, "GO:0008066" for glutamate receptors and "GO:0004970" for ionotropic glutamate receptors. Only annotated mRNA isoforms were analyzed. Statistics were calculated using GraphPad Prism (version 5; GraphPad, San Diego, CA, USA).

DATA AVAILABILITY

All datasets generated for this study are included in the manuscript.

AUTHOR CONTRIBUTIONS

RS and MK conceived, executed and discussed the research that is presented in this article. RS generated the figures, the table and wrote the manuscript. RS and MK edited together.

REFERENCES

- Aizenman, C. D., Manis, P. B., and Linden, D. J. (1998). Polarity of long-term synaptic gain change is related to postsynaptic spike firing at a cerebellar inhibitory synapse. *Neuron* 21, 827–835. doi: 10.1016/s0896-6273(00)80598-x
- Alberts, B., Johnson, A., Lewis, J., Morgan, D., Raff, M., Roberts, K., et al. (2014). *Molecular Biology of the Cell, 6th Edn.* New York and Abingdon: Garland Science.
- Anderson, W. F. (1969). The effect of tRNA concentration on the rate of protein synthesis. *Proc. Natl. Acad. Sci. U S A* 62, 566–573. doi: 10.1073/pnas.62.2.566
- Andreassi, C., and Riccio, A. (2009). To localize or not to localize: mRNA fate is in 3'UTR ends. *Trends Cell Biol.* 19, 465–474. doi: 10.1016/j.tcb.2009.06.001
- Balchin, D., Hayer-Hartl, M., and Hartl, F. U. (2016). *In vivo* aspects of protein folding and quality control. *Science* 353:aac4354. doi: 10.1126/science.aac4354
- Bassell, G. J., and Warren, S. T. (2008). Fragile X syndrome: loss of local mRNA regulation alters synaptic development and function. *Neuron* 60, 201–214. doi: 10.1016/j.neuron.2008.10.004
- Bidou, L., Hatin, I., Perez, N., Allamand, V., Panthier, J. J., and Rousset, J. P. (2004). Premature stop codons involved in muscular dystrophies show a broad spectrum of readthrough efficiencies in response to gentamicin treatment. *Gene Ther.* 11, 619–627. doi: 10.1038/sj.gt.3302211
- Bingol, B., and Schuman, E. M. (2006). Activity-dependent dynamics and sequestration of proteasomes in dendritic spines. *Nature* 441, 1144–1148. doi: 10.1038/nature04769
- Blair, J. D., Hockemeyer, D., Doudna, J. A., Bateup, H. S., and Floor, S. N. (2017). Widespread translational remodeling during human neuronal differentiation. *Cell Rep.* 21, 2005–2016. doi: 10.1016/j.celrep.2017.10.095
- Bliss, T. V. P., and Lomo, T. (1973). Long-lasting potentiation of synaptic transmission in the dentate area of the anaesthetized rabbit following stimulation of the perforant path. *J. Physiol.* 232, 331–356. doi: 10.1113/jphysiol.1973.sp010273
- Briese, M., Saal-Bauernschubert, L., Ji, C., Moradi, M., Ghanawi, H., Uhl, M., et al. (2018). hnRNP R and its main interactor, the noncoding RNA 7SK, coregulate the axonal transcriptome of motoneurons. *Proc. Natl. Acad. Sci. U S A* 115, E2859–E2868. doi: 10.1073/pnas.1721670115
- Burow, D. A., Martin, S., Quail, J. F., Alhusaini, N., Collier, J., and Cleary, M. D. (2018). Attenuated codon optimality contributes to neural-specific mRNA decay in *Drosophila*. *Cell Rep.* 24, 1704–1712. doi: 10.1016/j.celrep.2018.07.039
- Cajigas, I. J., Tushev, G., Will, T. J., tom Dieck, S., Fuerst, N., and Schuman, E. M. (2012). The local transcriptome in the synaptic neuropil revealed by deep sequencing and high-resolution imaging. *Neuron* 74, 453–466. doi: 10.1016/j.neuron.2012.02.036
- Cao, Q., Padmanabhan, K., and Richter, J. D. (2010). Pumilio 2 controls translation by competing with eIF4E for 7-methyl guanosine cap recognition. *RNA* 16, 221–227. doi: 10.1261/rna.1884610
- Castillo, P., C.Q. C., and Carroll, R. C. (2011). Long-term synaptic plasticity at inhibitory synapses. *Curr. Opin. Neurobiol.* 21, 328–338. doi: 10.1016/j.conb.2011.01.006
- Castrén, M., Tervonen, T., Kärkkäinen, V., Heinonen, S., Castrén, E., Larsson, K., et al. (2005). Altered differentiation of neural stem cells in fragile X syndrome. *Proc. Natl. Acad. Sci. U S A* 102, 17834–17839. doi: 10.1073/pnas.0508995102

FUNDING

This work was supported by the DFG (FOR2333, SPP1738 to MK) and the Boehringer Ingelheim Fonds (to RS).

ACKNOWLEDGMENTS

We apologize to all colleagues whose work could not be cited or discussed owing to space constraints. We thank members of the Kiebler lab for critical comments.

- Chen, E., Sharma, M. R., Shi, X., Agrawal, R. K., and Joseph, S. (2014). Fragile X mental retardation protein regulates translation by binding directly to the ribosome. *Mol. Cell* 54, 407–417. doi: 10.1016/j.molcel.2014.03.023
- Collart, M. A. (2016). The Ccr4-not complex is a key regulator of eukaryotic gene expression. *Wiley Interdiscip. Rev. RNA* 7, 438–454. doi: 10.1002/wrna.1332
- Costa-Mattioli, M., and Monteggia, L. M. (2013). mTOR complexes in neurodevelopmental and neuropsychiatric disorders. *Nat. Neurosci.* 16, 1537–1543. doi: 10.1038/nn.3546
- Darnell, J. C., and Klann, E. (2013). The translation of translational control by FMRP: therapeutic targets for FXS. *Nat. Neurosci.* 16, 1530–1536. doi: 10.1038/nn.3379
- Darnell, J. C., Van Driesche, S. J., Zhang, C., Hung, K. Y. S., Mele, A., Fraser, C. E., et al. (2011). FMRP stalls ribosomal translocation on mRNAs linked to synaptic function and autism. *Cell* 146, 247–261. doi: 10.1016/j.cell.2011.06.013
- de Luca, E., Ravasenga, T., Petrini, E. M., Polenghi, A., Nieuws, T., Guazzi, S., et al. (2017). Inter-synaptic lateral diffusion of GABAA receptors shapes inhibitory synaptic currents report inter-synaptic lateral diffusion of GABAA receptors shapes inhibitory synaptic currents. *Neuron* 95, 63–69.e5. doi: 10.1016/j.neuron.2017.06.022
- Doyle, M., and Kiebler, M. A. (2011). Mechanisms of dendritic mRNA transport and its role in synaptic tagging. *EMBO J.* 30, 3540–3552. doi: 10.1038/emboj.2011.278
- Fan, X. C., and Steitz, J. A. (1998). Overexpression of HuR, a nuclear-cytoplasmic shuttling protein, increases the *in vivo* stability of ARE-containing mRNAs. *EMBO J.* 17, 3448–3460. doi: 10.1093/emboj/17.12.3448
- Fedyunin, I., Lehnhardt, L., Böhmer, N., Kaufmann, P., Zhang, G., and Ignatova, Z. (2012). tRNA concentration fine tunes protein solubility. *FEBS Lett.* 586, 3336–3340. doi: 10.1016/j.febslet.2012.07.012
- Flexner, J., Flexner, L., and Stellar, E. (1963). Memory in mice as affected by intracerebral puromycin. *Science* 141, 57–59. doi: 10.1126/science.141.3575.57
- Floor, S. N., and Doudna, J. A. (2016). Tunable protein synthesis by transcript isoforms in human cells. *Elife* 5:e10921. doi: 10.7554/eLife.10921
- Flores, C. E., Nikonenko, I., Mendez, P., Fritschy, J., and Tyagarajan, S. K. (2015). Activity-dependent inhibitory synapse remodeling through gephyrin phosphorylation. *Proc. Natl. Acad. Sci. U S A* 112, 65–72. doi: 10.1073/pnas.1411170112
- Frey, U., and Morris, R. G. M. (1997). Synaptic tagging and long-term potentiation. *Nature* 385, 533–536. doi: 10.1038/385533a0
- Friend, K., Campbell, Z. T., Cooke, A., Kroll-Conner, P., Wickens, M. P., and Kimble, J. (2014). A conserved PUF-Ago-eEF1A complex attenuates translation elongation. *Nat. Struct. Mol. Biol.* 19, 176–183. doi: 10.1038/nsmb.2214
- Fritzsche, R., Karra, D., Bennett, K. L., Ang, F., Heraud-Farlow, J. E., Tolino, M., et al. (2013). Interactome of two diverse RNA granules links mRNA localization to translational repression in neurons. *Cell Rep.* 5, 1749–1762. doi: 10.1016/j.celrep.2013.11.023
- Gaiarsa, J., and Ben-Ari, Y. (2006). “Long-term plasticity at inhibitory synapses: a phenomenon that has been overlooked,” in *The Dynamic Synapse: Molecular Methods in Ionotropic Receptor Biology*, eds J. T. Kittler and S. J. Moss (Boca Raton, FL: CRC Press/Taylor & Francis).
- Gantois, I., Vandesompele, J., Speleman, F., Reyniers, E., D’Hooge, R., Severijnen, L. A., et al. (2006). Expression profiling suggests underexpression

- of the GABAA receptor subunit δ in the fragile X knockout mouse model. *Neurobiol. Dis.* 21, 346–357. doi: 10.1016/j.nbd.2005.07.017
- Gao, Y., Li, Y., Stackpole, E. E., Zhao, X., Richter, J. D., Liu, B., et al. (2018). Regulatory discrimination of mRNAs by FMRP controls mouse adult neural stem cell differentiation. *Proc. Natl. Acad. Sci. U S A* 115, E11397–E11405. doi: 10.1073/pnas.1809588115
- Ghosh, H., Auguadri, L., Battaglia, S., Thirouin, Z. S., Zemoura, K., Dieter, A., et al. (2016). Several posttranslational modifications act in concert to regulate gephyrin scaffolding and GABAergic transmission. *Nat. Commun.* 7:13365. doi: 10.1038/ncomms13365
- Grantham, R., Gautier, C., Gouy, M., Mercier, R., and Pavé, A. (1980). Codon catalog usage and the genome hypothesis. *Nucleic Acids Res.* 8, r49–r62. doi: 10.1093/nar/8.1.197-c
- Hanson, G., and Collier, J. (2018). Codon optimality, bias and usage in translation and mRNA decay. *Nat. Rev. Mol. Cell Biol.* 19, 20–30. doi: 10.1038/nrm.2017.91
- Hentze, M. W., Castello, A., Schwarzl, T., and Preiss, T. (2018). A brave new world of RNA-binding proteins. *Nat. Rev. Mol. Cell Biol.* 19, 327–341. doi: 10.1038/nrm.2017.130
- Heraud-Farlow, J. E., and Kiebler, M. A. (2014). The multifunctional Staufen proteins: conserved roles from neurogenesis to synaptic plasticity. *Trends Neurosci.* 37, 470–479. doi: 10.1016/j.tins.2014.05.009
- Heraud-Farlow, J. E., Sharangdhar, T., Li, X., Pfeifer, P., Tauber, S., Orozco, D., et al. (2013). Staufen2 regulates neuronal target RNAs. *Cell Rep.* 5, 1511–1518. doi: 10.1016/j.celrep.2013.11.039
- Hershkowitz, M., Wilson, J. E., and Glassman, E. (1975). The incorporation of radioactive amino acids into brain subcellular proteins during training. *J. Neurochem.* 25, 687–694. doi: 10.1111/j.1471-4159.1975.tb04389.x
- Howard, M. T., Shirts, B. H., Petros, L. M., Flanigan, K. M., Gesteland, R. F., and Atkins, J. F. (2000). Sequence specificity of aminoglycoside-induced stop codon readthrough: potential implications for treatment of Duchenne muscular dystrophy. *Ann. Neurol.* 48, 164–169. doi: 10.1002/1531-8249(200008)48:2%3C164::AID-ANA5%3E3.0.CO;2-B
- Huppertz, I., Attig, J., D'Ambrogio, A., Easton, L. E., Sibley, C. R., Sugimoto, Y., et al. (2014). iCLIP: protein-RNA interactions at nucleotide resolution. *Methods* 65, 274–287. doi: 10.1016/j.jymeth.2013.10.011
- Ingolia, N. T., Ghaemmghami, S., Newman, J. R. S., and Weissman, J. S. (2009). Genome-wide analysis *in vivo* of translation with nucleotide resolution using ribosome profiling. *Science* 324, 218–323. doi: 10.1126/science.1168978
- Ishimura, R., Nagy, G., Dotu, I., Zhou, H., Yang, X.-L., Schimmel, P., et al. (2014). RNA function. Ribosome stalling induced by mutation of a CNS-specific tRNA causes neurodegeneration. *Science* 345, 455–459. doi: 10.1126/science.1249749
- Jackson, R. J., Hellen, C. U. T., and Pestova, T. V. (2010). The mechanism of eukaryotic translation initiation and principles of its regulation. *Nat. Rev. Mol. Cell Biol.* 11, 113–127. doi: 10.1038/nrm2838
- Jung, H., Gkogkas, C. G., Sonenberg, N., and Holt, C. E. (2014). Remote control of gene function by local translation. *Cell* 157, 26–40. doi: 10.1016/j.cell.2014.03.005
- Kanai, Y., Dohmae, N., and Hirokawa, N. (2004). Kinesin transports RNA. *Neuron* 43, 513–525. doi: 10.1016/j.neuron.2004.07.022
- Kandel, E. R., Dudai, Y., and Mayford, M. R. (2014). The molecular and systems biology of memory. *Cell* 157, 163–186. doi: 10.1016/j.cell.2014.03.001
- Khoutorsky, A., Yanagiya, A., Gkogkas, C. G., Fabian, M., Prager-Khoutorsky, M., Cao, R., et al. (2013). Control of synaptic plasticity and memory via suppression of poly(A)-Binding protein. *Neuron* 78, 298–311. doi: 10.1016/j.neuron.2013.02.025
- Kiebler, M. A., and Bassell, G. J. (2006). Neuronal RNA granules: movers and makers. *Neuron* 51, 685–690. doi: 10.1016/j.neuron.2006.08.021
- Kimchi-sarfaty, C., Oh, J. M., Kim, I., Sauna, Z. E., Calcagno, A. M., Ambudkar, S. V., et al. (2007). A silent polymorphism in the MDR1 gene changes substrate specificity. *Science* 315, 525–528. doi: 10.1126/science.1135308
- Kirchner, S., Cai, Z., Rauscher, R., Kastelic, N., Anding, M., Czech, A., et al. (2017). Alteration of protein function by a silent polymorphism linked to tRNA abundance. *PLoS Biol.* 15:e2000779. doi: 10.1371/journal.pbio.2000779
- Klein, M. E., Castillo, P. E., and Jordan, B. A. (2015). Coordination between translation and degradation regulates inducibility of mGluR-LTD. *Cell Rep.* 10, 1459–1466. doi: 10.1016/j.celrep.2015.02.020
- Krug, M., Lössner, B., and Ott, T. (1984). Anisomycin blocks the late phase of long-term potentiation in the dentate gyrus of freely moving rats. *Brain Res. Bull.* 13, 39–42. doi: 10.1016/0361-9230(84)90005-4
- Lee, J. A., Damianov, A., Lin, C. H., Fontes, M., Parikshak, N. N., Anderson, E. S., et al. (2016). Cytoplasmic Rbfox1 regulates the expression of synaptic and autism-related genes. *Neuron* 89, 113–128. doi: 10.1016/j.neuron.2015.11.025
- Linden, D. J. (1996). A protein synthesis-dependent late phase of cerebellar long-term depression. *Neuron* 17, 483–490. doi: 10.1016/s0896-6273(00)80180-4
- Loughran, G., Chou, M. Y., Ivanov, I. P., Jungreis, I., Kellis, M., Kiran, A. M., et al. (2014). Evidence of efficient stop codon readthrough in four mammalian genes. *Nucleic Acids Res.* 42, 8928–8938. doi: 10.1093/nar/gku608
- Lu, J., and Deutsch, C. (2005). Folding zones inside the ribosomal exit tunnel. *Nat. Struct. Mol. Biol.* 12, 1123–1129. doi: 10.1038/nsmb1021
- Manuvakhova, M., Keeling, K., Bedwell, D. M., Manuvakhova, M., Keeling, K., and Bedwell, D. M. (2014). Aminoglycoside antibiotics mediate context-dependent suppression of termination codons in a mammalian translation system. *Cold Spring Harb. Lab. Press Oct.* 1, 1044–1055. Available at: <https://rnajournal.cshlp.org/content/6/7/1044.long>
- Mendez, R., and Richter, J. D. (2001). Translational control by CPEB: a means to the end. *Nat. Rev. Mol. Cell Biol.* 2, 521–529. doi: 10.1038/35080081
- Mircsof, D., Langouët, M., Rio, M., Moutton, S., Siquier-pernet, K., Bole-Feysot, C., et al. (2015). Mutations in NONO lead to syndromic intellectual disability and inhibitory synaptic defects. *Nat. Neurosci.* 18, 1731–1736. doi: 10.1038/nn.4169
- Murn, J., Zarnack, K., Yang, Y. J., Durak, O., Murphy, E. A., Cheloufi, S., et al. (2015). Control of a neuronal morphology program by an RNA-binding zinc finger protein, Unkempt. *Genes Dev.* 29, 501–512. doi: 10.1101/gad.258483.115
- Oh, W. C., Lutz, S., Castillo, P. E., and Kwon, H. B. (2016). De novo synaptogenesis induced by GABA in the developing mouse cortex. *Science* 353, 1037–1040. doi: 10.1126/science.aaf5206
- Parras, A., Anta, H., Santos-Galindo, M., Swarup, V., Elorza, A., Nieto-González, J. L., et al. (2018). Autism-like phenotype and risk gene mRNA deadenylation by CPEB4 mis-splicing. *Nature* 560, 441–446. doi: 10.1038/s41586-018-0423-5
- Peng, S. S.-Y., Chen, C. A., Xu, N., and Shyu, A. (1998). RNA stabilization by the AU-rich element binding, HuR, an ELAV protein. *EMBO J.* 17, 3461–3470. doi: 10.1093/emboj/17.12.3461
- Pernice, H. F., Schieweck, R., Kiebler, M. A., and Popper, B. (2016). mTOR and MAPK: from localized translation control to epilepsy. *BMC Neurosci.* 17:73. doi: 10.1186/s12868-016-0308-1
- Petrini, E. M., Ravasenga, T., Hausrat, T. J., Iurilli, G., Olcese, U., Racine, V., et al. (2014). Synaptic recruitment of gephyrin regulates surface GABAA receptor dynamics for the expression of inhibitory LTP. *Nat. Commun.* 5:3921. doi: 10.1038/ncomms4921
- Scheckel, C., Drapeau, E., Frias, M. A., Park, C. Y., Fak, J., Zucker-Scharff, I., et al. (2016). Regulatory consequences of neuronal ELAV-like protein binding to coding and non-coding RNAs in human brain. *Elife* 5:e10421. doi: 10.7554/eLife.10421
- Schieweck, R., Popper, B., and Kiebler, M. A. (2016). Co-translational folding: a novel modulator of local protein expression in mammalian neurons? *Trends Genet.* 32, 788–800. doi: 10.1016/j.tig.2016.10.004
- Sharangdhar, T., Sugimoto, Y., Heraud-Farlow, J., Fernández-Moya, S. M., Ehses, J., Ruiz de los Mozos, I., et al. (2017). A retained intron in the 3'-UTR of *Calm3* mRNA mediates its Staufen- and activity-dependent localization to neuronal dendrites. *EMBO Rep.* 18, 1762–1774. doi: 10.15252/embr.201744334
- Shashoua, V. E. (1976). Identification of specific changes in the pattern of brain protein synthesis after training. *Science* 193, 1264–1266. doi: 10.1126/science.959837
- Shiber, A., Döring, K., Friedrich, U., Klann, K., Merker, D., Zedan, M., et al. (2018). Cotranslational assembly of protein complexes in eukaryotes revealed by ribosome profiling. *Nature* 561, 268–272. doi: 10.1038/s41586-018-0462-y
- Sørensen, M. A., and Pedersen, S. (1991). Absolute *in vivo* translation rates of individual codons in *Escherichia coli*. The two glutamic acid codons GAA and GAG are translated with a threefold difference in rate. *J. Mol. Biol.* 222, 265–280. doi: 10.1016/0022-2836(91)90211-n
- Sosanya, N. M., Cacheaux, L. P., Workman, E. R., Niere, F., Perrone-Bizzozero, N. I., and Raab-Graham, K. F. (2015). Mammalian Target of

- Rapamycin (mTOR) tagging promotes dendritic branch variability through the capture of Ca²⁺/Calmodulin-dependent protein kinase II α (CaMKII α) mRNAs by the RNA-binding Protein HuD. *J. Biol. Chem.* 290, 16357–16371. doi: 10.1074/jbc.M114.599399
- Stefani, G., Fraser, C. E., Darnell, J. C., and Darnell, R. B. (2004). Fragile X mental retardation protein is associated with translating polyribosomes in neuronal cells. *J. Neurosci.* 24, 7272–7276. doi: 10.1523/JNEUROSCI.2306-04.2004
- Stergachis, A. B., Haugen, E., Shafer, A., Fu, W., Vernot, B., Reynolds, A., et al. (2013). Exonic transcription factor binding directs codon choice and affects protein evolution. *Science* 342, 1367–1372. doi: 10.1126/science.1243490
- Steward, O., Wallace, C. S., Lyford, G. L., and Worley, P. F. (1998). Synaptic activation causes the mRNA for the leg Arc to localize selectively near activated postsynaptic sites on dendrites. *Neuron* 21, 741–751. doi: 10.1016/s0896-6273(00)80591-7
- Sugimoto, Y., Vigilante, A., Darbo, E., Zirra, A., Militti, C., D'Ambrogio, A., et al. (2015). hiCLIP reveals the *in vivo* atlas of mRNA secondary structures recognized by Staufen 1. *Nature* 519, 491–494. doi: 10.1038/nature14280
- Tyagarajan, S. K., and Fritschy, J. M. (2014). Gephyrin: a master regulator of neuronal function? *Nat. Rev. Neurosci.* 15, 141–156. doi: 10.1038/nrn3670
- Ule, J., Jensen, K. B., Ruggiu, M., Mele, A., Ule, A., and Darnell, R. B. (2003). Identifies nova-regulated RNA networks in the brain. *Science* 302, 1212–1215. doi: 10.1126/science.1090095
- Van Etten, J., Schagat, T. L., Hrit, J., Weidmann, C. A., Brumbaugh, J., Coon, J. J., et al. (2012). Human Pumilio proteins recruit multiple deadenylases to efficiently repress messenger RNAs. *J. Biol. Chem.* 287, 36370–36383. doi: 10.1074/jbc.M112.373522
- Wagnon, J. L., Briese, M., Sun, W., Mahaffey, C. L., Curk, T., Rot, G., et al. (2012). CELF4 regulates translation and local abundance of a vast set of mRNAs, including genes associated with regulation of synaptic function. *PLoS Genet.* 8:e1003067. doi: 10.1371/journal.pgen.1003067
- Yang, G., Smibert, C. A., Kaplan, D. R., and Miller, F. D. (2014). An eIF4E1/4E-T complex determines the genesis of neurons from precursors by translationally repressing a proneurogenic transcription program. *Neuron* 84, 723–739. doi: 10.1016/j.neuron.2014.10.022
- Yarosh, C. A., Iacona, J. R., Lutz, C. S., and Lynch, K. W. (2015). PSF: nuclear busy-body or nuclear facilitator? *Wiley Interdiscip. Rev. RNA* 6, 351–367. doi: 10.1002/wrna.1280
- Yu, C. H., Dang, Y., Zhou, Z., Wu, C., Zhao, F., Sachs, M. S., et al. (2015). Codon usage influences the local rate of translation elongation to regulate co-translational protein folding. *Mol. Cell* 59, 744–754. doi: 10.1016/j.molcel.2015.07.018
- Zahr, S. K., Yang, G., Kazan, H., Borrett, M. J., Yuzwa, S. A., Voronova, A., et al. (2018). A translational repression complex in developing mammalian neural stem cells that regulates neuronal specification. *Neuron* 97, 520.e6–537.e6. doi: 10.1016/j.neuron.2017.12.045
- Zhang, M., Chen, D., Xia, J., Han, W., Cui, X., Neuenkirchen, N., et al. (2017). Post-transcriptional regulation of mouse neurogenesis by Pumilio proteins. *Genes Dev.* 31, 1354–1369. doi: 10.1101/gad.298752.117
- Zhang, G., and Ignatova, Z. (2011). Folding at the birth of the nascent chain: coordinating translation with co-translational folding. *Curr. Opin. Struct. Biol.* 21, 25–31. doi: 10.1016/j.sbi.2010.10.008

Conflict of Interest Statement: The authors declare that the research was conducted in the absence of any commercial or financial relationships that could be construed as a potential conflict of interest.

Copyright © 2019 Schieweck and Kiebler. This is an open-access article distributed under the terms of the Creative Commons Attribution License (CC BY). The use, distribution or reproduction in other forums is permitted, provided the original author(s) and the copyright owner(s) are credited and that the original publication in this journal is cited, in accordance with accepted academic practice. No use, distribution or reproduction is permitted which does not comply with these terms.

Manuscript I (Publication V): The RNA-binding protein Pumilio2 controls translation of the GABA_A receptor subunit GABRA2 to regulate neuronal excitation

This section contains the manuscript entitled **The RNA-binding protein Pumilio2 regulates expression of the GABA_A receptor subunit GABRA2 in the brain** by

Rico Schieweck, Therese Riedemann, Bernd Sutor, Tobias Straub and Michael A. Kiebler[‡]

[‡] corresponding author

Author contribution to this publication

Rico Schieweck and Michael A. Kiebler designed and conceptualized the study. Rico Schieweck performed all *in vitro* experiments (Figs. 1-4). Therese Riedemann and Bernd Sutor performed electrophysiological recordings. Tobias Straub analyzed microarray data (related to Fig. 1). Rico Schieweck and Michael A. Kiebler wrote and revised the manuscript.

(Rico Schieweck)

(Prof. Dr. Michael A. Kiebler)

(Prof. Dr. Heinrich Leonhardt)

The RNA-binding protein Pumilio2 regulates expression of the GABA_A receptor subunit GABRA2 in the brain

Rico Schieweck¹, Therese Riedemann², Bernd Sutor², Tobias Straub³ and Michael A. Kiebler^{1,*}

¹ Department for Cell Biology, Biomedical Center (BMC), Faculty of Medicine, LMU Munich, Germany

² Biomedical Center (BMC), Department of Physiological Genomics, Ludwig-Maximilians-University, Munich, Germany

³ Biomedical Center (BMC), Core Facility Bioinformatics, Ludwig-Maximilians-University, Munich, Germany

*Correspondence to

Michael Kiebler

Department for Cell Biology

Biomedical Center (BMC)

Medical Faculty, LMU

Großhaderner Straße 9, 82152 Planegg-Martinsried, Germany

Email: mkiebler@lmu.de

Word count abstract:

Word count text:

Key words: Pumilio2, Gabra2, epilepsy, posttranscriptional gene regulation

Running title: Pumilio2 regulates Gabra2 in neurons

Abstract

The RNA-binding protein (RBP) Pumilio2 (Pum2) is known to regulate neuronal excitability through translational repression of voltage-gated sodium channels. Pum2 deficiency is linked to epilepsy, a neurological disease characterized by neuronal hyperexcitability, in mice and humans. The underlying mechanisms of this process are, however, widely unknown. Here, we identified the $\alpha 2$ subunit of the GABA_A receptor (*Gabra2*) as mRNA target of the Pum2. Pum2 represses expression of *Gabra2* both in the brain and in cortical neurons. Interestingly, upregulation of *Gabra2* is responsible for dendritic branching deficits in Pum2 depleted neurons. Accordingly, enhanced *Gabra2* expression represses activity of presynaptic neurons. Together, our data strongly suggest that the Pum2 mediated repression of *Gabra2* expression represents a compensatory mechanism to counterbalance enhanced activity observed in Pum2 deficient neurons. Our study provides new insight into the regulatory network of RBPs and how they balance neuronal excitability.

Introduction

Neuronal inhibition is mediated by GABAergic interneurons that release γ -aminobutyric acid (GABA) from their presynaptic terminals to inhibit neuronal activity of their target cells, e.g. pyramidal cells. Therefore, GABA binding to the GABA_A receptor (GABAAR) leads to chloride ion influx and hyperpolarization¹. This process is essential for balancing neuronal activity in the brain². Dysregulation of this delicate equilibrium is linked to neurological and neuropsychiatric diseases such as epilepsy and autism spectrum disorders (ASD)^{3,4}. Thus, identifying physiologically relevant upstream regulators of GABAergic transmission is key to understand these diseases on a molecular level.

RNA-binding proteins (RBPs) bind numerous target mRNAs in the cell^{5,6}. Thereby, they regulate versatile processes in the RNA life cycle such as splicing, transport, stability and translation⁶. The RBP Pumilio2 (Pum2) is a known translation regulator⁷. It controls translation through distinct mechanisms⁸⁻¹². Pum2 represses excitatory synapse formation in cultured hippocampal neurons. Moreover, it inhibits the translation of voltage-gated sodium channels such as Nav1.6 (*Scn8a*)¹³. These results suggest a role of Pum2 in regulating neuronal excitability. Supportive for this notion is the finding that knock-down (KD) of Pum2 in mice causes epileptic seizures^{14,15}. Even though dysregulation of voltage-gated sodium (Nav) channels is a plausible explanation for epileptic seizures, electrophysiological recordings in Pum2 KD brains have shown that general excitability, which is mediated by Nav channels, is unaffected¹⁴. Instead, these recordings suggested impaired neuronal inhibition as possible cause for epilepsy in Pum2 KD mice. This is in line with recent findings showing that Pum2 is necessary for GABAergic transmission (Schieweck & Kiebler, *unpublished*). Thus, it is tempting to speculate that loss of Pum2 impacts GABAergic inhibition *in vivo*.

Here, we found that Pum2 binds and regulates the α 2 subunit of the GABAAR (Gabra2) in both mouse brain and in cultured cortical neurons. Interestingly, Gabra2 was upregulated in Pum2 depleted neurons. Knock-down of Gabra2 rescued dendritic branching deficits observed in Pum2 KD neurons. In line with this finding is the observation that double knock-down of Pum2 and Gabra2 enhanced neuronal activity. Together, these results suggest that upregulation of Gabra2 counteracts the increased

excitability observed in Pum2 KD neurons. We propose that this pathway represents a rescue mechanism to balance neuronal activity through decreased dendritic branching.

Materials and Methods

Animals

Pum2 gene trap (Pum2^{GT}) and WT mice (background: C57Bl6/J and C57Bl6/JRccHsd) were used throughout. All experiments were approved by the authors' institutional committee on animal care and performed according to German welfare legislation.

Polysome Profiling

One P21 mouse brain hemisphere was homogenized in polysome buffer (150 mM NaCl, 5 mM MgCl₂, 10 mM Tris-HCl pH 7.4, 1vol% NP-40, 1% (w/v) sodium deoxycholate supplemented with 100 µg/mL cycloheximide, CHX, and 2 mM dithiothreitol, DTT) on ice. Cultured cortical neurons (5 million cells per condition) were transduced with either shControl or shPum2 lentivirus after 10 days *in vitro* (DIV10) as described¹⁶. Medium was changed the day after and one day prior to lysis. Upon four days of shPum2 expression, cells were incubated with 100 µg/mL CHX for 10 min, washed 3 times with prewarmed Hank's Balances Salt Solution (HBSS) supplemented with 100 µg/mL CHX and then lysed in polysome buffer. Lysates were spun at 13,000 x *g* for 5 min at 4°C. Supernatant was layered onto a sucrose gradient (18% to 50% (w/v) sucrose in 100 mM KCl, 5 mM MgCl₂, 20 mM Hepes pH 7.4). Gradients were centrifuged at 35,000 rpm (SW55Ti, Beckman) for 1.5 h at 4°C and then fractionated using an automated fractionator (Piston Fractionator, Biocomp) with RNA detection at 254 nm. RNA was extracted using acidic phenol-chloroform¹⁷.

Western Blotting and Antibodies

Lysates were separated by SDS-PAGE, proteins were then transferred to nitrocellulose (pore size 0.2 µm). Membranes were blocked in blocking solution (2% (w/v) BSA, 0.1 vol% Tween 20, 0.1% (w/v) sodium azide in 1xTBS pH 7.5) for at least 1 h. Primary antibodies were diluted in blocking buffer and incubated overnight at 4°C. Membranes were washed in PBS supplemented with 0.2vol% Tween 20. Primary antibodies were detected using infrared dye labeled secondary anti-rabbit, anti-goat or anti-mouse antibodies (all 1:10,000, Li-COR Biosciences). Membranes were scanned using the Li-Cor Odyssey IR scanner.

The following antibodies were used: polyclonal rabbit anti-Pum2 1:10,000, rabbit anti-Rpl7a (both Abcam) 1:1,000, goat anti-Vinculin (Santa Cruz) 1:200, guinea pig anti-Gabra2 (Synaptic Systems) 1:1,000, mouse anti-Puromycin (PMY) (Millipore) 1:10,000, anti- β -III-Tubulin (Sigma Aldrich) 1:10,000 and monoclonal rat anti-GAPDH (Helmholtz Center Munich Antibody Core Facility) 1:20.

Immunoprecipitation of endogenous Pum2 granules

Pum2 immunoprecipitation was performed as previously described^{18,19}. In brief, one P21 mouse brain was homogenized in brain extraction buffer (25 mM HEPES pH 7.4, 150 mM KCl, 8% glycerol, 0.1% NP-40, 1 mM DTT supplemented with Complete Protease Inhibitor [Roche] and RNase Inhibitor) on ice using an hand-driven douncer. Homogenate was spun at 20.000 x g for 15 min at 4°C (S20). S20 lysate was loaded on continuous OptiPrep gradients (0% to 30% (v/v)) and spun at 40,000 rpm (SW 41 rotor, Beckman) for 2.5 h at 4°C. Gradients were fractionated in 900 μ L fractions by hand. To detect the fate of Pum2, proteins were isolated using methanol-chloroform extraction¹⁷. Pum2 enriched fractions were pooled and precleared with protein A Sepharose beads. For immunoprecipitation, anti-Pum2 or preimmune serum bound beads were blocked in brain extraction buffer supplemented with 1.25 mg/mL BSA. Precleared lysate was incubated with beads for 1.5 h at 4°C. Upon incubation, beads were washed four times in brain extraction buffer. RNA was isolated using TRIzol reagent according to manufactures manual. To control for antibody specificity, Pum2^{GT} brains¹⁵ were used for immunoprecipitation.

XRN1 treatment of total RNA

2 μ g of total RNA was incubated with 1 U of XRN1 for 1.5 h at 37°C. RNA was isolated using acidic phenol-chloroform according to the manufacturer's manual. RNA was subsequently reverse transcribed and then used for quantitative RT-PCR.

Quantitative real-time PCR (qRT-PCR)

RNA was isolated from DIV14 cultured cortical neurons using TRIzol according to the manufacturer's manual. cDNA synthesis and qRT-PCR were performed as described²⁰. *PPIA* was used as reference gene.

Schieweck *et al.* Pum2 regulates Gabra2 in neurons

Neuronal cell culture and transfection

Neuronal cell culture from rat was performed as previously described²¹ with slight modifications for cortical neurons. For transient transfection of shPum2 and control plasmids, DNA calcium phosphate coprecipitation²² was performed.

Immunostaining and image analysis

Upon fixation with 4% PFA, cells were washed with HBSS and permeabilized in 0.1% Triton X100 for 15 min at room temperature (RT) followed by washing in HBSS. Cells were immunostained as described²⁰. Antibodies were diluted in 10vol% blocking solution (rabbit polyclonal anti-Gabra2, Synaptic Systems, 1:500) and incubated overnight at 4°C. Cells were washed in HBSS and incubated with fluorescently labeled secondary antibodies (Dianova). Upon washing, coverslips were mounted in fluoromount (Sigma Aldrich). Fluorescence microscopy was performed using the Observer Z1 microscope (Zeiss) with a 63x planApo oil immersion objective (1.40 NA).

Statistics

For data analysis and statistics, prism software (version 5 GraphPad, San Diego, CA, USA) was used. Data was tested for normal distribution using either the Kolmogorov-Smirnov or the Shapiro-Wilk normality test. To calculate p-values, unpaired Student's t-test, Mann-Whitney or Kruskal-Wallis test were used, respectively. $p < 0.05$ was considered as statistically significant.

Results

Pum2 regulates *Gabra2* expression in the mouse brain

To get insight into the role of Pum2 into the regulation of neuronal excitability, we analyzed our transcriptome dataset from both wildtype (WT) and Pum2 KD (Pum2^{GT}) brains¹⁴. Interestingly, we observed a twofold increase in the mRNA expression of the $\alpha 2$ subunit of the GABAAR (*Gabra2*) (**Fig. 1A**). Surprisingly, we did not detect alterations in the expression of NMDA, AMPA receptors nor sodium and potassium channels (referred to as 'excitatory' genes). The GABAAR consists of different subunits¹. Therefore, we tested all subunits detected in our microarray dataset. Strikingly, *Gabra2* was selectively upregulated (**Fig. 1B**). We validated the effect of Pum2 on *Gabra2* expression by qRT-PCR in newborn (P0), juvenile (P21) and adult animals (**Supplementary Fig. 1A**). Importantly, we did not observe differences in the expression of vesicle release components or neuromodulatory receptors (**Supplementary Fig. 1B**). These findings point toward a unique role of Pum2 in regulating *Gabra2* expression. To get further insight into *Gabra2* expression, we performed polysome profiling by biochemically separating translationally active from dormant ribosomes. Here, we observed a similar upregulation of *Gabra2* mRNA in translationally active polysomes (**Fig. 1C**). Complementary, we found *Gabra2* protein to be starkly upregulated in Pum2^{GT} brain lysates compared to age-matched WT controls (**Fig. 1D** and **Supplementary Fig. 1C**). Next, we asked whether *Gabra2* is a Pum2 mRNA target in mouse brain. Supportive for this notion is the observation that mRNAs coding for subunits of the GABAAR exhibit a higher number of Pum2 binding sites²³ compared to transcripts coding for other receptors such as ionotropic glutamate or glycine receptors (**Supplementary Fig. 1D**). To experimentally test this hypothesis, we performed immunoprecipitation (IP) with self-made, affinity purified Pum2 antibodies upon density gradient fractionation as previously described for Stau2^{18,19} (**Supplementary Fig. 1E**). Density gradient fraction confirmed that the biochemically isolated Pum2 complexes indeed contain RNA as we observed a shift of Pum2 towards lighter fractions upon RNase1 treatment (**Fig. 1E**). In IPs of endogenous Pum2 complexes from mouse brain, we detected a threefold enrichment of *Gabra2* compared to Pum2-deficient brain tissue (**Fig. 1F**). As positive control, we included *eIF4E*, a known Pum2 mRNA target²⁴ that was enriched twofold. Importantly, other GABAAR

subunits such as *Gabra1* or transcripts coding for proteins involved in GABAergic inhibition such as *Slc12a5* (coding for KCC2) were not enriched. Moreover, we did not observe binding of Pum2 to *Grin1* coding for the NMDA receptor subunit Grin1 nor to the ribosomal RNA *18S rRNA* showing the selectivity for *Gabra2* in our Pum2 IP. Together, these results clearly show that Pum2 regulates *Gabra2* expression in the mouse brain.

Pum2 regulates translation of *Gabra2* in cultured cortical neurons

Next, we aimed at identifying the underlying mechanism of Pum2 mediated repression of *Gabra2* expression. Pum2 is able to destabilize mRNA through the recruitment of the deadenylase complex CCR4-NOT^{25,26}. To test whether depletion of Pum2 leads to an increase in mRNA stability, we measured the relative amount of uncapped mRNAs exploiting an XRN1 assay²⁷. In brief, XRN1 degrades uncapped mRNAs while capped mRNAs remain unaffected. Interestingly, we observed the same ratio of uncapped to capped mRNAs for WT and Pum2^{GT} brains (**Fig. 2A**) indicating that Pum2 does not affect *Gabra2* stability. To further investigate the impact of Pum2 on *Gabra2* expression, we downregulated Pum2 in cultured cortical neurons using either lentivirus transduction or transient transfection of an established shPum2 plasmid²⁴. Interestingly, *Gabra2* mRNA levels were not altered (**Fig. 2B**). The corresponding *Gabra2* protein levels, however, were found to be increased in Pum2 depleted neurons (**Fig 2C,D**). Importantly, this effect could be rescued by performing a double-knock down for Pum2 and *Gabra2* (**Fig. 2D** and **Supplementary Fig. 2A-D**). Together, these results suggest that Pum2 regulates *Gabra2* expression at the translational level rather than through decreasing RNA stability. To test this hypothesis, we exploited polysome profiling coupled with qRT-PCR to determine the amount of *Gabra2* mRNA in translationally active polysomes. Strikingly, we observed an increase in *Gabra2* mRNA levels associated with polysomes (**Fig. 2E**). Of note, the 50% increase of *Gabra2* mRNA in polysomes mirror the observed increase in *Gabra2* protein levels (**Fig. 2C,D**). In summary, our data strongly suggest that Pum2 regulates translation of *Gabra2* in neurons.

Gabra2 decreases dendritic branching

To determine the physiological role of Gabra2 upregulation in Pum2 depleted neurons, we simultaneously downregulated both Pum2 and Gabra2 using our shRNA tandem construct (**Fig. 2D**). First, we tested whether downregulation of Pum2 has an impact on dendritic branching in cortical neurons as shown for hippocampal neurons²⁴. Interestingly, we observed that Pum2 depleted neurons exhibited reduced dendritic branching (**Fig. 3A-C**). Next, we ask whether the upregulation of Gabra2 might be responsible for this effect. Gabra2 protein binds different proteins in the brain indicating an extra-receptor function. Amongst others, it binds ephexin-1 (Eph1)²⁸. Interestingly, Eph1 regulates growth cone collapse^{29,30}. Thus, it is tempting to speculate that increased expression of Gabra2 might recruit Eph1 to dendrites to cause growth cone collapse. To test this hypothesis, we downregulated Pum2 and Gabra2 in cortical neurons with our shRNA tandem construct. Interestingly, double knock-down completely rescued dendritic branching deficits (**Fig. 3A-C**). Together, our results clearly demonstrate that Gabra2 represses dendritic branching.

Gabra2 inhibits neuronal activity

Dendrites are essential for receiving synaptic input³¹. Hence, we speculated that decreased dendritic branching might inhibit synaptic input of Pum2 depleted neurons. To test this hypothesis, we stained against c-Fos, a known marker for neuronal activity, as it accumulates in the nucleus upon stimulation³². Strikingly, Gabra2 and Pum2 depleted cultures showed an higher number of c-Fos positive cells compared to shControl and shPum2 alone (**Fig. 4A,B**). Importantly, this effect was selectively detected in cells that surround the transfected pyramidal neuron (visualized in green). This finding indicates that postsynaptic neurons exhibit significantly higher neuronal activity. Thus, Gabra2 inhibits neuronal activity. This effect might counterbalance enhanced excitability in Pum2 depleted neurons (**Fig. 4C**).

Discussion

Pumilio2 controls translation of Gabra2 to regulate neuronal input

Pum2 is known to repress the expression of sodium channels such as Nav1.6¹³ thereby inhibiting neuronal excitability. It is generally accepted that this control might be the molecular basis for epileptic seizures in Pum2 KD animals. The role of Pum2 in neuronal inhibition, however, has not yet been addressed. Here, we show that Pum2 represses the translation of *Gabra2* in cortical neurons. *Gabra2* interacts with numerous proteins in the brain²⁸. One of its protein interactors is ephexin-1 (Eph1), a known growth cone regulator^{29,30}. It is therefore plausible that higher expression of *Gabra2* leads to enhanced Eph1 mediated growth cone collapse and, in turn, to decreased dendritic branching. Consequently, the dendritic input is reduced. Higher expression of voltage-gated sodium channels in the absence of Pum2 increase the frequency of action potentials¹³. Thus, it is tempting to speculate that decreased synaptic input balances increased sodium channel mediated excitability of Pum2 depleted neurons. Consequently, double-knock-down of Pum2 and *Gabra2* leads to enhanced neuronal activity. These findings together strongly suggest that the regulation of *Gabra2* represents a compensatory mechanism to inhibit neuronal activity. We propose that this effect is a rescue mechanism to avoid excitotoxicity in neurons. This dual regulator role of Pum2 in regulating mRNA coding for neuronal excitation and inhibition might also apply for other RBPs³³. Thus, it is tempting to speculate that RBPs balance neuronal activity through this mechanism. In summary, our study reveals an exciting, yet unexplored mechanism to regulate neuronal excitability through a dual role of RBPs in promoting and inhibiting neuronal activity. Of note, neurological and neuropsychiatric diseases such as epilepsy or ASD that are hallmarked by an imbalanced ratio of excitation and inhibition^{3,4}. Hence, Pum2 might also contribute to the pathology of these disorders. Future studies are clearly needed to unravel the role of Pum2 in ASD.

Acknowledgments

We thank Christin Illig for excellent technical assistance. We also thank Drs. Max Harner, Kai Kaila, Jan Medenbach, Dejana Mokranjac, Peter Scheiffele and members of the Kiebler lab for helpful discussions. This work was supported by the DFG (FOR2333 and SPP1738 to MAK) and the Boehringer Ingelheim Fonds (to RS). All authors read and approved the manuscript.

References

1. Möhler, H. GABA(A) receptor diversity and pharmacology. *Cell Tissue Res.* **326**, 505–16 (2006).
2. Farrant, M. & Nusser, Z. Variations on an inhibitory theme: Phasic and tonic activation of GABA A receptors. *Nat. Rev. Neurosci.* **6**, 215–229 (2005).
3. Staley, K. Molecular mechanisms of epilepsy. *Nat. Neurosci.* **18**, 367–372 (2015).
4. Rubenstein, J. L. R. & Merzenich, M. M. Model of autism: increased ratio of excitation/inhibition in key neural systems. *Genes Brain Behav.* **2**, 255–267 (2003).
5. Hentze, M. W., Castello, A., Schwarzl, T. & Preiss, T. A brave new world of RNA-binding proteins. *Nat. Rev. Mol. Cell Biol.* **19**, 327–341 (2018).
6. Jung, H., Gkogkas, C. G., Sonenberg, N. & Holt, C. E. Remote control of gene function by local translation. *Cell* **157**, 26–40 (2014).
7. Goldstrohm, A. C., Hall, T. M. T. & McKenney, K. M. Post-transcriptional Regulatory Functions of Mammalian Pumilio Proteins. *Trends Genet.* **34**, 972–990 (2018).
8. Van Etten, J. *et al.* Human Pumilio proteins recruit multiple deadenylases to efficiently repress messenger RNAs. *J. Biol. Chem.* **287**, 36370–83 (2012).
9. Miles, W. O., Tschöp, K., Herr, A., Ji, J. Y. & Dyson, N. J. Pumilio facilitates miRNA regulation of the E2F3 oncogene. *Genes Dev.* **26**, 356–368 (2012).
10. Chagnovich, D. & Lehmann, R. Poly(A)-independent regulation of maternal hunchback translation in the *Drosophila* embryo. *Proc. Natl. Acad. Sci. U. S. A.* **98**, 11359–64 (2001).
11. Friend, K. *et al.* A conserved PUF–Ago–eEF1A complex attenuates translation elongation. *Nat. Struct. Mol. Biol.* **15**, 98–116 (2014).
12. Cao, Q., Padmanabhan, K. & Richter, J. D. Pumilio 2 controls translation by competing with eIF4E for 7-methyl guanosine cap recognition. *RNA* **16**, 221–227 (2010).
13. Driscoll, H. E., Muraro, N. I., He, M. & Baines, R. A. Pumilio-2 Regulates

- Translation of Nav1.6 to Mediate Homeostasis of Membrane Excitability. *J. Neurosci.* **33**, 9644–9654 (2013).
14. Follwaczny, P. *et al.* Pumilio2-deficient mice show a predisposition for epilepsy. *Dis. Model. Mech.* **10**, 1333–1342 (2017).
 15. Siemen, H., Colas, D., Heller, H. C., Brustle, O. & Reijo Pera, R. A. Pumilio -2 Function in the Mouse Nervous System. *PLoS One* **6**, 1–14 (2011).
 16. Bauer, K. E. *et al.* Live cell imaging reveals 3'-UTR dependent mRNA sorting to synapses. *Nat. Commun.* **10**, 1–13 (2019).
 17. Wessel, D. & Flügge, U. I. A method for the quantitative recovery of protein in dilute solution in the presence of detergents and lipids. *Anal. Biochem.* **138**, 141–143 (1984).
 18. Heraud-Farlow, J. E. *et al.* Staufen2 regulates neuronal target RNAs. *Cell Rep.* **5**, 1511–8 (2013).
 19. Fritzsche, R. *et al.* Interactome of two diverse RNA granules links mRNA localization to translational repression in neurons. *Cell Rep.* **5**, 1749–1762 (2013).
 20. Sharangdhar, T. *et al.* A retained intron in the 3'- UTR of Calm3 mRNA mediates its Staufen2- and activity- dependent localization to neuronal dendrites. *EMBO Rep.* **18**, 1762–1774 (2017).
 21. Goetze, B. *et al.* The brain-specific double-stranded RNA-binding protein Staufen2 is required for dendritic spine morphogenesis. *J. Cell Biol.* **172**, 221–31 (2006).
 22. Goetze, B., Grunewald, B., Baldassa, S. & Kiebler, M. Chemically controlled formation of a DNA/calcium phosphate coprecipitate: Application for transfection of mature hippocampal neurons. *J. Neurobiol.* **60**, 517–525 (2004).
 23. White, E. K., Moore-Jarrett, T. & Ruley, H. E. PUM2, a novel murine puf protein, and its consensus RNA-binding site. *RNA* **7**, 1855–1866 (2001).
 24. Vessey, J. P. *et al.* Mammalian Pumilio 2 regulates dendrite morphogenesis and synaptic function. *Proc. Natl. Acad. Sci. U. S. A.* **107**, 3222–7 (2010).
 25. Goldstrohm, A. C., Hook, B. a, Seay, D. J. & Wickens, M. PUF proteins bind

- Pop2p to regulate messenger RNAs. *Nat. Struct. Mol. Biol.* **13**, 533–9 (2006).
26. Van Etten, J. *et al.* Human Pumilio proteins recruit multiple deadenylases to efficiently repress messenger RNAs. *J. Biol. Chem.* **287**, 36370–83 (2012).
 27. Wu, Y. *et al.* Function of HNRNPC in breast cancer cells by controlling the dsRNA-induced interferon response. *EMBO J.* **37**, 1–19 (2018).
 28. Nakamura, Y. *et al.* Proteomic characterization of inhibitory synapses using a novel phluorin-tagged γ -aminobutyric acid receptor, type a (GABAA), α 2 subunit knock-in mouse. *J. Biol. Chem.* **291**, 12394–12407 (2016).
 29. Sahin, M. *et al.* Eph-dependent tyrosine phosphorylation of ephexin1 modulates growth cone collapse. *Neuron* **46**, 191–204 (2005).
 30. Shamah, S. M. *et al.* EphA receptors regulate growth cone dynamics through the novel guanine nucleotide exchange factor ephexin. *Cell* **105**, 233–244 (2001).
 31. Nicholls, J. G. *et al.* *From Neuron to Brain, Fifth Edition.* (Sinauer Associates, 2012).
 32. Gehman, L. T. *et al.* The splicing regulator Rbfox1 (A2BP1) controls neuronal excitation in the mammalian brain. *Nat. Genet.* **43**, 706–711 (2011).
 33. Schieweck, R. & Kiebler, M. A. Posttranscriptional gene regulation of the GABA receptor to control neuronal inhibition. *Front. Mol. Neurosci.* **12**, 1–10 (2019).

Figure legends

Figure 1 Pum2 binds and regulates *Gabra2* in the brain

A. Volcano plot of transcripts that significantly changed in Pum2 deficient (Pum2^{GT}) brains compared to WT. **B.** Relative abundance of transcripts coding for subunits of the GABA_A receptor. **C.** Representative polysome profile of postnuclear brain lysates (left) and quantification of *Gabra2* mRNA in subpolysomal and polysomal fractions from WT and Pum2^{GT} brains (right). **D.** Representative immunoblot against Gabra2 from either WT or Pum2^{GT} brain lysates (n=3). Vinculin served as loading control. **E.** OptiPrep density gradient fractionation (0%-30%) of Pum2 RNA complexes. Proteins were either stained with Coomassie blue or Pum2 was detected by Western blot. **F.** Quantification of *Gabra2*, *eIF4E*, *Gabra1*, *Slc12a5*, *Grin1* and *18S* in eluates from Pum2 immunoprecipitates from either WT or Pum2^{GT} brain lysates from 2 independent experiments. P-values were calculated using unpaired Student's t-test, n=2-3 biological replicates. ** p < 0.01.

Figure 2 Pum2 regulates translation of *Gabra2* in cortical neurons

A. *Gabra2* mRNA quantification upon XRN1 treatment of isolated total RNA from WT or Pum2^{GT} brain lysates. **B.** Quantification of *Gabra2*, *Gabra1* and *Pum2* mRNA levels in total RNA isolated from shControl and shPum2 transduced cortical neurons. **C.-D.** Representative microscopy images of shControl and shPum2 transfected neurons (GFP positive) stained against endogenous Gabra2 (C) and quantification of the observed staining intensity (D). **E.** Quantification of *Gabra2* mRNA in polysomal fractions of either shControl or shPum2 transduced cortical neurons. P-values were calculated using unpaired Student's t-test. * p < 0.05, *** p < 0.001, **** p < 0.0001, ns not significant, n=3 biological replicates. Scale bar: 10 μm.

Figure 3 *Gabra2* balances activity of Pum2 depleted neurons

A.-C. Representative microscopy images (A) and Sholl analysis (B,C) of shControl, shPum2 and shPum2+shGabra2 transfected neurons. P-values were calculated using unpaired Student's t-test. * p < 0.05, ** p < 0.01, ns not significant, n=3 independent cultures. Scale bar: 10 μm.

Figure 4 Gabra2 inhibits neuronal activity

A. Representative microscopy images of shControl, shPum2 and shPum2+shGabra2 transfected neurons stained against the neuronal activity marker c-Fos. **B.** Quantification of the relative number of cFos positive cells surrounding the transfected cell (marked by an asterisk). **C.** Scheme showing how Gabra2 reduces neuronal activity in Pum2 depleted neurons. P-values were calculated using Kruskal-Wallis test. * $p < 0.05$, *** $p < 0.001$, ns not significant, n=3 independent cultures. Scale bar: 10 μm .

Supplementary Figure legends

Supplementary Figure 1 (*Related to Figures 1*)

A. Quantification of *Gabra2* mRNA in newborn (P0), juvenile (P21) and adult animals (3 month). mRNAs coding for KCC2, NKCC1 and eIF4E, respectively, were included as controls. **B.** Relative mRNA expression levels of vesicle release components and neuro-modulatory receptors in Pum2^{GT} brains. **C.** Representative Western blot against Gabra2 in three juvenile Pum2^{GT} and WT brains. **D.** Bioinformatic prediction of the Pum2 binding site (UGUANAUA) in the 3'-UTR of transcripts coding for the indicated receptors. **E.** Experimental scheme for the immunoprecipitation of endogenous Pum2 complexes from mouse brain. P-values were calculated using unpaired Student's t-test. * p < 0.05, ns not significant, n=3 biological replicates.

Supplementary Figure 2 (*Related to Figures 2*)

A./B. Representative microscopy images showing cortical neurons transfected with shControl or shGabra2 stained against endogenous Gabra2 (A) and quantification of Gabra2 staining intensity (B). **C.** Quantification of mRNAs upon *Gabra2* KD in cortical neurons. **D.** Quantification of *Gabra2* and *Pum2* mRNA, respectively in shPum2 or shPum2+shGabra2 transfected cells. P-values were calculated using unpaired Student's t-test. * p < 0.05, ** p < 0.01, *** p < 0.001, **** p < 0.0001, ns not significant, n=3-4 independent cultures. Scale bar: 10 μ m.

Figure 1: Pum2 binds and regulates *Gabra2* in the brain

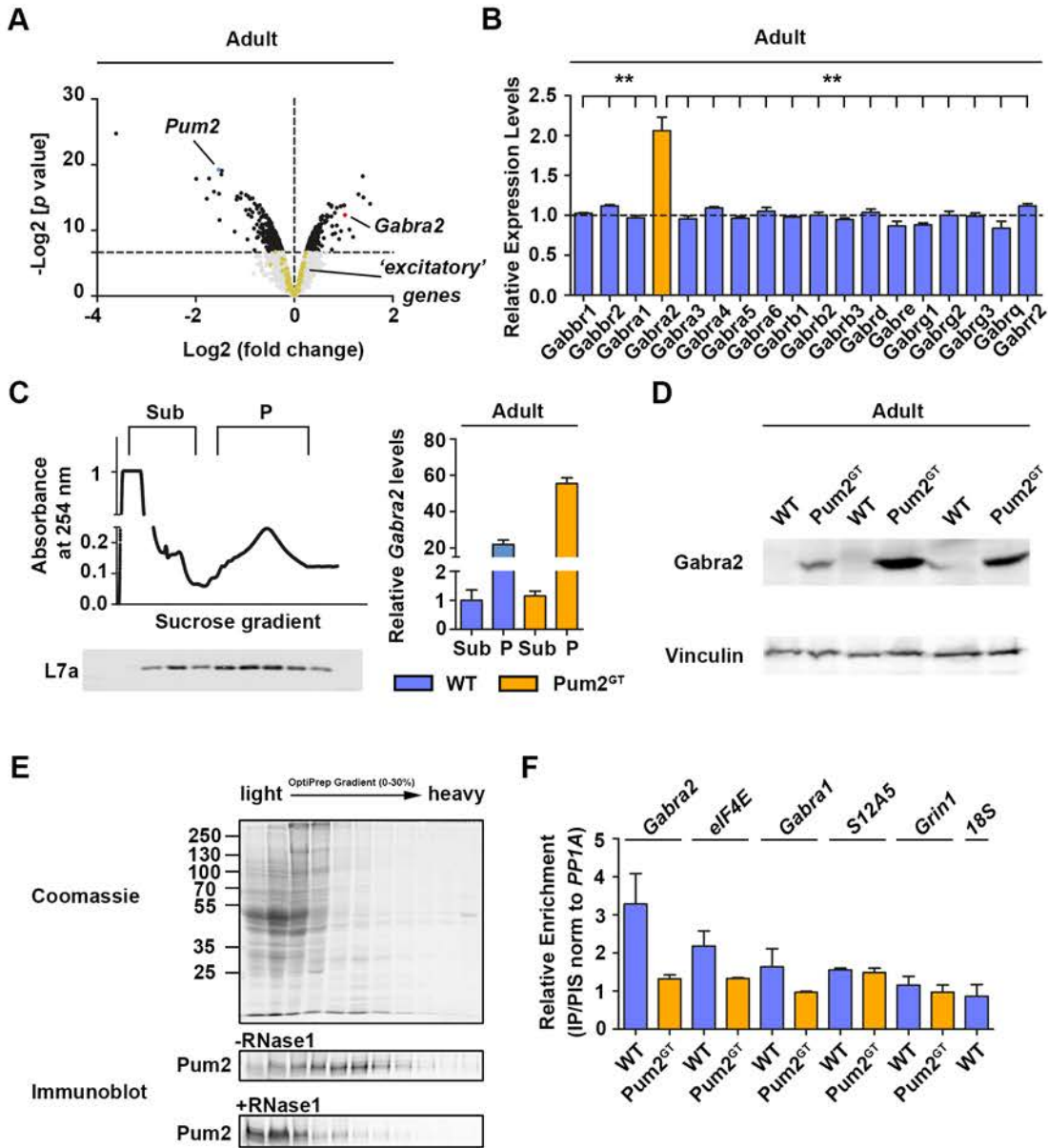


Figure 2: Pum2 regulates translation of *Gabra2* in cortical neurons

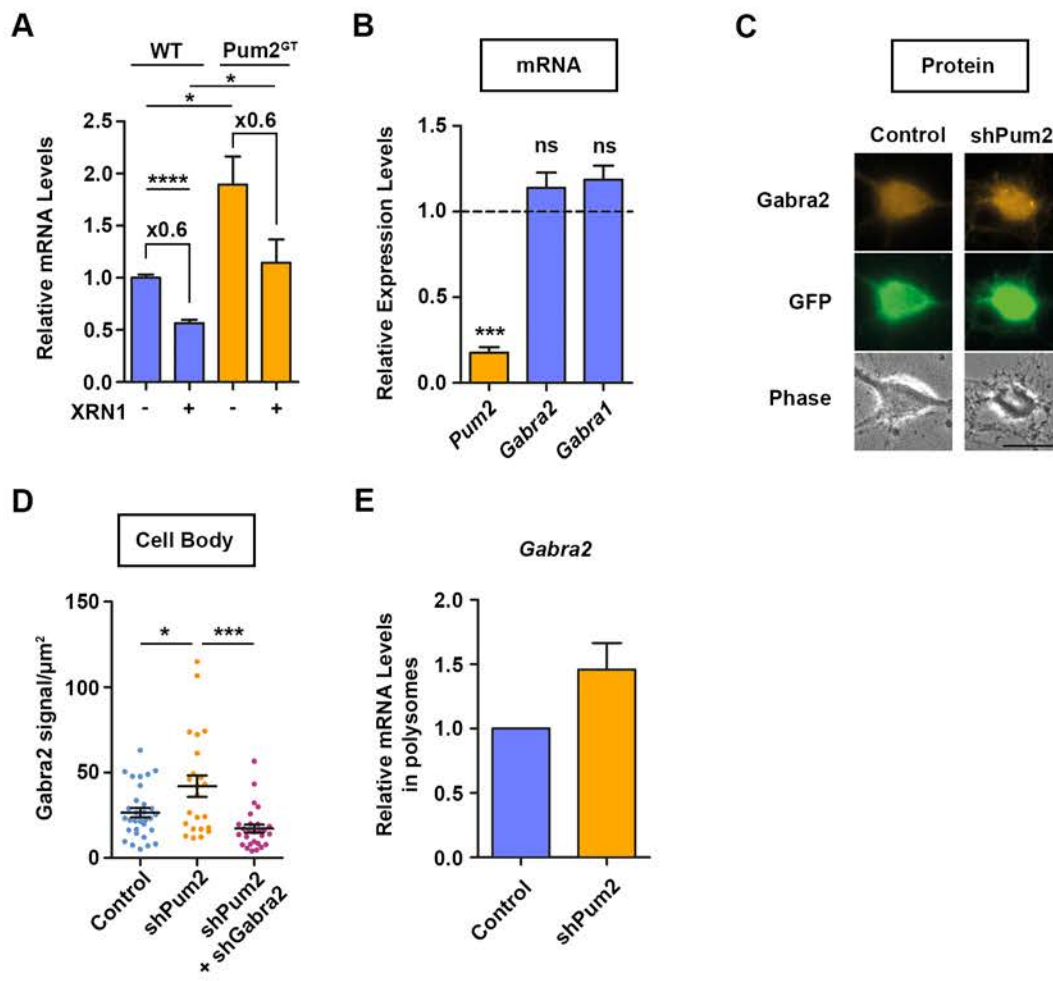


Figure 3: Gabra2 balances activity of Pum2 depleted neurons

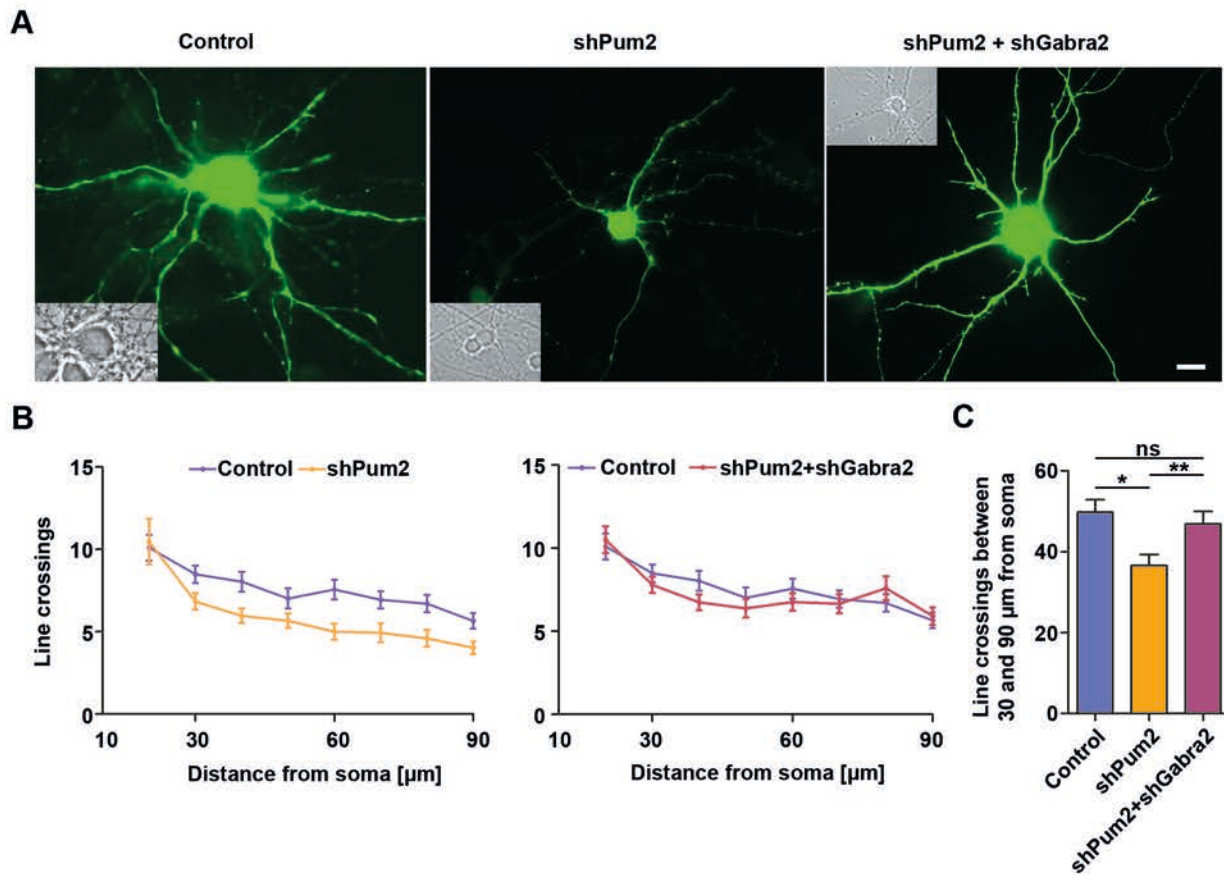
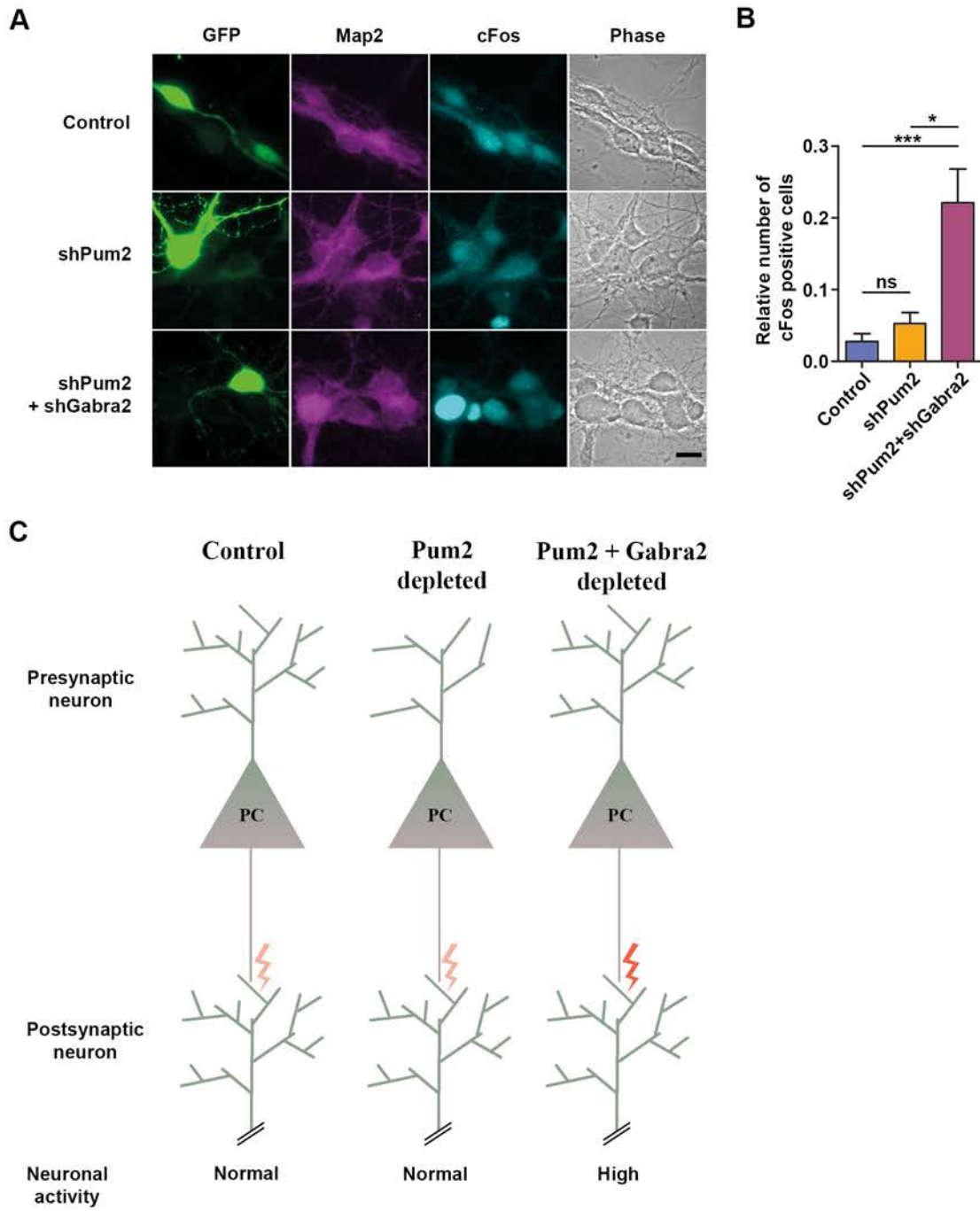
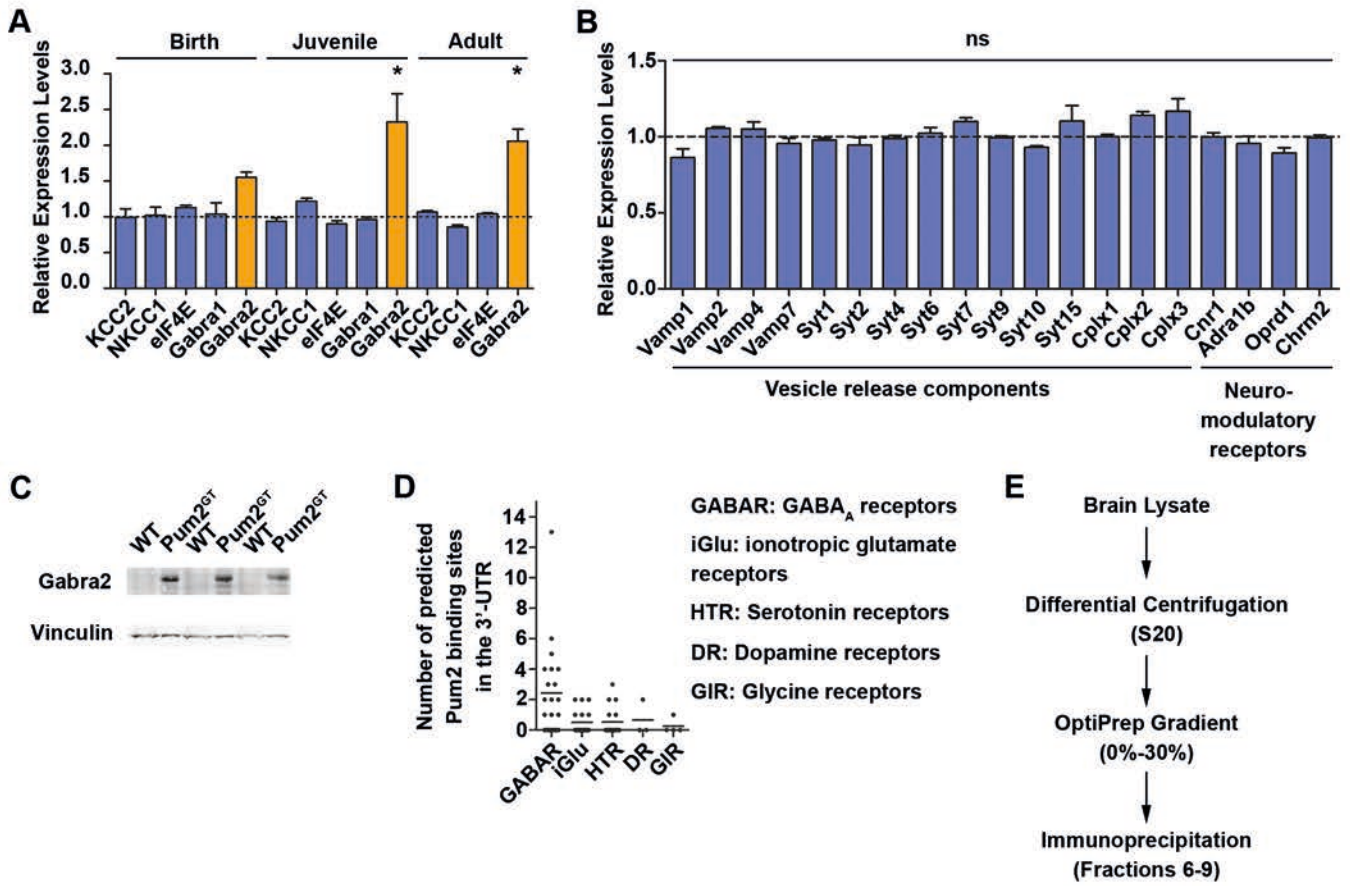


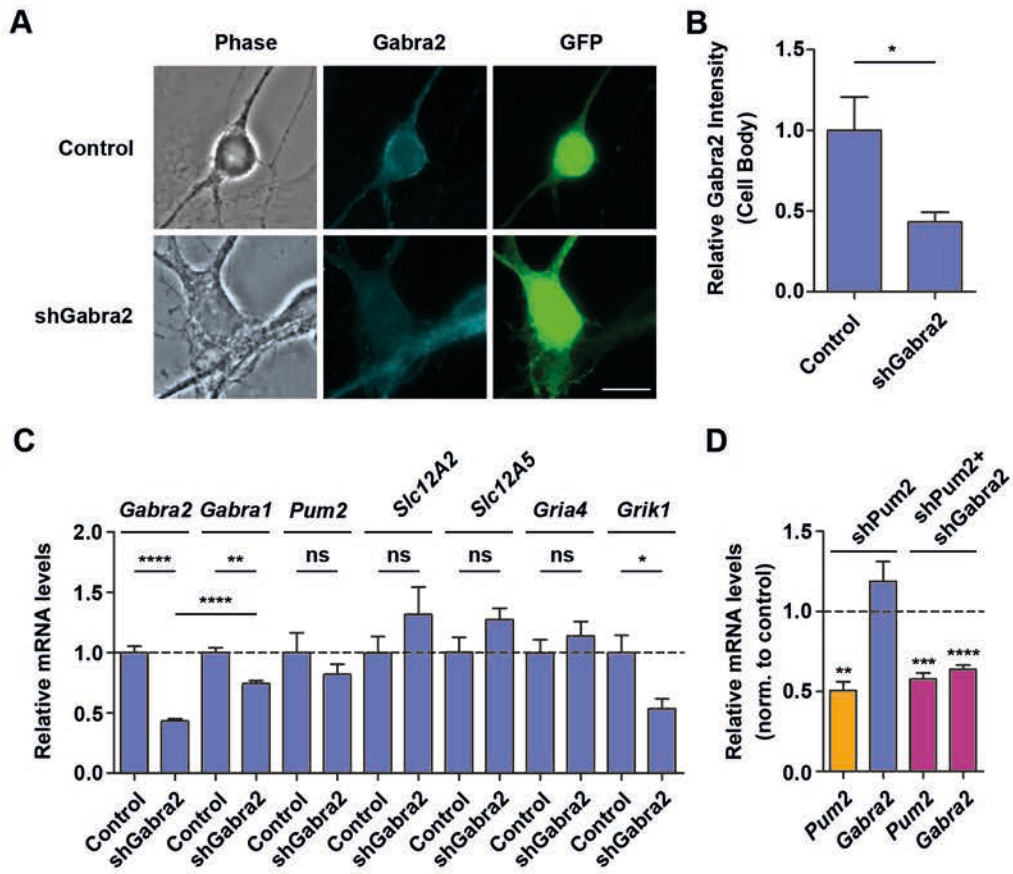
Figure 4: Gabra2 inhibits neuronal activity



Supplementary Figure 1



Supplementary Figure 2



Manuscript II (Publication VI): The RNA-binding protein Pumilio2 regulates GABAergic transmission

This section contains the manuscript entitled **The RNA-binding protein Pumilio2 regulates GABAergic transmission** by

Rico Schieweck, Therese Riedemann, Ignasi Forné, Daniela Rieger, Antonia F. Demleitner, Bastian Popper, Bernd Sutor, Axel Imhof and Michael A. Kiebler[‡]

[‡] corresponding author

Author contribution to this publication

Rico Schieweck and Michael A. Kiebler designed and conceptualized the study. Therese Riedemann and Bernd Sutor performed the electrophysiological recordings (Fig. 4). Ignasi Forné, Axel Imhof and Rico Schieweck generated and analyzed proteomics data (Fig. 3). Antonia F. Demleitner and Bastian Popper characterized the Pumilio2 deficient mouse line regarding body weight. Daniela Rieger purified Pumilio2 protein. Rico Schieweck performed all biochemical experiments, stainings and analyzed the data (Figs. 1-4). Rico Schieweck and Michael A. Kiebler wrote and revised the manuscript.

(Rico Schieweck)

(Prof. Dr. Michael A. Kiebler)

(Prof. Dr. Heinrich Leonhardt)

The RNA-binding protein Pumilio2 regulates GABAergic transmission

Rico Schieweck¹, Therese Riedemann², Ignasi Forné³, Daniela Rieger¹, Antonia F. Demleitner¹, Bastian Popper^{1,4}, Bernd Sutor², Axel Imhof³ and Michael A. Kiebler^{1,*}

¹ Biomedical Center (BMC), Department for Cell Biology & Anatomy, Medical Faculty, Ludwig-Maximilians-University, Planegg-Martinsried, Germany

² Biomedical Center (BMC), Department of Physiological Genomics, Ludwig-Maximilians-University, Planegg-Martinsried, Germany

³ Biomedical Center (BMC), Department for Molecular Biology (Protein Analysis Unit), Medical Faculty, Ludwig-Maximilians-University, Planegg-Martinsried, Germany

⁴ Biomedical Center (BMC), Core Facility Animal Models, Ludwig-Maximilians-University, Planegg-Martinsried, Germany

*Correspondence to

Michael Kiebler

Department for Cell Biology

Biomedical Center (BMC)

Medical Faculty, LMU

Großhaderner Straße 9, 82152 Planegg-Martinsried, Germany

Email: mkiebler@lmu.de

Biological sciences: neuroscience

Word count abstract:

Word count text:

Key words: Pumilio2, RNA-binding protein, translation activation, Gephyrin, neuronal inhibition

Short titles: Pumilio2 activates Gephyrin expression

Short Summary: Pum2 enhances global translation to promote GABAergic inhibition of neurons

Abstract (113 words)

The RNA-binding protein Pumilio2 (Pum2) is a known translational regulator in neurons and a well-established genetic risk factor for epilepsy. In this study, we aimed at identifying synaptic pathways that are functionally regulated by Pum2. Here, we show that Pum2 enhances global translation and activates the expression of key components of inhibitory synapses, e.g. the GABA_A receptor scaffold protein Gephyrin (Gphn), a well-known regulator of neuronal inhibition. Consequently, Pum2 depletion selectively reduces the amplitude of miniature inhibitory postsynaptic currents establishing a role of Pum2 in enhancing synaptic inhibition. As Pum2 controls neuronal excitability through voltage-gated sodium channels, it is reasonable to assume that Pum2 regulates both excitation and inhibition to balance neuronal activity.

Control of neuronal activity is a prerequisite for normal brain function. Dysregulation of the balance between excitation (E) and inhibition (I) has been linked to neurological and neuropsychiatric diseases such as epilepsy and autism spectrum disorders (ASD) (1, 2). The E/I balance is in part mediated through GABAergic inhibition, which is conveyed by the activation of γ -aminobutyric acid (GABA) type A receptors (GABAAR) (3). The molecular details, however, causing an imbalanced E/I ratio are essentially unknown. A reduction of the RNA-binding protein (RBP) Pumilio2 (Pum2) in the brain causes epileptic seizures in mice (4, 5) and has been linked to epilepsy in humans (6) suggesting that Pum2 might play a role in regulating the E/I balance.

To address this hypothesis, we investigated the impact of the translation regulator Pum2 on neuronal protein expression. First, we evaluated the interaction of Pum2 with translationally active polysomes. Differential centrifugation of mouse brain lysates (7) led to the preferential detection of Pum2 complexes in the pellet (P) compared to supernatant (S), whereas the RBP Barentsz (Btz) (8) was found exclusively in the supernatant (**Fig. 1A,B**). RNase1 treatment prior to centrifugation released Pum2 into the supernatant, whereas EDTA treatment did not, indicating that its association is RNA-mediated (**Fig. 1B**). This is not a general feature of all RBPs as the nuclear protein NeuN (Rbfox3) (9) were insensitive to RNase1 treatment. To further investigate the interaction of Pum2 with the translation machinery, we performed polysome profiling (**Fig. 1C**). When we separated translationally competent ribosomes from translationally silent ribosomes (**fig. S1A**), we could detect the majority of Pum2 in translationally dormant fractions (**Fig. 1D**) that are enriched for the translation initiation factor eIF4E. Together, our results suggest Pum2 regulates mRNA translation independently of its association with ribosomes. Moreover, our polysome profiling experiments indicate that Pum2 represses translation. Importantly, the mere association of RBPs with ribosomes does not allow to deduce its role in translational activity as recently shown for FMRP (10), a known Pum2 protein interactor (11).

We therefore performed polysome profiling (**Fig. 2A**) of Pum2-depleted versus control neurons (**Fig. 2B**). Interestingly, Pum2 knockdown significantly decreased the ratio between polysomes to monosomes, a commonly used index for translational activity (**Fig. 2C,D**). Such a decrease in the polysome to monosome ratio can also be observed when comparing Pum2 knock-down (KD) brains (Pum2^{GT}) with the corresponding tissue in WT mice (**Fig. 2E**). This indicates that the effect on translation is Pum2-dependent and not caused by shRNA expression. Accordingly, we observed a general

reduction of newly synthesized proteins (**Fig. 2F**) by performing puromycylation (PMY) assays using a PMY specific antibody (**fig. S2A,B**). This was not due to a reduction of the number of ribosomes or other essential translation factors as the levels of 18S rRNA or PABPC1 remained unaffected. In neurons lacking Pum2, we neither observed changes in phosphorylation of ribosomal protein S6, known to affect translation (12) (**fig. S2C,D**), nor in the levels of protein ubiquitination ruling out a Pum2-dependent effect on protein degradation (**fig. S2E**). Altogether, these results strongly suggest that Pum2 regulates global translation. Neuronal growth has been tightly linked to protein synthesis and protein degradation (13, 14). As decreased translation activity has an impact on cell size (15), we investigated whether Pum2 depletion in neurons affects their morphology. Consistent with its effect on translation, Pum2 depleted neurons showed a reduced cell size when compared to shControl transfected cells (**fig. S2F,G**). This seems to be a general effect as the body weight of Pum2^{GT} mice compared to age-matched WT animals is significantly reduced (**fig. S2H**). It is therefore tempting to speculate that enhanced Pum2-dependent translation critically contributes to neuronal growth.

Next, we aimed at identifying proteins affected by the Pum2 downregulation. In brief, we performed label-free mass spectrometry to determine protein abundance (**Fig. 3A**). Our analysis revealed that Pum2 significantly alters the neuronal proteome (**Fig. 3B,C**). In agreement with our results (**Fig. 2**), we observed a clear bias towards protein downregulation in Pum2 KD neurons (**Fig. 3D**). Most of the dysregulated proteins showed a moderate effect at the expression level (**Fig. 3D**). Importantly, this effect was specific for Pum2 as downregulation of Stau2 resulted in an increase in relative protein abundance (**Fig. 3E**). Accordingly, we detected a drop in peptide intensity in Pum2 depleted neurons compared to control or Stau2 depleted neurons (**Fig. 3F**). This not only confirms our polysome profiling results (**Fig. 2C,D**) but also further supports the notion of reduced general translational activity. Furthermore, we compared the proteins dysregulated in Pum2 depleted neurons with published Pum2 targets (11, 16). Surprisingly, there is only limited overlap with known Pum2 targets (**Fig. 3G**) indicating that loss of Pum2 has a global effect on mRNA translation and may not be restricted to its (direct) target mRNAs. This is in line with the finding that translation repressors such as Ago1 (17) and ZBP1 (18) were significantly upregulated while translational activators such as Impact (19) and YTHDF3 (19) were significantly downregulated (**fig. S3**). There is a subset of proteins, however, that is significantly downregulated upon

Pum2 depletion (**Fig. 3B**). Gene ontology (GO) analysis revealed the terms '*forebrain development*' and '*metabolic pathways*' to be significantly enriched. Notably, one of the strongest clusters are factors involved in GABAergic synaptic transmission (**Fig. 3C**). Importantly, protein synthesis plays an important role in releasing GABA from presynaptic terminals (20). Moreover, RBP mediated expression control has been suggested to control inhibition of the postsynaptic neuron (21). Together, these findings further support the notion that Pum2 plays a role in GABAergic synaptic transmission.

According to our proteomic data, several key regulators of GABAergic transmission were found to be downregulated: Gephyrin (Gphn), Vesicular inhibitory amino acid transporter (Vgat), Sodium- and chloride-dependent GABA transporter 1 (Gat1) and Glutamate decarboxylase 1 (Gad1) (**Fig. 4A**). Importantly, none of the detected proteins known to localize at glutamatergic synapses was affected (**Fig. 4B**). The four regulated proteins selectively contribute to GABAergic transmission, as Gphn is a key postsynaptic scaffold protein for the GABA_A receptor(22), Vgat transports GABA into presynaptic vesicles (23), Gat1 is involved in the reuptake of GABA into presynaptic terminals and Gad1 synthesizes GABA(24) (**Fig. 4C**). We decided to focus on Gphn as it is a known Pum2 target (16) and essential for GABAergic transmission (22). Pum2 KD cortical neurons were stained against Gphn (25). Interestingly, we did not see a reduction in somatic Gphn (**Fig. 4D,E**), but rather in dendrites of those neurons. The observed reduction in dendritic Gphn expression parallels those by our proteomic data (**Fig. 4A**).

Next, we tested whether this Pum2-dependent downregulation of proteins present at GABAergic synapses had any functional impact on GABAergic synaptic transmission. To this end, we recorded from shPum2- or shControl-treated neurons and analyzed spontaneous synaptic activity in these neurons. Strikingly, we observed a reduction in the amplitude of miniature inhibitory postsynaptic currents (mIPSCs), but not for inhibitory postsynaptic currents (IPSCs) or postsynaptic spontaneous postsynaptic currents (PSCs) (**Fig. 4F,G**). A similar reduction of the amplitude of GABAergic current has been reported in Gphn KO brains (26). In contrast, the frequency of mIPSCs, IPSCs and PSCs was comparable (**Fig. 4F,H**). Together, these findings argue for a postsynaptic role of Pum2 in GABAergic synaptic transmission. Moreover, we observed Gat1 to be downregulated (**Fig. 4A,C**). Accordingly, we found that the decay

time of mIPSCs and IPSCs was significantly prolonged in Pum2-depleted neurons (**Fig. 4I**), similar to Gat1 KO mouse brains (27).

In conclusion, our results provide strong experimental evidence that Pum2 activates expression of proteins independent of its ribosome association. Amongst others, Pum2 critically enhances abundance of key components of GABAergic synapses and crucially contributes to GABAergic transmission. Pum2 had previously been linked to neuronal excitation through its impact on voltage-gated sodium channels (28–30). Therefore, Pum2 appears to play a dual role in balancing excitability. This novel aspect of Pum2 mediated expression control explains in all likelihood the epileptic seizures observed in Pum2 depleted brains. Our results provide new insight into the unexpected role of the RBP Pum2 in neurological and neuropsychiatric diseases such as epilepsy or ASD thereby potentially initiating new therapeutic approaches for the treatment.

Acknowledgments

We thank Christin Illig and Sabine Thomas for excellent technical assistance. We also thank Drs. Julien Béthune, Max Harner, Jan Medenbach, Dejana Mokranjac and members of the Kiebler lab for helpful discussions. This work was supported by the DFG (FOR2333, SPP1738 to MAK and INST 86/1523 to AI) and the Boehringer Ingelheim Fonds (to RS). All authors read and approved the manuscript.

References

1. Rubenstein J L R, M. M. Merzenich, Model of autism: increased ratio of excitation/inhibition in key neural systems. *Genes Brain Behav.* **2**, 255–267 (2003).
2. C. Mullins, G. Fishell, R. W. Tsien, Unifying Views of Autism Spectrum Disorders: A Consideration of Autoregulatory Feedback Loops. *Neuron.* **89**, 1131–1156 (2016).
3. R. Tremblay, S. Lee, B. Rudy, GABAergic Interneurons in the Neocortex: From Cellular Properties to Circuits. *Neuron.* **91**, 260–292 (2016).
4. P. Follwaczny *et al.*, Pumilio2-deficient mice show a predisposition for epilepsy. *Dis. Model. Mech.* **10**, 1333–1342 (2017).
5. H. Siemen, D. Colas, H. C. Heller, O. Brustle, R. A. Reijo Pera, Pumilio -2 Function in the Mouse Nervous System. *PLoS One.* **6**, 1–14 (2011).
6. X. Wu *et al.*, Reduced Pumilio-2 expression in patients with temporal lobe epilepsy and in the lithium-pilocarpine induced epilepsy rat model. *Epilepsy Behav.* **50**, 31–39 (2015).
7. M. Mallardo *et al.*, Isolation and characterization of Staufen-containing ribonucleoprotein particles from rat brain. *Proc. Natl. Acad. Sci. U. S. A.* **100**, 2100–2105 (2003).
8. P. Macchi *et al.*, Barentsz, a new component of the Staufen-containing ribonucleoprotein particles in mammalian cells, interacts with Staufen in an RNA-dependent manner. *J. Neurosci.* **23**, 5778–5788 (2003).
9. K. K. Kim, J. Nam, Y. Mukoyama, S. Kawamoto, Rbfox3-regulated alternative splicing of Numb promotes neuronal differentiation during development. *J. Cell Biol.* **200**, 443–458 (2013).
10. E. J. Greenblatt, A. C. Spradling, Fragile X mental retardation 1 gene enhances the translation of large autism-related proteins. *Science.* **361**, 709–712 (2018).
11. M. Zhang *et al.*, Post-transcriptional regulation of mouse neurogenesis by Pumilio proteins. *Genes Dev.* **31**, 1354–1369 (2017).
12. P. E. Burnett, R. K. Barrow, N. A. Cohen, S. H. Snyder, D. M. Sabatini, RAFT1 phosphorylation of the translational regulators p70 S6 kinase and 4E-BP1. *Proc. Natl. Acad. Sci. U. S. A.* **95**, 1432–1437 (1998).
13. J. L. Franklin, E. M. Johnson, Jr., Control of neuronal size homeostasis by trophic factor-mediated coupling of protein degradation to protein synthesis. *J. Cell Biol.* **142**, 1313–1324 (1998).
14. A. C. Lloyd, The regulation of cell size. *Cell.* **154**, 1194 (2013).
15. D. C. Fingar, S. Salama, C. Tsou, E. Harlow, J. Blenis, Mammalian cell size is controlled by mTOR and its downstream targets S6K1 and 4EBP1 eIF4E. *Genes Dev.* **16**, 1472–1487 (2002).
16. S. K. Zahr *et al.*, A Translational Repression Complex in Developing Mammalian Neural Stem Cells that Regulates Neuronal Specification. *Neuron.* **97**, 520-537.e6 (2018).
17. K. S. Kosik, The neuronal microRNA system. *Nat. Rev. Neurosci.* **7**, 911–20 (2006).
18. S. Hüttelmaier *et al.*, Spatial regulation of β -actin translation by Src-dependent phosphorylation of ZBP1. *Nature.* **438**, 512–515 (2005).
19. C. M. Pereira *et al.*, IMPACT, a protein preferentially expressed in the mouse brain, binds GCN1 and inhibits GCN2 activation. *J. Biol. Chem.* **280**, 28316–28323 (2005).
20. T. J. Younts *et al.*, Presynaptic Protein Synthesis Is Required for Long-Term Plasticity of GABA Release. *Neuron.* **92**, 479–492 (2016).
21. R. Schieweck, M. A. Kiebler, Posttranscriptional gene regulation of the GABA receptor to control neuronal inhibition. *Front. Mol. Neurosci.* **12**, 1–10 (2019).
22. S. K. Tyagarajan, J. M. Fritschy, Gephyrin: A master regulator of neuronal function? *Nat. Rev. Neurosci.* **15**, 141–156 (2014).
23. S. L. McIntire, R. J. Reimer, K. Schuske, R. H. Edwards, E. M. Jorgensen, Identification and characterization of the vesicular GABA transporter. *Nature.* **389**, 870–876 (1997).
24. D. F. Owens, A. R. Kriegstein, Is there more to GABA than synaptic inhibition? *Nat. Rev. Neurosci.* **3**, 715–727 (2002).
25. E. M. Petrini *et al.*, Synaptic recruitment of gephyrin regulates surface GABA A receptor dynamics for the expression of inhibitory LTP. *Nat. Commun.* **5**, 1–19 (2014).
26. M. Kneussel *et al.*, Loss of postsynaptic GABA(A) receptor clustering in gephyrin-deficient mice. *J. Neurosci.* **19**, 9289–9297 (1999).
27. L. Bragina *et al.*, GAT-1 regulates both tonic and phasic GABAA receptor-mediated inhibition in the cerebral cortex. *J. Neurochem.* **105**, 1781–1793 (2008).
28. N. I. Muraro *et al.*, Pumilio binds para mRNA and requires Nanos and Brat to regulate sodium current in *Drosophila* motoneurons. *J. Neurosci.* **28**, 2099–109 (2008).
29. H. E. Driscoll, N. I. Muraro, M. He, R. A. Baines, Pumilio-2 Regulates Translation of Nav1.6 to

Schieweck *et al.* Pum2 activates Gephyrin expression

- Mediate Homeostasis of Membrane Excitability. *J. Neurosci.* **33**, 9644–9654 (2013).
30. W. Lin, C. N. G. Giachello, R. A. Baines, Seizure control through manipulation of Pumilio: a key component of neuronal homeostasis. *Dis. Model. Mech.* **10**, 141–150 (2017).
 31. M. A. Kiebler *et al.*, The Mammalian Staufen Protein Localizes to the Somatodendritic Domain of Cultured Hippocampal Neurons: Implications for Its Involvement in mRNA Transport. *J. Neurosci.* **19**, 288–297 (1999).
 32. K. E. Bauer *et al.*, Live cell imaging reveals 3'-UTR dependent mRNA sorting to synapses. *Nat. Commun.* **10**, 1–13 (2019).
 33. R. Fritzsche *et al.*, Interactome of two diverse RNA granules links mRNA localization to translational repression in neurons. *Cell Rep.* **5**, 1749–1762 (2013).
 34. T. Sharangdhar *et al.*, A retained intron in the 3'-UTR of Calm3 mRNA mediates its Staufen2- and activity-dependent localization to neuronal dendrites. *EMBO Rep.* **18**, 1762–1774 (2017).
 35. B. Goetze *et al.*, The brain-specific double-stranded RNA-binding protein Staufen2 is required for dendritic spine morphogenesis. *J. Cell Biol.* **172**, 221–31 (2006).
 36. J. P. Vessey *et al.*, Mammalian Pumilio 2 regulates dendrite morphogenesis and synaptic function. *Proc. Natl. Acad. Sci. U. S. A.* **107**, 3222–7 (2010).
 37. B. Goetze, B. Grunewald, S. Baldassa, M. Kiebler, Chemically controlled formation of a DNA/calcium phosphate coprecipitate: Application for transfection of mature hippocampal neurons. *J. Neurobiol.* **60**, 517–525 (2004).
 38. N. Shah *et al.*, Tyrosine-1 of RNA Polymerase II CTD Controls Global Termination of Gene Transcription in Mammals. *Mol. Cell.* **69**, 48-61.e6 (2018).
 39. X. Gao *et al.*, Quantitative profiling of initiating ribosomes in vivo. *Nat. Methods.* **12**, 147–153 (2015).
 40. J. S. Rothman, R. A. Silver, NeuroMatic: An Integrated Open-Source Software Toolkit for Acquisition, Analysis and Simulation of Electrophysiological Data. *Front. Neuroinform.* **12**, 1–21 (2018).

Figure legends

Figure 1 Pum2 granules co-migrate with translationally dormant mRNAs

(A) Experimental scheme. (B) Representative Western Blot showing Pum2, Btz and neuronal nuclei antigen (NeuN) in pellet and supernatant upon differential centrifugation of brain lysates. (C) Scheme of polysome profiling to separate translationally active from dormant ribosomes. (D) Representative polysome profile (18%-50%) of post-nuclear brain lysate and representative immunoblots for Pum2 (eIF4E as marker for the translation initiation machinery, Rpl7a for ribosomes, n=3 biological replicates).

Figure 2 Loss of Pum2 decreases translation in cultured cortical neurons

(A) Experimental scheme. (B) Representative Pum2 immunoblot from control and Pum2 depleted cortical neurons. Vinculin and β -III tubulin were used as loading controls. (C) Representative polysome profiles of post-nuclear lysates from Pum2 KD or control neurons as well as representative immunoblots for Pum2 (Rpl7a served as marker for ribosomes). (D) Polysome to monosome ratios determined by calculating the area under the polysome profile curves for cultured cortical neurons. (E) Polysome to monosome ratios calculated from polysome profiles of WT and Pum2 depleted (Pum2^{GT}) brains. Dots present individual profiles from individual brains. (F) Representative puromycin (PMY) immunoblot from control and Pum2 depleted neurons (DIV14). GAPDH served as loading control (left). Quantification of total PMY intensities from control and Pum2 KD lysates of cultured cortical neurons. P-values were calculated using paired (B, D), unpaired Student's t-test (E) or one sample t-test (F). *p < 0.05, ** p < 0.01, n=3-4 biological replicates, Scale bar: 10 μ m.

Figure 3 Pum2 promotes translation

(A) Experimental scheme. (B) Volcano plot of proteins showing differential expression in Pum2 KD neurons compared to controls. (C) GO term analysis of significantly up- and downregulated proteins in Pum2 depleted neurons. (D-E) Number (left) and histogram of relative fold change (right) of significantly up- and downregulated proteins in Pum2 (D) and Stau2 (E) KD neurons. (F) Cumulative plot of peptide intensities detected in shControl, shStau2 and shPum2 treated cells. (G) Number of significantly up- and downregulated proteins in Pum2 depleted neurons (shPum2) that are Pum2

mRNA targets identified in two independent studies (1 = Zhang *et al.*, 2 = Zahr *et al.*). P-values were calculated using unpaired Student's t-test (B) or Mann Whitney test (F). *** $p < 0.001$; ns, not significant, n=4 biological replicates.

Figure 4 Pum2 regulates GABAergic synapses

Relative abundance of proteins essential for GABAergic (A) and glutamatergic (B) transmission in Pum2 depleted neurons. Dots represent biological replicates. (C) Cartoon of an inhibitory synapse highlighting proteins that are downregulated in Pum2 deficient neurons. (D) Representative phase and fluorescence images of shControl and shPum2 transfected neurons. Cells were stained against Gphn. (E) Quantification of Gphn signal in the cell body (left) and in dendrites (right). Dots represent individual neurons. (F-I) Electrophysiological recordings of shControl and shPum2 transduced neurons. Representative current traces of IPSCs and mIPSCs (F, left) as well as representative averaged trace of IPSCs (grey) and mIPSCs (colored) (F, right). Quantification of amplitude, frequency and decay time of mIPSCs (G), IPSCs (H) and postsynaptic currents (I). P-values were calculated using unpaired Student's t-test, * $p < 0.05$, ** $p < 0.01$, *** $p < 0.001$, **** $p < 0.0001$, ns, not significant, n=3 biological replicates, Scale bar: 10 μm .

Supplementary Materials

Materials and Methods

Animals

Pum2 gene trap (Pum2^{GT}) and WT mice (background: C57Bl6/J and C57Bl6/JRccHsd) were used throughout. All experiments were approved by the institutional committee on animal care and performed according to German welfare legislation.

Differential centrifugation and sucrose cushion centrifugation

One brain hemisphere of postnatal day 21 (P21) mouse (Bl6/J) was homogenized in homogenization buffer (HB; 150 mM KCl, 50 mM Hepes pH 7.4, 1x complete protease inhibitor [Roche], 5 μ L Ribolock [ThermoFisher] per 10 mL HB) on ice using a hand-driven glass douncer. Homogenate was spun at 16,000 x *g* for 10 min at 4°C (S16, P16). Supernatant S16 was then spun at 100,000 x *g* for 20 min at 4°C (S100, P100). When required, samples were treated with RNase1 prior to centrifugation. P100 pellets were volume-even resuspended in RIPA buffer (150 mM NaCl, 50 mM Tris-HCl pH 8, 0.5% (w/v) sodium deoxycholate, 1vol% NP-40, 0.1% (w/v) SDS, 1x complete protease inhibitor [Roche]) at 37°C. All fractions used were methanol/chloroform extracted(31). Pum2 and Barentsz (Btz) were detected by Western blotting.

For sucrose cushion centrifugation, one P21 mouse brain was homogenized in polysome lysis buffer (150 mM NaCl, 5 mM MgCl₂, 10 mM Tris-HCl pH 7.4, 1vol% NP-40, 1% (w/v) sodium deoxycholate supplemented with 100 μ g/mL cycloheximide, CHX, and 2 mM dithiothreitol, DTT) at 4°C as described above. Lysate was spun at 13,000 x *g* for 5 min at 4°C. Postnuclear lysate was loaded on 2 mL 20% sucrose cushion (20%(w/v) sucrose, 100 mM KCl, 5 mM MgCl₂, 20 mM Hepes pH 7.4) and centrifuged for 2 h at 100,000 rpm (SW41Ti, Beckman rotor) at 4°C. Pellets were resuspended in SDS Laemmli buffer, separated by SDS PAGE and transferred to nitrocellulose by Western blotting.

Polysome Profiling

One P21 mouse brain hemisphere was homogenized in polysome buffer on ice as described above. Cultured cortical neurons (5 million cells per condition) were transduced with either shControl or shPum2 lentivirus after 10 days *in vitro* (DIV10) as

described (32). Medium was changed the day after and one day prior to lysis. Upon four days of shPum2 expression, cells were incubated with 100 µg/mL CHX for 10 min, washed 3 times with prewarmed Hank's Balances Salt Solution (HBSS) supplemented with 100 µg/mL CHX and then lysed in polysome buffer. Lysates were spun at 13,000 x *g* for 5 min at 4°C. Supernatant was layered onto a sucrose gradient (18% (w/v) to 50% (w/v) sucrose in 100 mM KCl, 5 mM MgCl₂, 20 mM Hepes pH 7.4) and centrifuged at 35,000 rpm (SW55Ti, Beckman) for 1.5 h at 4°C. Gradients were fractionated into 10x 500 µL fractions using an automated fractionator (Piston Fractionator, Biocomp) with RNA detection at 254 nm. 150 µL were used for protein extraction using methanol/chloroform extraction (31).

Western Blotting and Antibodies

Lysates were separated by SDS-PAGE. Proteins were transferred to nitrocellulose (pore size 0.2 µm). Membranes were incubated in blocking solution (2% (w/v) BSA, 0.1 vol% Tween 20, 0.1% (w/v) sodium azide in 1xTBS pH 7.5) for at least 1 h. Primary antibodies were diluted in blocking solution and incubated overnight at 4°C. Membranes were washed in PBS supplemented with 0.2vol% Tween 20. Primary antibodies were detected using infrared dye labeled secondary anti-rabbit, anti-goat or anti-mouse antibodies (all 1:10,000, Li-COR Biosciences). Membranes were scanned using the Licor Odyssey IR scanner.

The following antibodies were used: polyclonal antibodies: rabbit anti-Pum2 (Abcam) 1:10,000, self-made rabbit anti-Btz(33) 1:500, rabbit anti-Rpl7a (Abcam) 1:1,000, rabbit anti-Rps6 1:1,000, rabbit anti-phospho-Rps6 1:1,000, rabbit anti-PABP1 (all Cell Signaling) 1:1,000, goat anti-Vinculin (Santa Cruz) 1:200, mouse anti-Puromycin (PMY, Millipore) 1:10,000, anti-β-III-Tubulin (Sigma Aldrich) 1:10,000 and monoclonal rat anti-GAPDH (Helmholtz Center Munich Antibody Core Facility) 1:20.

Quantitative real-time PCR (qRT-PCR)

RNA was isolated from DIV14 cultured cortical neurons using TRIzol according to the manufacturer's manual. cDNA synthesis and qRT-PCR were performed as described (34). *PPIA* was used as reference gene.

Neuronal cell culture and transfection

Neuronal cell culture from rat was performed as described (35) with slight modifications for cortical neurons. For transient transfection of shPum2 and control plasmids (36), DNA calcium phosphate coprecipitation was performed (37).

Label-free mass spectrometry (LC-MS/MS)

For proteome analysis, 6 million cortical neurons were transduced with either shControl, shPum2 or shStau2 lentivirus as described (32). Proteins were digested with trypsin and analyzed by LC-MS as described (38). Data was analyzed by Maxquant 1.5.2.8 using default parameters. The String Database was used for Gene Ontology (GO) analysis.

Puromycylation of cultured cortical neurons

Puromycylation was performed as described (39). In brief, cultured cortical neurons were incubated with 25 μ M PMY for 15 min. Cells were washed 3 times with prewarmed HBSS and lysed in Laemmli buffer.

For immunostaining, cortical cells were plated on coverslips and incubated for 5 or 10 min with 1 μ M PMY. For controls, cells were either preincubated with 100 μ g/mL CHX for 10 min followed by 10 min 1 μ M PMY incubation or left untreated. For surface staining, anti-PMY antibody was used at 1:500.

Immunostaining and image analysis

Upon fixation with 4% PFA, cells were washed with HBSS and permeabilized in 0.1% Triton X100 for 15 min at room temperature (RT) followed by washing in HBSS. Cells were then incubated in blocking solution (2% FCS, 2% BSA, 0.2% fish gelatin [Sigma], in 1x PBS) for at least 30 min at RT. Antibodies were diluted in 10vol% blocking solution (mouse monoclonal anti-PMY [Millipore], mouse monoclonal anti-Gphn [Synaptic Systems] both 1:500) and incubated overnight at 4°C. Cells were washed in HBSS and incubated with fluorescently labeled secondary antibodies (Dianova). Upon washing, coverslips were mounted in fluoromount (Sigma Aldrich). Fluorescence microscopy was performed using the Observer Z1 microscope (Zeiss) with a 63x planApo oil immersion objective (1.40 NA). For distal dendrites, z-stacks were acquired (optimal step size 0.26 nm as suggested by the ZEN software, ZEISS). Images were subjected to deconvolution using the Zen software using default parameters.

Whole-cell patch-clamp recordings

All electrophysiological recordings were performed blindly. For whole-cell patch-clamp, coverslips with cultured cortical neurons were transferred to an organ bath mounted on the stage of an upright microscope (BX-RFA-1-5, Olympus, Japan). A single coverslip was continuously perfused with artificial cerebro-spinal fluid (ACSF) containing (in mM): NaCl (125), KCl (3), NaH₂PO₄ (1.25), NaHCO₃ (25), CaCl₂ (2), MgCl₂ (2) and D-Glucose (25 mM). The ACSF was saturated with 95% O₂ / 5% CO₂ to maintain a pH of 7.4. The osmolarity of the ACSF ranged between 305 to 318 mOsmol. The perfusion rate with ACSF was set to 3 mL / min and recordings were performed at 28°C. Cultured cells were visualized with a Dodt contrast tube (DGC, Scientifica, UK) that was attached to the microscope. Successfully transduced neurons were identified by RFP expression with the help of a fluorescence lamp (pE-300, CoolLED, UK) and epifluorescence optics for green fluorescence (filter: ZT473dcrb, Chroma, USA). Images were taken and displayed using a software-operated microscope camera (Evolve 512 Delta, Teledyne Photometrics, USA). The electrodes for whole cell patch-clamp recordings were fabricated from borosilicate glass capillaries (OD: 1.5 mm, ID: 0.86 mm, Hugo Sachs Elektronik-Harvard Apparatus, March-Hugstetten, Germany) and filled with a solution composed of (in mM): KCl (139), NaCl (2), EGTA (0.2), HEPES (10), Mg-ATP (4), Na-GTP (0.5), and phosphocreatine (10) (pH: 7.25 – 7.30, osmolarity: about 290 mOsmol). The electrodes (resistance: 4-5 MW) were connected to the headstage of a npi ELC-03XS amplifier (npi, Tamm, Germany). The recorded signals were amplified (x20), filtered at 3 kHz (voltage clamp), digitized at a sampling rate of 10 kHz and stored on a computer for off-line analysis. Data acquisition was performed by means of a CED 1401 Power 3 system in conjunction with the Signal6 data acquisition software (Cambridge electronic design, Cambridge, England).

All spontaneous synaptic activity was recorded at a holding potential of -60 mV for 5 minutes. Inhibitory postsynaptic currents (IPSCs) were recorded in the presence of the AMPA receptor blocker 2,3-dihydroxy-6-nitro-7-sulfamoyl-benzo[f]quinoxaline-2,3-dione (NBQX, 10 µM) and in the presence of the NMDA receptor blocker D-2-amino-5-phosphonopentanoate (D-AP5, 20 µM). Miniature inhibitory postsynaptic currents were recorded in the presence of tetrodotoxin (TTX, 0.5 µM). Data analysis was performed using IGOR Pro 6 (WaveMetrics, Lake Oswego, USA) together with the NeuroMatic IGOR plugin(40). Spontaneous synaptic events were automatically detected using the algorithm provided by the NeuroMatic plugin (version 2.00) for

IgorPro. The detection threshold was set to 15 pA. Only monophasic synaptic currents were analyzed, and the following parameters were determined: PSC frequency, peak amplitude and decay time.

All chemicals and drugs were obtained from Sigma-Aldrich (Munich, Germany) and Biotrend (Cologne, Germany), respectively. All drugs were added to the bathing solution.

Statistics

For data analysis and statistics, prism software (version 5 GraphPad, San Diego, CA, USA) was used. Data was tested for normal distribution using either the Kolmogorov-Smirnov or the Shapiro-Wilk normality test. To calculate p-values, paired, unpaired Student's t-test or Mann-Whitney test were used, respectively. Paired Student's t-test was used for paired, dependent samples to correct for variation in primary neuronal cultures. $p < 0.05$ was considered as statistically significant.

Supplementary Figure legends

Supplementary Figure 1 (Related to Figures 1) Pum2 does not associate with translating polysomes

Representative polysome profiles of cortical neurons upon incubation with CHX or Harringtonine, respectively, including representative Pum2 immunoblots (Rpl7a served as marker for ribosomes, n=2 biological replicates).

Supplementary Figure 2 (Related to Figures 2) Pum2 does not affect mTOR activity nor Ubiquitin-dependent proteolysis

(A) Representative immunostainings of cortical neurons upon puromycylation (1 μ M PMY treatment for 5 or 10 min) and labeling with anti-PMY antibody. Translation inhibitor CHX was added prior to PMY for 10 min. (B) PMY signal in cell bodies (>24 cells were quantified for each condition, two independent cultures). (C) Normalized qRT-PCR results for 18S rRNA from total RNA extracted from control and shPum2 transduced neurons (DIV14). *PPIA* was used as reference gene. (D) Representative immunoblots for Rpl7a, Rps6, p-Rps6 and PABPC1 (left). Quantification of immunoblots (right) normalized to Vinculin and β -III Tubulin (n=3). (E) Representative immunoblot against Ubiquitin (α -tubulin served as loading control, left) and quantification (right). (F/G) Representative phase and fluorescence images of shControl and shPum2 transfected mature cortical neurons (F) and quantification of cell body size (> 38 cells were measured for each condition, n > 4 cultures, G). (H) Body weight of WT and Pum2^{GT} animals (n=11-12). P-values were calculated using Mann-Whitney test. ** p < 0.01, **** p < 0.0001; ns, not significant; Scale bar: 10 μ m

Supplementary Figure 3 (Related to Figures 3) Pum2 affects expression of key translation regulators

Protein fold change of hand-selected translation regulators Ago1, ZBP1, Impact and YTHDF3. Dots represent biological replicates (n=4).

Figure 1: Pum2 granules co-migrate with translationally dormant mRNAs

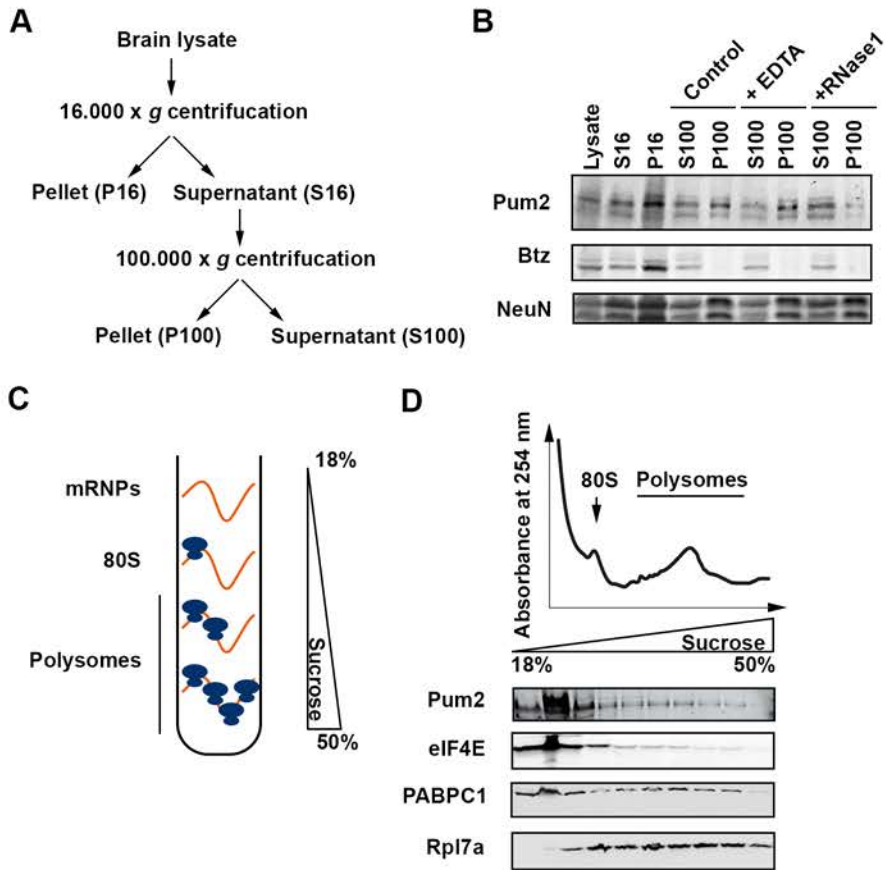


Figure 2: Loss of Pum2 decreases translation in cultured cortical neurons

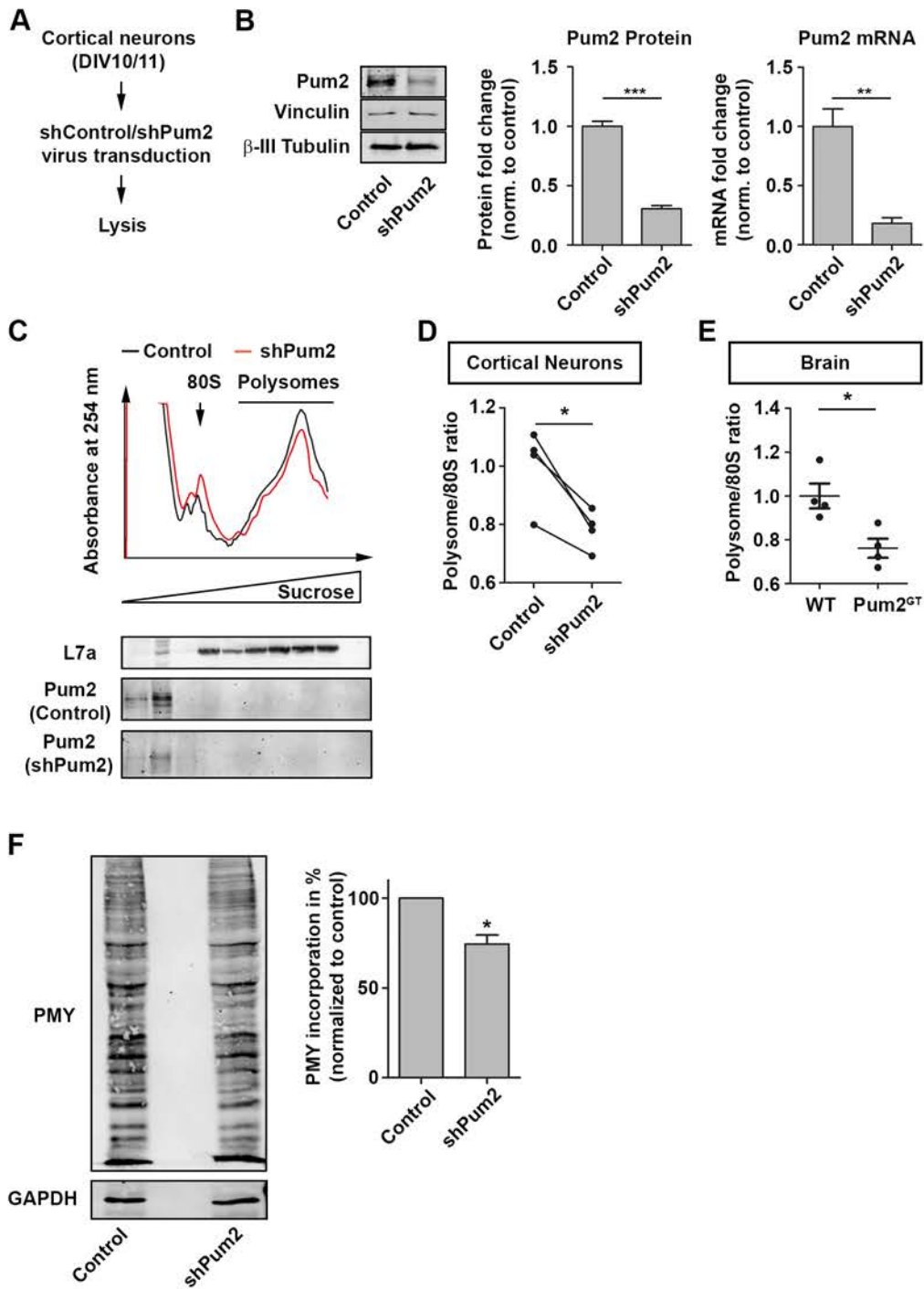


Figure 3: Pum2 promotes translation

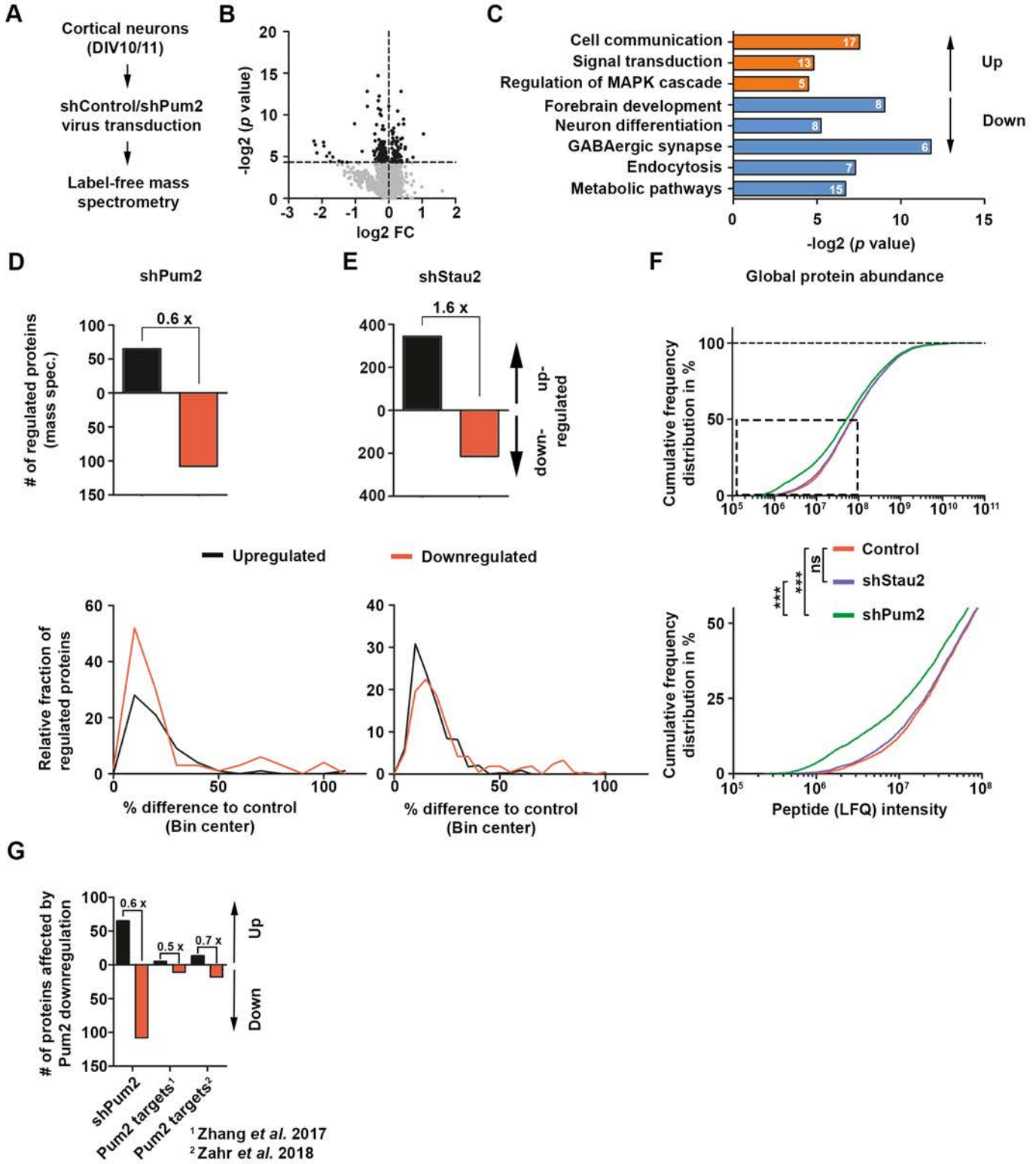


Figure 4: Pum2 regulates inhibitory synapses

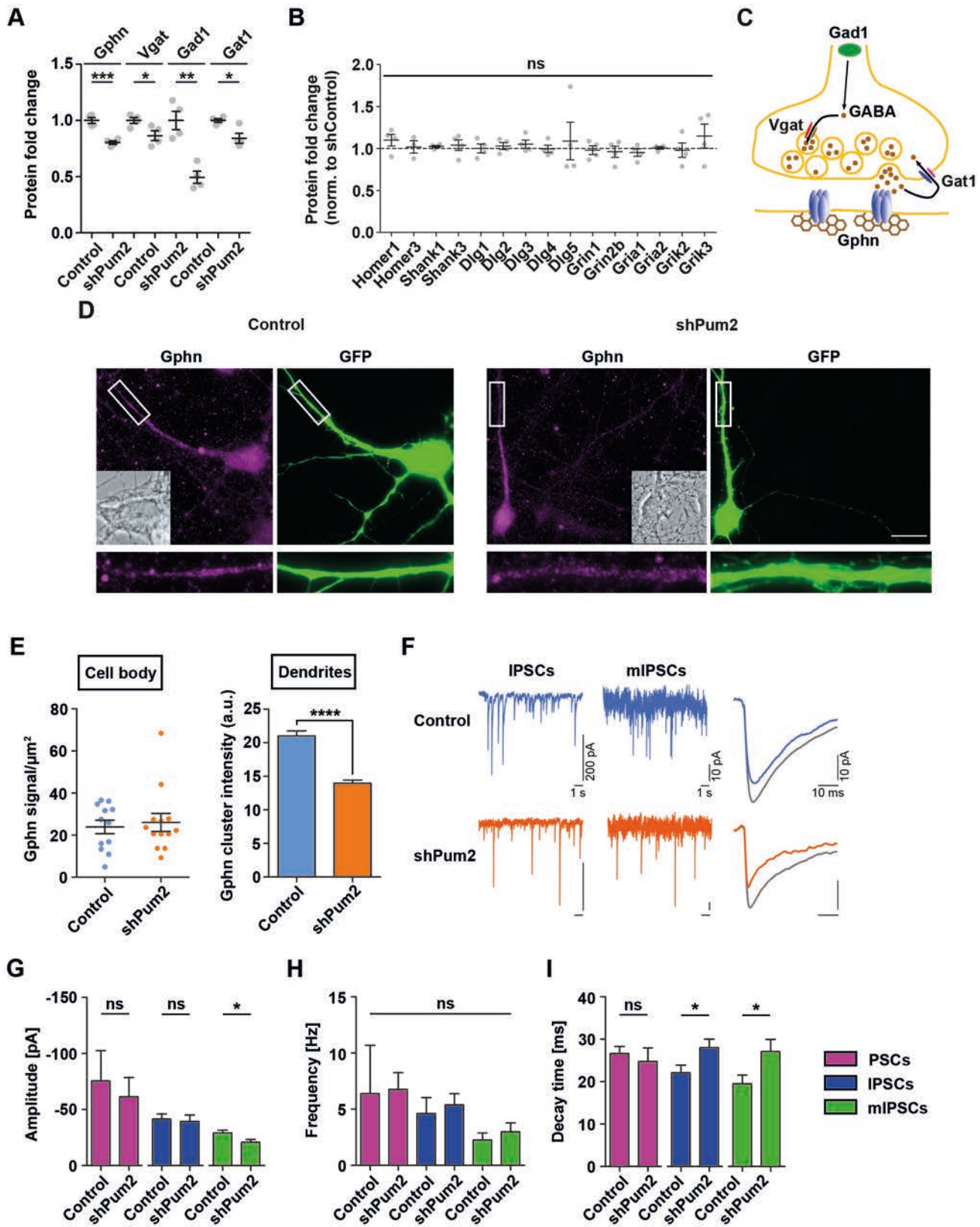


Figure S1: Pum2 does not associate with translating polysomes

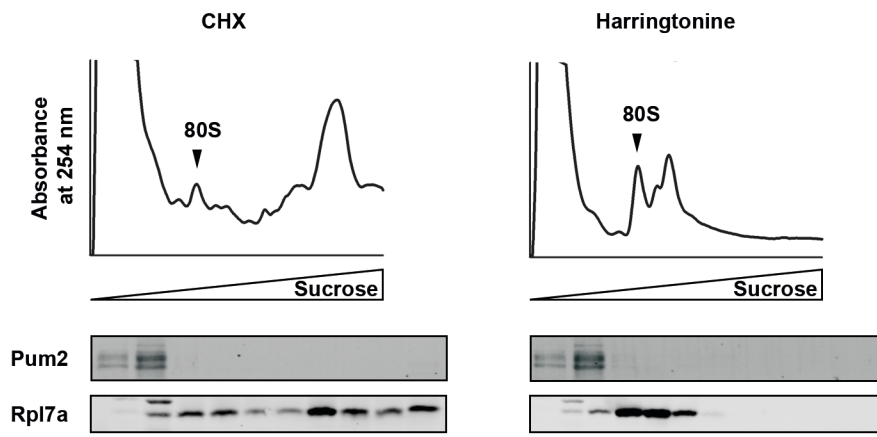
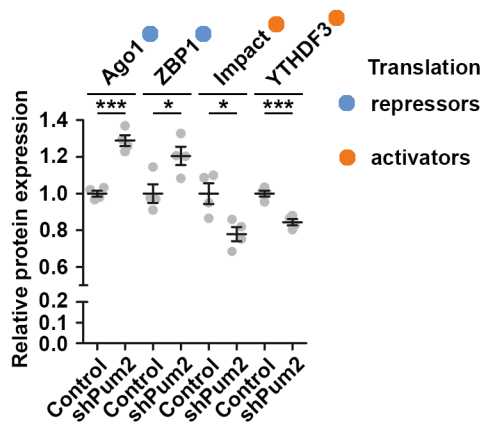


Figure S3: Pum2 affects expression of key expression regulators



Acknowledgments

First, I would like to thank Prof. Dr. Kiebler for giving me the opportunity to write my Ph.D. thesis in his lab, for his continuous support over the years and motivation. In addition, I like to thank my thesis committee for their helpful comments and inspiring discussions. A special thank goes to the Boehringer Ingelheim Fonds for their financial and intellectual supports over the last years.

Moreover, I am very grateful to Prof. Dr. Jovica Ninkovic, Dr. Max Harner and Dr. Bastian Popper for inspiring discussions and their challenging scientific questions. My sincere thanks also go to Antonia Demleitner, Philipp Follwaczny, Helena Pernice and Surina Frey for their experimental support. In addition, I thank all my collaborators for their help and support over the years. In particular, I thank Dr. Therese Riedermann, Dr. Tobias Straub, Prof. Dr. Axel Imhof and Dr. Ignasi Forné.

A special thank goes to Daniela Rieger and Christin Illig for their excellent experimental support. Moreover, I am very grateful to Sven Aschenbroich, Katja Eubler, Dr. Inmaculada Segura and Lydia Wunsch for critical comments on my thesis. Additionally, I would like to thank all members of the Kiebler lab for their intellectual input and helpful discussions.

Last but not least: I thank my family, my parents and my sister, as well as my friends for their support during the last 5 years.

Curriculum Vitae

Rico Schieweck

Dept. Cell Biology (Anatomy III), BioMedical Center
Ludwig-Maximilians University
Großhadener Str. 9
82152 Planegg

Education

University of Munich	PhD Thesis, Feb. 2015 – present
University of Potsdam	M.Sc. in Biochemistry and Molecular Biology, Feb. 2015
University of Potsdam	B.Sc. in Biochemistry, Aug. 2012

Research Experience

From December 2015 till present	PhD thesis entitled ‘RNA-binding proteins balance neuronal activity’ (Kiebler lab)
From 2014 till 2015	Master thesis entitled ‘Characterization of the translational landscape in neurons’ Topic: Investigating the translational control and nuclear translation in neurons with ribosome and polysome profiling (Ignatova lab)
From 2012 till 2014	Research Associate Topic: Investigation of tRNA levels and polysomes in different brain tissues (Ignatova lab)

From April 2012 till August 2012 Bachelor Thesis entitled ‘tRNA level dependent expression of EBNA-1’
Topic: Investigating the EBNA-1 expression in HEK cells dependant on transfected tRNAs (Ignatova lab)

Awards

Early Career Award FASEB Conference, 2019, Snowmass

Grants

DFG Grant ‘Pumilio2-mediated control of local protein expression in neurons’

LMU Research Grant (The role of regulation of translation in the regenerative response of *zebrafish* ependymogial cells)

Fellowship

Boehringer-Ingelheim Fellowship (2015-2017)

Teaching Activities

Neuroanatomy courses for medical students

Organ centred seminars for medical students

Histology courses for medical students

Supervision of Master thesis

Supervision of Medical thesis